
Chairman: Prof. Dr. Karin Coninx
Promotor: Prof. Dr. Thomas Junkers
Copromotors: Prof. Dr. Dirk Vanderzande
Dr. Laurence Lutsen
Members of the jury: Prof. Dr. Katja Loos, Rijksuniversiteit Groningen
Prof. Dr. Richard Hoogenboom, Universiteit Gent
Prof. Dr. Wouter Maes, UHasselt
Prof. Dr. Peter Adriaensens, UHasselt

If we knew what we were doing
It would not be called research, would it?

A. Einstein

TABLE OF CONTENTS

Chapter 1: General introduction

1.1. Polymers	2
1.2. Control in polymerizations	2
1.3. Conjugated polymers	4
1.3.1. Optical properties	4
1.3.2. Semiconductive properties	5
1.4. Complex architectures and self-assembly	6
1.5. Poly(<i>p</i> -phenylene vinylene)s	8
1.5.1. Synthesis of PPV materials <i>via</i> direct routes	9
1.5.2. Synthesis of PPV materials <i>via</i> indirect routes	10
1.5.3. Controlling PPV precursor polymerization	13
1.5.4. Synthesis of block copolymers containing one PPV block	13
1.6. Classical application of PPV materials in devices	16
1.6.1. Organic light emitting diodes	17
1.6.2. Organic photovoltaics	17
1.6.3. Organic field effect transistors	18
1.6.4. Biosensors	19
1.7. New biomedical applications	19
1.8. Aim and outline	20
1.9. References	23

Chapter 2: Discovery of an anionic polymerization mechanism for high molecular weight PPV derivatives *via* the sulfinyl precursor route

2.1. Introduction	35
2.2. Experimental section	37
2.2.1. Synthesis of monomer 4 1-(chloromethyl-4-[(<i>n</i> -octylsulfinyl)methyl] benzene)	37
2.2.2. Polymerization procedure	37
2.2.3. Influence of temperature	38
2.2.4. Anionic polymerization	38

2.2.5. Test the anionic nature of the polymerization with TEMPO	38
2.3. Results and discussion	39
2.3.1. Radical polymerization	39
2.3.2. Anionic polymerization	47
2.4. Conclusions	53
2.5. References	54

Chapter 3: Living polymerization *via* anionic initiation for the synthesis of well-defined PPV materials

3.1. Introduction	59
3.2. Experimental section	61
3.2.1. Synthesis of 1-chloromethyl-2,5-bis(2-ethylhexyloxy)-4-[(methylsulfinyl)methyl] benzene (7)	61
3.2.1.1. Synthesis of 1,4-bis(2-ethylhexyloxy) benzene (3)	61
3.2.1.2. Synthesis of 1,4-bis(chloromethyl)-2,5-bis(2-ethylhexyloxy)benzene (4)	61
3.2.1.3. Synthesis of 1,1'-[(2,5-bis(2-ethylhexyloxy)-1,4-phenylene)bis(methylene)] bis(tetrahydrothiophenium)chloride (5)	62
3.2.1.4. Synthesis of 1-chloromethyl-2,5-bis(2-ethylhexyloxy)-4-[(methylsulfinyl)methyl] benzene (7)	63
3.2.2. Synthesis of 1-(<i>tert</i> -butyl)-4-[(<i>n</i> -octylsulfinyl)methyl]benzene (10)	63
3.2.3. Polymerization procedure	64
3.2.4. Test the anionic nature of the polymerization with TEMPO	65
3.3. Results and discussion	66
3.4. Conclusions	74
3.5. References	75

Chapter 4: Anionic initiators and endcapping, looking at synthetic possibilities

4.1. Introduction	81
4.2. Experimental section	83
4.2.1. Synthesis of anionic initiators	83
4.2.1.1. Synthesis of 4-(<i>tert</i> -butyl)benzyl- <i>n</i> -octyl sulfane (2)	83
4.2.1.2. Synthesis of 1-(<i>tert</i> -butyl)-4-[(<i>n</i> -octyl sulfinyl)methyl]benzene (3)	84
4.2.1.3. Synthesis of 1-(<i>tert</i> -butyl)-4-[(<i>n</i> -octyl sulfonyl)methyl]benzene (4)	84
4.2.1.4. Synthesis of 1-(<i>tert</i> -butyl)-4-[(methylsulfinyl)methyl]benzene (6)	85
4.2.1.5. Synthesis of 1-bromo-4-[(<i>n</i> -octylsulfinyl)methyl]benzene (9)	86
4.2.1.6. Synthesis of 1-chloro-4-[(<i>n</i> -octylsulfinyl)methyl]benzene (12)	87
4.2.2. Synthesis of ¹³ C-labeled end-capper methyl-4-(chloromethyl)benzoate (14)	87
4.2.3. Polymerization	88
4.3. Results and discussion	90
4.3.1. Influence of monomer concentration	90
4.3.2. Influence of the polarizer functionality on the anionic initiator	91
4.3.3. Influence of the mode of compound addition	92
4.3.4. Effect of reaction temperature and time	96
4.3.5. Use of ¹³ C-labeled end-capper	99
4.4. Conclusions	105
4.5. References	106

Chapter 5: Anionic PPV polymerization from the sulfinyl precursor route: block copolymer formation from sequential addition of monomers

5.1. Introduction	111
-------------------	-----

5.2. Experimental section	113
5.2.1. Polymerization	113
5.2.2. Polymer and block copolymer synthesis with high vacuum line anionic polymerization setup (B → M + I)	113
5.2.3. Separation of polymers	114
5.3. Results and discussion	115
5.3.1. Anionic polymerization setup	115
5.3.2. Block copolymer synthesis on high vacuum line	118
5.4. Conclusions	128
5.5. References	129

Chapter 6: Synthesis of well-defined PPV containing block copolymers with precise endgroup control from a dual-initiator strategy

6.1. Introduction	135
6.2. Experimental section	138
6.2.1. Synthesis of anionic initiators for ESI-MS study	138
6.2.2. Synthesis of anionic initiator 6 (4-[(methylsulfinyl)methyl]phenyl-2-bromo-2-methylpropanoate)	138
6.2.3. PPV polymerization	139
6.2.4. Synthesis of PPV- <i>b</i> -P(<i>t</i> -BuA) block copolymer P4 <i>via</i> SET-LRP	140
6.2.5. Synthesis of PPV- <i>b</i> -PAA block copolymer P5	140
6.3. Results and discussion	141
6.3.1. ESI-MS assessment of initiation efficiency	141
6.3.2. Use of functionalized anionic initiators to synthesize block copolymers <i>via</i> the use of SET-LRP	153
6.4. Conclusions	163
6.5. References	165

Chapter 7: Synthesis of PPV-*b*-PEG block copolymers using Click chemistry

7.1. Introduction	171
-------------------	-----

7.2. Experimental section	174
7.2.1. General procedure for Sonogashira reaction	174
7.2.2. Synthesis of anionic initiator with TMS-protected alkyne-functionality, trimethyl[(4-[(octylsulfinyl)methyl]phenyl)ethynyl]silane (4)	174
7.2.3. Synthesis of alkyne initiator with spacer, trimethyl[3-(4-[(methylsulfinyl)methyl]phenoxy)propynyl]silane (9)	176
7.2.4. Synthesis of PPV block with alkyne functionality	178
7.2.5. Synthesis of PEG block with azide functionality	179
7.2.6. Synthesis of BEH-PPV- <i>b</i> -PEG <i>via</i> CuAAC coupling	179
7.3. Results and discussion	181
7.3.1. Synthesis of anionic initiator with alkyne functionality	181
7.3.2. Synthesis of block copolymers <i>via Click</i> coupling of an alkyne-functionalized PPV block (no spacer) and an azide-functionalized PEG block	183
7.3.3. Synthesis of block copolymers <i>via Click</i> coupling of an alkyne-functionalized PPV block (with spacer) and an azide-functionalized PEG block	187
7.4. Conclusions	193
7.5. References	194

Chapter 8: Anionic polymerization *via* the sulfinyl precursor route for other PPV premonomers and outlook towards functional block copolymers

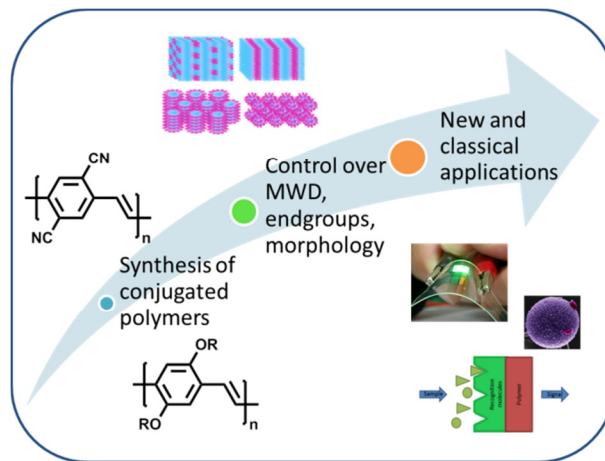
8.1. Introduction	199
8.2. Experimental section	202
8.2.1. Monomer synthesis	202
8.2.1.1. Synthesis of 1-chloromethyl-2-methoxy-5-(3,7-dimethyloctyloxy)-4-[(octylsulfinyl)methyl] benzene (6)	202

8.2.1.2.	Synthesis of 6-(2-chloromethyl-4-methoxy-5-[(octylsulfinyl)methyl]-phenoxy) hexanoic acid methyl ester (11)	202
8.2.1.3.	Synthesis of 1-bromomethyl-2,5-dicyano-4-[(octylsulfinyl)methyl] benzene (16)	203
8.2.2.	Synthesis of anionic initiators	204
8.2.2.1.	Synthesis of anionic initiators 17 , 18 and 19	204
8.2.2.2.	Synthesis of azide-functionalized anionic initiator 20	204
8.2.2.3.	Synthesis of anionic initiator 21 with deprotected alkyne function	205
8.2.3.	Anionic polymerization procedure	206
8.2.3.1.	General method	206
8.2.3.2.	Test the anionic nature of the polymerization with TEMPO	207
8.2.4.	Synthesis of block copolymers	207
8.2.4.1.	Block copolymers <i>via</i> SET-LRP	207
8.2.4.2.	Block copolymers <i>via</i> <i>Click</i> chemistry	208
8.2.5.	Hydrolysis of P3 to reach poly[1,4-(2-(5-carboxypentyloxy)-5-methoxyphenylene) vinylene] (CPM-PPV) P4	209
8.3.	Results and discussion	210
8.3.1.	Testing the anionic nature of the polymerization reactions for different sulfinyl monomers	210
8.3.1.1.	Anionic polymerization to obtain well-defined MDMO-PPV	211
8.3.1.2.	Anionic polymerization to obtain well-defined ester-functionalized PPV	212
8.3.1.3.	Anionic polymerization to obtain well-defined CN-PPV	214
8.3.1.4.	General overview for the anionic polymerization of different premonomers	215
8.3.2.	Outlook towards functionalized block copolymers	216

8.3.2.1. Block copolymers containing an ester-functionalized PPV polymer block	216
8.3.2.2. P-type–n-type block copolymers consisting of two PPV blocks <i>via</i> CuAAC coupling	219
8.4. Conclusions	225
8.5. References	226
Chapter 9: Materials and characterization	
9.1. Materials	230
9.2. Characterization	230
9.2.1. Standard characterization techniques for monomers and initiators	230
9.2.2. Specialized NMR measurements: (semi-) quantitative ¹³ C NMR and ¹³ C APT NMR	231
9.2.3. Spectroscopic techniques: UV-Vis and fluorescence spectroscopy	231
9.2.4. Size exclusion chromatography (SEC) / Gel permeation chromatography (GPC) / Multi angle laser light scattering (MALLS)	232
9.2.5. Electrospray ionization – mass spectrometry (ESI-MS)	233
9.2.6. Thermal analysis, DSC and TGA	234
9.2.7. Dynamic light scattering (DLS) for determination of hydrodynamic diameter of nanoparticles	234
Summary	237
Samenvatting	241
List of abbreviations	247
Publications and personal contribution	253
Dankwoord	259

CHAPTER 1

General Introduction



1.1. POLYMERS

Polymers or macromolecules are defined by IUPAC as 'a molecule of high relative molecular mass, the structure of which essentially comprises the multiple repetitions of units derived, actually or conceptually, from molecules of low relative molecular mass'.¹ The word polymer is also derived from the two Greek words '*poly*' which means 'many' and '*meros*' which means 'parts'.

In everyday life, mankind is confronted with polymers every second. Not only our body is full of polymers (e.g. DNA or proteins), also nature has provided us with a variety of polymeric materials like for instance wood, cotton or rubber. Synthetic polymers were first discovered by Leo Baekeland in 1907 with the synthesis of Bakelite (poly(oxybenzyl methylene glycol anhydride)), a phenol-formaldehyde polymer which was worldwide used for example as a plastic in telephone and radio casings or children's toys because of its heat-resistant and electrical insulating properties and because of its moldability and low-cost. From that moment on lots of synthetic polymers and polymer architectures with a variety of properties and benefits were, and are being developed.

1.2. CONTROL IN POLYMERIZATIONS

Based on the observed polymerization mechanism, a classification can be made based on two major possibilities: a step-growth mechanism or a chain-growth mechanism. In a step-growth mechanism (like polycondensation reactions), which is catalyzed by a proper catalyst, the formation of high molecular weight materials is only observed at large conversion (thus at the end of the polymerization reaction). In contrast, for a chain-growth polymerization mechanism, the reaction is started using an initiator and high molecular weight

polymers are obtained from the start because once a chain is started, it quickly polymerizes. If no termination, nor transfer occurs in this chain-growth polymerization reaction, a living polymerization is reached. Living polymerizations have some special characteristics: (i) because the propagating chain ends remain unchanged during the reaction, the degree of polymerization is equal to the monomer concentration divided by the initiator concentration ($DP_n = C_m / C_i$) after full conversion and (ii) the degree of polymerization is linearly proportional to the conversion. This means that once a chain is started, it keeps growing until depletion of monomer and if the initiation is much faster than the propagation, polymers with low polydispersity are formed. With tuning the amount of initiator, chain length (and thus molecular weight) of the polymer chains, synthesized *via* a living polymerization mechanism, can be controlled and also defined endgroups are obtained. In this respect block copolymers and complex architectures become readily available.

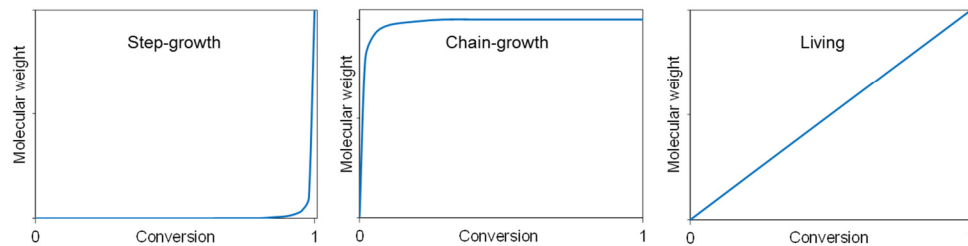


Figure 1.1: Molecular weight versus conversion for step-growth, chain-growth and living (fast initiation) polymerization mechanism

1.3. CONJUGATED POLYMERS

The IUPAC describes a conjugated polymer as 'a molecular entity whose structure may be represented as a system of alternating single and multiple bonds (e.g. $\text{CH}_2=\text{CH}-\text{CH}=\text{CH}-\text{CH}=\text{CH}_2$). In such systems, conjugation is the interaction of one p-orbital with another across an intervening σ -bond'.² Examples of the most common conjugated polymers³ are given in Figure 1.2.

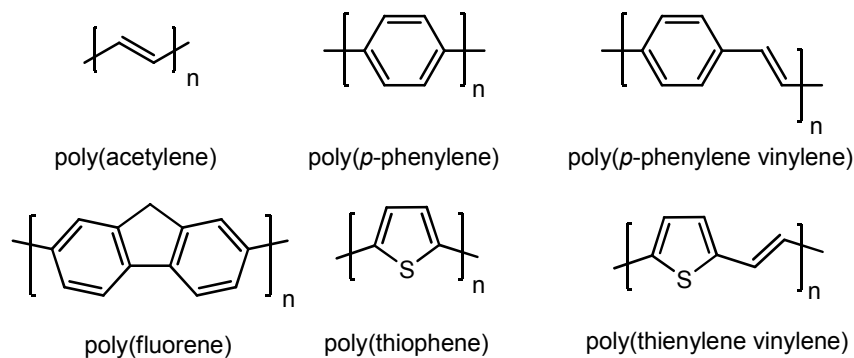


Figure 1.2: Structures for some of the most common conjugated polymers

1.3.1. Optical properties

One of the main optical properties of importance for conjugated polymers like poly(*p*-phenylene vinylene), is fluorescence. Fluorescence is a form of luminescence and is the emission of light by a substance that has absorbed light. In most cases the emitted light has a longer wavelength than the absorbed radiation (and thus lower energy). The main applications for fluorescent conjugated materials are based on chemical sensing or fluorescent labeling because, with introduction of specific functional groups on fluorescent polymers, specific interactions can be detected. For different polymer structures and functionalities also different emission colors can be obtained.⁴⁻⁶

1.3.2. Semiconductive properties

Because of the π -conjugation (electron delocalization along the polymer backbone) that is present in this material class, these conjugated polymers are intrinsically semiconducting. The π (bonding, HOMO) and π^* (anti-bonding, LUMO) orbitals arise from delocalized valence and conduction wavefunctions respectively, which support mobile charge carriers and the split between this valence and conduction band is defined as the bandgap (E_g). In order to achieve conductive materials electrochemical or chemical oxidation or reduction (so called doping) is necessary, in the latter case using simple oxidative or reductive species (so called dopants). Upon doping, the generated charges can delocalize over the π molecular orbitals and either p-type (oxidized, creation of holes) or n-type (reduced, creation of extra valence electrons) conductive materials can be obtained.⁷ In the pristine state, the bandgap of these semiconducting polymers typically varies between 0.5 and 3.5 eV (Figure 1.3). This conductivity, unique for doped conjugated polymers, was first observed for poly(acetylene)⁸ in the 1970's and for this discovery, Alan J. Heeger, Alan G. MacDiarmid and Hideki Shirakawa were awarded the Nobel Prize in Chemistry in 2000.⁹⁻¹¹

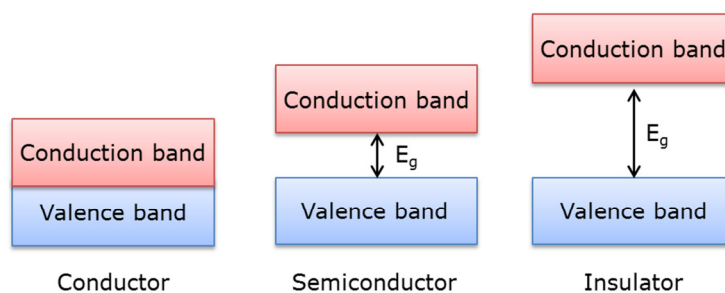


Figure 1.3: Energy bandgaps (E_g) for different materials (conductor, semiconductor and insulator)

By modifying the structure of the monomers, the HOMO and LUMO levels can be tuned, thereby changing the bandgap of the material. A second method to influence the bandgap of the material is by introducing side chains on the monomer which can, through sterical hindrance, disrupt the conjugation length of the polymer. Also defects in the polymer chains lead towards this disruption of the conjugated backbone again resulting in a change of the bandgap width.^{11,12}

The main advantages of conjugated polymer materials is that they combine the flexibility, light weight, great diversity of properties and easy processing (high solubility, thin layers) of plastics with semiconducting properties. The discovery of the use of poly(*p*-phenylene vinylene) (PPV) as a potential active element in large-area light emitting diode displays¹³ drew attention towards this material class.

1.4. COMPLEX ARCHITECTURES AND SELF-ASSEMBLY

The term complex architecture relates to the deviation from a linear chain by means of branching and thus corresponds to one macromolecule. This branching can occur either random or using specifically designed monomers to obtain precise architectures. With the development of living polymerization methods, and thereby the use of specially tailored monomers or initiators, polymers with specific architectures become readily available regarding functionality, composition and topology (Figure 1.4). The degree of branching of these macromolecules is determined by the functionality of the monomers and has a great influence on the physical and chemical (for example solubility, glass transition temperature (T_g) and viscosity) properties of the synthesized materials.

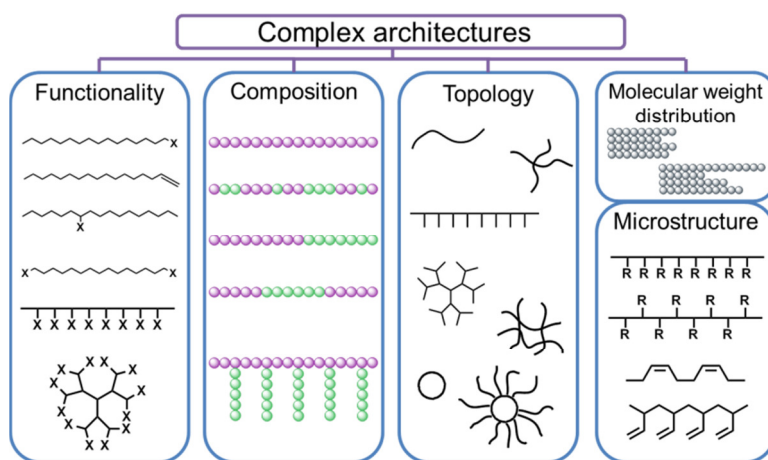


Figure 1.4: Overview of influences on complex architectures for polymers

Self-assembly is the spontaneous organization of different polymers into stable, well-defined structures for which the final structure is near or at the thermodynamic equilibrium. These structures are often held together using secondary interactions that are very specific and directional (hydrogen bonding, van der Waals interactions, π - π interactions, hydrophobic and hydrophilic interactions).¹⁴ In nature, self-assembly is very common, with the main examples being the folding of proteins or formation of the DNA double helix.

By using this self-assembly approach for conjugated polymers, stable and well-defined aggregates can be obtained which exhibit structural and morphological organization across multiple length scales. In this respect control could be gained over the aggregation and opto-electronic properties of these conjugated polymers because modifications could be obtained with differentiation in molecular weight, functionality (chain end or side chain) or combination of both.¹⁵

Block copolymers are defined by IUPAC by considering that, 'in the constituent macromolecules of a block copolymer, adjacent blocks are constitutionally

different, i.e. adjacent blocks comprise constitutional units derived from different species of monomer or from the same species of monomer but with a different composition or sequence distribution of constitutional units'.¹⁶ For this kind of polymer class, it is very well known that they are self-assembling materials (if they consist of blocks with distinct block properties) for which the self-assembled structures depend on the different polymer blocks and length of the blocks that are present. By using chemically distinct macromolecular blocks, self-assembly is driven by microphase separation behavior. The shape of the nanodomains (spheres, cylinders or lamellae) is determined by the relative volume fraction of the polymer blocks while the size of the domains is determined by the overall molecular weight of the block copolymers. In this respect, lots of possibilities arise when blocks with different chain lengths are coupled.¹⁷

1.5. POLY(*p*-PHENYLENE VINYLENE)s

Poly(arylene vinylene)s (PAVs) are an intensively studied material class mainly due to their (potential) application as active materials in organic electronics.¹⁸ Poly(*p*-phenylene vinylene) (PPV) for example has excellent electroluminescent properties and a plethora of PPV derivatives were studied and applied in organic light emitting diodes (oLEDs).^{19,20} For these PAVs, lots of synthesis routes were developed which can be divided into two major classes. The first ones are the direct routes, yielding the conjugated material in one step. This can be done using polycondensation reactions, palladium catalyzed coupling reactions, electrochemical methods or metathesis reactions. The second method to obtain PAV materials, is to use precursor methods where *p*-quinodimethanes are polymerized to form soluble precursor polymers which can, in a second step, be

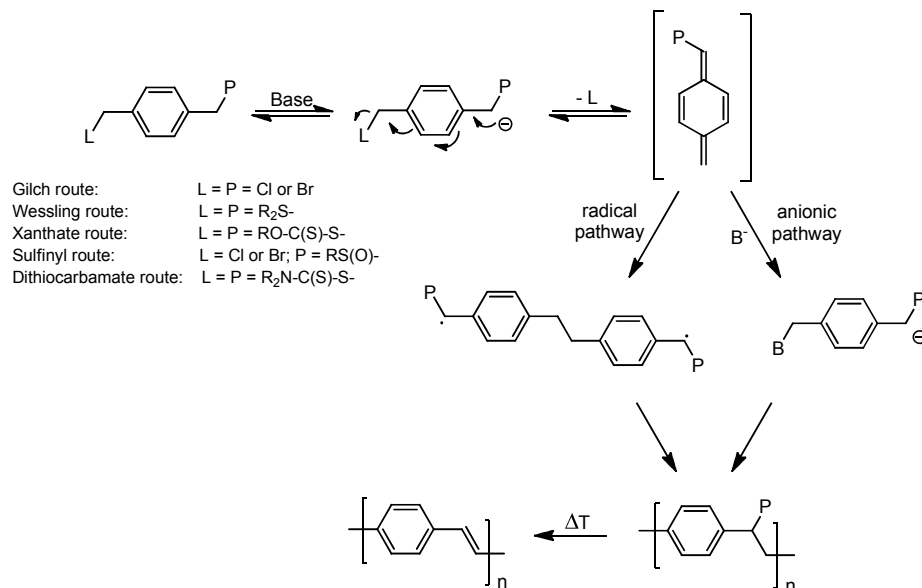
thermally converted into the conjugated polymer structure.²¹ Also some non-quinodimethane precursor methods were developed, based on ring opening metathesis polymerization (ROMP),^{22,23} but these methods will not further be described in this thesis.

1.5.1. Synthesis of PPV materials *via* direct routes

Examples of the direct routes towards PPVs are the Wittig,²⁴⁻²⁶ Horner,^{26,27} McMurry,^{28,29} Knoevenagel^{25,30,31} and Siegrist^{25,32} polycondensation reactions or the palladium catalyzed Heck,^{33,34} Stille³⁵ and Suzuki³⁶ coupling reactions. The main drawbacks of these methods are the bad chain length control, the low solubility of the conjugated material after polymerization due to interchain π stacking and the sensitivity towards the used conditions that lead to bad control over the polymerization reaction. The main advantage of the direct routes is the easy synthesis of alternating copolymers which can be accessed for the routes starting from two different monomers (e.g. Wittig and Knoevenagel polycondensations). A second method to gain the conjugated PPV polymers in one step is the electrochemical synthesis by the direct and mediated cathodic reduction of (halomethyl)arenes.^{37,38} Using ROMP³⁹⁻⁴¹ or acyclic diene metathesis (ADMET)⁴¹ as a polymerization method, starting from *para*-cyclophanediene or divinylbenzene respectively as the monomer, PPVs can also be obtained. *Via* these chain growth polymerization reactions high molecular weights are readily accessible but the rather complex monomer structures (especially for the ROMP polymerization) are synthetically challenging.

1.5.2. Synthesis of PPV materials via indirect route

To overcome the drawbacks of the direct synthesis routes towards PPV materials, indirect (or precursor) polymerization routes, based on *p*-quinodimethanes, were developed (see Scheme 1.1). This chain growth approach is advantageous because they allow for soluble polymers with higher molecular weights and large scale production because they are usually fast and cost effective.⁴²



Scheme 1.1: General scheme for the radical and anionic pathway for the different precursor routes towards PPV

In the first step a proton of the premonomer is abstracted by a base which is followed by a 1,6-elimination (second step) of the leaving group (L) to yield a *p*-quinodimethane system (*p*-QM), generating the actual monomer for the polymerization reaction.⁴³ In the third step, these unstable *p*-QMs will polymerize spontaneously without external initiation towards the soluble (non-conjugated) precursor polymer which can in a last step be converted to the

conjugated polymer using a thermal treatment or *via* base induced elimination.^{44,45} Over the last decades, different precursor routes were developed, for which the most important are the Gilch,⁴⁶ Wessling,⁴⁷⁻⁴⁹ xanthate,^{50,51} sulfinyl⁵²⁻⁵⁷ and the dithiocarbamate route.^{58,59} The sulfinyl route is distinguished from the other routes because it is the only route where the leaving group (L) and polarizer functionality (P) differ from each other, leading to an unsymmetrical premonomer. This is beneficial regarding the gain of control over the polymerization reaction and the very low defect level in the polymer chains since only head-to-tail couplings can occur during polymerization.^{60,61} For all the precursor routes (except for the xanthate route), a self-initiating radical mechanism was reported with the initiating moiety being a biradical formed by dimerization of two *p*-QMs.⁶²⁻⁶⁷ For the sulfinyl route, depending on the base and solvent used, either a radical mechanism (yielding high molecular weight polymers),^{68,69} or a combination of a radical and an anionic mechanism (yielding low molecular weight materials)^{70,71} was observed.

To render both the precursor polymer as well as the conjugated polymer soluble in organic solvents, long and flexible side chains are introduced on the aromatic core of the premonomer.⁷² The most studied PPV derivatives (see Figure 1.5 for structures) are poly[2-methoxy-5-(3,7-dimethyloctyloxy)-*p*-phenylene vinylene], (MDMO-PPV), poly[2-methoxy-5-(2-ethylhexyloxy)-*p*-phenylene vinylene], (MEH-PPV) and poly[2,5-bis(2-ethylhexyloxy)-*p*-phenylene vinylene], (BEH-PPV, the polymer that is mostly studied in this thesis)⁷³. Also poly[2-methoxy-5-(carboxypentyloxy)-*p*-phenylene vinylene], (CPM-PPV), a PPV derivative with an acid functionality in one of the side chains of the premonomer was developed. By synthesizing a copolymer of MDMO-PPV and CPM-PPV (9:1

ratio), a platform polymer could be obtained for further post-polymerization functionalization with various alcohols *via* an optimized DCC/DMAP procedure.⁷⁴

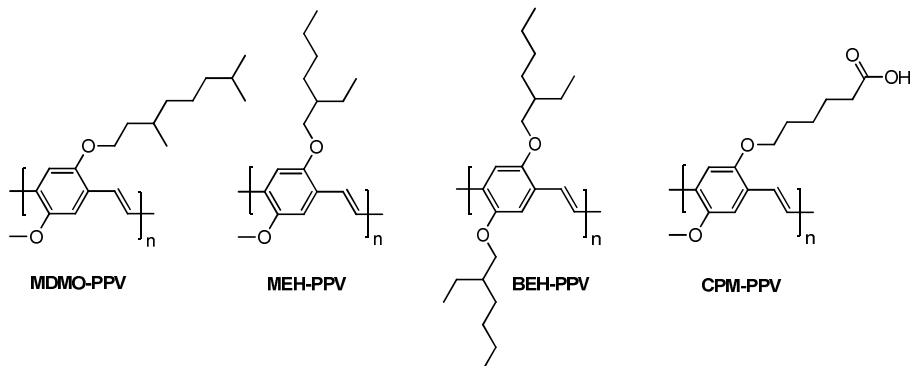


Figure 1.5: Most commonly studied PPV derivatives

Besides these p-type PPV derivatives, also a range of n-type derivatives were developed over the years. The main advantage of these materials as an alternative for PCBM ([6,6]-phenyl-butyrac acid methyl ester) in electronic devices is to facilitate the formation of an optimal morphology because polymers similar in structure are used. These n-type PAVs (Figure 1.6) can be obtained *via* the sulfinyl precursor route with the introduction of electron withdrawing groups on the aromatic core of the premonomer (CN-PPV)⁷⁵ or on the double bond (PP(CN)V, synthesized *via* the Knoevenagel polycondensation), or by using an electron accepting heterocyclic core like pyridine (poly(pyridine vinylene), PPyV) or derivatives hereof.⁷⁶

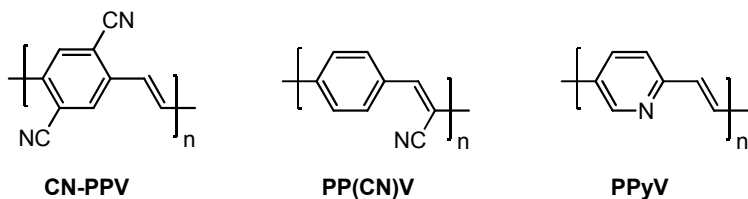


Figure 1.6: Possible n-type poly(*p*-arylene vinylenes)

1.5.3. Controlling PPV precursor polymerization

For all presented precursor routes (with the xanthate route as the only exception), so far a radical polymerization pathway was established⁶²⁻⁶⁷ for which the initiation was started from the formation of a biradical. For these very fast radical polymerization reactions, high molecular weight materials were obtained in high yields but with very little control. The only reported method of control is the use of a chain transfer agent, such as CBr_4 (carbon tetrabromide), for the radical sulfinyl precursor route.⁷⁷ Using this method, chain length and chain functionality (Br-functionalized chains) can more or less be controlled. This work was published in collaboration with J. Vandenberg during this thesis, but will further not be addressed.

For the sulfinyl route, not only a radical, but also a combined radical-anionic polymerization mechanism was reported earlier.^{70,71} Until the start of this thesis, no pure (living) anionic mechanism was reported nor the control over this kind of polymerization reaction in terms of molecular weight control, endgroup functionality or use of these precursor blocks in complex architectures or self-assembling block copolymers.

1.5.4. Synthesis of block copolymers containing one PPV block

Conjugated polymers are stiff polymers due to their delocalized electronic structures and generally have a limited solubility due to interchain π - π interactions. To increase the solubility and to gain more influence on the organization of the rod-like conjugated polymers, a second, flexible (or coil) block can be covalently bonded in order to obtain a rod-coil block copolymer. In this way all kinds of morphologies and nanostructured materials become available depending on the polymers and environment used (Figure 1.7).^{78,79}

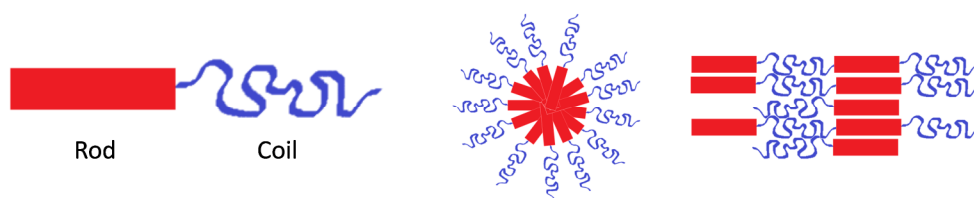


Figure 1.7: Schematic representation of a rod-coil block copolymer and some examples of self-assembly (micelle and lamellar conformation)

For PPV materials, rod-coil block copolymers were already reported, mostly starting from a PPV block synthesized using the Siegrist polycondensation method since it allows to introduce an aldehyde endgroup which can easily be coupled with an anion or by using a suitable linker. Block copolymers synthesized *via* this method are for instance: PPV-*b*-PS (polystyrene),^{80,81} PPV-*b*-PLA (poly(lactic acid)),⁸² PPV-*b*-PI (polyisoprene),^{83,84} PPV-*b*-PBA (poly(butyl acrylate))⁸⁵ and a triblock copolymer consisting of a poly(ferrocenyldimethylsilane), a poly(2-vinylpyridine) and a BEH-PPV block (PFS-*b*-P2VP-*b*-BEH-PPV).⁸⁶ Other examples starting from PPV blocks synthesized *via* the Siegrist polycondensation, which was post-polymerization functionalized with an alkyne bond in order to couple the second block using *Click* chemistry, were PPV-*b*-POM (polyoxomethalate)⁸⁷ and PPV-*b*-PMMA (poly(methyl methacrylate)).⁸⁸ Also a p-type-n-type block copolymer, namely PPV-*b*-P(*S-stat*-C₆₀MS) (statistical polymer of PS and C₆₀ decorated PS) was reported starting from a PPV block synthesized *via* Siegrist polycondensation.⁸⁹ These p-type-n-type block copolymers are particularly interesting for organic solar cells. To generate photocurrent first an exciton needs to be created by light absorption and in a second step, this exciton needs to dissociate to a donor-acceptor interface where charge separation can occur. Typically the exciton

diffusion length is 5-10 nm and in the case of a p-type–n-type block copolymer the requirement of this interface is easily reached because no phase separation in large donor or acceptor domains can occur. The main challenge for these kinds of block copolymers will be to reach an optimal morphology of the polymer layers in order to reach good charge transport through the layer towards the electrodes. Thus, self-assembly, that is found for block copolymers, provides a tool for patterning these p-type–n-type block copolymers leading towards nicely controlled layers for devices. So optimization of device behavior requires first of all control over nanodomain orientation and, to facilitate optimal charge transport, long-range order.⁹⁰ Alternatively Heck coupling was employed for the synthesis of block copolymers containing one PPV block such as PPV-*b*-PEG (polyethylene glycol), PEG-*b*-PPV-*b*-PEG and PPV-*b*-PPG (polypropylene glycol).^{91,92} A last literature example for a PPV-containing block copolymer is PEG-*b*-PPV, where first the PEG block was synthesized and the PPV block was attached in an anionic fashion using a strong base (diphenylmethyl potassium, DPMK).⁹³ For most of the given examples, also the morphology and self-assembly of the different blocks were described (for example micelles or lamellae).⁷⁸⁻⁸⁹ As can be concluded from all these examples, various PPV block copolymers have already been synthesized, but none of them started from a PPV precursor polymer, thus from a polymer with high molecular weight and potentially controlled microstructure. Development of block copolymer synthesis routes from precursor polymerization will allow for a multitude of novel materials with broad application range. Because of the high solubility of the PPV precursor block and the wide variety of possibilities (see later in this thesis the use of anionic initiators with custom-made functionalities) this method will be explored in this work.

1.6. CLASSICAL APPLICATION OF PPV MATERIALS IN DEVICES

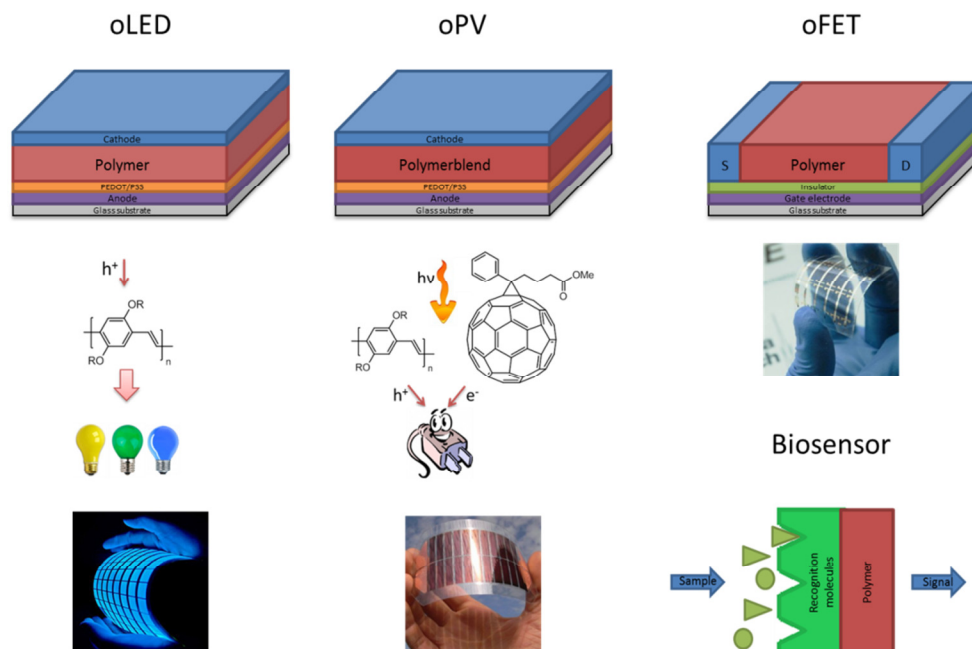


Figure 1.8: General overview of different electronic device applications of conducting polymers

As mentioned before, conjugated polymers combine the properties of plastics (light weight, flexible, low costs) with easy processing (spin-coating, spray coating and inkjet printing for large area thin films in roll-to-roll processing) and with the electrical and optical properties of metals or semiconductors. In this way they can easily be incorporated in all kinds of devices such as organic light emitting diodes, photovoltaics, field effect transistors and biosensors for which the main challenges are long-term stability and efficiency.^{94,95}

1.6.1. Organic light emitting diodes

The development of organic light emitting diodes (oLEDs) evolved because of the interest in the possibility of light emission for organic semiconductors. This could be achieved through charge injection under electroluminescence (a high applied field). Conjugated polymers are a good choice in this respect because of their excellent charge transport and their high quantum efficiency for luminescence. For these polymers, depending on the polymer structure which results in changes in the bandgap, the injected electrons and holes can emit light by recombination at different wavelengths.⁹⁶ Since the first oLED was reported in 1990, based on the use of PPV as the light emitting polymer (and a reported quantum efficiency below 0.1%)¹³ attention was drawn towards the development of better performing devices. This implies that polymers with low defect levels are preferred, because these defects result in an interruption of the conjugation length of the polymer (thereby changing the E_g) thus resulting in a lower operational lifetime of the devices.⁹⁷⁻⁹⁹ For a general device built-up and working principle of an oLED device see Figure 1.8.

Plain-PPV, with a bandgap around 2.2 eV, emits in the green-yellow region of the spectrum. By tuning the polymer structure, e.g. introducing substituents on the aromatic core (which also enhance the luminescence efficiency), on the vinyl bonds or by tuning the conjugation length of the polymers, the E_g of the polymer can be influenced yielding polymers with different emission colors.¹⁰⁰

1.6.2. Organic photovoltaics

Organic electronics are gaining more and more interest because of easy production, little material needed (thin layers of ~ 100 nm) and thus low cost. In an organic photovoltaic (oPV) device, electrons (e^-) and holes (h^+) are generated

in the active layer – consisting of a donor and acceptor material – which can migrate towards their respective electrodes and deliver energy (Figure 1.8). To do so, a phase separation of 5-10 nm is needed, if not, exciton recombination will occur and the absorbed energy is dissipated without generating photocurrent. Finally, the generated charges need to be able to transport to their respective electrodes. In this respect, morphological changes of the active layer and degradation (air, temperature, light) can drastically reduce the lifetime of the devices.⁹⁴ As for oLEDs, also for oPV materials defects in the polymer chains reduce the conjugation length and can act as a charge trap (reducing mobility of the charges and conductivity).^{101,102} To stabilize the initial nanomorphology of the active layer, four possible routes can be taken. First of all, one can think of using high T_g donor materials, introducing reduced flexibility in the polymer chain.^{103,104} A second possibility is the introduction of functional groups in the donor polymer so that cross-linking can occur to 'freeze' the morphology after a thermal or UV light treatment.¹⁰⁵ The third route is the use of p-type and n-type polymers (instead of fullerenes) because in this way improvement of the photovoltaic effect originates from fractal network geometry.¹⁰⁶⁻¹⁰⁸ A last option towards morphology stabilization is the use of donor–acceptor block copolymers instead of donor–acceptor bilayers or blends. By coupling both blocks, phase separation can not occur and bad electrode contact will be minimized if the nanomorphology can be controlled.^{89,109,110}

1.6.3. Organic field effect transistors

A field effect transistor (FET) is a transistor that uses an electric field to control the conductivity of a channel of one type of charge carriers. In this channel, the electrons or holes flow from the source to the drain which are connected to the

semiconductor through ohmic contacts. The conductivity of this channel is a function of the potential applied across the gate and source electrodes. In an oFET (Figure 1.8), the semiconducting material consists of an organic conjugated polymer such as PPV. oFET-based circuits are of particular interest because of their wide range of applications where high speeds are not critical such as flexible electronics. For PPV materials, a high degree of main-chain regularity and the introduction of non-branched side chains lead towards a higher mobility. After annealing (110–118 °C) mobility and stability – in air and dark conditions – were further enhanced.^{94,111,112}

1.6.4. Biosensors

Polymers are a key material in the construction of biosensors because they are used as transducer-active layer for the read-out of these devices (Figure 1.8). This was for instance successfully tested with MDMO-PPV as a transducer and immobilization layer for monoclonal mouse antibodies for binding of its specific antigens¹¹³ and non-conducting molecular imprinted polymers (MIPs) for nicotine sensing¹¹⁴ or the use of MEH-PPV for cholesterol sensing.¹¹⁵

1.7. NEW BIOMEDICAL APPLICATIONS

Because PPV materials have a low charge carrier mobility ($< 10^{-5} \text{ cm}^2 \cdot \text{V} \cdot \text{s}$), more and more, the switch is made from the classical electronic applications towards new applications where for instance, the very good fluorescence properties of PPV are used. In this respect, for instance the existing biomarkers can be replaced by PPV materials and therefore there's a high demand for controlled structures that can be reached using the block copolymer approach.⁴⁻⁶

1.8. AIM AND OUTLINE

The aim of the research presented in this thesis is a state-of-the-art study towards the synthetic possibilities for the anionic polymerization of PPV materials. The synthesis of poly[2,5-bis(2-ethylhexyloxy)-*p*-phenylene vinylene], (BEH-PPV) is described using various initiators (which will be shown to be very efficient). Also in this thesis, an efficient route towards block copolymer synthesis, again using functionalized anionic initiators in a bifunctional initiator strategy, is presented.

In **Chapter 2**, the shift from a radical towards a combined radical and anionic and finally a pure anionic polymerization pathway is described for plain-PPV. This goal could be reached using lithium hexamethyldisilazide (LHMDS) as the base and dry THF as the solvent during polymerization.

Chapter 3 describes the use of anionic initiators with a similar structure to the monomer to gain more control over the molecular weight and dispersity of the PPV polymers. Going from plain-PPV (non-substituted aromatic core) to a symmetrically bis(2-ethylhexyloxy) substituted monomer, not only a soluble precursor polymer, but also a soluble conjugated polymer is reached. Also for this monomer, use of anionic initiators shows good adjustability of molecular weight when using higher equivalents of initiator towards the monomer.

In **Chapter 4**, the use of anionic initiators and the order of adding the different components to the reaction mixture is further investigated. Different reaction temperatures and times are explored in order to study the kinetics of the anionic polymerization pathway for the sulfinyl precursor route. Also in this chapter, end-capping, to gain control over the ω -endgroup of the polymer, is studied using a ^{13}C -labeled endgroup.

Chapter 5 goes more into detail about the anionic polymerization setup. In collaboration with the University of Groningen, where a dedicated high-purity anionic polymerization setup is available, a study is performed comparing these results with results gained on conventional Schlenk lines. In a second part, block copolymer synthesis, making use of the anionic chain end of the PPV chain, is presented using an acrylate as the second monomer.

To prove the high initiator efficiency of the anionic polymerization approach, an ESI-MS study is performed and presented in **Chapter 6**. From this study, it became clear that a very high initiator reliability for the anionic initiators was found. In this way, synthetic possibilities arise towards block copolymers using a dual-initiator strategy. By introducing a bromine functionality on the initiator, single electron transfer – living radical polymerization (SET-LRP) becomes available to introduce a second (acrylate) polymer block and block copolymers are reached in good purity. After hydrolysis of the acrylate, pH responsive micelles can be obtained in aqueous solution.

In **Chapter 7**, synthetic routes towards *Click* reactions, coupling an alkyne-functionalized PPV block with an azide-functionalized poly(ethylene glycol) polymer block, are described. Results are discussed which reveal that a spacer between the aromatic core and the alkyne functionality of the anionic initiator is necessary to obtain a working *Click* reaction.

Chapter 8 describes the anionic polymerization for different premonomers. *Via* this pathway, well-defined MDMO-PPV, CPM-PPV and CN-PPV can be obtained as confirmed with the addition of TEMPO and different amounts of anionic initiator to the polymerization mixture. To finalize, an outlook is given towards functional block copolymers with preliminary results on the synthesis of block copolymers containing one CPM-PPV block with coupling of a second block (acrylates or

styrene) using SET-LRP in a dual-initiator strategy. The synthesis of all-PPV p-type-n-type block copolymers, using CuAAC coupling, is so far not very efficient as it is shown, *via* ESI-MS that for the anionically synthesized CN-PPV precursor polymer insufficient initiation efficiency is found.

In **Chapter 9**, the used materials and all characterization methods that are used during this thesis are described.

To finalize, a **summary** of the thesis in English and Dutch is given, followed by a **list of abbreviations** and an overview of **publications, posters and conference contributions**. Last but not least, the '**dankwoord**' is addressed to all the people that helped me, in a 'chemical way' or not, to finalize my thesis as it is now.

1.9. REFERENCES

- ¹ <http://goldbook.iupac.org/M03667.html> [June 2013].
- ² <http://goldbook.iupac.org/C01267.html> [June 2013].
- ³ K. Okamoto, C. K. Luscombe, *Polym. Chem.* **2011**, *2*, 2424–2434.
- ⁴ C. S. Fischer, M. C. Baier, S. Mecking, *J. Am. Chem. Soc.* **2013**, *135*, 1148–1154.
- ⁵ F. Schütze, B. Stempfle, C. Jüngst, D. Wöll, A. Zumbusch, S. Mecking, *Chem. Comm.* **2012**, *48*, 2104–2106.
- ⁶ J. Pecher, S. Mecking, *Polym. Prepr.* **2008**, *49*, 363–364.
- ⁷ P. Chandrasekhar, *Conducting polymers, fundamentals and applications. A practical approach*, Kluwer Academic Publisher, **1999**, Chapter 1.
- ⁸ C. K. Chang, C. R. Fincher, Y. W. Park, A. J. Heeger, H. Shirakawa, E. J. Louis, S. C. Gau, A. G. MacDiarmid, *Phys. Rev. Lett.* **1977**, *39*, 1098–1101.
- ⁹ H. Shirakawa, *Angew. Chem. Int. Ed.* **2001**, *40*, 2574–2580.
- ¹⁰ A. MacDiarmid, *Angew. Chem. Int. Ed.* **2001**, *40*, 2581–2590.
- ¹¹ A. Heeger, *Angew. Chem. Int. Ed.* **2001**, *40*, 2591–2611.
- ¹² H. Becker, H. Speitzer, K. Ibrom, W. Kreuder, *Macromolecules* **1999**, *32*, 4925–4932.
- ¹³ J. H. Burroughes, D. D. C. Bradley, A. R. Brown, R. N. Marks, K. Mackay, R. H. Friend, P. L. Burns, A. B. Holmes, *Nature* **1990**, *347*, 539–541.
- ¹⁴ C. E. Carraher Jr., *Polymer chemistry*, 6th ed; Marcel Dekker Inc., **2003**, Chapter 15.
- ¹⁵ R. C. Evans, *J. Mater. Chem. C* **2013**, *1*, 4190–4200.
- ¹⁶ <http://goldbook.iupac.org/B00683.html> [June 2013].
- ¹⁷ B. H. Kim, J. Y. Kim, S. O. Kim, *Soft Matter* **2013**, *9*, 2780–2786.

- ¹⁸ S. Günes, H. Neugebauer, N. S. Sariciftci, *Chem. Rev.* **2007**, *107*, 1324–1388.
- ¹⁹ A. P. Kulkarni, C. J. Tonzola, A. Babel, S. A. Jenekhe, *Chem. Mater.* **2004**, *16*, 4556–4573.
- ²⁰ T. A. Skotheim, J. R. Reynolds, *Handbook of conducting polymers: Conjugated polymers: processing and applications*, 3th ed; CRC Press, **2007**, Chapter 5.
- ²¹ T. A. Skotheim, J. R. Reynolds, *Handbook of conducting polymers: Conjugated polymers: theory, synthesis, properties and characterization*, 3th ed; CRC Press, **2007**, Chapter 4.
- ²² V. P. Conticello, D. L. Gin, R. H. Grubbs, *J. Am. Chem. Soc.* **1992**, *114*, 9708–9710.
- ²³ A. M. Spring, C.-Y. Yu, M. Horie, M. L. Turner, *Chem. Commun.* **2009**, 2676–2678.
- ²⁴ R. N. McDonald, T. W. Campbell, *J. Am. Chem. Soc.* **1960**, *82*, 4669–4671.
- ²⁵ G. Kossmehl, *J. Phys. Chem.* **1979**, *83*, 417–426.
- ²⁶ A. P. Davey, A. Drury, S. Maier, H. J. Byrne, W. J. Blau, *Synth. Met.* **1999**, *103*, 2478–2479.
- ²⁷ S. Pfeiffer, H.-H. Hörhold, *Macromol. Chem. Phys.* **1999**, *200*, 1870–1878.
- ²⁸ W. J. Feast, I. S. Millichamp, R. H. Friend, M. E. Horton, D. Phillips, S. D. D. V. Rughooputh, G. Rumbles, *Synth. Met.* **1985**, *10*, 181–191.
- ²⁹ M. Rehahn, A. D. Schlüter, *Makromol. Chem., Rapid Commun.* **1990**, *11*, 375–379.
- ³⁰ N. C. Greenham, S. C. Moratti, D. D. C. Bradley, R. H. Friend, A. B. Holmes, *Nature* **1993**, *365*, 628–630.

- ³¹ S. C. Moratti, R. Cervini, A. B. Holmes, D. R. Baigent, R. H. Friend, N. C. Greenham, J. Grüner, P. J. Hamer, *Synth. Met.* **1995**, *71*, 2117–2120.
- ³² H. Kretzschmann, H. Meier, *Tetrahedron Lett.* **1991**, *32*, 5059–5062.
- ³³ Z. Bao, Y. Chen, R. Cai, L. Yu, *Macromolecules* **1993**, *26*, 5281–8286.
- ³⁴ M. Pan, Z. Bao, L. Yu, *Macromolecules* **1995**, *28*, 5151–5153.
- ³⁵ F. Babudri, S. R. Cicco, G. M. Farinola, F. Naso, A. Bolognesi, W. Porzio, *Macromol. Rapid Commun.* **1996**, *17*, 905–911.
- ³⁶ F. Koch, W. Heitz, *Macromol. Chem. Phys.* **1997**, *198*, 1531–1544.
- ³⁷ J. H. P. Utley, J. Gruber, *J. Mater. Chem.* **2002**, *12*, 1613–1624.
- ³⁸ E. K. C. Yoshikawa, L. S. Roman, I. A. Hümmelgen, J. Gruber, *Synth. Met.* **2003**, *135-136*, 3–4.
- ³⁹ Y.-J. Miao, G. C. Bazan, *J. Am. Chem. Soc.* **1994**, *116*, 9379–9380.
- ⁴⁰ H. Hopf, *Angew. Chem.* **2008**, *120*, 9954–9958.
- ⁴¹ M. Porz, D. Mäker, K. Brödner, U. Bunz, *Macromol. Rapid Commun.* **2013**, *34*, 873–878.
- ⁴² G. Odian, *Principles of polymerization*, 4th ed; Wiley–Interscience, **2004**, Chapter 3.
- ⁴³ L. Hermosilla, S. Catak, V. Van Speybroeck, M. Waroquier, J. Vandenberg, F. Motmans, P. Adriaensens, L. Lutsen, T. Cleij, D. Vanderzande, *Macromolecules* **2010**, *43*, 7424–7433.
- ⁴⁴ E. Kesters, L. Lutsen, D. Vanderzande, J. Gelan, *Synth. Met.* **2001**, *119*, 311–312.
- ⁴⁵ A. J. J. M. van Breemen, A. D. J. Issaris, M. M. de Kok, M. J. A. N. Van Der Borght, P. J. Adriaensens, J. M. J. V. Gelan, D. J. M. Vanderzande, *Macromolecules* **1999**, *32*, 5728–5735.

- ⁴⁶ H. G. Gilch, W. L. Weelwright, *J. Polym. Sci. Polym. Chem. Ed.* **1966**, *4*, 1337–1349.
- ⁴⁷ R. A. Wessling, R. G. Zimmerman, *US Patent 3401152*, **1968**.
- ⁴⁸ R. A. Wessling, R. G. Zimmerman, *US Patent 3706677*, **1972**.
- ⁴⁹ F. R. Denton, A. Serker, P. M. Lathi, R. O. Garay, F. E. Karasz, *J. Polym. Sci.: Part A: Polym. Chem.* **1992**, *30*, 2233–2240.
- ⁵⁰ S. Son, A. Dodabalapur, A. J. Lovinger, M. E. Galvin, *Science* **1995**, *269*, 376–378.
- ⁵¹ E. Kesters, S. Gilissen, F. Motmans, L. Lutsen, D. Vanderzande, *Macromolecules* **2002**, *35*, 7902–7910.
- ⁵² F. Louwet, D. Vanderzande, J. Gelan, J. Mullens, *Macromolecules* **1995**, *28*, 1330–1331.
- ⁵³ F. Louwet, D. Vanderzande, J. Gelan, *Synth. Met.* **1995**, *69*, 509–510.
- ⁵⁴ A. Issaris, D. Vanderzande, P. Adriaensens, J. Gelan, *Macromolecules* **1998**, *31*, 4426–4431.
- ⁵⁵ A. Van Breemen, D. Vanderzande, P. Adriaensens, J. Gelan, *J. Org. Chem.* **1999**, *64*, 3106–3112.
- ⁵⁶ L. Lutsen, A. Van Breemen, W. Kreuder, D. Vanderzande, J. Gelan, *Helv. Chem. Acta* **2000**, *83*, 3113–3121.
- ⁵⁷ M. Van Der Borght, D. Vanderzande, P. Adriaensens, J. Gelan, *J. Org. Chem.* **2000**, *65*, 284–289.
- ⁵⁸ A. Henckens, I. Duyssens, L. Lutsen, D. Vanderzande, T. Cleij, *Polymer* **2006**, *47*, 123–131.
- ⁵⁹ A. Henckens, L. Lutsen, D. Vanderzande, M. Knipper, J. Manca, T. Arnouts, J. Poortman, *J. Proc. SPIE Int. Soc. Opt. Eng.* **2004**, *5464*, 52–59.

- ⁶⁰ H. Roex, P. Adriaensens, D. Vanderzande, J. Gelan, *Macromolecules* **2003**, *36*, 5613–5622.
- ⁶¹ E. Kesters, L. Lutsen, D. Vanderzande, J. Gelan, T. P. Nguyen, P. Molinié, *Thin Solid Films* **2002**, *403-404*, 120–125.
- ⁶² L. Hontis, V. Vrindts, L. Lutsen, D. Vanderzande, J. Gelan, *Polymer* **2001**, *42*, 5793–5796.
- ⁶³ L. Hontis, L. Lutsen, D. Vanderzande, J. Gelan, *Synth. Met.* **2001**, *119*, 135–136.
- ⁶⁴ J. Wiesecke, M. Rehahn, *Angew. Chem. Int. Ed.* **2003**, *42*, 567–570.
- ⁶⁵ B. R. Cho, Y. K. Kim, M. S. Han, *Macromolecules* **1998**, *31*, 2098–2106.
- ⁶⁶ T. Schwalm, J. Wiesecke, S. Immel, M. Rehahn, *Macromol. Rapid Commun.* **2009**, *30*, 1295–1322.
- ⁶⁷ J. Vandenberg, J. Wouters, P. Adriaensens, R. Mens, T. Cleij, L. Lutsen, D. Vanderzande, *Macromolecules* **2009**, *42*, 3661–3668.
- ⁶⁸ A. Issaris, J. Gelan, D. Vanderzande, *Synth. Met.* **1997**, *85*, 1149–1150.
- ⁶⁹ A. Issaris, D. Vanderzande, J. Gelan, *Polymer* **1997**, *38*, 2571–2574.
- ⁷⁰ L. Hontis, M. Van Der Borcht, D. Vanderzande, J. Gelan, *Polymer* **1999**, *40*, 6615–6617.
- ⁷¹ L. Hontis, V. Vrindts, D. Vanderzande, L. Lutsen, *Macromolecules* **2003**, *36*, 3035–3044.
- ⁷² I. Van Severen, M. Breselge, S. Fourier, P. Adriaensens, J. Manca, L. Lutsen, T. J. Cleij, D. Vanderzande, *Macromol. Chem. Phys.* **2007**, *208*, 196–206.
- ⁷³ I. Cosemans, J. Wouters, T. Cleij, L. Lutsen, W. Maes, T. Junkers, D. Vanderzande, *Macromol. Rapid Commun.* **2012**, *33*, 242–247.

- ⁷⁴ J. Duchateau, L. Lutsen, W. Guedens, T. J. Cleij, D. Vanderzande, *Polym. Chem.* **2010**, *1*, 1313–1322.
- ⁷⁵ S. Gillissen, L. Lutsen, D. Vanderzande, J. Gelan, *Synth. Met.* **2001**, *119*, 137–138.
- ⁷⁶ S. Gillissen, M. Jonforsen, E. Kesters, T. Johansson, M. Theander, M. R. Andersson, O. Inganäs, L. Lutsen, D. Vanderzande, *Macromolecules* **2001**, *34*, 7294–7299.
- ⁷⁷ J. Vandenberg, I. Cosemans, L. Lutsen, D. Vanderzande, T. Junkers, *Polym. Chem.* **2012**, *3*, 1722–1725.
- ⁷⁸ M. Lee, B.-K. Cho, W.-C. Zin, *Chem. Rev.* **2001**, *101*, 3869–3892.
- ⁷⁹ A. de Cuendias, R. C. Hiorns, E. Cloutet, L. Vignau, H. Cramail, *Polym. Int.* **2010**, *59*, 1452–1476.
- ⁸⁰ N. Sary, R. Mezzenga, C. Brochon, G. Hadziioannou, J. Ruokolainen, *Macromolecules* **2007**, *40*, 3277–3286.
- ⁸¹ C. Brochon, N. Sary, R. Mezzenga, C. Ngov, F. Richard, M. May, G. Hadziioannou, *J. Appl. Polym. Sci.* **2008**, *110*, 3664–3670.
- ⁸² C. H. Braun, B. Schöpf, C. Ngov, C. Brochon, G. Hadziioannou, E. J. W. Crossland, S. Ludwigs, *Macromol. Rapid Commun.* **2011**, *32*, 813–819.
- ⁸³ B. D. Olsen, R. A. Segalman, *Macromolecules* **2005**, *38*, 10127–10137.
- ⁸⁴ W. Li, H. Wang, L. Yu, T. L. Morkved, H. M. Jaeger, *Macromolecules* **1999**, *32*, 3034–3044.
- ⁸⁵ U. Stalmach, B. de Boer, A. D. Post, P. F. van Hutten, G. Hadziioannou, *Angew. Chem. Int. Ed.* **2001**, *40*, 428–430.
- ⁸⁶ F. He, T. Gädt, M. Jones, G. D. Scholes, I. Manners, M. A. Winnik, *Macromolecules* **2009**, *42*, 7953–7960.

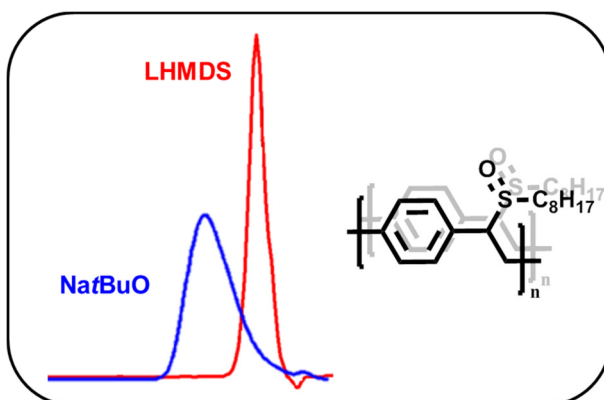
- ⁸⁷ S. Chakraborty, A. Keightley, V. Dusevich, Y. Wang, Z. Peng, *Chem. Mater.* **2010**, *22*, 3995–4006.
- ⁸⁸ C.-C. Ho, Y.-H. Lee, C.-A. Dai, R. A. Segalman, W.-F. Su, *Macromolecules* **2009**, *42*, 4208–4219.
- ⁸⁹ M. H. van der Veen, B. de Boer, U. Stalmach, K. I. van de Wetering, G. Hadziioannou, *Macromolecules* **2004**, *37*, 3673–3684.
- ⁹⁰ R. A. Segalman, B. McCulloch, S. Kirmayer, J. J. Urban, *Macromolecules* **2009**, *42*, 9205–9216.
- ⁹¹ H. Wang, H. H. Wang, V. S. Urban, K. C. Littrell, P. Thiyagarajan, L. Yu, *J. Am. Chem. Soc.* **2000**, *122*, 6855–6861.
- ⁹² H. Wang, Q. You, P. Jiang, L. Yu, H. H. Wang, *Chem. Eur. J.* **2004**, *10*, 986–993.
- ⁹³ C. Bianchi, B. Grassl, B. François, C. Dragon-Lartigau, *J. Polym. Sci., Part A: Polym. Chem.* **2005**, *43*, 4337–4350.
- ⁹⁴ T. A. Skotheim, J. R. Reynolds, *Handbook of conducting polymers: Conjugated polymers: processing and applications*, 3th ed; CRC Press, **2007**, Chapter 4.
- ⁹⁵ W.-P. Chang, W.-T. Whang, *Polymer* **1996**, *37*, 4229 – 4234.
- ⁹⁶ C. Adachi, T. Tsutsui, S. Saito, *Appl. Phys. Lett.* **1999**, *55*, 1489–1491.
- ⁹⁷ H. Becker, O. Gelsen, E. Kluge, W. Kreuder, H. Schenk, H. Spreitzer, *Synth. Met.* **2000**, *111-112*, 145–149.
- ⁹⁸ H. Becker, H. Spreitzer, W. Kreuder, E. Kluge, H. Schenk, I. Parker, Y. Cao, *Adv. Matter.* **2000**, *12*, 42–48.
- ⁹⁹ H. Becker, H. Spreitzer, W. Kreuder, E. Kluge, H. Vestweber, H. Schenk, K. Treacher, *Synt. Met.* **2001**, *122*, 105–110.

- ¹⁰⁰ M. Van Der Borght, P. Adriaensens, D. Vanderzande, J. Gelan, *Polymer* **2000**, *41*, 2743–2753.
- ¹⁰¹ T. Munters, T. Martens, L. Goris, V. Vrindts, J. Manca, L. Lutsen, W. De Ceuninck, D. Vanderzande, L. De Schepper, J. Gelan, N. S. Sariciftci, C. J. Brabec, *Thin Solid Films* **2002**, *403-404*, 247–251.
- ¹⁰² H. Hoppe, N. S. Sariciftci, *J. Mater. Res.* **2004**, *19*, 1924–1945.
- ¹⁰³ S. Bertho, G. Janssen, T. J. Cleij, B. Conings, W. Moons, A. Gadisa, J. D'Haen, E. Goovaerts, L. Lutsen, J. Manca, D. Vanderzande, *Sol. Energy Mater. Sol. Cells* **2008**, *92*, 753–760.
- ¹⁰⁴ J. Vandenberg, B. Conings, S. Bertho, J. Kesters, D. Spoltore, S. Esiner, J. Zhao, G. Van Assche, M. M. Wienk, W. Maes, L. Lutsen, B. Van Mele, R. A. J. Janssen, J. Manca, D. J. M. Vanderzande, *Macromolecules* **2011**, *44*, 8470–8478.
- ¹⁰⁵ B. Campo, W. Oosterbaan, J. Gilot, T. Cleij, L. Lutsen, R. A. J. Janssen, D. Vanderzande, *Proc. SPIE* **2009**, *7416*, 74161G.
- ¹⁰⁶ J. J. M. Halls, C. A. Walsh, N. C. Greenham, E. A. Marseglia, R. H. Friend, S. C. Moratti, A. B. Holmes, *Nature* **1995**, *376*, 498–500.
- ¹⁰⁷ K. Tada, K. Hirohata, R. Hidayat, T. Kawai, M. Onoda, M. Teraguchi, T. Musada, A. A. Zakhidov, K. Yoshino, *Synth. Met.* **1997**, *85*, 1305–1306.
- ¹⁰⁸ Y. Greenwald, X. Xu, M. Fourmigué, G. Srdanov, C. Koss, F. Wudl, A. J. Heeger, *J. Polym. Sci., Part A: Polym. Chem.* **1998**, *36*, 3115–3120.
- ¹⁰⁹ R. McCoy, F. E. Karasz, *Chem. Mater.* **1991**, *3*, 941–947.
- ¹¹⁰ P. A. Troshin, O. A. Mukhacheva, Ö. Usluer, A. E. Goryachev, A. V. Akkuratov, D. K. Susarova, N. N. Demova, S. Rathgeber, N. S. Sariciftci, V. F. Razumov, D. A. M. Egbe, *Adv. Energy Mater.* **2013**, *3*, 161–166.

- ¹¹¹ A. J. J. M. van Breemen, P. T. Herwig, C. H. T. Chlon, J. Sweelssen, H. F. M. Schoo, E. M. Benito, D. M. de Leeuw, C. Tanase, J. Wildeman, P. W. M. Blom, *Adv. Funct. Mater.* **2005**, *15*, 872–876.
- ¹¹² H. Kayashima, T. Yasuda, K. Fujita, T. Tsutsui, *J. Phys. D.: Appl. Phys.* **2007**, *40*, 1646–1648.
- ¹¹³ P. Cooreman, R. Thoelen, J. Manca, M. vandeVen, V. Vermeeren, L. Michiels, M. Ameloot, P. Wagner, *Biosens. Bioelectron.* **2005**, *20*, 2151–2156.
- ¹¹⁴ R. Thoelen, R. Vansweevelt, J. Duchateau, F. Horemans, J. D’Haen, L. Lutsen, D. Vanderzande, M. Ameloot, M. vandeVen, T. J. Cleij, P. Wagner, *Biosens. Bioelectron.* **2008**, *23*, 913–918.
- ¹¹⁵ Z. Matharu, S. K. Arya, S. P. Singh, V. Gupta, B. C. Malhotra, *Anal. Chim. Acta* **2009**, *634*, 243–249.

CHAPTER 2

Discovery of an Anionic Polymerization Mechanism for High Molecular Weight PPV Derivatives *via* the Sulfinyl Precursor Route



The polymerization of PPV *via* the sulfinyl precursor route has been investigated with respect to its mechanism. When polymerized in *sec*-butanol, a purely radical polymerization mechanism is observed as in most precursor polymerization routes. Accordingly an increase in the reaction temperature, an increase in the overall yield alongside with a reduction of the average molecular weight of the polymer was found. Upon changing the monomer concentration in solution before addition of the base Na^tBuO , an increase in molecular weight is observed, signifying that the polymerization is faster than the mixing of the two reaction components. When changing the solvent to NMP, a competition of anionic and radical polymerization has been established while in THF an anionic polymerization mechanism occurs exclusively. To prevent termination reactions, LDA and LHMDs were introduced as base whereby LHMDs shows less propensity to initiate anionic chain growth due to higher steric hindrance. With polymerizations in presence of the radical quencher TEMPO, the anionic polymerization mechanism could unambiguously be proven.

Published in:

* J. Wouters, *PhD thesis*, Universiteit Hasselt, **2012**.

* D. Vanderzande, L. Hontis, A. Palmaerts, D. Van Den Berghe, J. Wouters, L. Lutsen, T. Cleij, *Proc. SPIE 5937* **2005**.

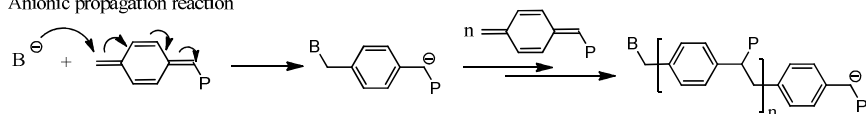
* Reviewed in: I. Cosemans, L. Hontis, D. Van Den Berghe, A. Palmaerts, J. Wouters, T. Cleij, L. Lutsen, W. Maes, T. Junkers, D. Vanderzande, *Macromolecules* **2011**, *44*, 7610–7616.

2.1. INTRODUCTION

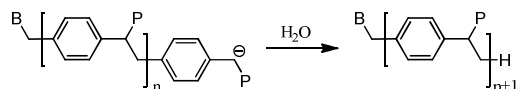
Some years ago the sulfinyl precursor route was studied in our group in N-methylpyrrolidone (NMP) as the solvent and sodium *tert*-butoxide (Na*t*BuO) was applied as the required base. Thereby bimodal polymer product distributions were observed and indication was given that a competition between a radical (resulting in high molecular weight polymer) and an anionic (resulting in low molecular weight material) polymerization mechanism was responsible for this bimodality.¹⁻⁴ In order to find pathways towards a purely anionic PPV polymerization, detailed studies into the exact reaction mechanism also for the radical pathway⁵⁻¹¹ are important. Only if the latter process is understood, then a differentiation between both reaction modes can be made on the basis of the resulting polymer distributions. Scheme 2.1 summarizes the reactions that can take place in each case. In the anionic pathway, the base that is added to form the quinodimethane from the premonomer can also act as an anionic chain initiator as in classical anionic polymerization. Subsequently, the chains are growing until either all monomer is consumed or until the reaction is quenched dedicatedly with an end-capper molecule. In the radical polymerization mode, a biradical species is formed from the monomer (see Scheme 2.1), whereby a dimerization of the monomer was proposed to self-initiate the reaction. The so-obtained biradicals can subsequently undergo chain propagation, growing on both sides of the chain. Upon termination of the reaction, again a biradical is formed (alongside a chain defect in the final polymer due to head-to-head coupling), thus reducing the overall radical concentration but not terminating chain growth. It is for this reason that the reaction can also be referred to as a "pseudo" termination, since it reduces radical concentration, but does not constitute a chain breaking event.

Anionic PPV polymerization

Anionic propagation reaction

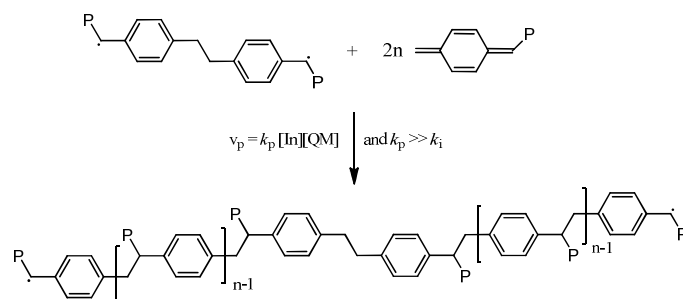


Anionic quenching reaction

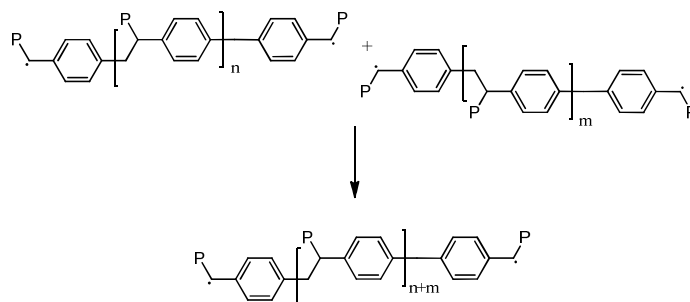


Radical PPV polymerization

Radical propagation reaction



Radical recombination reaction

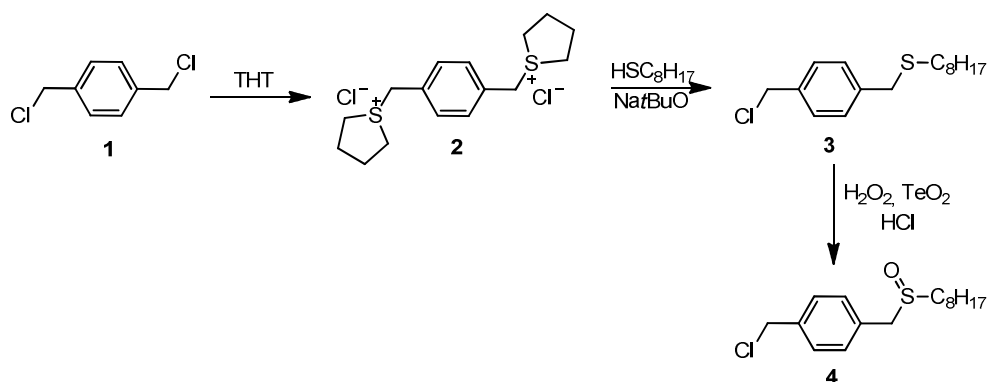


Scheme 2.1: Anionic polymerization compared to radical polymerization reactions in p -quinodimethane polymerization

In this chapter, a polymerization of a monosubstituted p -quinodimethane system is reported that purely proceeds *via* an anionic polymerization mechanism, which is achieved *via* careful selection of reaction conditions and type of base employed to form the monomer.

2.2. EXPERIMENTAL SECTION

2.2.1. Synthesis of monomer **4** (1-chloromethyl-4-[(*n*-octylsulfanyl)methyl] benzene)



Scheme 2.2: Synthesis of monomer **4**

Monomer **4** was synthesized according to a known procedure.¹⁶⁻¹⁸ In the final step a few drops of concentrated HCl (37%) were added to catalyze the reaction. Premonomer purity is of utmost importance for the polymerization outcome, so special attention was devoted to the purification of monomer **4**. Monomer **4** was purified using column chromatography (silica, eluent CHCl_3) and subsequently recrystallized twice from a hexane/chloroform mixture.

2.2.2. Polymerization procedure

Standard radical polymerization procedure with sudden base addition:

All glassware was dried overnight in a drying oven at 110 °C and flamed under vacuum prior to use. A solution of premonomer **4** (0.6 g, 2 mmol) in *sec*-butanol (10 mL) and a solution of Na^tBuO (0.5 g, 5 mmol) in *sec*-butanol (25 mL) were flushed with N_2 . The base solution was then added in one go to the monomer solution at a given temperature and was stirred for 1 h. The reaction mixture

was poured in water (50 mL), neutralized with 1.0 M HCl and extracted with CH₂Cl₂. The solvent of the combined organic layers was removed under reduced pressure and the prepolymer was analyzed without further purification. To gain the conjugated polymer, the prepolymer was dissolved in toluene (10 mL) and heated at 110 °C for 3 h. After cooling down, the polymer was precipitated in ice cold methanol (100 mL) and filtered on a Teflon[®] filter. The polymer was obtained as a red powder.

For the test using reversed addition the premonomer solution was added as fast as possible to the base solution.

2.2.3. Influence of temperature

The general procedure for fast addition of base to monomer was followed. The different polymerization temperatures were obtained as follows: 0 °C with an ice/water mixture; -64 °C with a CHCl₃/liquid nitrogen mixture. The polymerizations at 30 °C, 50 °C and 75 °C were performed in a thermostatic flask.

2.2.4. Anionic polymerization

The general procedure for fast base addition was followed. In this case 1.2 equivalents of base (LDA (2M in THF/*n*-heptane) or LHMDs (1M in THF)) were used during polymerization.

2.2.5. Test the anionic nature of the polymerization with TEMPO

The procedure was similar to the standard polymerization procedure, but 0.5 equivalents of TEMPO were added to the premonomer solution.

2.3. RESULTS AND DISCUSSION

In the next section, first of all the radical polymerization is described with respect to the outcome of the polymerization upon variation of certain reaction conditions. From the fact that high molecular weight material is typically obtained with a low defect level in the product (stemming from head-to-head couplings) the propagation rate constant (k_p) has to be much larger than the rate constant for initiation (k_i).¹² Self-termination reactions that would indeed lead to a stop in chain growth, like cyclization, are unlikely to occur once the formation of high molecular weight material is reached (although macrocyclization at the end of the polymerization reaction is possible, but hard to analyze). For smaller (bi-)radical species, such reaction was however observed.¹³ Also, termination by disproportionation, which would eliminate one of the radical centers per chain is not possible due to the absence of β -hydrogen atoms, so recombination is the only mode of termination.

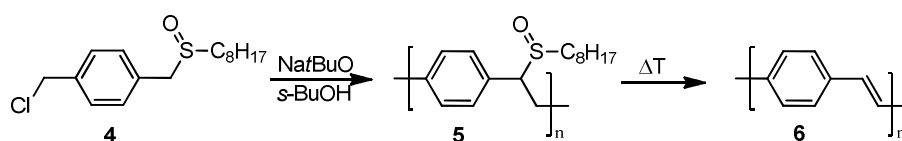
For most quinodimethane polymerizations, the radical polymerization pathway is postulated.¹⁴

2.3.1. Radical polymerization

To assess if there was a possibility to achieve a purely anionic PPV polymerization, more information on the radical mechanism and particularly on the influence of certain reaction parameters on the outcome of the polymerization is required. It was demonstrated earlier that if *sec*-butanol was used as the solvent, polymerization proceeds exclusively along a radical pathway.¹⁵ So far, however, it was not yet systematically studied how the outcome of these polymerizations is changed when the reaction conditions are varied. In order to identify conditions for anionic polymerizations, it is of high

importance to understand these influences as only then a truly anionic PPV polymerization can be characterized and discerned from a “conventional” radical polymerization.

As a proof-of-concept the polymerization of 1-chloromethyl-4-[(*n*-octylsulfinyl)methyl]benzene **4** as the premonomer, in *sec*-butanol as the solvent employing Na*t*BuO as the base, was studied, affording plain-PPV which is insoluble when eliminated (Scheme 2.3). The full three step synthesis and characterization of the sulfinyl premonomer **4** is described elsewhere.¹⁶⁻¹⁸



Scheme 2.3: Synthesis of plain-PPV **6** via the sulfinyl precursor route

To start, the effect of temperature on the radical polymerization was investigated. Results for polymerizations performed at temperatures between 0 °C and 75 °C are collated in Table 2.1. All reactions have been carried out twice to ensure reproducibility. All polymerizations, except stated otherwise, were started by sudden addition of the entire base solution to the monomer solution. All reported molecular weights (based on polystyrene calibration of the SEC) are given for the non-eliminated PPV material **5** because of the insolubility of the conjugated plain-PPV **6**.

Table 2.1: Effect of temperature on the polymerization of premonomer^a in *sec*-butanol, results given for precursor polymers

T / °C	Procedure 1 ^b			Procedure 2 ^c		
	$M_w^{app} / \text{g}\cdot\text{mol}^{-1}$	<i>PDI</i>	Yield / %	$M_w^{app} / \text{g}\cdot\text{mol}^{-1}$	<i>PDI</i>	Yield / %
75	150000	1.8	90			
	145000	2.0	89			
50	370000	2.3	88			
	450000	2.9	83			
30	535000	3.0	78	620000	2.8	83
	560000	2.7	80	590000	3.0	78
0	685000	2.5	73	780000	2.5	63
	680000	3.0	65	810000	2.5	65

^a Polymerizations with 1-chloromethyl-4-[(*n*-butylsulfinyl)methyl]benzene as premonomer

^b Premonomer dissolved in *sec*-butanol (14 mL), initial premonomer concentration $[M]_i = 143 \text{ mM}$; base (Na*t*BuO) dissolved in *sec*-butanol (6 mL), initial base concentration $[B]_i = 434 \text{ mM}$; $[B]_i/[M]_i = 3.03$

^c Premonomer dissolved in *sec*-butanol (10 mL), $[M]_i = 200 \text{ mM}$; base (Na*t*BuO) dissolved in *sec*-butanol (10 mL), $[B]_i = 260 \text{ mM}$; $[B]_i/[M]_i = 1.30$

It must be noted that only apparent molecular weights (M^{app}) are reported in this thesis since the polymers were measured on a GPC with conventional polystyrene (PS) calibration.

With conventional SEC, the hydrodynamic volume is measured versus retention time relative towards PS (Mark-Houwink parameters (MHKS) *a* and *K* known for PS). This means that, to obtain the real molecular weight of a sample, recalculation of the achieved result is necessary using the Mark-Houwink constants for the measured polymer, which depend on polymer-solvent interaction and temperature of viscosity determination in following Mark-Houwink relationship:

$$[\eta] = K \cdot M^a$$

These constants (a and K) can experimentally be determined by measuring the intrinsic viscosity ($[\eta]$) – using a viscometer – for several polymer samples of known molecular weight (determined using an independent method, e.g. light scattering) and plotting $\log [\eta]$ versus $\log M$. From the straight line thus obtained, the slope corresponds to the a value and the intercept is equal to $\log K$. This means that determination of a and K should be performed for all different polymers (thus all polymers with different initiators used) which is not straightforward. The independent method that can be used to obtain absolute molecular weights is the use of MALLS (multi-angle laser light scattering) measurements which requires dn/dc (this is the specific refractive index increment for a change of solute concentration). This dn/dc value is difficult to determine and a big batch-to-batch variation is found (for which the reason is still unknown).^{19,20} For this reason, dn/dc was not determined for BEH-PPV and the MALLS results presented in Chapter 5 were based on the dn/dc value determined for MDMO-PPV in our lab.²⁰

Nevertheless, conventional GPC – which only results in relative molecular weight values – allows for qualitative discussion of results and to discern trends.

The obtained data for radical polymerizations performed at different reaction temperatures (Table 2.1) show good reproducibility. The obtained yields increase with the reaction temperature and this can be interpreted as a result of an increased propagation rate compared to the initiation or termination rate with increasing temperature. At the same time, the average degree of polymerization increases with decreasing temperature which may as well be attributed to a lower initiation rate towards lower temperatures. Analysis of the filtrate confirms

that all monomer is consumed and that only paracyclophanes are present as a side product from the initiating biradical.¹³ This species effectively limits the achievable yield and hence an increase in initiation (as expected with increasing temperature) must not necessarily be followed by a higher yield. In addition to the change in temperature, also the effect of varying the initial base $[B]_i$ and premonomer concentration $[M]_i$ (resulting however in constant total concentrations in the mixture) upon the outcome of the reaction was investigated at 30 °C and 0 °C. Also here, a good reproducibility is given. It should be noted that both sets of experiments represent solutions that result in identical base and monomer concentrations after mixing. Still, a moderate increase of ~15% in molecular weight can be observed when $[B]_i/[M]_i$ is decreased. Thus, it may be concluded that the polymerization must proceed with a very high overall rate of polymerization; otherwise the initial concentrations of both components could not have an influence on the outcome of the polymerization. It should be noted that such effect complicates the kinetic analysis tremendously since mixing effects must be considered as a rate limiting step, a task that is not easily done.

To clarify unambiguously the effect of concentration of base and premonomer on the molecular weight further experiments were performed whereby the same amount of premonomer **4** (2 mmol) was systematically dissolved in an increasing amount of solvent. The Na^tBuO base (2.1 mmol in 10 mL solvent) was added without delay. The results for these polymerizations are collated in Table 2.2.

Table 2.2: Effect of premonomer concentration on the polymerization of premonomer **4** in *sec*-BuOH, results for precursor polymers

Conc. premonomer / mmol·L ⁻¹ ^a	Initial solvent volume / mL ^b	Yield / %	M_w^{app} / g·mol ⁻¹	<i>PDI</i>
80	15	56	399000	3.4
66.7	20	66	328000	3.8
50	30	73	265000	3.3
40	40	68	213000	3.2
25	70	57	145000	2.9
18.2	100	61	119000	2.9

^a Concentration premonomer **4** after addition of base solution

^b 2 mmol premonomer **4** dissolved in *sec*-BuOH; base dissolved in *sec*-BuOH (10 mL), [B]_i = 210 mM; T = 30 °C; all experiments were performed *in duplo* and results are given as averages

The results indicate that the initial premonomer concentration has only a minor effect on the overall yield of the polymerization, however a monotonous decrease of the molecular weight with decreasing the premonomer concentration can be clearly observed. Higher premonomer concentrations afford higher concentrations of the intermediate *p*-quinodimethane system thus accelerating the propagation reaction and consequently allowing the chains to grow to higher molecular weights. All these results are indicative of a radical chain growth mechanism

In the next step, it was tested if a termination reaction is operational. Whether termination occurs or not can be probed by sequential polymerization reactions. If no termination occurs, then addition of a new batch of premonomer to an already polymerized solution should afford for polymers of higher molecular weight due to chain extension reactions. Hence premonomer **4** (2 mmol in 15 mL *sec*-BuOH) and base solutions (2.1 mmol Na^tBuO in 10 mL *sec*-BuOH) were added to fully polymerized reaction mixtures (after 40 min of the initial

reaction). This process was repeated five times. Before adding the monomer and base solution, 5 mL of the reaction mixture was quenched to provide a sample for comparison. The results for the experiments are given in Table 2.3.

Table 2.3: Effect of sequential polymerizations of premonomer **4** in *sec*-BuOH, results given for precursor polymers

Polymerization step	Conc. premonomer / mmol·L ⁻¹ ^a	Initial solvent volume / mL ^b	M_w^{app} / g·mol ⁻¹	PDI
1	80	15	394000	3.7
2	44.4	35	319000	3.4
3	30.8	55	270000	3.4
4	23.5	75	242000	3.0
5	19.1	95	209000	3.1

^a Concentration premonomer **4** of the complete reaction mixture after addition of base solution

^b Total solvent volume of given reaction step, $[B]_i = 210 \text{ mM}$; $T = 30 \text{ }^\circ\text{C}$; all experiments were performed *in duplo* and results are given as averages

The obtained results reveal that the molecular weight drops after each sequential addition of monomer. Clearly no chain extension takes place and thus it can be concluded that a termination process is active during polymerization. When the results of the molecular weights in function of the premonomer concentration of the last two sets of experiments are compared, it is evident that the slope for the sequential polymerization experiment is less steep than the slope for the premonomer concentration experiment (Figure 2.1). This difference can be explained by the fact that every time a sample is taken out of the reaction medium for GPC analysis, the GPC sample will also contain polymeric material obtained in the previous polymerization step and an accumulation of several individual polymerizations is seen. It should be noted

that the above experiments demonstrate that a chain-terminating reaction clearly takes place, the nature of this reaction remains however unclear. Transfer reactions could be in principle also responsible, but also termination related to traces of oxygen in the reaction mixture. Anyhow, no living polymerization is observable under the chosen reaction conditions and the polymerization behavior is in line with a radical chain growth mechanism.

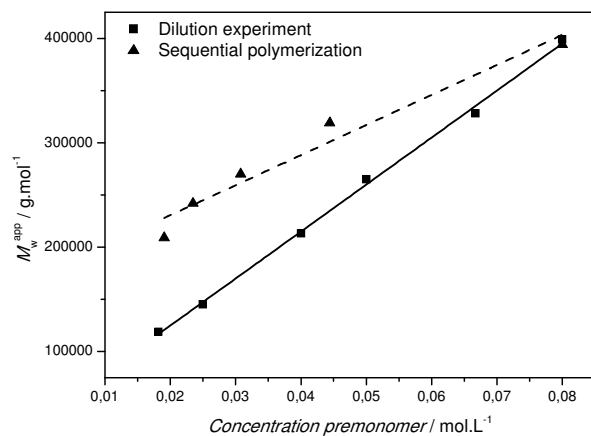


Figure 2.1: Radical propagation and termination reactions: dilution experiment (squares, see Table 2.2) and sequential polymerizations (triangles, see Table 2.3)

2.3.2. Anionic polymerization

To the best of our knowledge there are no literature examples in which unambiguously an anionic polymerization mechanism was so far observed for *p*-quinodimethane systems, except for the procedure in which the sulfinyl route is performed in a solvent like dry NMP¹⁻⁴ (see Figure 2.2). In this case, bimodal behavior was observed and attributed to simultaneous occurrence of an anionic and a radical polymerization pathway.

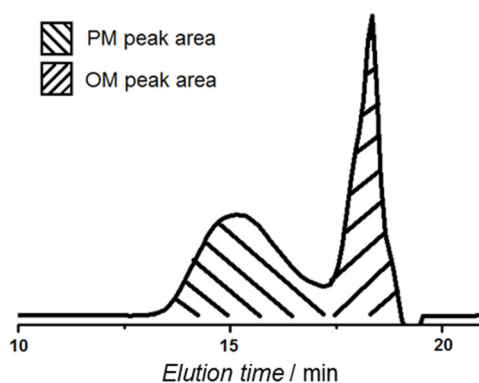


Figure 2.2: Typical GPC chromatogram for the polymerization of a sulfinyl premonomer in NMP (PM = polymeric material, OM = oligomeric material)

To describe the extent of competition between the radical and the anionic polymerization mechanism, this reaction was subsequently further investigated in NMP as the solvent. The relative integrated surface in the GPC chromatogram of the polymeric versus the oligomeric fraction was calculated and the sum of both surfaces was taken as 100%. This practical approach may not be fully correct since the distributions overlap with each other. Nevertheless, for a qualitative comparison such evaluation is sufficient. In Table 2.4 the results are illustrated for a series of experiments for which the dependence of the

competition between anionic and radical polymerization on the initial premonomer and base concentration was investigated. All experiments were performed *in duplo* and results are given as averages.

Table 2.4: Overview of polymeric (PM) and oligomeric (OM) fractions (precursor polymers) for the various premonomer **4** and base concentrations^a

Ratio mL(M) ^b /mL(B) ^c	Total yield / %	[B] _i / mM	[M] _i / mM	[B] _i /[M] _i	<i>M_w</i> ^{app} (PM) /g·mol ⁻¹	% PM	<i>M_w</i> ^{app} (OM) /g·mol ⁻¹
14/6	33	0.37	0.14	2.6	73000	67	3100
14/8	44	0.28	0.14	2.0	117000	80	3100
10/10	65	0.22	0.20	1.1	176000	89	3300

^a T = room temperature

^b Amount of solvent (NMP) in which the premonomer was dissolved, [M]_i= initial premonomer concentration

^c Amount of solvent (NMP) in which the base was dissolved, [B]_i= initial base concentration

It is clear that there is a high sensitivity for the competition between the two polymerization mechanisms and that already small changes in the reaction preparation have a profound influence on the transition in mechanism. In the analysis of the results, the relative peak areas for the oligomeric (OM) and polymeric (PM) material is used to assess the predominance of each mechanism. The OM material is assigned (as previously done) to material stemming from anionic polymerization, while PM is the result of the radical growth mode as described in the previous section. It should hereby be noted that the peak areas from SEC analysis do not represent true ratios of concentration of polymers due to the weighting of the molecular weight distributions. Transformation into the number distribution is required for that purpose, which however requires absolute molecular weight detection. Thus, with the numbers in Table 2.4, the

amount of oligomers is underestimated. Also, the given molecular weights are only crude estimates since the selection of integration limits are only arbitrary. A full deconvolution of the distributions is not easily done but the presented data are good enough to clearly show the underpinning trends. Small changes in initial concentrations of base and premonomer have pronounced effects on the molecular weight and the relative amount of the polymeric fraction. In comparison with Table 2.2 (radical polymerization only), changes of initial base or premonomer concentration do not give rise to strong variations in the outcome of the polymerization reaction. However, the more competitive the anionic mechanism becomes, the lower the molecular weight of the polymeric fraction is. A higher amount of the oligomeric material seems to go along with a high ratio of initial base concentration versus initial premonomer concentration. In an anionic polymerization, a sensitivity for the initial base versus premonomer concentration can be expected because the base concentration directly influences the rate of initiation (compared to the radical pathway where the rate of initiation is dependent on the *p*-quinodimethane concentration and hence only indirectly coupled with the amount of base). An experiment that demonstrates this hypothesis unambiguously is an experiment in which the effect of a reversed addition (addition of premonomer **4** solution to the base solution) is studied (Table 2.5).

Table 2.5: Addition of base versus reversed addition^a, results for molecular weights of polymeric and oligomeric fraction for the precursor polymers

Addition	Yield / %	M_w^{app} (PM) / $\text{g}\cdot\text{mol}^{-1}$	% PM	M_w^{app} (OM) / $\text{g}\cdot\text{mol}^{-1}$
Normal	61	170000	87	3500
Reversed	41	10400	36	2900

^a T = room temperature

Clearly, reversed addition has a tremendous effect on the molecular weight and on the relative contribution of the polymeric fraction. When mixed, the monomer faces a comparatively high base concentration, which apparently favors the anionic initiation over the radical pathway. An alternative experiment that demonstrates that the reaction can be directed towards one specific mechanism is to perform the polymerization at low temperature (see Table 2.6 for results). Anionic initiation typically is associated with a low activation energy, thus decreasing the temperature should increase the amount of oligomeric material. As can be seen from the data in Table 2.6, this hypothesis can be confirmed.

Table 2.6: Effect of temperature on the amount of the oligomeric (OM) fraction, molecular weights given for precursor polymers

T / °C	Yield / %	M_w^{app} (PM) / $\text{g}\cdot\text{mol}^{-1}$	% PM	M_w^{app} (OM) / $\text{g}\cdot\text{mol}^{-1}$
RT	68	182000	90	3000
0	43	54000	52	3300

To identify reaction conditions that allow for a purely anionic polymerization mechanism, all radical initiation events must be suppressed and termination reactions of an anionic polymerization eliminated. There are two possible (anionic) termination reactions that can potentially occur, *i.e.* quenching from deprotonation of the solvent or reaction with the protonated base, which is formed during the *p*-quinodimethane formation. This reasoning implies that strong bases (which will be less likely to terminate an anionic chain growth in its protonated form) and an aprotic solvent are essential conditions for a living anionic polymerization.

Consequently, lithium diisopropylamide (LDA) was tested as a base in dry THF. In such reaction, only low molecular weight oligomers were formed, indicating that anionic polymerization occurs exclusively. LDA has been reported in literature as being an initiator for the anionic polymerization of methacrylate monomers.²¹ For this reason LDA was exchanged for a more sterically hindered base, *i.e.* lithium hexamethyldisilazide (LHMDS), and used as the base during the polymerization. For the polymerization of premonomer **4**, plain-PPV polymers with ten times higher molecular weight were obtained with LHMDS compared to LDA as a base in dry THF (Table 2.7). This increase in molecular weight is indicative of a largely reduced anionic initiation rate with the sterically more hindered base. In consequence, less chains are initiated and thus each individual chain can grow to higher degree of polymerization due to the changed ratio of initiated species over the total monomer concentration.

Table 2.7: Results for precursor polymers obtained from polymerization^a of premonomer **4** in THF with LDA or LHMDS

Base	T / °C	M_w^{app} / $g \cdot mol^{-1}$	<i>PDI</i>
LDA	-64	1800	1.3
LDA	0	3600	1.9
LHMDS	-64	46100	2.1
LHMDS	0	64000	3.2

^a T = room temperature; $[M]_i = 0.05M$

To verify the anionic character of the polymerization procedure using LHMDS in THF, the effect of 2,2,6,6-tetramethylpiperidin-1-oxyl (TEMPO) on the molecular weight was investigated and compared to a classical radical polymerization of PPV (Na^tBuO in *sec*-butanol) (Table 2.8 and Figure 2.3) since a stable nitroxide should inhibit polymerization if a radical mechanism is operational.

Table 2.8: Results for the verification of the anionic nature of the polymerization of premonomer **4** with LHMDS as a base in THF^{a,b}

Base	Solvent	Additive	M_w^{app} / $\text{g}\cdot\text{mol}^{-1}$	PDI	Yield / %
NatBuO	sec-BuOH	none	208400	4.0	52
NatBuO	sec-BuOH	TEMPO	9800	1.4	<1
NatBuO	THF	none	1324100	6.9	79
NatBuO	THF	TEMPO	111800	2.7	21
LHMDS	THF	none	43300	2.5	84
LHMDS	THF	TEMPO	49400	3.5	82

^a T = room temperature; $[M]_i = 0.05 \text{ M}$

^b Molecular weights given for precursor polymers

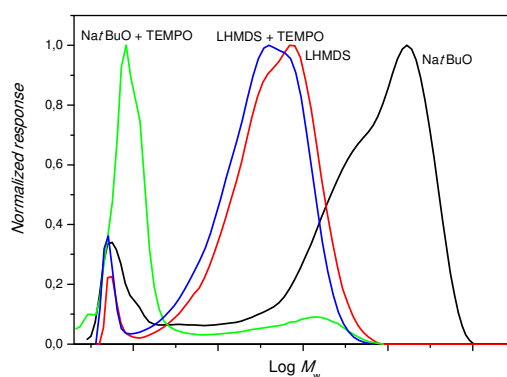


Figure 2.3: GPC results for the polymerization of premonomer **4** with NatBuO or LHMDS as the base. Verification of the anionic nature with TEMPO.

As is clear from Table 2.8 and Figure 2.3, for the polymerizations conducted with LHMDS no major changes were observed, nor on the molecular weight, nor in the yields of the reactions. This nicely verifies that the polymers were indeed obtained through an anionic polymerization mechanism. To further illustrate that the base is responsible for the change to an anionic mechanism, the effect of TEMPO was also studied on the polymerization in THF using NatBuO as a base. Again high molecular weight material was obtained in absence of the radical inhibitor and a drastic decrease of both yield and molecular weight was observed

in the presence of TEMPO. It was shown earlier on that one equivalent of TEMPO is needed to stop the radical polymerization completely.²² This explains the observed reduced molecular weight but still the presence of oligomers when 0.5 equivalents of TEMPO are used.

It can hence be concluded that the polymerization of PPVs in THF proceeds entirely *via* an anionic polymerization mechanism if a strong base such as LDA or LHMDS is used for the formation of the active *p*-quinodimethane monomer. The base acts at the same time as reagent to form the monomer, but also to some extent initiates the polymerization reaction.

2.4. CONCLUSION

The polymerization mechanism and the change in the outcome of the polymerizations upon variation of the reaction conditions was demonstrated for the sulfinyl precursor route. When polymerized in *sec*-butanol with a base such as Na^tBuO, a purely radical polymerization mechanism is observed. In this case, the polymer molecular weight can be systematically varied by changing the reaction temperature or *via* changing the initial monomer concentration in solution before mixing with the base. A purely anionic polymerization mechanism for PPVs can be obtained when the reaction conditions are chosen carefully to exclude radical initiation and quenching reactions of an anionic polymerization. This is achievable when the sulfinyl precursor route is performed in dry THF as the solvent and LHMDS is used as the base. LDA also leads to an exclusive anionic polymerization, but does result in overall lower molecular weights due to an increased propensity to initiate the polymerization compared to the sterically more hindered LHMDS.

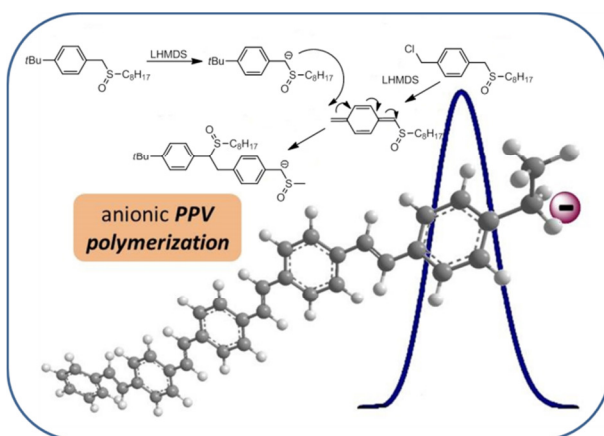
2.5. REFERENCES

- ¹ F. Louwet, D. Vanderzande, J. Gelan, *Synth. Met.* **1995**, *69*, 509–510.
- ² L. Hontis, M. Van Der Borght, D. Vanderzande, J. Gelan, *Polymer* **1999**, *40*, 6615–6617.
- ³ M. Van Der Borght, P. Adriaensens, D. Vanderzande, J. Gelan, *Polymer* **2000**, *41*, 2743–2753.
- ⁴ P. Adriaensens, M. Van Der Borght, L. Hontis, A. Issaris, A. van Breemen, M. de Kok, D. Vanderzande, J. Gelan, *Polymer* **2000**, *41*, 7003–7009.
- ⁵ L. Hontis, V. Vrindts, L. Lutsen, D. Vanderzande, J. Gelan, *Polymer* **2001**, *42*, 5793–5796.
- ⁶ T. Schwalm, J. Wiesecke, S. Immel, M. Rehahn, *Macromolecules* **2007**, *40*, 8842–8854.
- ⁷ B. Cho, Y. Kim, M. Han, *Macromolecules* **1998**, *31*, 2098–2106.
- ⁸ A. Issaris, D. Vanderzande, J. Gelan, *Polymer* **1997**, *38*, 2571–2574.
- ⁹ A. Issaris, D. Vanderzande, P. Adriaensens, J. Gelan, *Macromolecules* **1998**, *31*, 4426–4431.
- ¹⁰ L. Hontis, L. Lutsen, D. Vanderzande, J. Gelan, *Synth. Met.* **2001**, *119*, 135–136.
- ¹¹ J. Vandenbergh, J. Wouters, P. Adriaensens, R. Mens, T. Cleij, L. Lutsen, D. Vanderzande, *Macromolecules* **2009**, *42*, 3661–3668.
- ¹² H. Becker, H. Spreitzer, K. Ibrom, W. Kreuder, *Macromolecules* **1999**, *32*, 4925–4932.
- ¹³ J. Wiesecke, M. Rehahn, *Angew. Chem., Int. Ed.* **2003**, *42*, 567–570.
- ¹⁴ T. Schwalm, J. Wiesecke, S. Immel, M. Rehahn, *Macromol. Rapid Commun.* **2009**, *30*, 1295–1322.

- ¹⁵ A. van Breemen, A. Issaris, M. de Kok, M. Van Der Borght, P. Adriaensens, J. Gelan, D. Vanderzande, *Macromolecules* **1999**, *32*, 5728–5735.
- ¹⁶ A. van Breemen, D. Vanderzande, P. Adriaensens, J. Gelan, *J. Org. Chem.* **1999**, *64*, 3106–3112.
- ¹⁷ M. Van Der Borght, D. Vanderzande, P. Adriaensens, J. Gelan, *J. Org. Chem.* **2000**, *65*, 284–289.
- ¹⁸ L. Lutsen, A. van Breemen, W. Kreuder, D. Vanderzande, J. Gelan, *Helv. Chim. Acta* **2000**, *83*, 3113–3121.
- ¹⁹ L. Hontis, *PhD thesis*, Limburgs Universitair Centrum, **2002**, Chapter 4.
- ²⁰ J. Vandenbergh, unpublished results.
- ²¹ S. Antoun, P. Teyssié, R. Jérôme, *J. Polym. Sci. Part A* **1997**, *35*, 3637–3644.
- ²² J. Wiesecke, M. Rehahn, *Macromol. Rapid Commun.* **2007**, *28*, 78–83.

CHAPTER 3

Living Polymerization *via* Anionic Initiation for the Synthesis of Well-Defined PPV Materials



The anionic polymerization of PPV *via* the sulfinyl precursor route is further investigated in this chapter. When LHMDs is employed as the base to form the actively propagating quinodimethane system and THF as the solvent, anionic polymerizations can be observed. With the use of a *tert*-butyl substituted anionic initiator, specific functional groups can be built in the polymer chain and the chain length can be efficiently controlled, which is demonstrated here for the first time. With introduction of branched side chains on the aromatic core, soluble conjugated PPV material can be obtained with molecular weights in the range of 5000 – 16000 g·mol⁻¹.

Published in:

* Part on plain-PPV: J. Wouters, *PhD thesis*, Universiteit Hasselt, **2012**.

* I. Cosemans, J. Wouters, T. Cleij, L. Lutsen, W. Maes, T. Junkers, D. Vanderzande, *Macromol. Rapid Commun.* **2012**, *33*, 242–247.

3.1. INTRODUCTION

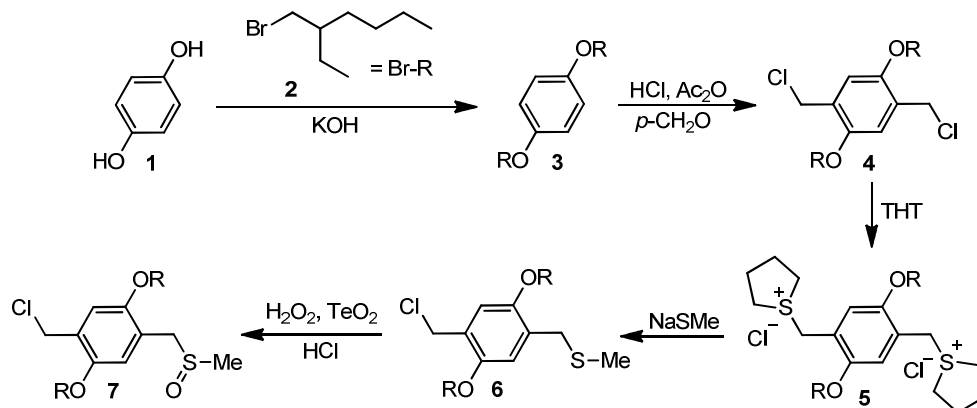
To date, no precursor polymerization method¹⁻⁹ has been developed that grants facile access to well-defined PPV polymers in a controlled fashion, which means control over molecular weight, functionality and polydispersity. In these precursor routes, a substituted and non-conjugated polymer is synthesized which may however be eliminated to yield PPV, either *in situ* or *via* postprocessing of the polymer.^{10,11} The radical polymerization of *p*-quinodimethanes proceeds in a largely uncontrolled fashion and only recently a method was introduced to gain limited control over the reactions by employing CBr₄ (carbon tetrabromide) as a chain length regulator.⁹ Otherwise, molecular weights can only be slightly adjusted via a change in monomer concentration, solvent or reaction temperature, whereby the dispersity and endgroup functionality of the polymers are not defined.¹² Therefore, it is a matter of priority to identify more efficient control methodologies for PPV polymerization.¹³ In Chapter 2 it was shown that a selective anionic polymerization to reasonable yields and molecular weights could be achieved. Still, although polymerization solely proceeded *via* an anionic polymerization mechanism, broad molecular weight distributions and only little control over the molecular weight could be obtained because the base acted both as the co-initiator of the reaction (by formation of the quinodimethane) and as the anionic initiator of the polymerization.

In this chapter, the possibility to use specific anionic initiators to gain more precise control over the functionality and the molecular weight of the obtained PPV is reported, which is required to target specific molecular weights, a prerequisite for further macromolecular design. Only if specific endgroups can be introduced to the polymer chains, more complex macromolecular designs

become accessible. In addition, utilization of specific initiators allows for a better understanding of the underpinning process. As defined for a truly living polymerization, not only termination events must be suppressed (as is the case in anionic polymerization without doubt), but also initiation must be decoupled from monomer formation and should be faster than propagation in order to allow for low dispersities. As will be show, the latter prerequisite is not yet fully fulfilled, but the data presented herein mark a significant advancement toward such goal. Also, in Chapter 2 research was focused on plain, unsubstituted PPV (which is insoluble in its conjugated form; work performed by J. Wouters), which will be extended in this chapter towards well-soluble materials by addition of two 2-ethylhexyloxy side chains to the monomer structure to obtain poly[2,5-bis(2-ethylhexyloxy)-*p*-phenylene vinylene], (BEH-PPV, work performed by I. Cosemans).^{14,15}

3.2. EXPERIMENTAL SECTION

3.2.1. Synthesis of 1-chloromethyl-2,5-bis(2-ethylhexyloxy)-4-[(methyl sulfinyl)methyl] benzene (**7**)



Scheme 3.1: Synthesis of BEH-substituted monomer **7**.

3.2.1.1. Synthesis of 1,4-bis(2-ethylhexyloxy)benzene (**3**)

Synthesis and characterization has already been described elsewhere.¹⁶ Material identity and purity were confirmed by ¹H and ¹³C NMR. FT-IR (NaCl, cm⁻¹): 2959, 2929, 2873, 2860, 1508, 1228; DIP MS (EI, *m/z*): 334 [M⁺], 110 [M⁺ - 2 C₈H₁₇].

3.2.1.2. Synthesis of 1,4-bis(chloromethyl)-2,5-bis(2-ethylhexyloxy)benzene (**4**)

A mixture of **3** (54.8 g, 0.16 mol) and *p*-formaldehyde (39.4 g, 1.31 mol) was brought to 0 °C under nitrogen atmosphere. HCl (37%, 90.3 mL, 1.08 mol) and acetic anhydride (246 mL, 2.62 mol) were added dropwise. The reaction mixture was stirred overnight at reflux temperature. After cooling of the reaction mixture water was added. The water layer was extracted with CH₂Cl₂. The combined

organic layers were washed with a saturated NaHCO₃ solution, dried over MgSO₄ and filtered. In the last step the solvent was removed under reduced pressure. The product was purified by column chromatography (silica, eluent hexane/CHCl₃ 7/3) and isolated as a colorless oil. Yield: 79% (54.4 g). ¹H NMR (300 MHz, CDCl₃, δ): 6.89 (s, 2H; ArH), 4.61 (s, 4H; CH₂Cl), 3.85 (d, *J* = 5.4 Hz, 4H; CH₂O), 1.79–1.71 (m, 2H; CH), 1.52–1.21 (m, 16H; CH₂), 0.92 (t, *J* = 7.7 Hz, 6H; CH₃), 0.89 (t, *J* = 7.2 Hz, 6H; CH₃); ¹³C NMR (75 MHz, CDCl₃, δ): 151.3 (C4), 127.6 (C4), 114.6 (CH), 71.7 (CH₂), 42.1 (CH₂), 40.3 (CH), 31.3 (CH₂), 29.8 (CH₂), 24.7 (CH₂), 23.7 (CH₂), 14.8 (CH₃), 11.9 (CH₃); FT-IR (NaCl, cm⁻¹): 2959, 2929, 2873, 2860, 1509, 1416, 1228; DIP MS (EI, *m/z*): 430 [M⁺], 318 [M⁺ - C₈H₁₇], 206 [M⁺ - 2 C₈H₁₇].

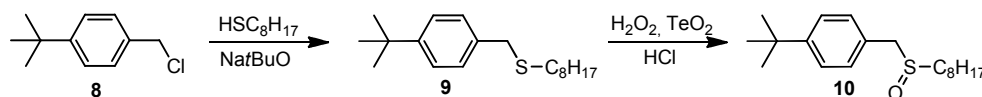
3.2.1.3. Synthesis of 1,1'-[(2,5-bis(2-ethylhexyloxy)-1,4-phenylene)bis(methylene)] bis(tetrahydrothiophenium)chloride (**5**)

Reaction of **4** with tetrahydrothiophene (THT) was conducted as previously reported.¹⁷⁻¹⁹ Precursor **5** was precipitated in ice cold diethyl ether and isolated as a white powder. Yield: 60% (44.4 g). ¹H NMR (300 MHz, D₂O, δ): 7.10 (s, 2H; ArH), 4.41 (s, 4H; CH₂S), 3.92 (d, *J* = 5.5 Hz, 4H; CH₂O), 3.54-3.26 (m, 8H; CH₂), 2.31–2.09 (m, 8H; CH₂), 1.75–1.60 (m, 2H; CH), 1.46–1.15 (m, 16H; CH₂), 0.82 (t, *J* = 7.5 Hz, 6H; CH₃), 0.77 (t, *J* = 7.5 Hz, 6H; CH₃); ¹³C NMR (75 MHz, D₂O, relative to 3-(trimethylsilyl)-1-propanesulfonic acid sodium salt, δ): 154.1 (C4), 122.3 (C4), 118.7 (CH), 74.2 (CH₂), 45.6 (CH₂), 44.2 (CH₂), 41.5 (CH), 32.7 (CH₂), 31.1 (CH₂), 26.2 (CH₂), 25.1 (CH₂), 16.1 (CH₃), 13.1 (CH₃); FT-IR (NaCl, cm⁻¹): 2959, 2929, 2873, 1512, 1222; DIP MS (EI, *m/z*): 607 [M⁺], 430 [M⁺ - CH₂-THT⁺ 2Cl⁻].

3.2.1.4. Synthesis of 1-chloromethyl-2,5-bis(2-ethylhexyloxy)-4-[(methylsulfinyl)methyl]benzene (**7**)

Synthesis was performed as earlier described.¹⁷⁻¹⁹ NaSMe in H₂O (21%) was used to synthesize compound **6** instead of HSC₈H₁₇ and Na^tBuO. Monomer **7** was purified by column chromatography (silica, eluent hexane/ethyl acetate 6/4) followed by two cold recrystallizations in hexane. Yield: 39% (10.8 g). Mp: 52–54°C; ¹H NMR (300 MHz, CDCl₃, δ): 6.91 (s, 1H; ArH), 6.79 (s, 1H; ArH), 4.61 (s, 2H; CH₂Cl), 4.02 (s, 2H; CH₂S), 3.83 (d, *J* = 5.5 Hz, 4H; CH₂O), 2.45 (s, 3H; CH₃), 1.78–1.61 (m, 2H; CH), 1.53–1.19 (m, 16H; CH₂), 0.91 (t, *J* = 7.4 Hz, 6H; CH₃), 0.90 (t, *J* = 7.2 Hz, 6H; CH₃); ¹³C NMR (75 MHz, CDCl₃, δ): 150.8 (C4), 150.6 (C4), 126.8 (C4), 119.3 (C4), 115.3 (CH), 113.6 (CH), 71.1 (CH₂), 70.8 (CH₂), 54.9 (CH₂), 41.4 (CH₂), 39.6 (CH), 37.6 (CH₃), 30.6 (CH₂), 29.1 (CH₂), 24.0 (CH₂), 23.0 (CH₂), 14.1 (CH₃), 11.2 (CH₃); FT-IR (NaCl, cm⁻¹): 2959, 2928, 2873, 1509, 1418, 1212, 1051; DIP MS (CI, *m/z*): 459 [MH⁺], 395 [M⁺ - SOCH₃].

3.2.2. Synthesis of 1-(*tert*-butyl)-4-[(*n*-octylsulfinyl)methyl]benzene (**10**)



Scheme 3.2: Synthesis of anionic initiator **10**.

A solution of octanethiol (5.9 g, 40 mmol) and Na^tBuO (4.0 g, 42 mmol) in ethanol (40 mL) was stirred for 1 h at room temperature. This solution was then added dropwise to a solution of 4-(*tert*-butyl)benzyl chloride (**8**, 3.7 g, 20 mmol) and NaI (0.6 g, 4 mmol) in ethanol (60 mL) and heated to reflux

overnight. The reaction mixture was poured in water and extracted with CH_2Cl_2 . The combined organic layers were washed with a NaOH solution (10%), dried over MgSO_4 and filtered. The solvent was evaporated under reduced pressure. The obtained yellow oil (5.6 g, 18 mmol) was dissolved in 1,4-dioxane (10 mL). TeO_2 (0.3 g, 1.8 mmol) and HCl (2M, 0.9 mL) were added. Finally H_2O_2 (35%, 3.1 mL, 36 mmol) was added dropwise. The reaction was followed on TLC and quenched with a saturated NaCl solution when overoxidation became apparent. The reaction mixture was extracted with CH_2Cl_2 . The combined organic layers were dried over MgSO_4 , filtered and the solvent was removed under reduced pressure. The crude product was dissolved in ethyl acetate and precipitated in hexane (100 mL). In the last step, initiator **10** was purified by recrystallization from a hexane/ethyl acetate (4/1) mixture and isolated as white crystals. Yield: 53% (3.3 g). Mp: 37–38°C; ^1H NMR (300 MHz, CDCl_3 , δ): 7.36 (d, $J = 8.3$ Hz, 2H; ArH), 7.19 (d, $J = 8.3$ Hz, 2H; ArH), 3.92 (q, $J = 12.9$ Hz, 2H; ArCH_2S), 2.54 (t, $J = 7.8$ Hz, 2H; SCH_2), 1.79–1.61 (m, 2H; CH_2), 1.43–1.16 (m, 19H; $\text{CH}_2 + \text{CH}_3$), 0.84 (t, $J = 7.0$ Hz, 3H; CH_3); ^{13}C NMR (CDCl_3 , δ): 151.8 (C4), 130.4 (CH), 127.5 (C4), 126.5 (CH), 58.4 (CH_2), 51.5 (CH_2), 35.2 (C4), 32.3 (CH_2), 31.9 (CH_3), 29.8 (CH_2), 29.6 (CH_2), 29.4 (CH_2), 23.2 (CH_2), 23.1 (CH_2), 14.7 (CH_3); FT-IR (NaCl, cm^{-1}): 2957, 2921, 2856, 1516, 1465, 1413, 1363, 1043; DIP MS (CI, m/z): 309 [MH^+], 147 [$\text{M}^+ - \text{SOC}_8\text{H}_{17}$].

3.2.3. Polymerization procedure

All glassware was dried overnight in a drying oven at 110 °C, flamed under vacuum and flushed three times with vacuum/ N_2 prior to use. The premonomer (0.2 g, 0.7 mmol) and the given amount of initiator **10** were dissolved in dry THF providing a premonomer concentration of 0.05 M and brought at 0 °C under

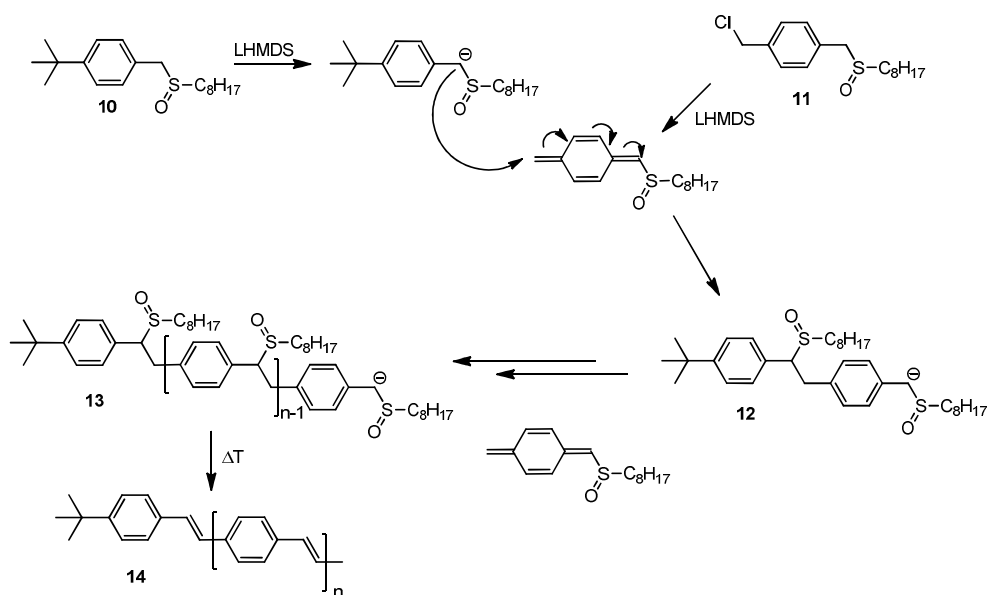
nitrogen atmosphere. The polymerization was started by adding 1.2 equivalents of LHMDS (1M in THF) by syringe. After 1 h, the reaction mixture was precipitated in water, neutralized with 1.0 M HCl, extracted with CH₂Cl₂ and analyzed without further purification. The prepolymer was then dissolved in toluene (10 mL) and heated at 110 °C for 3 h. After cooling down, the polymer was precipitated in cold methanol (100 mL) and filtered on a Teflon[®] filter. The polymer was obtained as a red powder.

3.2.4. Test the anionic nature of the polymerization with TEMPO

The procedure was similar to the standard polymerization procedure (without the use of initiator), but 0.5 equivalents of TEMPO (2,2,6,6-tetramethylpiperidin-1-oxyl) were added to the premonomer solution.

3.3. RESULTS AND DISCUSSION

One of the advantages of anionic polymerization over radical processes is the good control over the obtained molecular weight in terms of size and dispersity as well as the high chain-end fidelity usually found in polymers made by anionic polymerization. To allow for these features also in the quinodimethane polymerization, dedicated initiators must be introduced so that the functionality and the number of growing chains can be more precisely tuned. To reach this aim, the free energy of the initiation step must be favorable, and to have a narrow polydispersity, the initiation has to be faster than propagation. In the case of the anionic polymerization of PPV *via* the sulfinyl precursor route, there is an energy gain when the *p*-quinodimethane system of the monomer becomes aromatic. Therefore, it is not necessary that the initiator is a stronger nucleophile than the propagating anion for the polymerization to take place. The anionic polymerization of PPVs is, however, yet somewhat more complicated. A strong nucleophile, such as *s*-butyl lithium, would be immediately protonated by the rather acidic benzylic protons of the premonomer. Therefore, no substance can be used as initiating moiety that is a stronger base than the deprotonated premonomer. Still, the initiating anion must be reactive enough to add efficiently to the active *p*-quinodimethane monomer. An initiator similar in structure to the growing chain end, namely 1-*tert*-butyl-4-[(*n*-octylsulfinyl)methyl]benzene **10** (Scheme 3.3), therefore seemed to be a good choice to fulfill these criteria.



Scheme 3.3: Anionic polymerization of monomer **11** with anionic initiator **10** to obtain functionalized plain-PPV

Table 3.1 summarizes the outcome of polymerization (averages over three polymerizations) when various amounts of the above initiator are employed to start the reaction. It is obvious that the additive has a strong effect on the molecular weight. When the inverse molecular weight is plotted versus the amount of additive used, a clear linear relationship is observed (Figure 3.1). This provides strong evidence that the initiator indeed works in the initiation step of the polymerization. It should be noted that all data given represent polymers that were obtained after full conversion of all monomer. Because of the high energy gain from restoration of aromaticity in the propagation step, both the radical and the anionic polymerization *p*-quinodimethanes are very rapid. Thus, taking samples at different monomer conversions, which is usually done to demonstrate the typical increase of molecular weight in a living polymerization, cannot easily be performed. In fact, as for the radical polymerization mode,

reactions are rapid enough so that already the mixing of the components has an effect on the outcome of polymerization.¹² Even when polymerizations are carried out at $-78\text{ }^{\circ}\text{C}$, almost full monomer conversion is reached within seconds, demonstrating the extremely high driving force to polymerize and the therewith connected difficulties to reach good control (see Chapter 4).

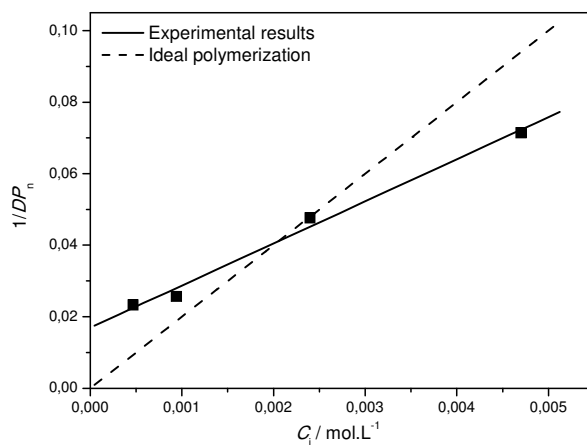


Figure 3.1: Linear relationship of $1/DP_n$ versus the initial initiator concentration in the reaction mixture

Table 3.1: Results for the anionic polymerization of premonomer **11** (precursor polymer) with the aid of anionic initiator **10**. Initiator concentration is given in relation to monomer concentration ($0.05\text{ mol}\cdot\text{L}^{-1}$).

$[\text{In}] / \text{mmol}\cdot\text{L}^{-1}$	$M_n^{\text{app}} / \text{g}\cdot\text{mol}^{-1}$	<i>PDI</i>	DP_n
0	20000	3.2	76
0.5	11700	4.3	44
1	10600	3.6	40
2.5	5900	2.5	22
5	4100	2.2	15

In an ideal anionic polymerization, the degree of polymerization of the residual polymer (obtained at full conversion of monomer) should be proportional to the ratio of the initial monomer concentration to the initiator concentration. Neglecting the molar mass of the initiator itself, the following relation should hence be fulfilled and consequently be used to assess the quality of the polymerization:

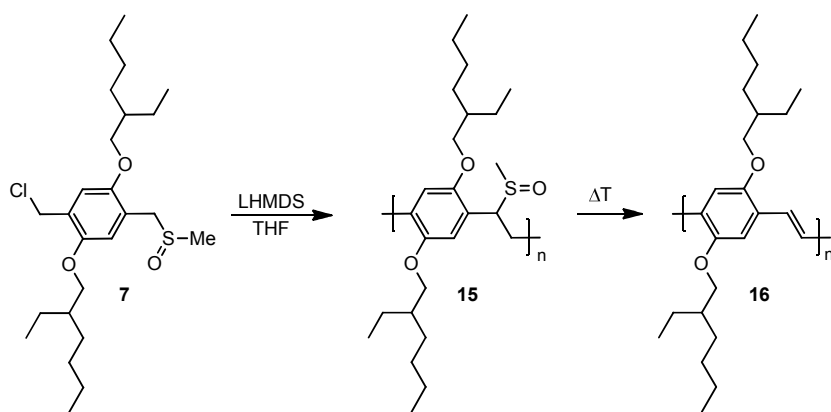
$$1/DP_n = 1/C_m \cdot C_i$$

As follows from the equation, plotting the inverse of the average degree of polymerization versus the initiator concentration employed should yield a linear plot whereby the slope of the best fit to the data should in principle be equivalent to the monomer concentration. As can be seen from Figure 3.1, indeed a linear relationship is observed and the results are hence in line with a living anionic polymerization. Unfortunately, the slope of the fit does however not return the monomer concentration and an almost twice as steep slope should be expected if the above equation would fully hold. This deviation may potentially be explained by the presence of a (constant) base concentration in the whole series of experiments. As already seen and discussed before, the base that is used to form the *p*-quinodimethane itself can potentially also initiate the anionic chain addition, leading to a constant chain initiation during polymerization. This hypothesis will later, in Chapter 6, be probed using ESI-MS (electrospray ionization – mass spectrometry) measurements but can also be addressed to imperfect GPC calibration (samples measured towards PS standards).

Thus, while the reaction proceeds entirely *via* an anionic pathway, a constant offset to the theoretical values is observed, which lowers the slope of the graph.

The influence of the base is also seen in the dispersity indices given in Table 3.1. At low initiator concentrations, relatively broad molecular weight distributions are obtained because of the high competition between initiation by the added initiator and the base, while somewhat better defined material is obtained when more initiator is added. Additional disturbance might be given by the high reaction rate. During mixing of base and monomer solution, comparatively higher base concentrations are present locally and thus an increased proportion of chains is started compared to what would be expected from the bulk concentrations. Also, the data given in the figure and the table are based on polystyrene calibration of the size exclusion apparatus and are hence associated with a considerable error. Nevertheless, within the given limits, a good control over the molecular weight is obtained. Low molecular weights could be accessed and good tunability of chain length is given by addition of the initiator.

In a final step, it was tested if the above-mentioned procedure could also be extended to other monomers and efficient anionic polymerizations could still be achieved if the monomer structure is changed. Plain-PPV is only poorly soluble and *via* introduction of suitable side chains on the aromatic ring, the final polymer becomes soluble in common organic solvents. Good solubility is generally a prerequisite for many applications of these polymers and hence it was a matter of priority to test whether such polymers can also be controlled. The material under investigation was therefore the symmetrically substituted analogue with two 2-ethylhexyloxy side chains on the aromatic ring, BEH-PPV (poly[2,5-bis(2-ethylhexyloxy)*p*-phenylene vinylene], **16**) (see Scheme 3.4 for structures).

Scheme 3.4: Synthesis of BEH-PPV **16**

First of all, the anionic nature for the polymerization of premonomer **7** was tested by performing three test reactions (Table 3.2). A first test was the standard anionic polymerization method which then could be compared to the second test, where 0.5 equivalents of TEMPO were added to the monomer mixture. If the same molecular weights are reached in high yields, it can safely be concluded that no radicals were present and a pure anionic pathway is followed. To confirm, a third test using Na^tBuO as the base in THF as the solvent was performed, resulting in sample of high molecular weight thus polymerized *via* the radical pathway (see similar experiment for plain-PPV in Chapter 2).

Table 3.2: Results for the conjugated polymers (after precipitation in cold MeOH) synthesized starting from premonomer **7** in THF as the solvent at 0 °C

Base	Additive	$M_n^{\text{app}} / \text{g}\cdot\text{mol}^{-1}$	<i>PDI</i>	Yield / %
LHMDS	none	15600	2.4	95
LHMDS	TEMPO	15600	2.7	95
Na^tBuO	none	81400	4.5	80

The results from these polymerizations are in good agreement with the above-described behavior. Anionic polymerizations were indeed carried out (Table 3.2) in comparable quality as in the plain-PPV polymerization. Reasonable high molecular weights are obtained, being indicative of an undisturbed anionic polymerization (e.g. that the side chains that were introduced do not interfere with the anions). In this way it is also possible to polymerize premonomer **7** together with anionic initiator **10** to gain polymers with a defined molecular weight and functionality (Table 3.3 and Figure 3.2).

Table 3.3: Results for the anionic polymerization of premonomer **7** with the aid of anionic initiator **10** after thermal elimination. Initiator concentration is given in relation to monomer concentration ($50 \text{ mmol}\cdot\text{L}^{-1}$).

$T / ^\circ\text{C}$	$[\text{In}] / \text{mmol}\cdot\text{L}^{-1}$	$M_n^{\text{app}} / \text{g}\cdot\text{mol}^{-1}$ ^a	<i>PDI</i>	DP_n
RT	--	13900	2.5	39
0	--	15600	2.4	44
0	2.5	8300	2.2	23
0	5	4600	1.7	13

^a Nearly quantitative yields

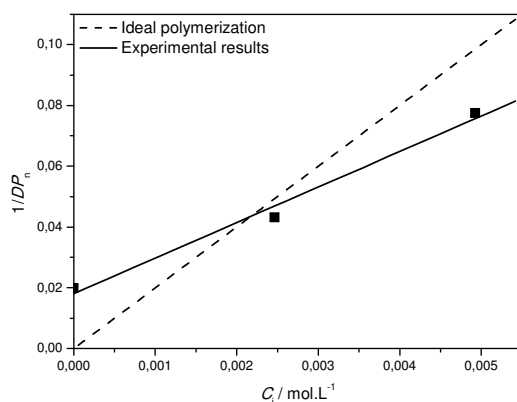


Figure 3.2: Inverse of degree of polymerization (M_n^{app} determined after precipitation of the conjugated materials) for the anionic polymerization of BEH-PPV

As in the other polymerizations, the molecular weight distributions are relatively broad for a living process, which can again be interpreted as initiation being not completely instantaneous. However, also here, moderate polydispersities were obtained. When initiator **10** is added, a similar behavior as with the unsubstituted PPV is observed, that is, a reduction in overall molecular weight and polydispersity with increasing content of the initiator. Also here, a deviation from the ideal polymerization is, however, observed with qualitatively similar deviations (Figure 3.2). This deviation can also be ascribed to the SEC measurements that were performed towards polystyrene standards because Mark-Houwink parameters are not available for this system (see discussion in Chapter 2). Also, it must be stressed that different polymerizations can give different outcome in molecular weights for repeated experiments. This can for instance be due to a small variation in premonomer purity and small differences in monomer to initiator ratios.

3.4. CONCLUSION

In conclusion it can be stated the use of dedicated anionic initiators, with a similar structure to the monomer, can be employed to gain better control over the molecular weight and a clear relation between degree of polymerization and initial initiator concentration is established. For the first time, PPVs with preselectable molecular weight are obtained from the anionic polymerization mode, which marks a very important milestone in the ongoing endeavor to establish living polymerization procedures for the design of conjugated materials with complex structures. On the basis of the above-presented results, block copolymers should be directly obtainable, giving access to materials with the ability to undergo self-assembly. Small deviations from ideal living polymerization character are still observed in the polymerization, for which no exact nature could be revealed so far. Through the introduction of branched alkoxy side chains on the monomer, a soluble conjugated BEH-PPV polymer is obtained with preselectable molecular weight when different amounts of anionic initiator are used.

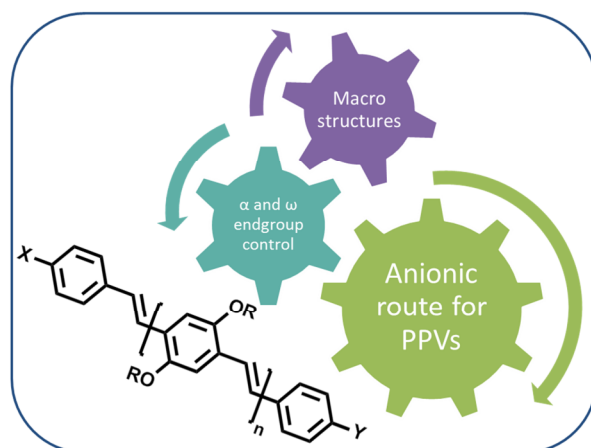
3.5. REFERENCES

- ¹ H. G. Gilch, W. L. Weelwright, *J. Polym. Sci. Polym. Chem. Ed.* **1966**, *4*, 1337–1349.
- ² R. A. Wessling, R. G. Zimmerman, *US Patent 3401152* **1968**.
- ³ R. A. Wessling, R. G. Zimmerman, *US Patent 3706677* **1972**.
- ⁴ F. Louwet, D. Vanderzande, J. Gelan, J. Mullens, *Macromolecules* **1995**, *28*, 1330–1331.
- ⁵ A. Henckens, I. Duyssens, L. Lutsen, D. Vanderzande, T. Cleij, *Polymer* **2006**, *47*, 123–131.
- ⁶ A. Henckens, L. Lutsen, D. Vanderzande, M. Knipper, J. Manca, T. Aernouts, J. Poortman, *Proc. SPIE Int. Soc. Opt. Eng.* **2004**, *5464*, 52–59.
- ⁷ T. Schwalm, J. Wiesecke, S. Immel, M. Rehahn, *Macromol. Rapid Commun.* **2009**, *30*, 1295–1322.
- ⁸ T. Junkers, J. Vandenberg, P. Adriaensens, L. Lutsen, D. Vanderzande, *Polym. Chem.* **2012**, *3*, 275–285.
- ⁹ J. Vandenberg, I. Cosemans, L. Lutsen, D. Vanderzande, T. Junkers, *Polym. Chem.* **2012**, *3*, 1722–1725.
- ¹⁰ E. Kesters, S. Gillissen, F. Motmans, L. Lutsen, D. Vanderzande, *Macromolecules* **2002**, *35*, 7902–7910.
- ¹¹ E. Kesters, D. Vanderzande, L. Lutsen, H. Penxten, R. Carleer, *Macromolecules* **2005**, *38*, 1141–1147.
- ¹² I. Cosemans, L. Hontis, D. Van Den Berghe, A. Palmaerts, J. Wouters, T. Cleij, L. Lutsen, W. Maes, T. Junkers, D. Vanderzande, *Macromolecules* **2011**, *44*, 7610–7616.
- ¹³ J. Wiesecke, T. Schwalm, *Angew. Chem. Int. Ed.* **2003**, *42*, 567–570.

- ¹⁴ A. van Breemen, P. Herwig, C. Chlon, J. Sweelssen, H. Schoo, E. Benito, D. De Leeuw, C. Tanase, J. Wildeman, P. Blom, *Adv. Funct. Mater.* **2005**, *15*, 872–876.
- ¹⁵ L. Breban, L. Lutsen, G. Vanhoyland, J. D’Haen, J. Manca, D. Vanderzande, *Thin Solid Films* **2006**, *511-512*, 695–700.
- ¹⁶ R. Palacias, W. Chang, J. Grey, Y. Chang, W. Miller, C. Lu, G. Henkelman, D. Zepeda, J. Ferraris, P. Barbara, *J. Phys. Chem. B* **2009**, *113*, 14619–14628.
- ¹⁷ A. van Breemen, D. Vanderzande, P. Adriaensens, J. Gelan, *J. Org. Chem.* **1999**, *64*, 3106–3112.
- ¹⁸ M. Van der Borght, D. Vanderzande, P. Adriaensens, J. Gelan, *J. Org. Chem.* **2000**, *65*, 284–289.
- ¹⁹ L. Lutsen, A. van Breemen, W. Kreuder, D. Vanderzande, J. Gelan, *Helv. Chim. Acta* **2000**, *83*, 3113–3121.

CHAPTER 4

Anionic initiators and end-capping,
looking at synthetic possibilities



The use of dedicated anionic initiators with similar structure to the monomer is studied in more detail in this chapter. Differences were made in polarizer functionality, addition mode, initiator functionality, reaction temperature and reaction time. From these experiments it is found that a sulfinyl polarizer functionality is preferred and that the addition mode, that is the order of addition of reactants to the mixture, is crucial for the built in of anionic initiators with different functionalities. By studying the kinetics of the anionic polymerization reaction for the sulfinyl precursor route, it is clear that even at $-78\text{ }^{\circ}\text{C}$ and “zero” minutes (direct quenching with acid after addition of base) reaction time, high molecular weights and conversions are reached and that the polymerization takes place upon mixing of the different components. With making use of a ^{13}C -labeled end-capper, it became evident that the ω -endgroup functionality is difficult to control in comparison to the initiator group.

Some parts (different addition modes and results at $-78\text{ }^{\circ}\text{C}$) published in:

* I. Cosemans, J. Vandenberg, V. S. D. Voet, K. Loos, L. Lutsen, D. Vanderzande, T. Junkers, *Polymer* **2013**, *54*, 1298–1304.

4.1. INTRODUCTION

In Chapters 2 and 3, a good and reliable method was described to synthesize PPV materials *via* the anionic sulfinyl precursor route¹ and also more control over the molecular weights could be gained using anionic initiators with a similar structure to the monomer (a molecule with a sulfinyl polarizer functionality on one side of the aromatic core). In this way, it is possible to introduce specific functionalities on the α -position of the polymer chain (which in Chapter 6 will be proved to be highly successful). It was also shown that high initiator concentrations lead towards polymers with lower molecular weights (and *PDI*s). A linear behavior was found if the inverse of the degree of polymerization was plotted against the initiator concentration.² Still, a deviation from the ideal anionic polymerization was found, so doubts remained about the initiation efficiency of the anionic initiators used. Furthermore, the ω -endgroup of the polymer chains still remained unclear. Because of the low abundance of the endgroups in the relatively long polymer chains, it is difficult to draw conclusions from conventional NMR measurements.³ To overcome this drawback, the use of ¹³C-labeled compounds opens possibilities.^{4,5} With labeling a specific functionalized endgroup molecule that is added to end the anionic chain growth (with only a chlorine leaving group and no sulfinyl polarizer group) it should be possible to investigate the effectiveness of such approach. In this way, an extra feature is given to go towards functionalized polymers leading towards e.g. block copolymer synthesis, self-assembly or surface modification.

In order to achieve end-capping, a rate reduction in polymerization should be favorable. To date,^{6,7} only a reaction temperature of 0 °C was investigated (see Chapter 3). By lowering the temperature and reaction time, kinetics can be influenced and reactions are slowed down. It is expected that lower conversions

would be reached at these reaction conditions, allowing for more detailed kinetic investigations, also in absence of specific end-cappers.

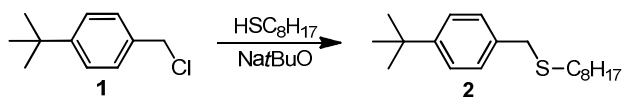
To gain better insights in the anionic polymerization route for PPV materials, different experiments are described in this chapter:

- i. Variation of monomer concentration.
- ii. Variation of the polarizer functionality on the anionic initiator (thioether, sulfinyl with long and short alkyl chains and sulfonyl)
- iii. The anionic polymerizations are extremely fast and polymerizations occur on the timescale of mixing the individual components (initiator and base). Thus, three different reaction procedures – that is the mode of addition of the initiator and base to the reaction mixture – are investigated for differently functionalized initiators (*tert*-butyl, bromine and chlorine functionality).
- iv. In a further attempt to gain more control over the polymerization reactions, different reaction temperatures (-78 °C, 0 °C and RT) were studied at different reaction times to see if better control might be achievable. Also kinetics can be studied at these low temperatures.
- v. In a last section, control over the ω -endgroup of the polymer was studied using a ^{13}C -labeled compound.

4.2. EXPERIMENTAL SECTION

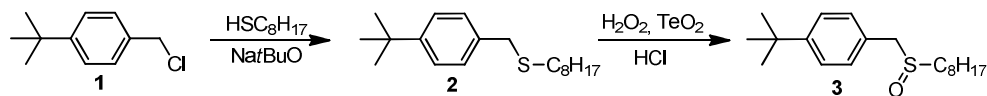
4.2.1. Synthesis of anionic initiators

4.2.1.1. Synthesis of 4-(*tert*-butyl)benzyl-*n*-octylsulfane (**2**)

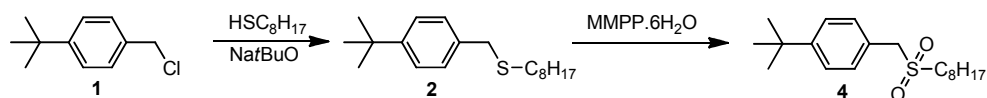


Scheme 4.1: Synthesis of anionic initiator with thioether polarizer group **2**

A solution of *n*-octanethiol (5.9 g, 40 mmol) and NaOBu (4.0 g, 42 mmol) in ethanol (40 mL) was stirred for 1 h at room temperature. This solution was then added dropwise to a solution of 4-(*tert*-butyl)benzyl chloride **1** (3.7 g, 20 mmol) and NaI (0.6 g, 4 mmol) in ethanol (60 mL) and heated to reflux overnight. The reaction mixture was poured in water and extracted with CH₂Cl₂. The combined organic layers were washed with a NaOH solution (10%), dried over MgSO₄ and filtered. The solvent was evaporated under reduced pressure. The obtained yellow oil was purified by column chromatography (silica, eluent hexane/chloroform 6/4). Pure **2** was isolated as a colorless oil. Yield: 56% (3.2 g). ¹H NMR (300 MHz, CDCl₃, δ): 7.30 (d, *J* = 8.4 Hz, 2H; ArH), 7.21 (d, *J* = 8.4 Hz, 2H; ArH), 3.66 (s, 2H; ArCH₂S), 2.40 (t, *J* = 7.5 Hz, 2H; SCH₂), 1.54 (m, 2H; CH₂), 1.40–1.10 (m, 19H; CH₂ and CH₃), 0.86 (t, *J* = 7.4 Hz, 3H; CH₃); ¹³C NMR (75 MHz, CDCl₃, δ): 150.4 (C4), 136.3 (C4), 129.2 (CH), 126.1 (CH), 36.5 (CH₂), 35.2 (C4), 32.5 (CH₂), 32.2 (CH₂), 32.1 (CH₃), 30.0 (CH₂), 29.9 (CH₂), 29.8 (CH₂), 29.6 (CH₂), 23.4 (CH₂), 14.8 (CH₃); FT-IR (NaCl, cm⁻¹): 2957, 2928, 2855, 1651, 1515, 1418, 1363, 1268; DIP MS (EI, *m/z*): 292 [M⁺], 147 [M⁺ - SOC₈H₁₇].

4.2.1.2. Synthesis of 1-(tert-butyl)-4-[(n-octylsulfinyl)methyl]benzene (**3**)Scheme 4.2: Synthesis of anionic initiator with sulfinyl polarizer group **3**

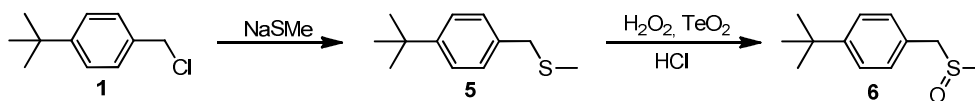
Synthesis and characterization of compound **3**, starting from 4-(tert-butyl)benzyl chloride (**1**), was already described in Chapter 3.

4.2.1.3. Synthesis of 1-(tert-butyl)-4-[(n-octylsulfonyl)methyl]benzene (**4**)Scheme 4.3: Synthesis of anionic initiator with sulfonyl polarizer group **4**

Thioether **2** (1.5 g, 5 mmol) was dissolved in 1,4-dioxane (25 mL) and cooled to 0 °C. MMPP·6H₂O (magnesium bis(monoperoxyphthalate) hexahydrate^{8,9}, 80%; 5 mmol, 4.5 g) was added and the reaction was followed on TLC and quenched with a saturated NaHCO₃ solution. The reaction mixture was extracted with CH₂Cl₂ and the combined organic layers were dried over MgSO₄, filtered and the solvent was removed under reduced pressure. The crude product was purified by column chromatography (silica, eluent hexane/chloroform 1/1) and initiator **4** was isolated as a white solid. Yield: 62% (1.0 g). Mp: 35 °C; ¹H NMR (300 MHz, CDCl₃, δ): 7.40 (d, *J* = 8.5 Hz, 2H; ArH), 7.30 (d, *J* = 8.5 Hz, 2H; ArH), 4.16 (s, 2H; ArCH₂S), 2.80 (t, *J* = 7.9 Hz, 2H; SCH₂), 1.78 (m, 2H; CH₂), 1.44–1.10 (m, 19H; CH₂ and CH₃), 0.85 (t, *J* = 7.0 Hz, 3H; CH₃); ¹³C NMR (75 MHz, CDCl₃, δ): 152.8 (C4), 130.9 (CH), 126.7 (CH), 125.7 (C4), 59.7 (CH₂), 51.6 (CH₂), 35.3

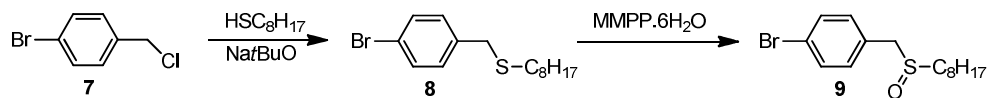
(C4), 32.4 (CH₂), 31.9 (CH₃), 29.7 (CH₂), 29.6 (CH₂), 29.1 (CH₂), 23.3 (CH₂), 22.5 (CH₂), 14.7 (CH₃); FT-IR (NaCl, cm⁻¹): 2957, 2925, 2856, 1512, 1465, 1411, 1364, 1308, 1268, 1124, 1108; DIP MS (EI, *m/z*): 324 [M⁺], 147 [M⁺ - SO₂C₈H₁₇].

4.2.1.4. Synthesis of 1-(*tert*-butyl)-4-[(methylsulfinyl)methyl]benzene (**6**)

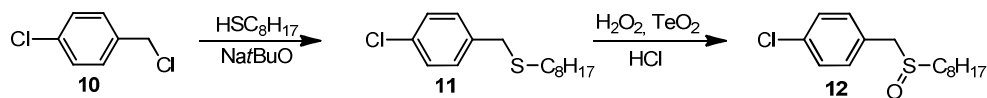


Scheme 4.4: Synthesis of anionic initiator **6** with short alkyl chain on polarizer functionality

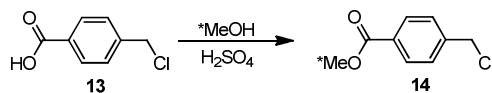
Synthesis was repeated as described for **3**. Compound **5** was synthesized starting from **1** (5.0 g, 27.4 mmol) and NaSMe (21% in H₂O; 2.3 g, 32.8 mmol) and oxidized without purification to gain **6**. The product was purified by column chromatography (silica, eluent hexane/chloroform 3/7) followed by a recrystallization in hexane/ethyl acetate (9/1). Pure **6** was isolated as white crystals. Yield: 17% (0.9 g). Mp: 48 °C; ¹H NMR (300 MHz, CDCl₃, δ): 7.37 (d, *J* = 8.5 Hz, 2H; ArH), 7.20 (d, *J* = 8.5 Hz, 2H; ArH), 3.94 (q, *J* = 12.8 Hz, 2H; ArCH₂S), 2.44 (s, 3H; SCH₃), 1.29 (s, 9H; CH₃); ¹³C NMR (75 MHz, CDCl₃, δ): 151.9 (C4), 130.5 (CH), 127.3 (C4), 126.5 (CH), 60.3 (CH₂), 37.9 (CH₃), 35.2 (C4), 31.9 (CH₃); FT-IR (NaCl, cm⁻¹): 2954, 2910, 2868, 1516, 1465, 1415, 1269, 1043; DIP MS (CI, *m/z*): 211 [MH⁺], 147 [M⁺ - SOCH₃].

4.2.1.5. Synthesis of 1-bromo-4-[(*n*-octylsulfinyl)methyl]benzene (**9**)Scheme 4.5: Synthesis of bromine-functionalized anionic initiator **9**

Compound **8** was synthesized according to the described procedure for **2** (without purification) starting from **7** (30 mmol, 6.2 g). To a solution of **8** (20 mmol, 6.3 g) in MeOH (50 mL) at 0 °C, MMPP·6H₂O (80%; 10 mmol, 8.9 g) was added in small portions. Reaction was followed on TLC and quenched with a saturated NaHCO₃ solution when overoxidation became apparent. The reaction mixture was extracted with CH₂Cl₂ and the combined organic layers were dried over MgSO₄. After evaporation of the solvent, the product was purified by column chromatography (silica, eluent hexane/CHCl₃ 1/9) and recrystallized in a hexane/ethyl acetate (3/1) mixture. Initiator **9** was isolated as white crystals. Yield: 55% (5.31 g). Mp: 101 °C; ¹H NMR (300 MHz, CDCl₃, δ): 7.49 (d, *J* = 8.5 Hz, 2H; ArH), 7.15 (d, *J* = 8.5 Hz, 2H; ArH), 3.88 (s, 2H; ArCH₂S), 2.54 (t, *J* = 7.0 Hz, 2H; SCH₂), 1.77–1.67 (m, 2H; CH₂), 1.30–1.18 (m, 10H; CH₂), 0.85 (t, *J* = 6.8 Hz, 3H; CH₃); ¹³C NMR (75 MHz, CDCl₃, δ): 132.8 (CH), 132.3 (CH), 129.7 (C4), 123.3 (C4), 58.0 (CH₂), 51.8 (CH₂), 32.4 (CH₂), 29.8 (CH₂), 29.7 (CH₂), 29.5 (CH₂), 23.3 (CH₂), 23.2 (CH₂), 14.8 (CH₃); FT-IR (NaCl, cm⁻¹): 2958, 2918, 2848, 1488, 1073, 1025; DIP MS (CI, *m/z*): 330/332 [MH⁺], 169/171 [M⁺ - SOC₈H₁₇].

4.2.1.6. Synthesis of 1-chloro-4-[(*n*-octylsulfinyl)methyl]benzene (**12**)Scheme 4.6: Synthesis of chlorine-functionalized initiator **12**

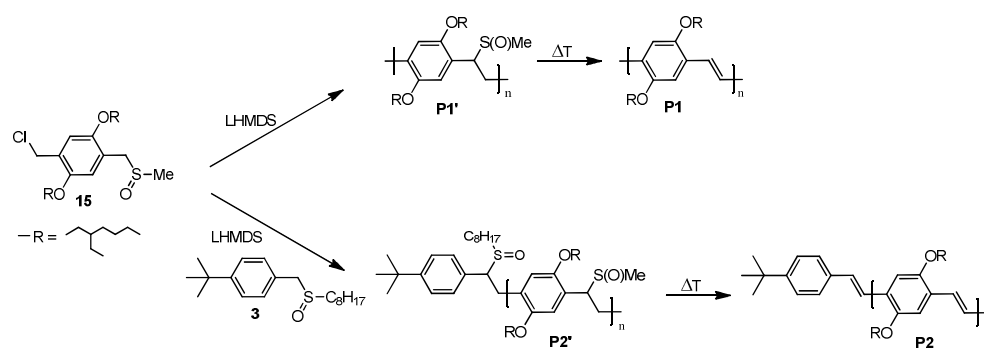
Synthesis was performed as described for **2** (without purification) and **3**. Synthesis was started with **10** (10.0 g, 62 mmol). After column chromatography purification (silica, eluent chloroform) and recrystallization in hexane/ethyl acetate (9/1), pure **12** could be isolated as white crystals. Yield: 39% (6.9 g). Mp: 92 °C; ¹H NMR (300 MHz, CDCl₃, δ): 7.33 (d, *J* = 8.6 Hz, 2H; ArH), 7.20 (d, *J* = 8.6 Hz, 2H; ArH), 3.89 (s, 2H; ArCH₂S), 2.54 (t, *J* = 7.3 Hz, 2H; SCH₂), 1.72 (m, 2H, CH₂), 1.50–1.10 (m, 10H; CH₂), 0.85 (t, *J* = 7.0 Hz, 3H; CH₃); ¹³C NMR (75 MHz, CDCl₃, δ): 134.9 (C₄), 132.0 (CH), 129.7 (CH), 129.2 (C₄), 57.8 (CH₂), 51.7 (CH₂), 32.3 (CH₂), 29.8 (CH₂), 29.6 (CH₂), 29.4 (CH₂), 23.2 (CH₂), 23.1 (CH₂), 14.7 (CH₃); FT-IR (NaCl, cm⁻¹): 2958, 2912, 2849, 1598, 1493, 1468, 1416, 1025; DIP MS (CI, *m/z*): 211 [MH⁺], 126 [M⁺ - SOC₈H₁₇].

4.2.2. Synthesis of ¹³C-labeled end-capper methyl-4-(chloromethyl)benzoate (**14**)Scheme 4.7: Synthesis of ¹³C-labeled end-capper **14**

To a solution of **13** (1.70 g, 10 mmol) in ¹³C-labeled methanol (*MeOH; 5 g), H₂SO₄ (1.11 g; 11.3 mmol) was added and the resulting mixture was refluxed

for 5 h. After the reaction was completed, methanol was distilled from the mixture and water was added. The water layer was extracted with CH_2Cl_2 , dried over MgSO_4 and filtered. After evaporation of the solvent and purification using column chromatography (silica, eluent $\text{CHCl}_3/\text{hexane}$ 1/1) pure **14** was obtained as white crystals. Yield: 90% (1.7 g). Mp: 39 °C; ^1H NMR (300 MHz, CDCl_3 , δ): 8.01 (d, $J = 8.4$ Hz, 2H; ArH), 7.44 (d, $J = 8.4$ Hz, 2H; ArH), 4.60 (s, 2H; CH_2Cl), 4.08 + 3.72 (d, $J = 147.1$ Hz, 3H; $^*\text{CH}_3$); ^{13}C NMR (75 MHz, CDCl_3 , δ): 166.6 (C4), 142.2 (C4), 130.1 (C4), 130.0 (CH), 128.5 (CH), 52.2 ($^*\text{CH}_3$), 45.4 (CH_2); FT-IR (NaCl, cm^{-1}): 2989, 2948, 1719, 1613, 1432, 1282, 1180, 1104; DIP MS (EI, m/z): 185 [M^+], 153 [$\text{M}^+ - \text{O}^*\text{CH}_3$], 125 [$\text{M}^+ - \text{COO}^*\text{CH}_3$].

4.2.3. Polymerization



Scheme 4.8: Anionic polymerization of monomer **15**¹⁰ without (**P1'** and **P1**) and with anionic initiator (**P2'** and **P2**)

All polymerization and elimination reactions were carried out as described before.² The polymerization temperature of -78 °C was reached with an isopropanol / dry ice bath. The synthesis of the precursor polymer was quenched by the addition of 0.2 mL concentrated HCl solution (37%). During polymerization, three different addition modes were used to add the initiator to

the mixture. The first method exists from the fast addition of a mixture of base and initiator (in THF (2/3)) to the monomer (in THF (1/3)) using a cannula. This method is indicated as $I + B \rightarrow M$. In the second method the base is directly added to a mixture of initiator and monomer in THF and is indicated as $B \rightarrow M + I$. In the third method, the monomer solution (1/3 of the THF) is added as fast as possible to a solution of initiator mixed with base (2/3 of the THF) using a cannula. This last method is indicated as $M \rightarrow I + B$.

For the reactions quenched with ^{13}C -labeled end-capper **14**, a solution of 0.2 eq of the end-capper dissolved in 0.5 mL of THF was added after stirring for a certain time (see Table 4.6 below) and again stirred for 15 min. The resulting mixture was poured in acidified water before extraction of the prepolymer.

4.3. RESULTS AND DISCUSSION

4.3.1. Influence of monomer concentration

The influence of the monomer concentration on the molecular weight and the polydispersity of the polymers was checked for the anionic polymerization without using an initiator. As can be seen from Table 4.1 and Figure 4.1, for higher monomer concentrations, a higher molecular weight was reached, but also an increase in *PDI* was observed. For concentrations of 50 mmol·L⁻¹ and lower, there is more or less no change in molecular weight and *PDI*, therefore this concentration ($[M]_i = 50 \text{ mmol}\cdot\text{L}^{-1}$) was chosen as the standard concentration in all further experiments.

Table 4.1: MWD and *PDI* for polymers synthesized with different monomer concentrations at 0 °C and a reaction time of 15 min

$[M]_i / \text{mmol}\cdot\text{L}^{-1}$	Precursor polymer		Conjugated polymer	
	$M_n^{\text{app}} / \text{g}\cdot\text{mol}^{-1}$	<i>PDI</i>	$M_n^{\text{app}} / \text{g}\cdot\text{mol}^{-1}$	<i>PDI</i>
25	11500	2.6	14200	2.4
50	13600	2.7	15600	2.4
80	14300	3.2	18300	2.5
110	22800	4.4	31900	2.7

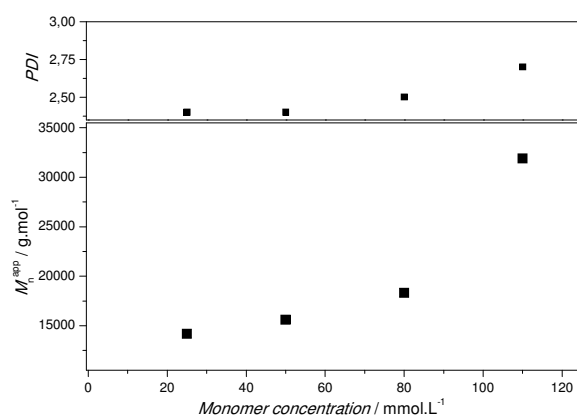


Figure 4.1: M_n^{app} and *PDI* vs monomer concentration for conjugated BEH-PPV

As is clear from Table 4.1, higher molecular weights are measured with conventional GPC for the conjugated polymers as for the precursor polymers, although the sulfinyl group is removed from the chain and lower molecular weights would be expected for the conjugated polymer. This difference is due to the difference in hydrodynamic volume between the precursor and conjugated polymer (measured relative to polystyrene standards and thus only relative determination of MWD).

4.3.2. Influence of the polarizer functionality on the anionic initiator

One of the advantages of anionic chain-growth polymerization is that the endgroups of the polymer chains are well-defined. In the case of PPV, the use of dedicated anionic initiators leads towards better defined polymer chains concerning molecular weights and polydispersities (*PDI*s) as described before.² As shown in Chapter 3, an initiator with a structure similar to the growing chain end is required to have an efficient initiation in the anionic polymerization route. Therefore, three slightly different functionalized initiators on the polarizer side were tested. One with a thioether functionality (**2**), a second one with a sulfinyl (**3** or **6**) and a third initiator with a sulfonyl (**4**) polarizer group. For the sulfinyl polarizer group also long and short alkyl chains were tested (initiators **3** and **6**, see Figure 4.2). Results regarding molecular weight and polydispersity are given in Table 4.2 (addition mode $I + B \rightarrow M$, 0 °C, 0.1 equivalents of initiator and $[M]_i = 50 \text{ mmol}\cdot\text{L}^{-1}$).

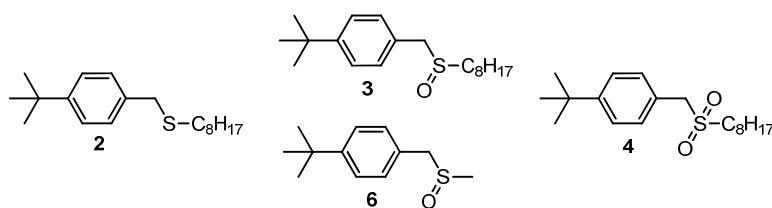


Figure 4.2: Initiators with different polarizer functionalities

Table 4.2: Results regarding MW and *PDI* for anionic initiators with different polarizer functionalities

Initiator	Precursor polymer		Conjugated polymer	
	$M_n^{\text{app}} / \text{g}\cdot\text{mol}^{-1}$	<i>PDI</i>	$M_n^{\text{app}} / \text{g}\cdot\text{mol}^{-1}$	<i>PDI</i>
--	13500	2.7	15600	2.4
2	7600	2.4	12500	1.9
3	4100	2.2	6700	2.1
6	3100	2.0	6500	1.9
4	3400	1.8	7100	1.6

As is clear from the results for the conjugated polymers given in Table 4.2, the molecular weight of the polymer synthesized using initiator **2** is closer to the molecular weight obtained for the polymerization performed without addition of initiator (entry 1) while the MWDs obtained for initiators **3**, **6** and **4** are more or less comparable. These results are indicative for the fact that the length of the alkyl chain on the polarizer group does not have an influence on built in of the initiator, but that an oxidized polarizer group is needed to have a proper initiation efficiency.

4.3.3. Influence of the mode of compound addition

An important aspect of PPV polymerization is that the associated reactions are particularly fast, proceeding on the timescale of seconds. Thus, the employed procedure of adding compounds may have a significant influence on the

outcome of the polymerization reaction. If the base is added to a mixture of monomer and initiator, then both elimination/deprotonation reactions occur at the same instance. If the initiator is premixed with the base, then chain initiation can in principle start faster and only the monomer precursor elimination (i.e. formation of the *p*-quinodimethane system) is rate-limiting. Therefore, the effect of the addition of initiator **3** (in different concentrations) to the reaction mixture was investigated by means of three different addition modes for which the results regarding MWD and *PDI* were collated in Table 4.3. In the first series of experiments (Figure 4.3, green triangles, I + B → M), the base and initiator were mixed first (in 2/3 of the amount of solvent) and then added in one batch to the monomer in solution using a cannula. The reaction was stirred for 15 min at 0 °C. For the second series of experiments (Figure 4.3, red circles, B → M + I), the monomer was mixed with the initiator and dissolved in dry THF. The base (LHMDS (1M solution in THF)) was added directly to this mixture by syringe and stirred for 15 min at 0 °C. In a last experiment, the addition mode was changed to adding the monomer solution (1/3 of the solvent) to the initiator and base solution (M → I + B; 15 min at 0 °C).

Table 4.3: Results for MW and *PDI* for the polymers after elimination using different addition modes and initiator concentrations

$[I]_i / \text{mmol}\cdot\text{L}^{-1}$	I + B → M		B → M + I		M → I + B	
	$M_n^{\text{app}} / \text{g}\cdot\text{mol}^{-1}$	<i>PDI</i>	$M_n^{\text{app}} / \text{g}\cdot\text{mol}^{-1}$	<i>PDI</i>	$M_n^{\text{app}} / \text{g}\cdot\text{mol}^{-1}$	<i>PDI</i>
0	15600	2.4	15600	2.4		
1.25			12300	2.2		
2.5	13000	2.2	8600	2.0		
5	6700	2.1	7400	2.1	5600	2.1
10	4600	1.4	4200	1.4		

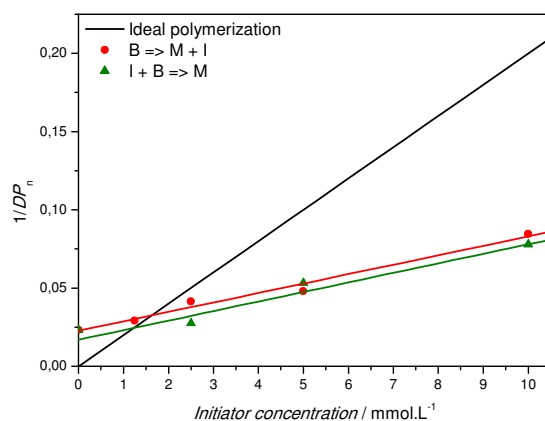


Figure 4.3: Inverse of the degree of polymerization reached in polymerizations at different initiator concentrations and different addition modes of initiator **3**

From Table 4.3 and Figure 4.3 it could be concluded that all addition modes show – within limits of accuracy – the same results regarding molecular weights and polydispersities and no improvement over the reaction could be gained by changing the reaction procedure. At first glance, these results appears to be little surprising since monomer formation as well as polymerization take place on the timescale of mixing of the components. Differences in the product depending on the practical procedure have, however, been observed for initiators functionalized with a halogen atom (bromine, **9** and chlorine, **12**). Molecular weights and polydispersities for the different addition modes for these initiators can be found in Table 4.4. Polymerizations were performed with 0.1 eq of initiator at 0 °C with a reaction time of 15 min and $[M]_i = 50 \text{ mmol}\cdot\text{L}^{-1}$.

Table 4.4: Results regarding molecular weight and *PDI* for anionic PPV polymerizations with *tert*-butyl (**3**), bromine (**9**) and chlorine (**12**) functionalized initiators compared to results for polymerization without initiator

In	Precursor polymer				Conjugated polymer			
	I + B → M		B → M + I		I + B → M		B → M + I	
	$M_n^{\text{app}} / \text{g}\cdot\text{mol}^{-1}$	<i>PDI</i>	$M_n^{\text{app}} / \text{g}\cdot\text{mol}^{-1}$	<i>PDI</i>	$M_n^{\text{app}} / \text{g}\cdot\text{mol}^{-1}$	<i>PDI</i>	$M_n^{\text{app}} / \text{g}\cdot\text{mol}^{-1}$	<i>PDI</i>
--	13500	2.7	13500	2.7	15600	2.4	15600	2.4
3	4100	2.2	4500	2.0	6700	2.1	7400	2.0
9	7500	1.9	5100	1.8	13100	1.9	7800	1.8
12	6700	1.9	4200	1.7	10400	1.9	6700	1.7

If the results in Table 4.4 are compared, it is clear that addition mode I + B → M resulted in higher molecular weight material for initiators **9** and **12** compared to addition mode B → M + I, where low MW material was gained (the clearest trends can be derived from the MWDs reported for the conjugated polymers). Incorporation of the anionic initiator with bromine functionality for this second method was confirmed *via* ^{13}C APT (attached proton test) NMR measurements (Figure 4.4, positive signals for C4 and CH₂ and negative signals for CH and CH₃) where the aromatic peaks, originating from the bromine-substituted anionic initiator, were only found for method B → M + I. It can thus be concluded that no (or very little) incorporation of the anionic initiator for the halogen-substituted initiators **9** and **12** occurs if initiator and base are primarily mixed. For the addition mode where the base was added to a mixture of monomer and initiator (B → M + I), more or less the same molecular weights were found for all initiators used during the polymerization reactions. This result is surprising because one would expect that initiation would be more straightforward when the initiator is first mixed with the base before addition to the monomer.

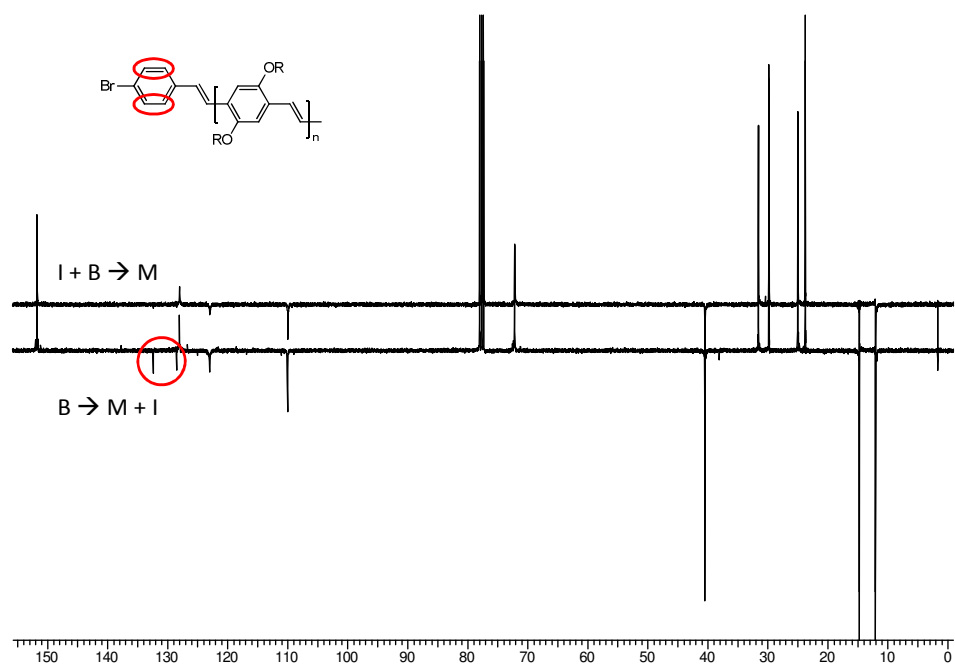


Figure 4.4: ^{13}C APT NMR (CDCl_3) spectrum for the polymer with bromine-functionalized initiator **9** for the different addition modes ($\text{I} + \text{B} \rightarrow \text{M}$, upper spectrum and $\text{B} \rightarrow \text{M} + \text{I}$, lower spectrum)

4.3.4. Effect of reaction temperature and time

To further examine the anionic polymerization pathway for the synthesis of defined PPV materials, polymerizations were studied at different reaction temperatures and times. In order to understand the polymerization mechanism better, the reaction temperature was decreased to slow down the reaction. Therefore, the reaction initiated by 0.1 equivalents of initiator **3** was repeated at $-78\text{ }^\circ\text{C}$ for 15, 2 and virtually zero (“0”) minutes reaction time (zero meaning that the reaction was quenched *via* insertion of an acid solution right after addition of the base). If the reaction could be slowed down in this way, molecular weights and yields should become lower than observed at $0\text{ }^\circ\text{C}$ and a progress in molecular weight with time may become observable. This would be

important results because kinetics for this living process could be studied. The results regarding molecular weight, polydispersity and yield for the polymerizations performed at $-78\text{ }^{\circ}\text{C}$ are summarized in Table 4.5 (addition mode $\text{I} + \text{B} \rightarrow \text{M}$). The same experiments were also repeated at $0\text{ }^{\circ}\text{C}$ (reaction times 15 min, 5 min, 2 min, 30 sec and "0"; results see Table 4.5 and Figure 4.5) and at room temperature (reaction times 15 min, 2 min, 30 sec and "0"; results see Table 4.5 and Figure 4.5) to have a full overview regarding kinetics for the anionic polymerization of PPVs with the use of 0.1 eq of initiator **3**.

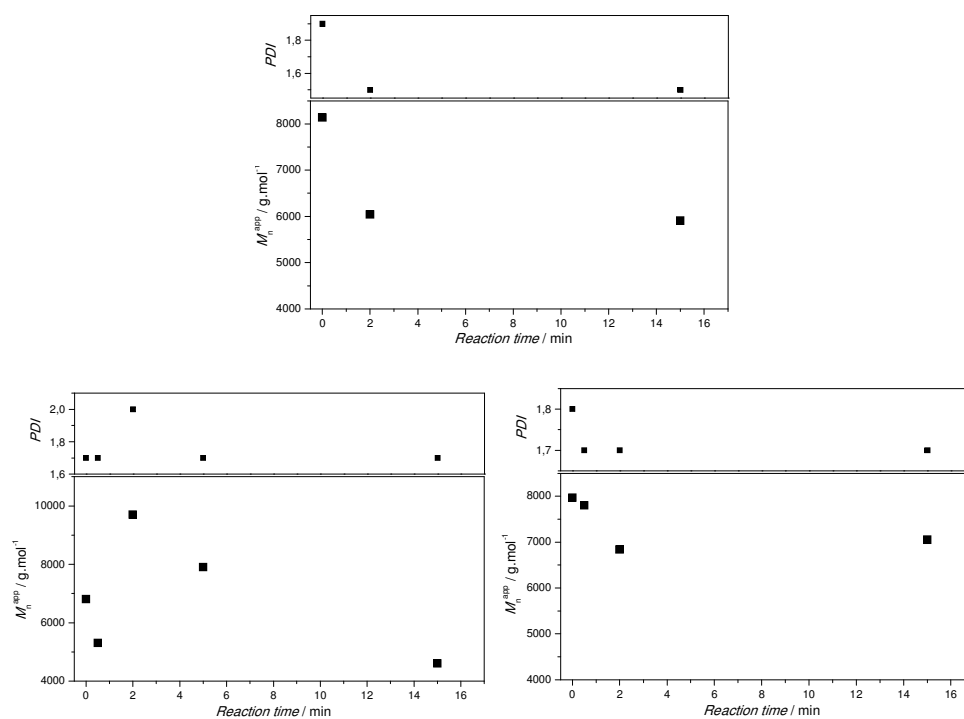


Figure 4.5: M_n^{app} and PDI (conjugated polymers) vs reaction time at $-78\text{ }^{\circ}\text{C}$ (top), $0\text{ }^{\circ}\text{C}$ (bottom, left) and RT (bottom, right)

Table 4.5: Results regarding molecular weight, polydispersity and yield for the conjugated polymers polymerized at different reaction temperatures and times (I + B → M) using 0.1 eq of initiator **3**

Time / min	-78 °C			0 °C			RT		
	$M_n^{app} / \text{g}\cdot\text{mol}^{-1}$	<i>PDI</i>	Yield / %	$M_n^{app} / \text{g}\cdot\text{mol}^{-1}$	<i>PDI</i>	Yield / %	$M_n^{app} / \text{g}\cdot\text{mol}^{-1}$	<i>PDI</i>	Yield / %
15	5900	1.5	93	4600	1.7	95	7100	1.7	95
5				7900	1.7	90			
2	6000	1.5	94	9700	2.0	94	6800	1.7	89
0.5				5300	1.7	84	7800	1.7	92
"0"	8100	1.9	80	6800	1.7	89	8000	1.8	89

From the results in Table 4.5 and Figure 4.5 it can be concluded that even at -78 °C, the molecular weights and yields are – within some scatter – practically identical compared to the results gained for the reactions at 0 °C and room temperature. The only advantage of doing the reaction at lower temperatures is the observed slight drop in polydispersity from 1.7 to 1.5. But even if the polymerization reaction was quenched with acid directly after addition of the base ("0" minutes reaction time) at -78 °C, the obtained molecular weight (8100 g·mol⁻¹) and yield (80%) were very high. It can thus be concluded that the anionic polymerization of PPV materials *via* the sulfinyl precursor route cannot be delayed by means of lowering the reaction temperature and is practically already finished upon mixing of the components. This also implies that the progression of polymerization in terms of kinetics and molecular weight evolution in the anionic polymerization reaction cannot directly be studied without significant effort.

4.3.5. Use of ^{13}C -labeled end-capper

To check if also the ω -endgroup of the polymer chain can be controlled, a ^{13}C -labeled end-capper was synthesized and added to the polymerization mixture after different reaction times. In this respect, a label was added to the chains which could be studied using ^{13}C NMR measurements. Polymers were synthesized using 0.1 equivalents of initiator **3** using the addition method $\text{I} + \text{B} \rightarrow \text{M}$ at 0 °C. Reaction was quenched with 0.2 equivalents of end-capper dissolved in a small amount of THF and stirred for another 15 min. Results regarding MWD and *PDI* were collated in Table 4.6.

Table 4.6: Molecular weights and polydispersities for precursor and conjugated polymers quenched with ^{13}C -labeled end-capper **14** after different reaction times

Time / min	Precursor polymer		Conjugated polymer	
	$M_n^{\text{app}} /$ $\text{g}\cdot\text{mol}^{-1}$	<i>PDI</i>	$M_n^{\text{app}} /$ $\text{g}\cdot\text{mol}^{-1}$	<i>PDI</i>
15	3100	1.5	5300	1.4
2	3100	1.6	5500	1.4
0.5	3800	2.2	8000	1.6
"0" ^a	4500	2.0	7600	1.9

^a Addition of initiator and base mixture to end-capper and monomer mixture ($\text{I} + \text{B} \rightarrow \text{M} + \text{E}$)

As expected, molecular weights reported for the conjugated polymers in Table 4.6 are comparable with the results discussed in Table 4.5 for polymerizations performed at 0 °C (within the error margins of the GPC profiles measured towards PS standards) because the same reaction conditions were used with the only difference being the quenching method.

To investigate the end-capper efficiency, ^{13}C NMR measurements were used to determine if the end-capper was built in the polymer chain and if the reaction was quantitative or not. First of all, ^{13}C APT NMR spectra were investigated,

because with this method, it is comparatively easy to distinguish between C4 and CH₂ (positive) and CH and CH₃ (negative) peaks. From these measurements, it became clear that the end-capper was not incorporated in the polymers quenched after a reaction time of 15 or 2 min. For shorter reaction times (30 sec and "0" (direct addition of the end-capper to the monomer before adding the initiator and base mixture)) a clear signal for the ¹³C-labeled endgroup was found in the ¹³C APT NMR spectrum (signal 'z' in Figure 4.6, spectrum given for polymerization quenched after a reaction time of 30 sec).

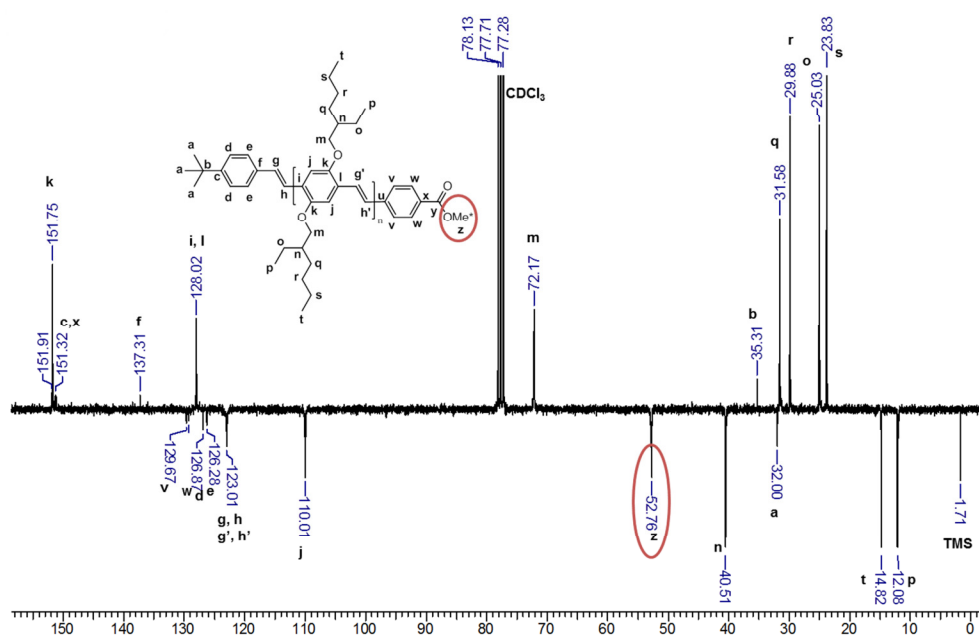


Figure 4.6: ¹³C APT NMR spectrum for PPV with *tert*-butyl initiator and ¹³C-labeled end-capper for a reaction time of 30 sec

In this (qualitative) ¹³C APT NMR spectrum (Figure 4.6), first of all the signals for the repeating monomer unit could be found. The aromatic carbon atoms (signals i – l) were found in the high ppm region between 151 and 100 ppm and

the signals for the 2-ethylhexyloxy side chain were found around 72 ppm (signal m) and in the low ppm region between 32 and 12 ppm (signals n – t). The signals corresponding to the carbon atoms of the double bond (g' and h') were found around 123 ppm. For the initiating moiety, the *tert*-butyl carbon atoms were found around 35 and 32 ppm and the aromatic signals between 137 and 126 ppm. The ^{13}C -labeled methyl group (z) showed a clear presence with a signal around 62 ppm. However, the ester functionality (normally with a signal around 160 ppm), was not present in the spectrum. Next a quantitative ^{13}C NMR spectrum was recorded (as shown in Figures 4.7–4.9) in order to determine the α - and ω -endgroups of the polymer chain and to determine whether they are quantitatively incorporated in all polymer chains. If the integration for the initiator-signals correspond to the integration for the endgroup-signals, one can assume that quantitative built in of both functional groups is obtained.

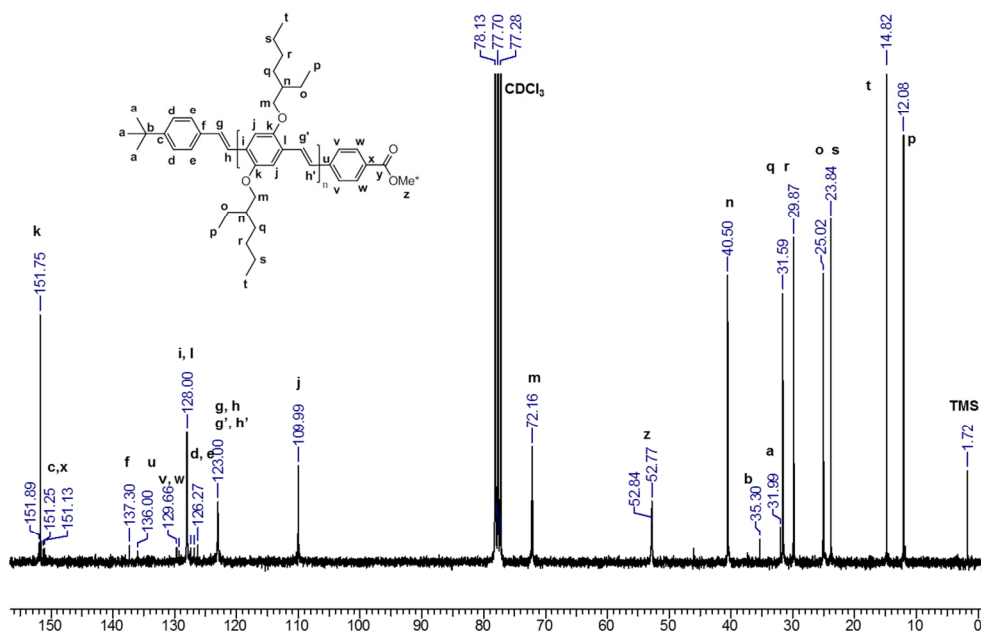


Figure 4.7: Quantitative ^{13}C NMR spectrum for PPV with ^{13}C -labeled end-capper (reaction time 30 sec)

As can be seen from Figure 4.7, exactly the same signals were found for the polymer carbon atoms and with comparable ppm values as described in the ^{13}C APT spectrum presented in Figure 4.6. Again, only the labeled methyl group (signal assigned as z) is found for the end-capping moiety and the ester carbon atom (signal y) is not present. In Figure 4.8, a zoom is given for the high ppm region, while in Figure 4.9 a zoom is given for the low ppm region. In Figures 4.8 and 4.9, the integration of the peaks is also given.

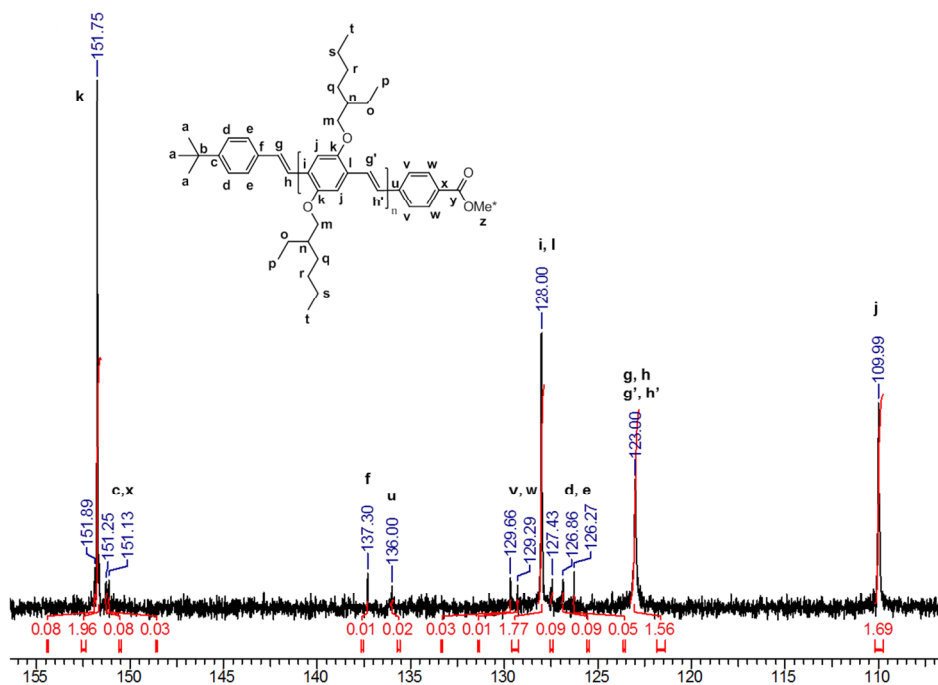


Figure 4.8: Quantitative ^{13}C NMR spectrum, zoom of high ppm region

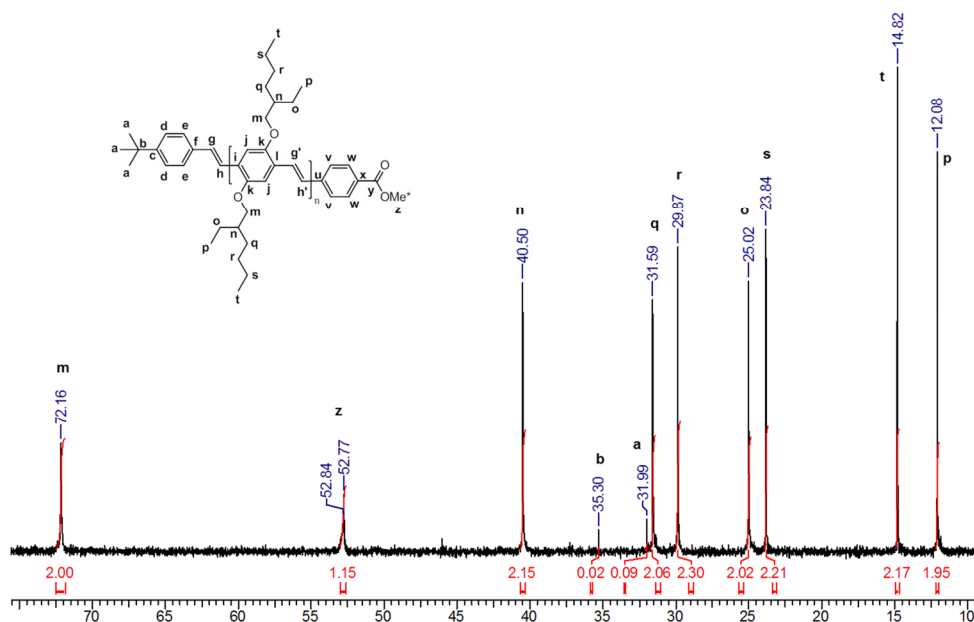


Figure 4.9: Quantitative ^{13}C NMR spectrum, zoom of low ppm region

From Figures 4.8 and 4.9 it is clear that the integration of the signals for the carbon atoms, present in the repeating monomer unit, fit the expected values. For the *tert*-butyl functionalized initiator, all carbon atoms were found, but integration was not straightforward because of their low abundance in the polymer chains. If for instance the integration for signals a and b are compared, there already is a disagreement (0.09 for a (3 carbon atoms) and 0.02 for b (1 carbon atom)) and no conclusions regarding quantitative built in of this moiety can be drawn. In order to look at ω -endgroup fidelity, the integration of signal z would in a second step be compared to the integration of signals a and b. If the same value for this integration is found, quantitative built in of both groups can be assumed because the initiator and end-capper should appear in the same ratio in the polymer chains. For this comparison, recalculation of the integrated value for signal z for the natural abundance would be necessary (natural

abundance of ^{13}C is only 1.1%). This already indicates a very low presence of this ω -endgroup in the polymer chain and no conclusions can be drawn regarding built in and nature of the ω -endgroup of all polymer chains. In Chapter 6, an ESI-MS study will be presented which will reveal more about the initiator efficiency and endgroup fidelity of the polymer chains.

4.4. CONCLUSION

It can be concluded that for high monomer concentrations, high molecular weights are found with high *PDI*s. This is why a standard initial monomer concentration of $50 \text{ mmol}\cdot\text{L}^{-1}$ is chosen for all further experiments. The anionic initiators – with a similar structure to the monomer – with a sulfinyl (or sulfonyl) polarizer group, seem to be the most efficient initiators compared to a thioether polarizer group for which a less efficient initiation for the anionic chains is found. For a *tert*-butyl functionalized initiator, using different addition modes for monomer, initiator and base to the reaction mixture, no differences in outcome of the reactions is found regarding MWD and *PDI*. In contrast, for halogen-substituted anionic initiators, a drastic influence on molecular weight is observed for different addition modes. By using very low temperatures, it became clear that the anionic polymerization proceeds upon mixing of the different components and the reaction cannot be slowed down by using temperatures of $-78 \text{ }^\circ\text{C}$ and even after very short reaction times high yields are observed. It is still not fully understood if a high initiator efficiency is indeed found (deviation of the ideal polymerization plot). Although with using different amounts of the anionic initiator a good linear correlation of the chain length with the initiator concentration is found.

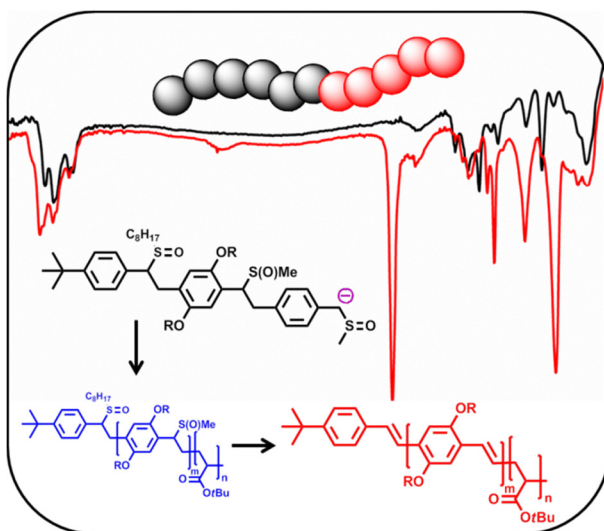
In a last part, it is revealed that the efficiency for the built in of a functionalized ^{13}C labeled end-capper molecule is low and only possible using very short reaction times as confirmed *via* ^{13}C NMR measurements. This finding is in-line with the low-temperature experiments and indicates that end-capping does not allow to quantitatively form ω -functionalized PPV chains.

4.5. REFERENCES

- ¹ I. Cosemans, L. Hontis, D. Van Den Berghe, A. Palmaerts, J. Wouters, T. Cleij, L. Lutsen, W. Maes, T. Junkers, D. Vanderzande, *Macromolecules* **2011**, *44*, 7610–7616.
- ² I. Cosemans, J. Wouters, T. Cleij, L. Lutsen, W. Maes, T. Junkers, D. Vanderzande, *Macromol. Rapid Commun.* **2012**, *33*, 242–247.
- ³ R. N. Ibbett, *NMR spectroscopy of Polymers*, 1st ed; Chapman & Hall, **1993**, Chapter 3.
- ⁴ H. Diliën, S. Chambon, T. J. Cleij, L. Lutsen, D. Vanderzande, P. J. Adriaenssens, *Macromolecules* **2011**, *44*, 4711–4720.
- ⁵ J. E. Baldwin, *J. Label. Compd. Radiopharm.* **2007**, *50*, 947–960.
- ⁶ C. E. Carraher, Jr., *Seymour/Carraher's Polymer Chemistry*, 7th ed; CRC Press, **2008**, Chapter 5.
- ⁷ G. Odian, *Principles of polymerization*, 4th ed; Wiley-Interscience, **2004**, Chapter 5.
- ⁸ O. Arjona, R. Menchaca, J. Plumet, *J. Org. Chem.* **2001**, *66*, 2400–2413.
- ⁹ R. F. de la Pradilla, M. V. Buergo, P. Manzano, C. Montero, J. Priego, A. Viso, F. H. Cano, M. P. Martínez-Alcázar, *J. Org. Chem.* **2003**, *68*, 4797–4805.
- ¹⁰ Synthesis of the bis-(2-ethylhexyloxy) substituted monomer, see Chapter 3.

CHAPTER 5

Anionic PPV Polymerization from the Sulfinyl Precursor Route: Block Copolymer Formation from Sequential Addition of Monomers



The sulfinyl precursor route for the synthesis of poly(*p*-phenylene vinylene) (PPV) materials *via* an anionic polymerization procedure employing dedicated initiators is evaluated in depth. Since polymerization proceeds to full conversion on the timescale of mixing of the reaction components (even at -78 °C), a closer look was taken into the polymerization setup. Comparison was made between the usual Schlenk line setup and a specialized setup for anionic polymerizations. BEH-PPVs could be obtained in the range of 3000 to 16 000 g·mol⁻¹, whereby dispersity decreases with decreasing molecular weight, allowing for materials with a *PDI* of 1.1 for the smallest PPV chain. Block copolymerizations were performed *via* sequential addition of monomers to make use of the living PPV chain ends. Bimodal product mixtures are obtained, consisting of block copolymer as well as PPV homopolymer. The block copolymer PPV-*b*-poly(*tert*-butyl acrylate) could nevertheless be separated by selective precipitation as well as preparative chromatography techniques.

Published in:

* I. Cosemans, J. Vandenberg, V. S. D. Voet, K. Loos, L. Lutsen, D. Vanderzande, T. Junkers, *Polymer* **2013**, *54*, 1298–1304.

5.1. INTRODUCTION

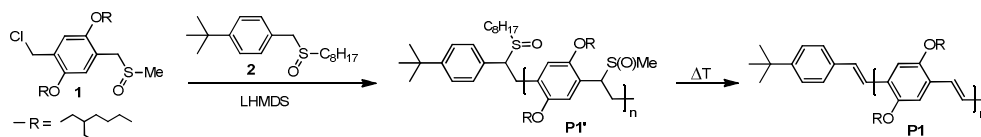
In the previous chapters it was demonstrated that a pure anionic PPV polymerization can be achieved.^{1,2} However, deviations from ideal polymerization were still observed and doubts remained about the initiation efficiency of the employed initiator. In this chapter the polymerization efficiency, with respect to endgroup functionality in order to find methodologies to utilize the polymerization procedure for block copolymer synthesis and self-assembly of materials, is further elucidated. Generally, the field of semiconducting polymers runs behind that of classical polymers with respect to advanced macromolecular design and closing this gap will open up new avenues also outside the classical fields of application of conjugated materials. For PPV materials, a self-initiated free-radical mechanism is observed for the different precursor routes gaining materials for which little or no control on molecular weight, endgroups or dispersity could be reached.³⁻¹⁰ To allow for the synthesis of advanced macromolecular structures with sophisticated materials properties, good control over these parameters are, however, required. Defined block or graft polymers will only be accessible if endgroup and molecular weight control is achieved. Different strategies for the synthesis of complex architectures and block copolymers have already been described, for instance *via* the Wittig reaction, resulting in difficult reaction-deprotection-reaction methods yielding complex oligomers. These are complicated stepwise reactions, with thorough monomer synthesis to start from.^{11,12}

To overcome these observed difficulties, two aspects of the polymerization were targeted in this chapter. First of all a deeper look was taken into the polymerization setup. In collaboration with the University of Groningen, where a specialized anionic polymerization setup is available, influences from small

impurities on the polymerization was examined. In this chapter the results gained with the use of regular Schlenk lines (vacuum/N₂, Hasselt technique) are compared to these reached in Groningen on the specialized setup,^{13,14} which allows to avoid the use of syringes and thus water and/or oxygen intake as much as possible. In the second part, the synthesis of block copolymers by addition of a second monomer to the living PPV polymers is described. Namely *tert*-butyl acrylate (*t*-BuA) was used as the second monomer during the synthesis of the block copolymer. As will be demonstrated, the high reactivity of the living PPV chain ends makes block copolymer synthesis very challenging, but not entirely impossible. Block copolymers can indeed be gained if remaining homopolymers are removed *via* selective precipitation and advanced chromatography techniques (frequently applied for semiconducting polymer materials). It should be noted that of course such approach is not the most desirable, but may, however, yield interesting materials.

5.2. EXPERIMENTAL SECTION

5.2.1. Polymerization



Scheme 5.1: Anionic polymerization of BEH-PPV **P1**

All polymerization and elimination reactions were carried out as described before ($[M]_i = 50 \text{ mmol}\cdot\text{L}^{-1}$; $0 \text{ }^\circ\text{C}$; $\text{B} \rightarrow \text{M} + \text{I}$).² The synthesis of the precursor polymer was quenched after 15 minutes by addition of 0.2 mL concentrated HCl solution (37%).

5.2.2. Polymer and block copolymer synthesis with high vacuum line anionic polymerization setup ($\text{B} \rightarrow \text{M} + \text{I}$)

A dried 50 mL flask was degassed by evacuation on a high vacuum system and backfilled with nitrogen. To this flask monomer **1** (0.5 mmol, 0.23 g) and initiator **2** were added and was again evacuated and filled with nitrogen. THF was added by direct distillation of dried THF under reduced pressure and the full mixture was subjected to three freeze-pump-thaw cycles. The concentration was kept around $50 \text{ mmol}\cdot\text{L}^{-1}$ but could not exactly be controlled in this way. The flask was then cooled to $0 \text{ }^\circ\text{C}$ and LHMDS (1M in THF, 1.3 equivalents, 0.65 mL) was added using a degassed syringe. The mixture was stirred for 15 minutes and quenched with concentrated HCl (37%). Work-up and elimination of the prepolymer was performed as earlier reported.²

For the block copolymer synthesis, the reaction was not quenched with acid, but *tert*-butyl acrylate (5 equivalents, 2.5 mmol, 0.36 mL) was added using a degassed syringe and the reaction was consequently stirred for another 15 min at 0 °C and quenched with methanol. Work-up and elimination was again performed as described before.² The conjugated polymer was precipitated in a MeOH/HCl (2/1) mixture and was filtered as a sticky red solid. Afterwards the dried polymer was separated with the use of recycling preparative HPLC.

It must be noted that only apparent molecular weights M_n^{app} are reported since the polymers were measured on a GPC with conventional polystyrene calibration, which nevertheless allows for qualitative discussion of results and to discern trends. Absolute molecular weights were determined for selected samples *via* light scattering; those results will be discussed below.

5.2.3. Separation of polymers

Separation of polymers after selective precipitation were performed on a recycling preparative HPLC LC-9210 NEXT system in the manual injection mode (3 mL) comprising a JAIGEL-2H and JAIGEL-3H column and a NEXT series UV detector using CHCl_3 as the eluent with a flow rate of $3.5 \text{ mL}\cdot\text{min}^{-1}$. Fractions were collected manually.

5.3. RESULTS AND DISCUSSION

5.3.1. Anionic polymerization setup

Because no control could be gained over the anionic polymerization reaction by lowering the reaction temperature to $-78\text{ }^{\circ}\text{C}$,¹⁵ insights were taken into the polymerization setup. All earlier published polymers^{1,2} (and polymers described in this thesis) were synthesized *via* the anionic route using regular Schlenk lines (vacuum/ N_2). For comparison, experiments using different equivalents of anionic initiator **2** were repeated on a high vacuum line anionic polymerization setup with a high vacuum pump which is available at the University of Groningen. Results for molecular weights and *PDI*s for the eliminated polymer **P1** (Figure 5.1) are collated in Table 5.1 and summarized in Figure 5.2.

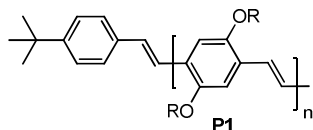


Figure 5.1: *Tert*-butyl functionalized BEH-PPV **P1**

Table 5.1: Comparison of molecular weight and *PDI* for eliminated BEH-PPV **P1** synthesized on Schlenk lines or on a high vacuum anionic polymerization setup measured with conventional GPC compared to MALLS

[In] / mmol·L ⁻¹	Schlenk lines				High Vacuum Line			
	Conventional GPC		MALLS		Conventional GPC		MALLS	
	$M_n^{\text{app}} /$ g·mol ⁻¹	<i>PDI</i>	$M_n /$ g·mol ⁻¹	<i>PDI</i>	$M_n^{\text{app}} /$ g·mol ⁻¹	<i>PDI</i>	$M_n /$ g·mol ⁻¹	<i>PDI</i>
0	15600	2.4	15500	1.4	13100	2.2	13300	1.5
2.5	8600	2.0	9600	1.3				
5	7400	2.1	7800	1.3	5200	1.7	6000	1.4
10	4200	1.4	4500	1.3				
15					3400	1.3	3900	1.2
25	2800	1.2	3000	1.1	2600	1.2	3000	1.1

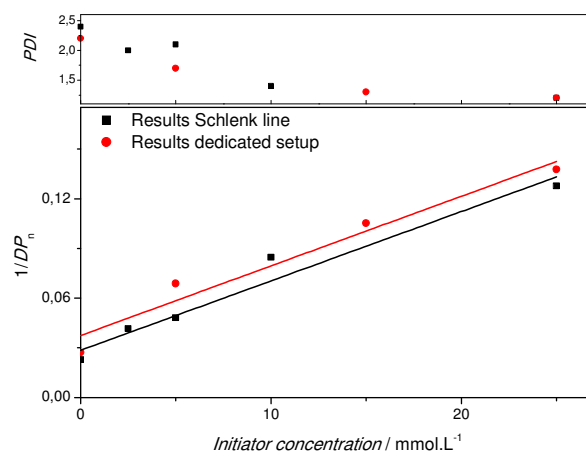


Figure 5.2: Comparison of the inverse of the degree of polymerization (DP_n) and PDI for PPVs synthesized on Schlenk lines (black squares) or with high vacuum line (red circles) measured on conventional GPC

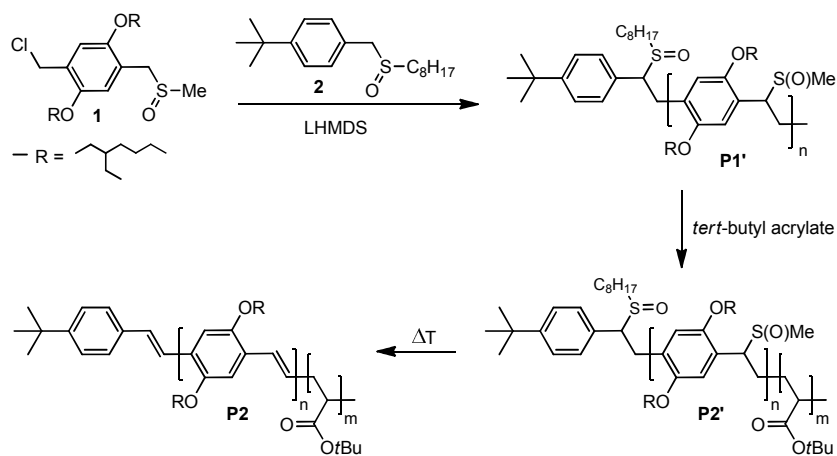
From Table 5.1 and Figure 5.2, it is clear that the same trends regarding molecular weight and polydispersity are observed regardless the setup used for the synthesis of the polymer. If the initiator concentration is plotted against the inverse of the degree of polymerization, the same linear trend is found. With the use of higher amounts of anionic initiator, lower molecular weights and dispersities were gained in both cases. It can thus be concluded that similar results were generated for both setups and that the method, using a conventional Schlenk line to synthesize PPV materials *via* the anionic pathway, may not be the conventional way at first sight but leads to reproducible and reliable results for the anionic polymerization pathway. If the results of the conventional GPC (measured towards polystyrene standards) are compared to results gained with MALLS (multi angle laser light scattering) detection (absolute determination of MWD using dn/dc determined for MDMO-PPV^{16,17}), it can be seen that the number average molecular weights are in good agreement for both characterization techniques. This agreement is essentially coincidental, but

is of course advantageous since it simplifies further investigations tremendously. When analyzing the polydispersities, however, one sees a significant difference. MALLS reveals that the molecular weight distributions are associated with a significantly lower dispersity than they appear to be in conventional GPC. The MALLS data show that for all samples *PDI*s of <1.5 are obtained, which underpins that the polymerization indeed proceeds *via* a living polymerization pathway.¹⁸ At the highest initiator concentration, a dispersity of 1.1 is reached, which is an exceptionally narrow distribution for a conjugated polymer material. This observation should not be underestimated. Self-assembly of materials may only become possible when precise and narrow block length distributions are accessible. *Via* the radical pathway mentioned above, so far only PPV blocks with a dispersity of minimal 2 were obtainable, thus the present data reveal a significant advantage of the anionic polymerization route, that was previously not acknowledged.

As can be concluded from Figure 5.2, a linear correlation is found for both setups when the inverse of the degree of polymerization is plotted versus the initiator concentration which deviates from the ideal polymerization ($1/DP_n = 1/C_m \cdot C_i$). From Table 5.1 it is clear that similar molecular weights are found for conventional GPC (relative towards PS) and MALLS measurements but large deviation in *PDI* is found. With these findings, the initiation efficiency of the polymer chains still remains unclear.

5.3.2. Block copolymer synthesis on high vacuum line

By synthesizing PPVs *via* the anionic polymerization pathway, a living chain end is created and can be used to synthesize block copolymers by addition of a second monomer to the polymerization mixture. For the synthesis of the PPV-*b*-P(*t*-BuA) block copolymer, the same anionic initiator with *tert*-butyl functionality (**2**) is used and polymerized with monomer **1** (Scheme 5.2).



Scheme 5.2: Synthesis of BEH-PPV-*b*-P(*t*-BuA) block copolymer **P2**

After 15 minutes of reaction time at 0 °C, 5 equivalents of *tert*-butyl acrylate were added to the reaction mixture and further stirred for 15 minutes at 0 °C. The polymerization reaction was then quenched with methanol and extracted with CH₂Cl₂. After evaporation of the solvent the precursor block copolymer **P2'** was obtained as a sticky yellow solid. After elimination (3 h reflux in toluene), precipitation and filtration, the conjugated polymer **P2** was obtained as a red solid.

With the goal to synthesize block copolymers *via* the living chain end of the PPV block, also styrene was tested as the monomer for sequential polymerization.

The same procedure was followed as described above, but no block copolymer could be identified in the product mixture. The reason for the failure of this experiment could not be identified so far and it can only be speculated that the anionic chain end of the PPV precursor polymer chain does not favour styrene addition. In a different attempt to synthesize a block copolymer with a PPV and a polystyrene (PS) block, styrene was polymerized first, initiated by *sec*-BuLi (*sec*-butyllithium), followed by addition of the sulfinyl monomer **2** after 15 minutes of reaction time at -78 °C. In this case a bimodal (no addition of LHMDS to initiate PPV polymerization) or even a trimodal (addition of LHMDS directly after addition of monomer **1**) GPC profile was measured. The different peaks in the chromatogram could essentially be assigned to homopolymers rather than block copolymers. The reason for the failure of this method lies in the basic nature of the active anionic polystyrene chain ends. These resemble themselves species that can deprotonate the sulfinyl monomer, thus activating the PPV polymerization while concomitantly deactivating the polystyrene chains. Thus, before PPV can be added to the chain ends, all anionic centers have already been quenched.

The only successful method to obtain block copolymers *via* the use of the anionic PPV chain end, was the first described block extension of the PPV precursor chains with *tert*-butyl acrylate (see Scheme 5.2). Still, the chromatogram measured for the non-purified precursor polymer **P2'** shows a bimodal molecular weight distribution (see Figure 5.3 and Table 5.2 for MW values), indicating that not all PPV chains were able to react further and form a block copolymer. Thus, the reaction product resembles a mixture of PPV homopolymer and block copolymer (homopolymer of the acrylate cannot be formed, since no other initiator was present to start chain growth).

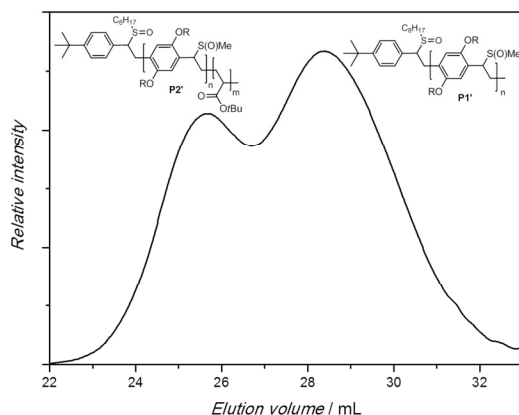


Figure 5.3: GPC profile for the precursor block copolymer prePPV-*b*-P(*t*-BuA) **P2'**

After elimination of the materials to form the conjugated PPV blocks, copolymer **P2** could not be precipitated in MeOH (the usual non-solvent for PPV materials) but only in a MeOH/HCl (2/1) mixture. This indicates successful chain addition of the acrylate because pure acrylate homopolymer would dissolve in this solvent mixture. After precipitation, again a bimodal GPC profile is observed (Figure 5.4 and Table 5.2), however, the bimodality is less pronounced due to the selective precipitation. For comparison, the molecular weight of pure BEH-PPV (synthesized with 0.1 equivalents of anionic initiator **1**) is also collated in Table 5.2. For the precursor and conjugated PPV polymer, respectively, an apparent molecular weight of 3400 and 5200 $\text{g}\cdot\text{mol}^{-1}$ was found. In this way, it becomes evident that the low molecular weight part (high elution volumes) of the bimodality for **P2'** and **P2** is in agreement with these values. It must be pointed out that the molecular weights, measured by means of GPC towards polystyrene standards, for the roid-coil block copolymers **P2'** and **P2** are only a rough estimation of the real molecular weights because of the difference in hydrodynamic volume for the different polymer blocks.

To further purify the polymer obtained, the conjugated block copolymer **P2** was subjected to recycling preparative GPC, a standard technique for the separation of conjugated polymer materials.^{19,20} In this way, the block copolymer **P2** could be separated from the homopolymer **P1**. The polymers were fractionated during the second cycle (collected from 88.7 – 95.1 min, see Figure 5.4 and Table 5.2).

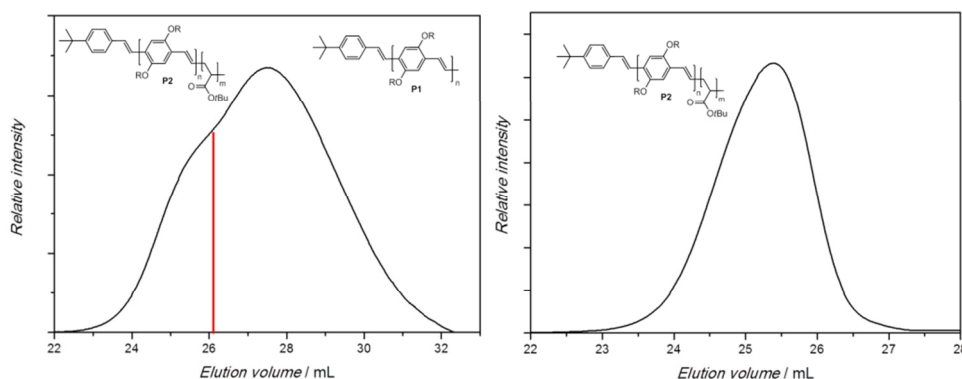


Figure 5.4: GPC profile for the eliminated PPV-*b*-P(*t*-BuA) **P2** before (left) and after (right) separation on recycling HPLC

Table 5.2: Molecular weights and polydispersities obtained from conventional SEC for block copolymers **P2'** and **P2** and the purified block copolymer fraction of **P2** compared to BEH-PPV

	Precursor polymer		Conjugated polymer	
	$M_n^{\text{app}} / \text{g}\cdot\text{mol}^{-1}$	<i>PDI</i>	$M_n^{\text{app}} / \text{g}\cdot\text{mol}^{-1}$	<i>PDI</i>
Pure BEH-PPV	3400	1.8	5200	1.7
Before purification	6600	4.7	8900	3.2
After purification, high MW fraction			48300	1.2

After fractionation, the high molecular weight fraction was characterized using ^1H NMR, FT-IR, UV-Vis and fluorescence spectrometry, TGA (thermogravimetric analysis) and DSC (differential scanning calorimetry) measurements. From the selective precipitation of the conjugated polymer **P2**, it was already clear that a PPV-*b*-P(*t*-BuA) block copolymer was formed. This was further proven with the use of FT-IR and ^1H NMR spectroscopy. When the FT-IR spectra for the pure BEH-PPV **P1** (black line, Figure 5.5) and BEH-PPV-*b*-P(*t*-BuA) **P2** (red line, Figure 5.5) were compared, signals at 1728, 1368 and 1150 cm^{-1} clearly appear, which could be assigned to the carbonyl functionality of the acrylate block that was attached to the PPV block.

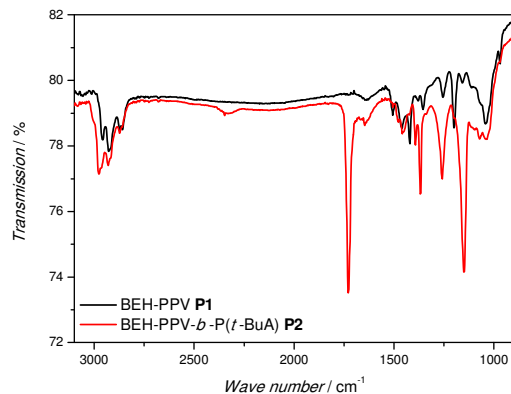


Figure 5.5: FT-IR spectra for BEH-PPV **P1** (black line) and BEH-PPV-*b*-P(*t*-BuA) **P2** (red line)

In the ^1H NMR spectrum for the high molecular weight fraction of **P2** (Figure 5.6) signals for both the PPV and the poly(*tert*-butyl acrylate) block could be distinguished. From this NMR spectrum the length of the different blocks of **P2** could be calculated by integrating the signals for the aromatic protons of the PPV main chain and comparing this to the signal corresponding to the hydrogen

atoms of the acrylate main chain (2.23 ppm). For the eliminated BEH-PPV, synthesized with the use of 0.1 equivalents of initiator, an average molecular weight of around $5200 \text{ g}\cdot\text{mol}^{-1}$ is found (see Table 5.2). This translates to an average of 15 PPV units present in the first polymer block (molecular weight of one unit $\sim 357 \text{ Da}$) and thus integration of the aromatic protons was set to 15. To calculate the acrylate block length, the integration value thus obtained for the peak at 2.23 ppm (the signal for the three protons present in the main chain of P(*t*-BuA)) was used (256 protons which is equal to 85 acrylate units). It can hence be calculated that the acrylate block (MWD one unit $\sim 128 \text{ Da}$) should have a molecular weight of $10900 \text{ g}\cdot\text{mol}^{-1}$ resulting in a total molecular weight of $16100 \text{ g}\cdot\text{mol}^{-1}$ for the synthesized BEH-PPV-*b*-P(*t*-BuA) block copolymer.

In comparison to these calculated values, the molecular weight determined with conventional GPC ($48300 \text{ g}\cdot\text{mol}^{-1}$, relative towards PS standards) does not match. This observed difference is probably due to the big difference in hydrodynamic volume between the stiff PPV block and the coiled acrylate block which results in an erroneous result when measured towards PS standards on a conventional GPC.

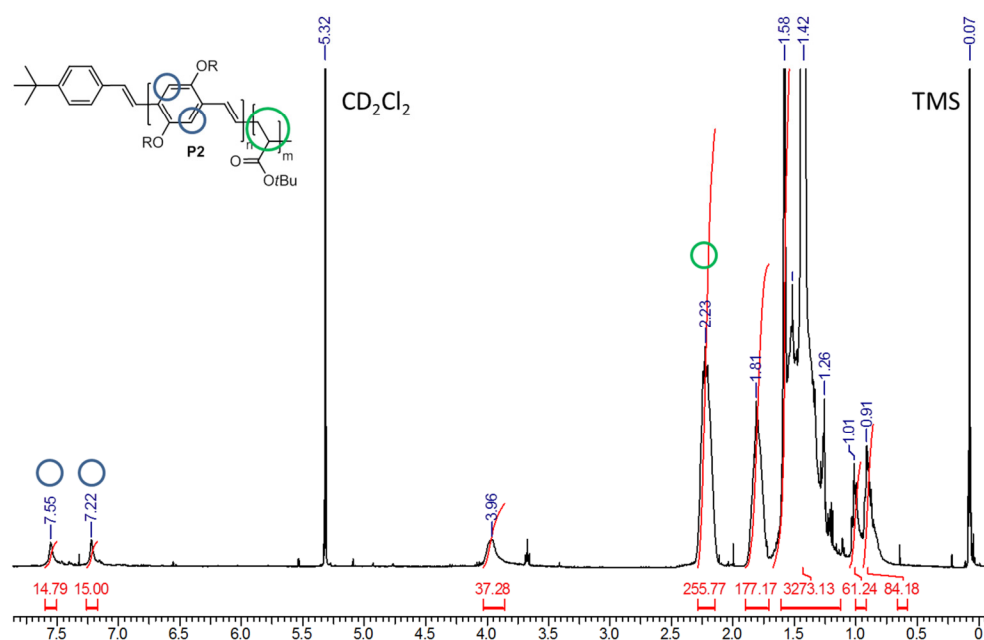


Figure 5.6: $^1\text{H-NMR}$ spectrum of block copolymer **P2** in CD_2Cl_2

In contrast, however, if one would calculate the theoretical amount of acrylate units for full conversion (5eq acrylate towards PPV premonomer), the molecular weight of the acrylate block should be around $6400 \text{ g}\cdot\text{mol}^{-1}$. This mismatch between the theoretically expected composition and the experimentally derived MWD can be explained by only partial reinitiation of the chains (as already indicated by the bimodality) as well as preparative separation of the polymers, which have cut out systematically lower molecular weight blocks, thus also shifting the average molecular weights.

In the UV-Vis spectrum (Figure 5.7, left), a blue-shift in λ_{max} is observed if the block copolymer **P2** (466 nm) is compared to the pure PPV **P1** (495 nm). Possible explanations for this blue-shift are that the *tert*-butyl acrylate block is slightly disrupting the optimal conjugation of the PPV block (resulting in a shorter average conjugation length), or that the acrylate block quenches the

light absorption of the PPV block in the block copolymer. The same result is found in the fluorescence spectrum (Figure 5.7, right), where also a blue-shifted maximum wavelength is found for the BEH-PPV-*b*-P(*t*-BuA) block copolymer compared to the pure BEH-PPV.

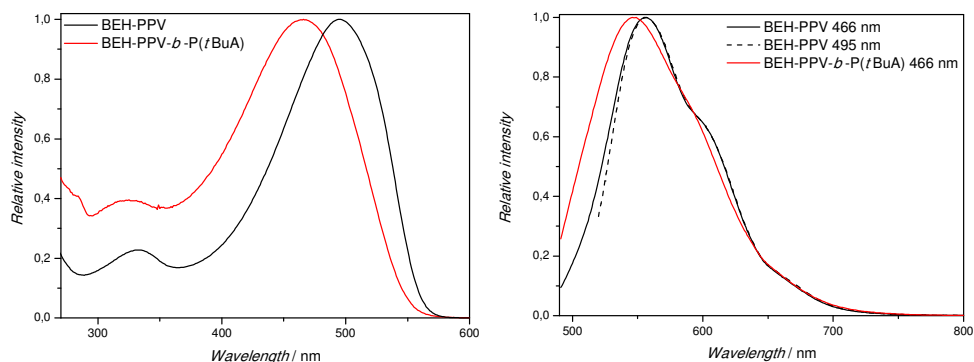


Figure 5.7: UV-Vis (left) and fluorescence (right) spectra measured in CHCl_3 solution for BEH-PPV **P1** (red line) and BEH-PPV-*b*-P(*t*-BuA) **P2** (black line)

To confirm the presence of a block copolymer also a GPC trace (CB as eluent) was measured with UV detection at the maximum absorption wavelength for **P2** (466 nm; see Figure 5.7, left). If a monomodal peak of high MWD is found, the presence of a block copolymer is unambiguously proven because at 466 nm, only the PPV block will absorb light and thus the acrylate must be attached to the PPV block. From the data in Figure 5.8 and Table 5.3 it can thus be concluded that a PPV-*b*-P(*t*-BuA) block copolymer is formed.

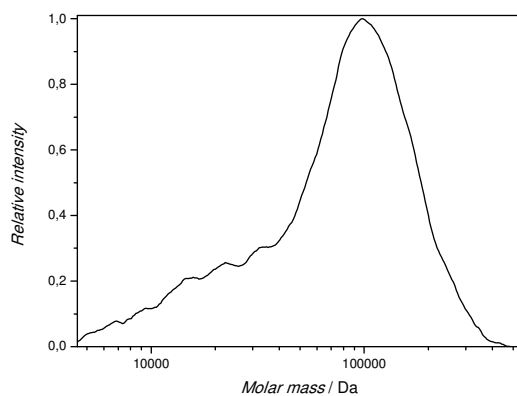


Figure 5.8: GPC profile of **P2** for UV detection at 466 nm in CB as the solvent

Table 5.3: Molecular weight and *PDI* for **P2** (UV detection at 466 nm) measured on conventional GPC using CB as the eluent (PS standards)

	Conjugated polymer	
	$M_n^{app} / \text{g}\cdot\text{mol}^{-1}$	<i>PDI</i>
After purification, high MW fraction	43900	2.1

In the DSC profile (Figure 5.9), a glass transition (T_g) is visible at 34.7 °C which can be addressed to the acrylate block. For the PPV block, no T_g could be observed in this measurement.

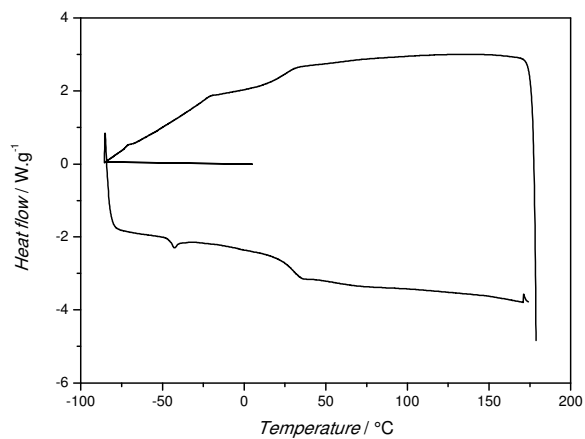


Figure 5.9: DSC profile for BEH-PPV-*b*-P(*t*-BuA) **P2**

To study the thermal stability of the polymers, the weight loss is recorded as a function of temperature in thermogravimetric analysis. From the TGA profile (Figure 5.10), decomposition can be observed with a start around 210 °C. The second major weight loss, with a maximum around 432 °C, accounts for the degradation of the conjugated system.

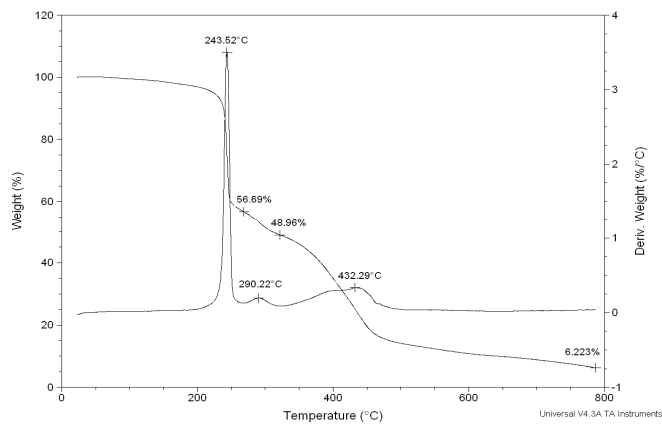


Figure 5.10: TGA profile for BEH-PPV-*b*-P(*t*-BuA) **P2**

5.4. CONCLUSION

PPV formation *via* the anionic polymerization mode in the sulfinyl precursor route is very fast and yields narrowly distributed PPV materials as confirmed *via* MALLS measurements. When the PPV polymerizations are repeated on a dedicated high vacuum anionic polymerization setup, gained molecular weights and polydispersities are similar. The use of regular Schlenk lines is thus a good synthetic tool to reach reproducible results for the anionic PPV polymerization *via* the sulfinyl route. For the synthesis of block copolymers, making use of the living chain end of the PPV chain was not fully successful. Formation of block copolymer occurred, but also PPV homopolymer remained in the product mixture. After selective precipitation and fractionation on a preparative recycling GPC, a high molecular weight block copolymer could nevertheless be successfully isolated. Block structure and composition were confirmed via FT-IR and ^1H NMR measurements.

This study marks a significant step towards further investigations into PPV-containing block copolymer materials. While still essentially successful in the goal of producing block copolymers (at least on small scale), it is clear from the above described investigations that sequential monomer addition is not suitable to prepare block structures efficiently.

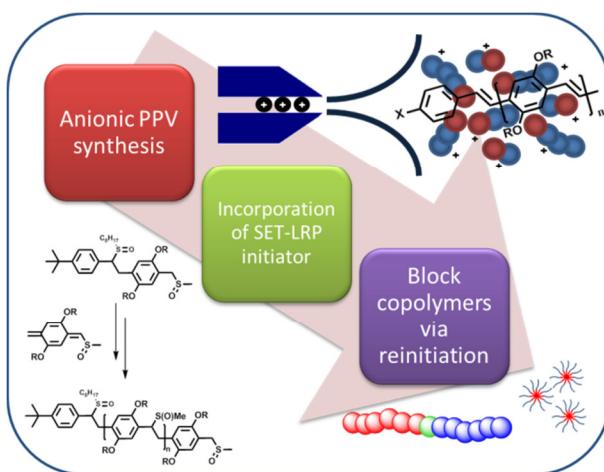
5.5. REFERENCES

- ¹ I. Cosemans, L. Hontis, D. Van Den Berghe, A. Palmaerts, J. Wouters, T. Cleij, L. Lutsen, W. Maes, T. Junkers, D. Vanderzande, *Macromolecules* **2011**, *44*, 7610–7616.
- ² I. Cosemans, J. Wouters, T. Cleij, L. Lutsen, W. Maes, T. Junkers, D. Vanderzande, *Macromol. Rapid Commun.* **2012**, *33*, 242–247.
- ³ L. Hontis, V. Vrindts, L. Lutsen, D. Vanderzande, J. Gelan, *Polymer* **2001**, *42*, 5793–5796.
- ⁴ T. Schwalm, J. Wiesecke, S. Immel, M. Rehahn, *Macromolecules* **2007**, *40*, 8842–8854.
- ⁵ B. Cho, Y. Kim, M. Han, *Macromolecules* **1998**, *31*, 2098–2106.
- ⁶ A. Issaris, D. Vanderzande, J. Gelan, *Polymer* **1997**, *38*, 2571–2574.
- ⁷ A. Issaris, D. Vanderzande, P. Adriaensens, J. Gelan, *Macromolecules* **1998**, *31*, 4426–4431.
- ⁸ L. Hontis, L. Lutsen, D. Vanderzande, J. Gelan, *Synth. Met.* **2001**, *119*, 135–136.
- ⁹ J. Vandenbergh, J. Wouters, P. Adriaensens, R. Mens, T. Cleij, L. Lutsen, D. Vanderzande, *Macromolecules* **2009**, *42*, 3661–3668.
- ¹⁰ T. Schwalm, J. Wiesecke, S. Immel, M. Rehahn, *Macromol. Rapid Commun.* **2009**, *30*, 1295–1322.
- ¹¹ M. Jorgensen, F. Krebs, *J. Org. Chem.* **2005**, *70*, 6004–6017.
- ¹² O. Hagemann, M. Jorgensen, F. Krebs, *J. Org. Chem.* **2006**, *71*, 5546–5559.
- ¹³ G. Gobius du Sart, I. Vukovic, G. Alberda van Ekenstein, E. Polushkin, K. Loos, G. ten Brink, *Macromolecules* **2010**, *43*, 2970–2980.

- ¹⁴ M. Faber, V. S. D. Voet, G. ten Brinke, K. U. Loos, *Soft Matter* **2012**, *8*, 4479–4485.
- ¹⁵ For results of polymerizations performed at -78 °C, see Chapter 4.
- ¹⁶ L. Hontis, *PhD thesis*, Limburgs Universitair Centrum, **2002**, Chapter 4.
- ¹⁷ J. Vandenberg, unpublished results.
- ¹⁸ G. Odian, In *Principles of polymerization*, 4th ed; Wiley Interscience, **2004**, Chapters 1 and 5.
- ¹⁹ J. Lesec, *J. Liq. Chromatogr.* **1985**, *8*, 875–923.
- ²⁰ M. Sommer, H. Komber, S. Huettner, R. Mulherin, P. Kohn, N. C. Greenham, W. T. S. Huck, *Macromolecules* **2012**, *45*, 4142–4151.

CHAPTER 6

Synthesis of Well-Defined PPV Containing Block Copolymers with Precise Endgroup Control from a Dual-Initiator Strategy



Poly(2,5-bis(2-ethylhexyloxy)*p*-phenylene vinylene)-*b*-poly(*tert*-butyl acrylate) (BEH-PPV-*b*-P(*t*-BuA)) block copolymers with various block compositions have been synthesized from a dual initiator strategy. PPV polymerizations are performed *via* the anionic polymerization mode of the so-called sulfinyl precursor synthesis route with a dedicated initiator carrying a moiety that is able to reinitiate polymer chains under conditions of a single electron transfer living radical polymerization (SET-LRP). In order to prove that such route can be taken, a detailed study on the initiator efficiency in the anionic polymerization based on post-mortem analysis of materials with ESI-MS is presented. Almost quantitative incorporation of the initiator in alpha position of the chains is confirmed. Block copolymers are subsequently obtained from a BEH-PPV building block with an apparent M_n of 5300 g·mol⁻¹ and block copolymers with apparent M_n between 6800 and 25000 g·mol⁻¹ are synthesized. Hydrolysis of the acrylate ester block yields amphiphilic block copolymers with a poly(acrylic acid) block, which can be self-assembled in methanolic solution to form micelles with a mean diameter of 81 nm. The micelles respond to changes in pH and ionic strength, leading to significant expansion of the micelles in both cases.

Published in:

* I. Cosemans, J. Vandenberg, L. Lutsen, D. Vanderzande, T. Junkers, *Polym. Chem.* **2013**, *4*, 3471–3479.

6.1. INTRODUCTION

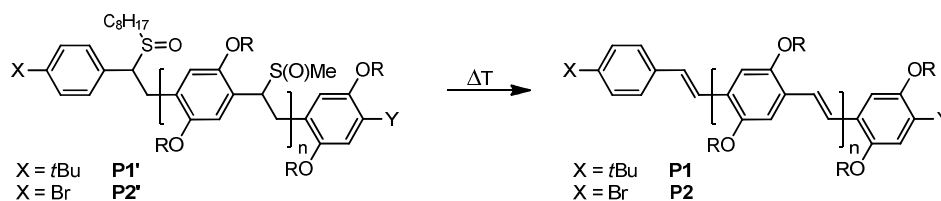
In the previous chapter it was demonstrated that direct anionic polymerization of a second monomer (*tert*-butyl acrylate, *t*-BuA), with the aim to obtain block copolymers of the structure PPV-*b*-P(*t*-BuA) was possible, but did not yield pure diblock structures, but bimodal mixtures of block copolymer and PPV homopolymer.¹ Thus, further investigations towards block copolymers containing one PPV block were still necessary. Such materials can be used for self-assembly and can thus give direct access to interesting nanostructured materials with unique semiconducting properties.

Generally, knowledge over the endgroups of polymers and their control is of high importance for such aim since by influencing the endgroup fidelity of a polymer, access is given to selective introduction of endgroups that can later be used to synthesize block copolymers, either *via Click*-chemistry methods^{2,3} or chain extension *via* reinitiation.^{4,5} Either way, successful introduction of distinct functional groups in alpha or omega position of the PPV chain are a prerequisite. The alpha position can be modified *via* dedicated initiators while the other chain end might be controllable *via* end-cappers that are added to the polymerization as a quencher. In Chapter 4, however, it was shown that the latter approach is not efficient enough to yield polymers with an endgroup purity close to what would be required (> 90%).

Before, deviation from ideal anionic polymerization behavior was observed and doubts remained about the initiation efficiency of the employed initiator. To gain better understanding of the initiation process, ESI-MS (electrospray ionization mass spectrometry)^{6,7} was employed to fully characterize the polymerization products obtained with various initiators. With this soft ionization mass spectrometry technique it is possible to perform a detailed study on the

endgroups of the polymer chains and thus to elucidate the initiation pathways. As mentioned above, it is imperative to elucidate the initiation pathways of the polymerization reaction not only to understand the mechanism fully, but also to learn how the obtained PPVs can be utilized for block copolymer synthesis or self-assembly.

The polymer under investigation in this study is poly[2,5-bis(2-ethylhexyloxy)*p*-phenylene vinylene] (BEH-PPV **P1** & **P2**, Scheme 6.1)⁸ which is a symmetrically substituted derivative that leads to a soluble polymer both at the precursor as the eliminated stage. For the sake of the ESI-MS study, the introduced functionalities from the anionic initiators are a *tert*-butyl function (**P1**) and a bromine group (**P2**), since these two groups can be well distinguished *via* MS methods.



Scheme 6.1: BEH-PPV with different anionic initiators

As will be demonstrated, efficient initiation can be confirmed with quantitative introduction of the initiator in the polymer chain. By employment of an initiator carrying a suitable group for reinitiation under the conditions of a copper mediated polymerization like ATRP (atom transfer radical polymerization) or SET-LRP (single electron transfer living radical polymerization), block copolymers become accessible. SET-LRP is a robust and versatile method that can proceed at room temperature and below to polymerize a large variety of monomers.^{9,10} Mild reaction temperatures are interesting for precursor PPV

materials because if long reaction times are required, elimination will already prematurely start, which might interfere with the reaction. In the second part of this paper, we thus report on the synthesis of block copolymers synthesized *via* the above described procedure in which *tert*-butyl acrylate (*t*-BuA) was used as the second monomer. After hydrolysis of the acrylate block, a PPV-*b*-PAA (poly(acrylic acid)) block copolymer could be formed and self-assembly of the polymers in micelles was studied with the use of DLS (dynamic light scattering) measurements.

6.2. EXPERIMENTAL SECTION

6.2.1. Synthesis of anionic initiators for ESI-MS study

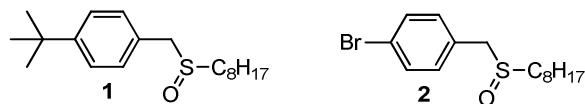
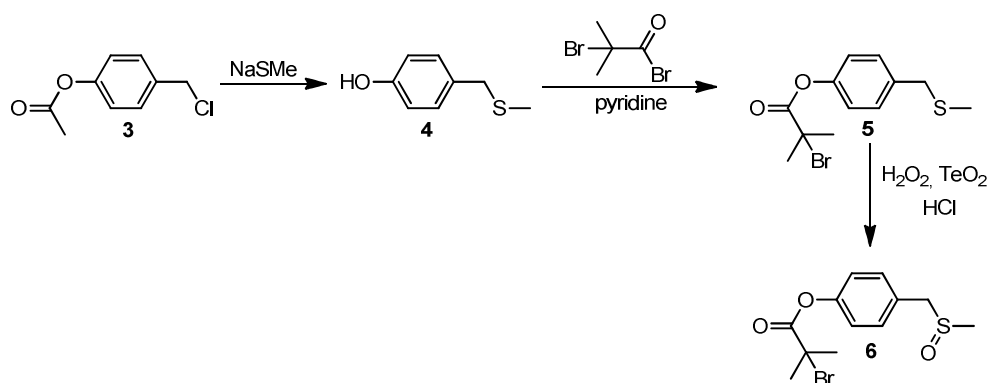


Figure 6.1: Anionic initiators with *tert*-butyl (**1**) and bromine (**2**) functionality

Anionic initiators **1** (*tert*-butyl functionality) and **2** (bromine functionality) were synthesized as described in Chapters 3 and 4 respectively.

6.2.2. Synthesis of anionic initiator **6** (4-[(methylsulfinyl)methyl]phenyl-2-bromo-2-methylpropanoate)

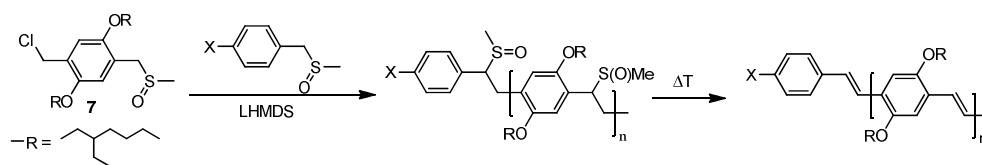


Scheme 6.2: Synthesis of functionalized initiator **6**

A literature procedure¹¹ was followed to synthesize product **4** and optimized using NaSMe (21% in H₂O) during the reaction and workup by stirring for 1 h in a KOH-solution (in H₂O; 10 equivalents) before extraction. In the second step, a solution of **4** (0.16 g, 1.1 mmol) and pyridine (0.17 mL, 2.1 mmol) in CH₂Cl₂ (20 mL) was cooled to 0 °C. To this mixture 2-bromo-2-methylpropanoyl bromide

(0.31 g, 1.4 mmol) in CH_2Cl_2 (5 mL) was slowly added and the resulting solution was stirred overnight at room temperature. After addition of water, extraction with CH_2Cl_2 and drying over MgSO_4 , the solvent was evaporated and the resulting yellow oil was used without further purification. In a last step, **5** was oxidized as described before.⁸ The crude product was purified by recrystallization from a hexane/ethyl acetate (3/1) mixture and initiator **6** was isolated as white crystals. Yield: 50% (0.16 g). Mp: 79 °C; ^1H NMR (300 MHz, CDCl_3 , δ): 7.33 (d, $J = 8.7$ Hz, 2H; ArH), 7.15 (d, $J = 8.7$ Hz, 2H; ArH), 3.97 (q, $J = 13.1$ Hz, 2H; ArCH₂S), 2.46 (s, 3H; SCH₃), 2.05 (s, 6H; CH₃); ^{13}C NMR (75 MHz, CDCl_3 , δ): 162.7 (C4), 143.5 (C4), 123.8 (CH), 120.2 (C4), 114.3 (CH), 51.9 (CH₂), 47.8 (C4), 29.8 (CH₃), 23.2 (CH₃); FT-IR (NaCl, cm^{-1}): 3005, 2977, 2925, 1751, 1504, 1464, 1267, 1210, 1035, 1017; DIP MS (CI, m/z): 319/321 [MH^+], 255/257 [M^+ -SOMe].

6.2.3. PPV polymerization



Scheme 6.3: General anionic polymerization pathway

All polymerization and elimination reactions were carried out as described earlier starting from monomer **7**.⁸ The synthesis of the precursor polymers was quenched after 5 minutes by addition of 0.2 mL concentrated HCl solution (37%). To obtain low molecular weight materials (**P1** and **P2**) for ESI-MS measurements, 0.5 equivalents of initiator **1** were used. For the synthesis of **P3'**, 0.2 eq of initiator **6** were used during prepolymer synthesis.

6.2.4. Synthesis of PPV-*b*-P(*t*-BuA) block copolymer P4 via SET-LRP

For the block copolymerization with *tert*-butyl acrylate the non-purified precursor polymer **P3'** was used. A Schlenk tube was filled with Cu(0) (45 μ mol; 2.8 mg), *tert*-butyl acrylate (50, 100 or 200 equivalents towards **P3'**), Me₆tren (tris[2-(dimethylamino) ethyl]amine, 45 μ mol; 12 μ L) and **P3'** ($M_n^{app} = 2200$ Da, 0.1 g, 45 μ mol) dissolved in DMF (1 mL). The Schlenk tube was subjected to three freeze-pump-thaw cycles and transferred into the glovebox. The reaction mixture was stirred for 1 hour at room temperature and after reaction it was poured in an aluminium tray to evaporate the solvent. Polymer **P4'** was filtered over a small alumina column to remove all copper and the solvent was evaporated. To obtain the conjugated block copolymer **P4**, precursor polymer **P4'** was eliminated as described before.⁸ **P4** was isolated as a red solid after precipitation in a MeOH/H₂O (4/1) mixture and filtration.

6.2.5. Synthesis of PPV-*b*-PAA block copolymer P5

For the hydrolysis of the *tert*-butyl group of the acrylate polymer, **P4** (synthesized with 200 eq of *t*-BuA; 0.1 g) was dissolved in dry CH₂Cl₂ (10 mL) and trifluoroacetic acid (TFA, 16 equivalents relative towards acrylate, calculated from GPC result, 0.75 mL) was added. The reaction mixture was stirred overnight at room temperature. After precipitation in water and filtration (washing with water and THF to remove all homopolymers), **P5** was isolated as a red solid. For dispersion and DLS measurements, 5 mL MeOH was added to 7.5 mg **P5**. 1 mL of this solution was further diluted with MeOH (5mL) and filtered (0.45 μ m). To this solution a few drops of a 1M NaOH solution (in H₂O) were added (pH \sim 6).

6.3. RESULTS AND DISCUSSION

6.3.1. ESI-MS assessment of initiation efficiency

From polymerization reactions at $-78\text{ }^{\circ}\text{C}$ that were quenched immediately after base addition it became clear that the anionic polymerization reaction proceeds upon mixing of the different components.¹² Since monitoring of the polymerization progress failed, two different polymers were synthesized with low molecular weights so they could be studied by means of ESI-MS and hence allow for a post-mortem analysis of the initiator, a strategy that was before also used to assess the initiator efficiency of radical initiators¹³ and as well very often used to assess the livingness of polymers.¹⁴ With this sensitive technique, it is possible to distinguish between polymer endgroup distributions directly, which is mostly impossible with conventional techniques. To reach molecular weights that fall into the analysis window of below 2000 Da, 0.5 equivalents of initiator had to be used for the polymerization reaction. M_n^{app} and PDI for the analyzed polymers are given in Table 6.1. The first polymer (**P1**) contains a *tert*-butyl functionalized initiator (**1**), the second polymer (**P2**) a bromine-functionality (**2**) (Figure 6.2).

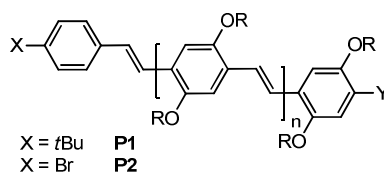


Figure 6.2: Conjugated polymers for ESI-MS study

Because the reaction is quenched with a concentrated HCl solution (37%), it is to be expected that the endgroup of the polymer chains (Y) is that of a sulfinyl group (the propagating center is a carbanion with a sulfinyl group substituent). The obtained results regarding molecular weights and dispersities of (unpurified)

precursor polymers **P1'** and **P2'** and (precipitated) conjugated polymers **P1** and **P2** (relative towards polystyrene standards) are summarized in Table 6.1. The differences in molecular weight are reflections of the substantial change in hydrodynamic volume of the chains after formation of the conjugated system. It should be noted that the values in Table 6.1 are based on conventional calibration of the SEC. Previous MALLS (multi angle laser light scattering) studies have shown that number average molecular weights are in good agreement with conventional calibration, but polydispersity is overestimated and that the true distributions are considerably more narrow.^{1,15}

Table 6.1: Results for measurements on conventional GPC regarding molecular weight and *PDI* for the anionic polymerization of premonomer **7** (structure see Scheme 6.4)⁸ with 0.5 eq of initiator **1** (**P1'** and **P1**) and **2** (**P2'** and **P2**)

Init	Precursor polymer		Conjugated polymer	
	$M_n^{app} / \text{g}\cdot\text{mol}^{-1}$	<i>PDI</i>	$M_n^{app} / \text{g}\cdot\text{mol}^{-1}$	<i>PDI</i>
t-Bu	1200	1.4	2800	1.2
Br	1400	1.4	2900	1.2

For all polymers, ESI-MS spectra were recorded and analyzed. The first spectra investigated were these for the polymers synthesized with *tert*-butyl functional initiator **1**. It can be observed that the spectrum for the (unpurified) precursor polymer **P1'** (see Figure 6.3 and Table 6.2) contains more peaks than the one for the eliminated polymer **P1** (see Figure 6.4). This difference can be attributed to the presence of several sulfinyl groups in the polymer chains which can eliminate in minor amount either already during the synthesis of the precursor polymer (base induced elimination because of slight excess of base used during synthesis of precursor polymer)¹⁶ as well as during the ESI-MS recording itself (tip temperature of 275 °C).

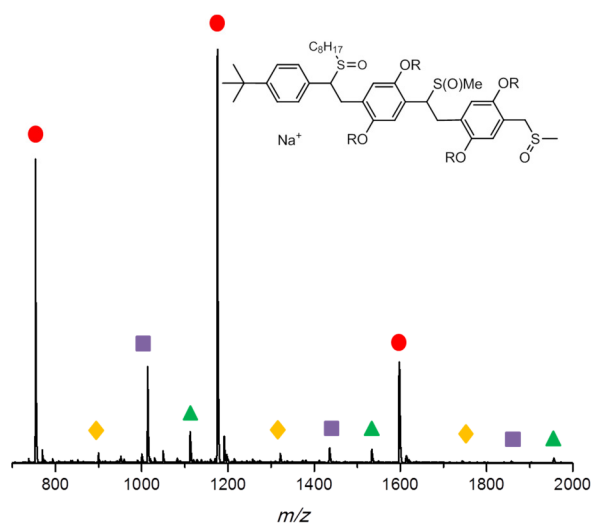
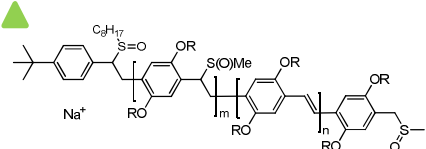
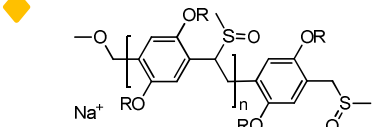


Figure 6.3: ESI-MS spectrum of precursor polymer **P1'** with *tert*-butyl functionalized initiator **1** and structure of most abundant species

Table 6.2: Comparison between measured and calculated values for different polymer structures found in ESI-MS spectrum of **P1'**

Structure	n	Peak in spectrum	Peak calculated
	0	753.67	753.49
	1	1175.67	1175.78
	2	1598.17	1598.06
Structure	n	Peak in spectrum	Peak calculated
	1	1013.67	1013.67
	2	1436.33	1435.96
	3	1858.17	1858.24

Structure	m	n	Peak in spectrum	Peak calculated
	0	1	1112.50	1111.78
	1	1	1534.33	1534.06
	2	1	1956.25	1956.35

Structure	n	Peak in spectrum	Peak calculated
	1	899.58	899.59
	2	1321.33	1321.87
	3	1744.00	1744.16

For **P1'** mass differences regarding the non-eliminated monomer unit (422.29 Da) are observed, thus the spacing expected for identical species that differ only in chain length. The ESI-MS spectrum of **P1'** as given in Figure 6.3 exhibits four main series of peaks which correspond to different polymer structures with a sodium counter ion. Three of them correspond to the main polymer structure with *tert*-butyl initiator **1** in α -position of the polymer chain and a sulfanyl endgroup (see insert of the structure in Figure 6.3 and Table 6.2). The signals denoted by the red circle ($m/z = 753.67, 1175.67$ and 1598.17 Da) correspond to the main structure in which none of the sulfanyl groups were eliminated. The purple squares correspond to polymer chains where the sulfanyl group of the initiator moiety is already eliminated and all monomer units still contain their sulfanyl groups (note that a differentiation can be readily made since initiator and monomer carry different sulfanyl groups). The third series of peaks, indicated with green triangles, corresponds to polymer chains in which one of the monomer units underwent elimination and the sulfanyl group of the initiator and other monomer units are still present. The assignment of the peak according

to the last polymer structure (indicated with an orange diamond), which is only present in minor amounts, is less clear. Different polymer structures were taken into account and the signals could formally be assigned to a polymer structure with a sulfinyl endgroup and a methoxy function in alpha position of the chain. However, mechanistically there is no motivation how this structure would be obtained. Nevertheless, this fourth series is not very abundant and hence the majority of material in the spectrum of **P1'** can be regarded to be well assigned to the expected (initiated) polymer structure.

The picture for the eliminated polymer **P1** is, however, on first glance more confusing. Based on Figure 6.3 one would expect only one series of peaks if all sulfinyl groups were eliminated. Clearly, two series of peaks are observed in Figure 6.4 and Table 6.3. Also in this spectrum, series of peaks are distinguished based on the mass differences of the conjugated monomer unit (358.29 Da). The first series of peaks (red circle) correspond to the expected polymer chains with a *tert*-butyl initiator and a sulfinyl endgroup and thus the expected successful product of elimination. For the second series of peaks (blue star) the structure remains unclear. All earlier described endgroups occurring in PPV polymers (aldehyde, methyl, chloromethyl, hydrogen, methoxy, carboxylic acid)¹⁷ were taken into account, but none of these endgroups correspond in mass to the polymer peaks seen in the spectra. Also the conjugated polymer with methoxy initiator and sulfinyl endgroup was taken into account, but also this structure did not correspond to the measured values. Therefore – even though the spectrum in Figure 6.3 indicated almost quantitative incorporation of initiator into the chains – it is from the spectrum in Figure 6.4 not possible to conclude with absolute certainty that the initiator efficiency is indeed high.

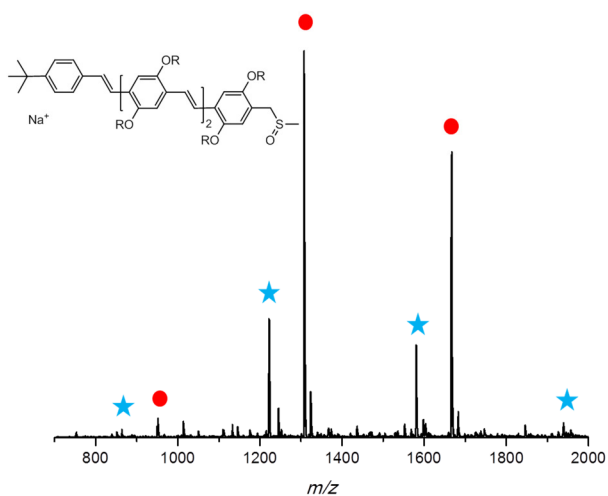
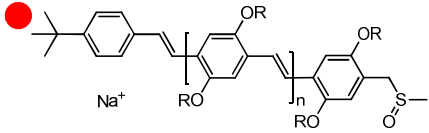
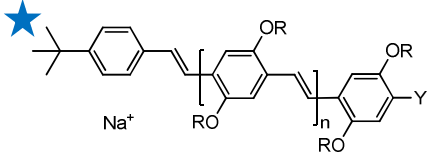


Figure 6.4: ESI-MS spectrum of conjugated polymer **P1** with *tert*-butyl functionalized initiator

Table 6.3: Comparison between measured and calculated values for different polymer structures found in ESI-MS spectrum of **P1**

Structure	n	Peak in spectrum	Peak calculated
	1	949.73	949.67
	2	1307.73	1307.96
	3	1666.67	1666.25
Structure	n	Peak in spectrum	Peak calculated
		863.80	
		1221.87	
		1580.93	
		1938.93	

Because no corresponding peaks could be found in the spectrum of the precursor polymer **P1'**, it is to be expected that these polymer structures must be formed during the elimination of the polymer (although no reaction could be assigned to occur that could explain the observed mass difference between both series of peaks) or fragmentation must be occurring during the ESI-MS measurements. To gain better insights in the polymer structures and therewith the incorporation of the anionic initiator in the synthesized polymers, the ESI-MS spectrum of **P2'** with a bromine-substituted initiator (Figure 6.5 and Table 6.4) was studied regarding the different polymer structures. Bromine can in this case be used as a marker due to its specific isotopic pattern that allows for a clear distinction of peaks of species containing bromine from those that do not. In this way, a second sensor is built in the chains to check if the initiator is present in the product independent of a clear assignment of the total m/z .

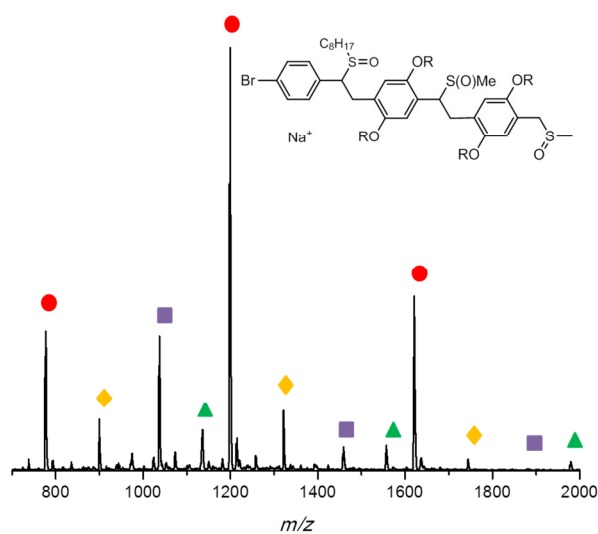


Figure 6.5: ESI-MS spectrum of precursor polymer **P2'** with bromine functionalized initiator **2** and structure of most abundant species

Table 6.4: Comparison between measured and calculated values for different polymer structures found in ESI-MS spectrum of **P2'**

Structure	n	Peak in spectrum	Peak calculated	
	0	777.50	777.34	
	1	1199.33	1199.63	
	2	1621.33	1621.91	
Structure	n	Peak in spectrum	Peak calculated	
	1	1037.50	1037.52	
	2	1459.17	1459.80	
	3	1881.92	1882.09	
Structure	m	n	Peak in spectrum	Peak calculated
	0	1	1135.33	1135.63
	1	1	1557.17	1557.91
	2	1	1980.08	1980.20
Structure	n	Peak in spectrum	Peak calculated	
	1	899.58	899.59	
	2	1321.33	1321.87	
	3	1744.00	1744.16	

Again, for the unpurified precursor polymer with bromine initiator **P2'** (Figure 6.5), the same four polymer structures could be found in the mass spectrum as in the spectrum of **P1'** (Figure 6.3). As expected, the typical isotope pattern for bromine atoms is observed for all polymer structures designated with the red

circle, purple square and green triangle which correspond all to a polymer structure with bromine functionalized initiator group and sulfinyl endgroup (red circle = non-eliminated precursor polymer, purple square = sulfinyl group at initiator eliminated and green triangle = one of the sulfinyl groups at a monomer unit being eliminated). A second confirmation of a good initiation efficiency is that the whole spectrum of **P2'** is simply shifted by the mass difference between the *tert*-butyl group and the halogen (21.85 Da) when compared to the spectrum of **P1'**. The only exception in the whole spectrum is the series of peaks represented by the orange diamond, (methoxy functionality in α -position of the chain and sulfinyl endgroup) for which exactly the same masses are found in both the spectra of **P1'** and **P2'**. Additionally no bromine-isotope pattern could be observed for this peak series (see Figure 6.6). It can safely be concluded that this species does not carry the initiator group and hence stems from an alternative initiation of chains (which is unknown for achieving a methoxy group). For **P2'** this peak series is somewhat more abundant than for **P1'**, but still this species must be clearly seen as a minor side product.

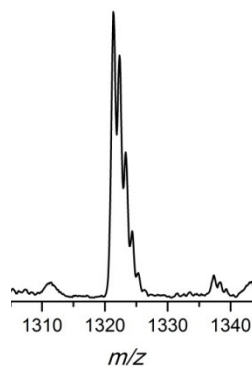


Figure 6.6: Zoom of mass peak at 1321.58 Da (indicated with orange diamond) in the spectrum of precursor polymer **P2'**

For the conjugated polymer with bromine functionality **P2** (see Figure 6.7 and Table 6.5), again the typical pattern for the natural abundant bromine isotopes could be studied in the mass spectrum. As expected, in all these peaks, the typical isotope pattern for bromine atoms is observed (see insert of zoom of one of the peaks in Figure 6.7), concluding that bromine, and thus the initiator, is built in in all polymer chains. Again a first series of peaks (red circle) is found corresponding to polymer chains containing the bromine functionalized initiator **2** and the expected sulfinyl endgroup. For the other series of peaks (blue star) the endgroup is still unknown, but it is clear from the isotopic pattern that also these chains contain the desired bromine initiator group. Thus, while the omega chain end remains unknown, the alpha position can be clearly assigned to the functional initiator used. The mass difference between the two series of peaks in **P2** is identical to the two series observed for **P1**, thus whatever causes the rise of this species must occur in identical ways for both polymer species and is independent of the initiator employed.

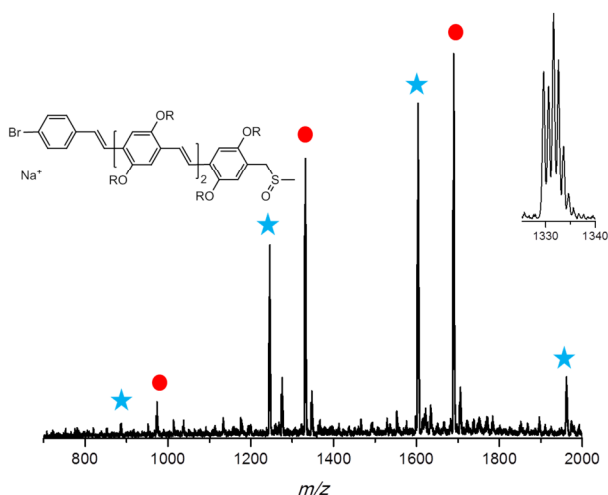
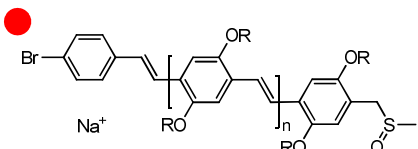
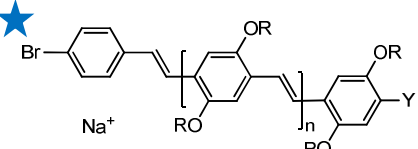


Figure 6.7: ESI-MS spectrum of conjugated polymer **P2** with bromine functionalized initiator and zoom of one of the peaks (others have the same pattern)

Table 6.5: Comparison between measured and calculated values for different polymer structures found in ESI-MS spectrum of **P2**. Again the values for the most intense peaks are reported

Structure	n	Peak in spectrum	Peak calculated
	1	973.53	973.52
	2	1331.60	1331.81
	3	1689.67	1690.09
Structure	n	Peak in spectrum	Peak calculated
		887.67	
		1245.73	
		1603.87	
		1961.93	

Interestingly, the series of peaks containing no initiator moiety (indicated with orange diamond in spectra of **P1'** and **P2'**) is not present in both the spectra of **P1** or **P2**, which means that this species is removed from the product mixture during the elimination procedure or by the selective precipitation following the elimination reaction. Potentially, chains without initiator moiety are only formed as low molecular weight compounds which stay in solution during precipitation. Even though this hypothesis is hard to prove, the conclusion can be drawn that the eliminated PPV product is more clean than the precursor material.

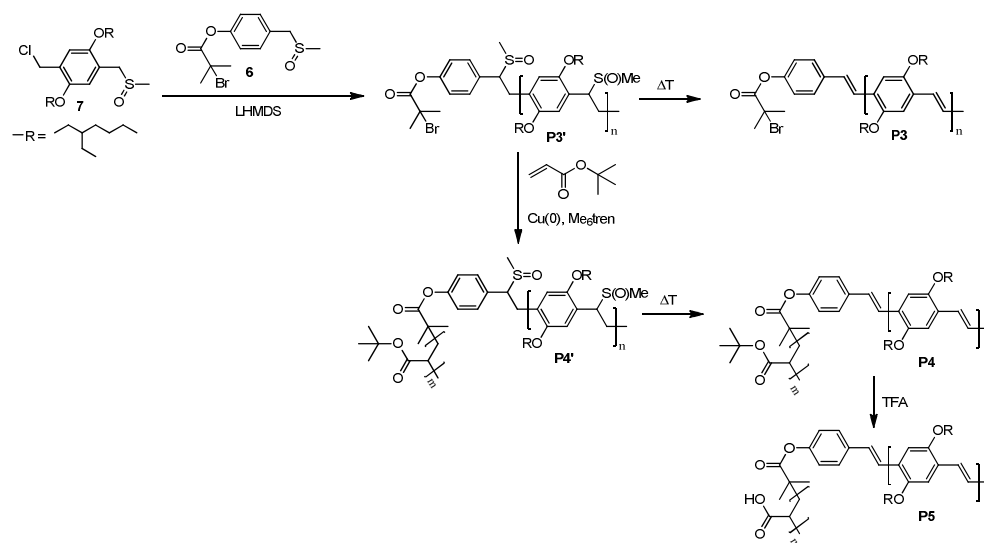
Regarding the unassigned peak series for the conjugated polymers marked with the blue stars an interesting observation can be made: Samples made under virtually identical reaction conditions and workup procedures exhibit different abundances of this peak series, whereby, however, the desired product with the known structure remains always the more abundant one. Tests regarding

ionizability were performed and no significant change in intensity ratios could be achieved *via* a change in the instrument setting of the spectrometer. Since no comparable peak exists in the precursor polymer materials and no reasonable structure corresponding to the m/z of these peaks could be drawn, the assumption may be made that this peak corresponds to an adduct rather than a purely covalently bonded polymer structure, which would also explain the changing abundances of these peaks. PPV is known to readily form aggregates, making appearance of such adducts in the spectrum less surprising. MS² experiments on the other hand required relatively large collision energies, which is again more in-line with a covalently bonded species. Regardless, it is important to note that in terms of endgroup functionality presence of this species is completely inconsequential since it is unambiguously demonstrated by the shift of the spectra when going from **P1** to **P2** as well as by the isotopic pattern that all material analyzed contains the initiator moiety and that thus a practically complete functionalization of chains can be safely assumed.

Because ESI-MS measurements are not possible for polymer samples with higher molecular weights (thus synthesized with lower initiator content) and because of the linear behavior that was shown for the molecular weight relative towards the amount of initiator used during polymerization (Chapter 3),⁸ it can be assumed that this very high initiation efficiency can be extended to all samples synthesized *via* the anionic sulfinyl precursor route.

6.3.2. Use of functionalized anionic initiators to synthesize block copolymers *via* the use of SET-LRP

First of all, functionalized initiator **6** (Scheme 6.2) was synthesized in an easy three-step synthesis route starting from 4-(chloromethyl)phenyl acetate. In a first step the thioether functionality was introduced using NaSMe (21% in H₂O) following a literature procedure.¹¹ In a second step, 2-bromo-2-methylpropionyl bromide was built in as the wanted functionality on the initiator moiety and in a last step, the thioether polarizer group was oxidized and pure initiator **6** was isolated as white crystals. For the synthesis of the PPV block with initiator **6** (0.2 eq), an earlier described procedure was followed (B → M + I; 0 °C, 5 min, [M]_i = 50 mmol·L⁻¹)⁸ (see Scheme 6.4). Molecular weights and polydispersity values (*PDI*s) for the (unpurified) precursor **P3'** and eliminated PPV polymer block **P3** are given in Table 6.6. Note that dispersities are overestimated due to conventional calibration.¹⁵

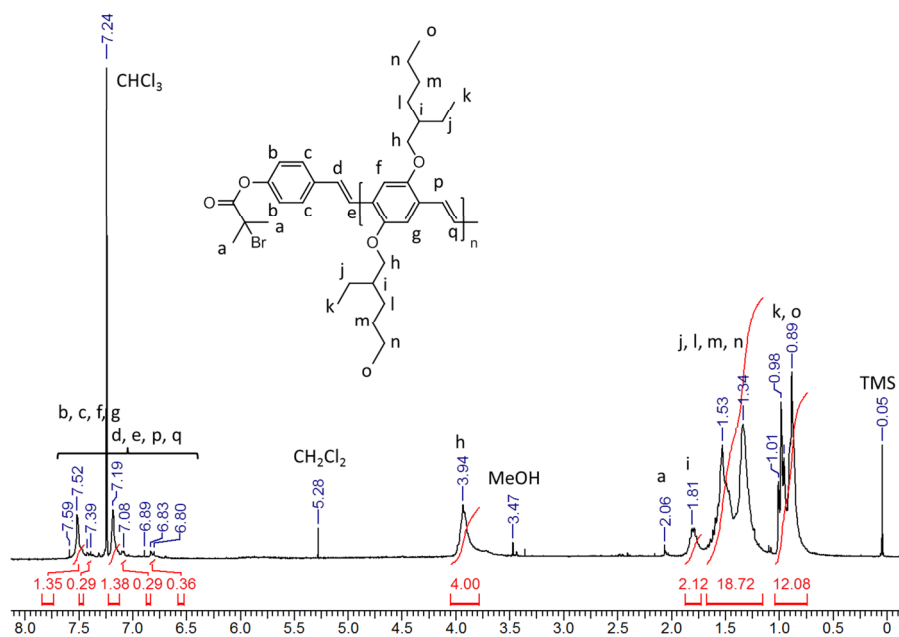


Scheme 6.4: Synthesis of BEH-PPV-*b*-P(*t*-BuA) block copolymer **P4** and hydrolyzed block copolymer PPV-*b*-PAA **P5**

Table 6.6: Molecular weights and *PDI*s for precursor and eliminated PPV polymers **P3'** and **P3**

	$M_n^{\text{app}} / \text{g}\cdot\text{mol}^{-1}$	<i>PDI</i>
P3'	2200	1.9
P3	5300	1.5

The obtained molecular weights for **P3'** and **P3** are within the expected range for the given initiator concentration, indicating success of the anionic polymerization. Based on the ESI study described above, complete incorporation of the initiator into the prepolymer chains was assumed which was also confirmed by means of ^1H NMR for the final conjugated polymer **P3** (Figure 6.8).

Figure 6.8: ^1H NMR spectrum (CDCl_3) of BEH-PPV **P3**

Since **6** is both an initiator for the PPV polymerization as well as for SET-LRP (or ATRP for that instance), **P3'** was subjected to a SET-LRP reaction (see Scheme 6.4) to obtain block copolymers. A mixture of Cu(0), **P3'**, Me₆tren and *t*-BuA in DMF was allowed to polymerize under inert conditions. For completion of the polymerization, the reactions were stirred for 1 hour at room temperature. Different amounts of the acrylate (50, 100 and 200 equivalents relative to the precursor polymer) were added in the experiments. Results regarding molecular weight and *PDI* for the PPV-*b*-P(*t*-BuA) block copolymers **P4'** (precursor) and **P4** (conjugated, after thermal elimination and precipitation) are collated in Table 6.7 and GPC profiles are shown in Figure 6.9.

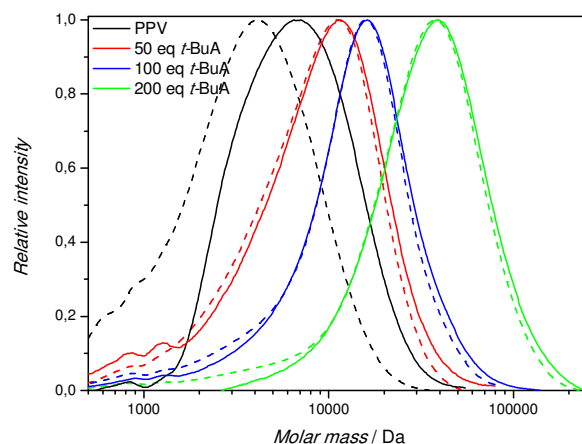


Figure 6.9: GPC profiles (RI detection, THF) for **P3'** (dashed black line) and **P3** (solid black line) compared to **P4'** (dashed colored lines) and **P4** (solid colored lines) synthesized with different equivalents of *t*-BuA

Table 6.7: Molecular weights and polydispersities for SET-LRP reactions (**P4'** (unpurified) and **P4**) for different equivalents of *t*-BuA added

Eq <i>t</i> -BuA	Precursor polymer P4'		Conjugated polymer P4	
	$M_n^{\text{app}} / \text{g}\cdot\text{mol}^{-1}$	<i>PDI</i>	$M_n^{\text{app}} / \text{g}\cdot\text{mol}^{-1}$	<i>PDI</i>
50	4900	2.1	6800	2.1
100	7600	2.1	8900	1.9
200	14900	2.7	24900	1.8

To look more closely into the characterization of the block copolymers, UV-Vis spectrometry measurements were performed (Figure 6.10). Here it could be seen that only a very slight blue shift for λ_{max} was found for the different block copolymers (493, 493 and 490 nm respectively for 50, 100 and 200 eq *t*-BuA added) compared to the pure PPV (494 nm).

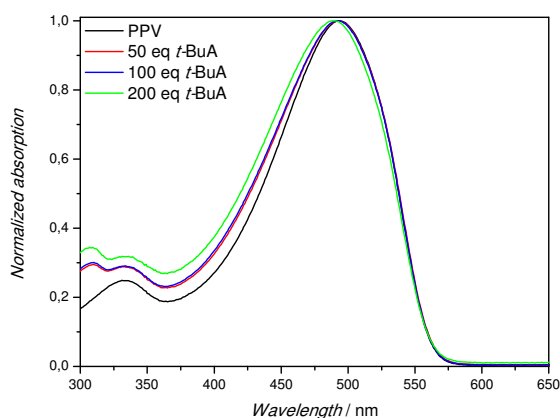


Figure 6.10: UV-Vis spectra (right) for conjugated polymers **P3** (black line) compared to **P4** (colored lines) synthesized with different equivalents of *t*-BuA

As derived from Table 6.7, a clear correlation between monomer concentration and molecular weight achieved is observed both for the precursor polymer as well as for the eliminated PPV block copolymers. Increasing the amount of *t*-BuA leads to longer acrylate blocks and thereby larger overall molecular weights.

Polydispersities appear to be somewhat high, but taking into account that polymerizations were carried out to full conversions appear acceptable. Figure 6.9 depicts the precursor polymers in dashed lines and the eliminated polymers as solid lines. As can be seen only the polymer before block extension appears to shift in the elugrams after elimination (which is commonly observed for PPVs due to rather strong changes in the hydrodynamic volume upon conjugation of the chains¹⁸). All PPV-*b*-P(*t*-BuA) block copolymers do not significantly shift after elimination, allowing for the conclusion that the acrylate blocks seemingly dominates the hydrodynamic volume of the total chains. It should also be noted that the M_n^{app} values given are based on conventional calibration and block compositions might be inadequately represented. Lower molecular weight material is nevertheless removed after elimination due to selective precipitation, explaining the change in overall M_n^{app} observed.

Calculation of block composition based on NMR analysis was performed to check similarity with the obtained GPC results. The ¹H NMR spectrum for the PPV-*b*-P(*t*-BuA) block copolymer **P4** synthesized with 50 eq of *t*-BuA can be found in Figure 6.11. To check for block lengths of the different polymer blocks in **P4**, integration of the peaks for signals k and o (CH₃ groups in the side chain of the PPV block) and for r and s (main chain of the acrylate block) was compared. Per PPV unit, approximately three acrylate units were identified in this manner. From the M_n^{app} of the pure BEH-PPV (5300 g·mol⁻¹, value measured using conventional GPC after elimination of the precursor), it was calculated that 15 PPV units (MWD 1 unit ~ 357 g·mol⁻¹) were supposedly present. This would result in presence of 45 acrylate units (MWD 1 unit ~ 128 g·mol⁻¹) which translates in a molecular weight of approximately 5700 g·mol⁻¹ for the acrylate block. In total this gives an average M_n of 11000 g·mol⁻¹ which deviates from the

measured $6800 \text{ g}\cdot\text{mol}^{-1}$ using GPC (towards PS standards). This difference can be addressed to the difference in hydrodynamic volume, which is very different for the stiff PPV block and the coiled acrylate block.

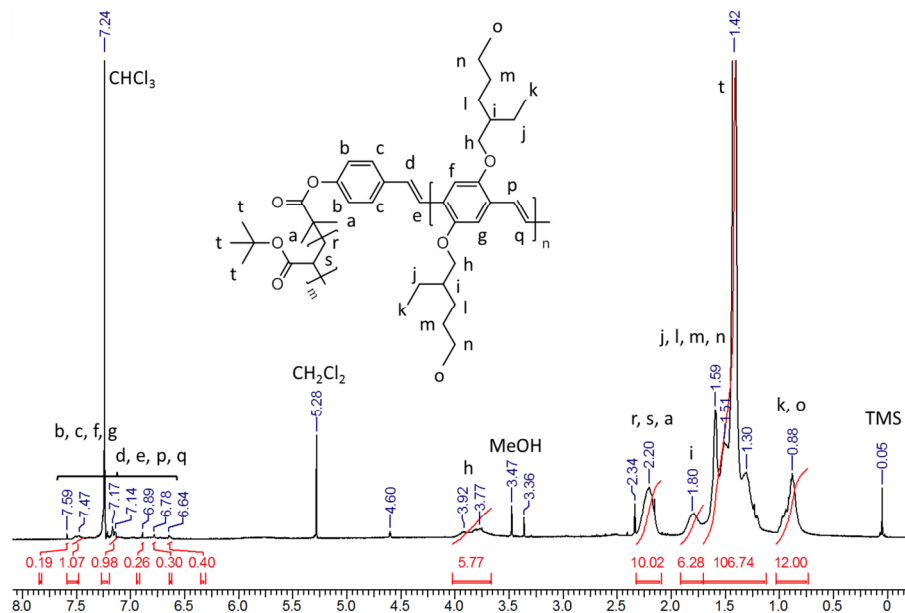


Figure 6.11: ^1H NMR spectrum (CDCl_3) of BEH-PPV-*b*-P(*t*-BuA)
P4 (50 eq of *t*-BuA)

From the GPC profiles and NMR analysis, it can hence be concluded that block copolymers with sufficient efficiency are formed. To prove that a block copolymer was indeed synthesized, GPC profiles were measured with detection at λ_{max} of the polymers (493 nm, only PPV absorption; Figure 6.12). If a monomodal peak is found, with comparable molecular weight as for RI detection, it can be concluded that the acrylate is attached to the PPV block and indeed a block copolymer is formed.

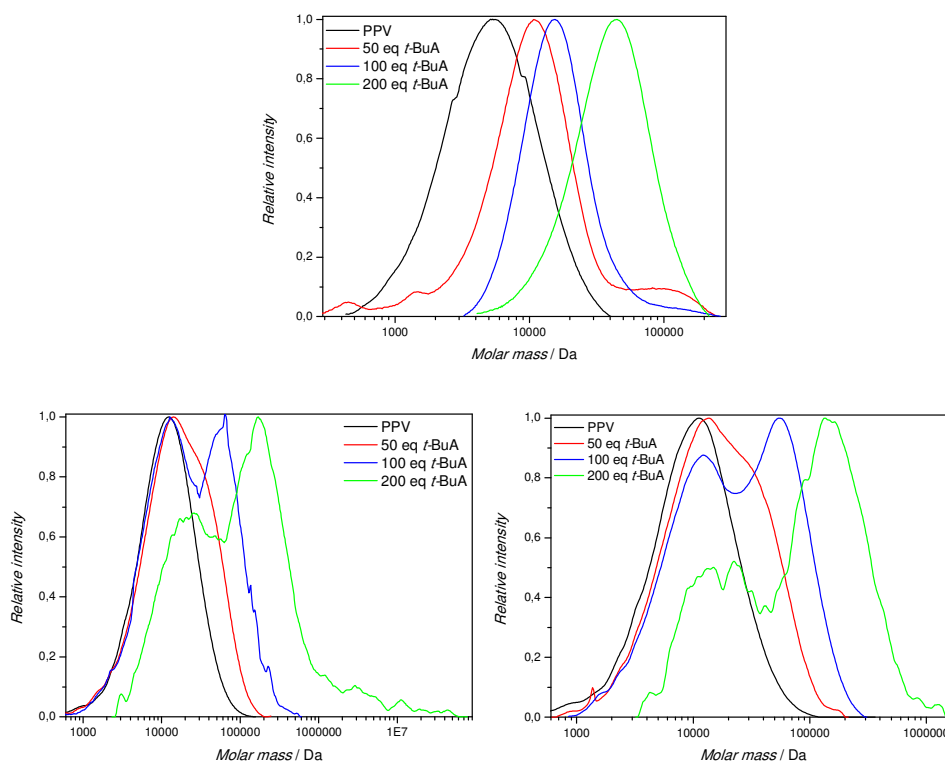


Figure 6.12: GPC profiles for **P3** and **P4** measured on chlorobenzene GPC with RI (top) and UV (bottom left: 493 nm and bottom right: 465 nm) detection

However, the expected result is not found for the block copolymers (samples measured with CB as the solvent). For RI detection, a monomodal GPC profile is measured and a nice shift in molecular weight is seen with the addition of a higher amount of acrylate to the polymerization reaction (Figure 6.12, top). If UV detection is used at the maximal wavelength (493 nm) of the polymers (Figure 6.12, left) and also at the maximal wavelength that was found for a very pure PPV-*b*-P(*t*-BuA) block copolymer,^{1,19} 465 nm (Figure 6.12, right), a bimodal profile is observed for the block copolymers. The more acrylate added to the system, the more pronounced the bimodality. It is clear that the low molecular weight peak originates from a pure PPV block (black line), indicating that no

complete reinitiation for the SET-LRP occurs. Because only the PPV block absorbs the light at this wavelength, an overestimation is, however, made for the presence of the PPV homopolymer. Quantification of the presence of PPV homopolymer is difficult, because of the difference in signal measured at both wavelengths. When compared to the RI measurements, a nice shift of the monomodal peak is found, indicating a very small PPV homopolymer weight fraction.

With changing the parameters of the reaction (initiator, ligand, monomer concentrations) it may be possible to overcome this observed bimodality. Also – as we demonstrated in our previous study on block copolymers from consecutive anionic polymerization – recycling preparative GPC can be used to remove the PPV homopolymer. It should be noted though that a further refinement of conditions was so far not required, since the block copolymers show distinct behaviour after hydrolysis of chains and form pH-responsive micelles (see below), which underpins the good structural integrity of the materials.

Another way to elucidate the quality of the synthesized block copolymers is to test for self-assembly behavior. To perform such study, the *tert*-butyl acrylate block was subsequently hydrolyzed using TFA to yield poly(acrylic acid) blocks. In this way, an amphiphilic block copolymer is created that should display strong self-assembly behavior in solution. For the hydrolysis of **P4** ($M_n^{\text{app}} = 24900$; 200 eq of *t*-BuA) (see Scheme 6.4), one must first of all note that the spacer (the functionality on anionic initiator **6**) between the two polymer blocks also consists of an ester functionality. It is thus possible that, by treating block polymer **P4** with TFA, the two polymer blocks are separated from each other. Thus, the obtained polymer **P5** was washed with H₂O and THF to remove the homopolymer contents. Block copolymer **P5** was analyzed by ATR (attenuated

total reflectance) FT-IR spectroscopy (GPC measurement was not possible because of solubility issues). Comparison of the infrared spectra is made for the pure BEH-PPV (**P3**) and block copolymers **P4** and **P5** (Figure 6.13). It is clear that for **P4** the C=O ester peak (1722 cm^{-1}) of the acrylate is present and compared to **P5**, this peak is shifted to lower wavenumber (C=O acid, 1696 cm^{-1}). Additionally, a broad peak appears between 3400 and 2400 cm^{-1} , resulting from $-\text{COOH}$ complexation.

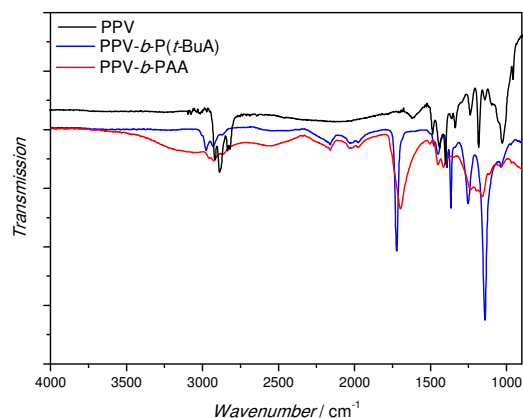


Figure 6.13: ATR FT-IR spectra for BEH-PPV **P3**, BEH-PPV-*b*-P(*t*-BuA) **P4** and BEH-PPV-*b*-PAA **P5**

For self-assembly, polymer **P5** was dispersed in MeOH to which a few drops of a NaOH solution (1 M in H_2O) were added. In such solution ($\text{pH} \sim 6$), rather small micelles with reasonable dispersity were measured as confirmed by DLS measurements (see Table 6.8).

Table 6.8: Mean hydrodynamic diameter and polydispersity of measured nanoparticles by DLS for dispersions of **P5**

pH	Added solution^a	Mean diameter / nm	PDI
6	Few drops NaOH	81	0.149
14	NaOH	1003	0.096
6	HCl	775	0.048
6	NaCl ^b	1343	0.155

^a NaOH: 1 M solution in H₂O; HCl: 2 M solution in H₂O

^b NaCl: saturated solution in H₂O; added to starting solution

Upon addition of NaOH (1 M in H₂O), increasing pH to 14, the diameter of the micelles increased from 81 to roughly 1000 nm. Thus addition of base results in a swelling of the micelles, which is easily explained by the stronger repulsion between single acrylic acid segments after deprotonation. Decreasing pH again to 6 (using 2 M HCl solution in H₂O), results in particles with a somewhat smaller diameter than at pH 14 but the original state of the micelles could not be reached again. The formed NaCl results in an increase of ionic strength in the solution and thus again to a swelling of the micelles compared to the particles measured in the starting solution. This is confirmed by addition of a saturated NaCl solution to the starting solution (pH ~ 6), resulting in mean diameters of 1343 nm, exemplifying that ionic strength alone can account for significant expansion of the micellar structures. Regardless, the above data nicely demonstrate the ability of the synthesized block copolymers to self-assemble thereby confirming the high definition of the block structures. It is noteworthy to add that the performed measurements of the micellar solutions were only performed to prove the above point. Shapes of the micelles were not elucidated and of course also the partial change from methanolic to aqueous solution will account for shifts in the diameter size.

6.4. CONCLUSION

The initiation of the anionic polymerization pathway *via* the sulfinyl precursor route to obtain PPV materials is very efficient as confirmed by means of an ESI-MS study on different polymer samples with *tert*-butyl and bromine functional groups built in on the initiating moiety. For both precursor and eliminated polymers almost quantitative presence of the initiator group in the chains is confirmed, even though some uncertainty remains regarding the ω -endgroup of the polymer chain in the eliminated PPV. Since the ambiguity of the second endgroup only exists for the eliminated polymers, it is well possible that the unknown series of peaks resemble aggregates, but further studies into the origin of this peak may be required to fully understand the elimination process. The proof of high initiation efficiency is by itself a very important observation.

While this is an important conclusion from a mechanistic viewpoint alone (initiation efficiency was unresolved before and significant side reactions could not be ruled out), this has very large consequences with respect to polymer synthesis. With this high initiator fidelity, a synthetic handle is created that gives access to complex polymer structures when more specific functionalities are incorporated into the chains *via* functionalized anionic initiators, beyond the block copolymerizations that have been demonstrated herein.

Successful synthesis of a PPV-*b*-P(*t*-BuA) block copolymer of sufficient purity is achieved *via* introduction of a initiator for SET-LRP reaction *via* the anionic initiator moiety of the PPV polymerization. Block copolymers of various block length composition can be obtained, from which amphiphilic polymers can be reached *via* hydrolysis of the acrylate ester. pH-responsive block copolymers are obtained that change in mean diameter of the micelles formed upon addition of

a base or salt, thereby nicely demonstrating the self-assembly behavior of the target structures and the high definition of block copolymers that are obtained.

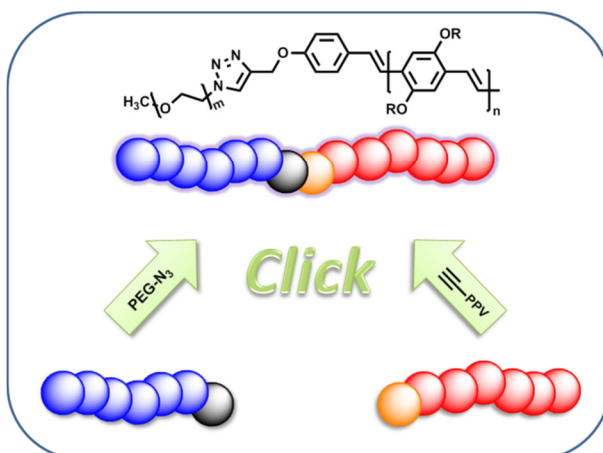
6.5. REFERENCES

- ¹ I. Cosemans, J. Vandenberg, V. S. D. Voet, K. Loos, L. Lutsen, D. Vanderzande, T. Junkers, *Polymer* **2013**, *54*, 1298–1304.
- ² C. Barner-Kowollik, F. E. Du Prez, P. Espeel, C. J. Hawker, T. Junkers, H. Schlaad, W. Van Camp, *Angew. Chem. Int. Ed.* **2011**, *50*, 60–62.
- ³ H. C. Kolb, M. G. Finn, K. B. Sharpless, *Angew. Chem. Int. Ed.* **2001**, *40*, 2004–2021.
- ⁴ W. A. Braunecker, K. Matyjaszewski, *Prog. Polym. Sci.* **2007**, *32*, 93–146.
- ⁵ K. Okamoto, C. K. Luscombe, *Polym. Chem.* **2011**, *11*, 2424–2434.
- ⁶ S. J. Gaskell, *J. Mass Spectrom.* **1997**, *32*, 677–688.
- ⁷ S. D. Hanton, *Chem. Rev.* **2001**, *101*, 527–569.
- ⁸ I. Cosemans, J. Wouters, T. Cleij, L. Lutsen, W. Maes, T. Junkers, D. Vanderzande, *Macromol. Rapid Commun.* **2012**, *33*, 242–247.
- ⁹ V. Percec, T. Guliashvili, J. Ladislaw, A. Wistrand, A. Stjerndahl, M. Sienkowska, M. Montiero, S. Sahoo, *J. Am. Chem. Soc.* **2006**, *128*, 14156–14165.
- ¹⁰ B. Rosen, V. Percec, *Chem. Rev.* **2009**, *109*, 5069–6323.
- ¹¹ H. L. Holland, F. M. Brown, B. G. Larsen, *Tetrahedron: Asymmetry* **1995**, *6*, 1561–1567.
- ¹² For results regarding polymerizations performed at -78 °C, see Chapter 4.
- ¹³ D. Voll, T. Junkers, C. Barner-Kowollik, *J. Polym. Sci. Part A: Polym. Chem.* **2012**, *50*, 2739–2757.
- ¹⁴ C. Barner-Kowollik, T. P. Davis, M. H. Stenzel, *Polymer* **2004**, *45*, 7791–7805.
- ¹⁵ For some MALLS results, see Chapter 5.

- ¹⁶ A. J. J. M. van Breemen, A. D. J. Issaris, M. M. de Kok, M. J. A. N. Van Der Borght, P. J. Adriaensens, J. M. J. V. Gelan, D. J. M. Vanderzande, *Macromolecules* **1999**, *32*, 5728 – 5735.
- ¹⁷ T. Junkers, J. Vandenberg, P. Adriaensens, L. Lutsen, D. Vanderzande, *Polym. Chem.* **2012**, *3*, 275–285.
- ¹⁸ L. Hontis, *PhD thesis*, Limburgs Universitair Centrum, **2002**.
- ¹⁹ See Chapter 5.

CHAPTER 7

Synthesis of PPV-*b*-PEG Block Copolymers Using *Click* Chemistry



In this chapter, the synthesis of amphiphilic rod-coil semiconductive block copolymers with a poly(*p*-phenylene vinylene) (PPV) block as rod-block using a *Click* chemistry approach is investigated and a facile reaction pathway towards poly(*p*-phenylene vinylene)-*block*-poly(ethylene glycol) (PPV-*b*-PEG) block copolymers is presented. To reach this aim, an alkyne-functionalized PPV block (produced from anionic sulfinyl precursor route polymerization) was synthesized and subsequently coupled to azide-functionalized poly(ethylene glycol) of different lengths. Self-assembly of these materials in aqueous solution demonstrate the potential to form micelles with different morphologies and sizes for these PPV-*b*-PEG block copolymers.

To be submitted:

I. Cosemans, J. Vandenberg, L. Lutsen, D. Vanderzande, T. Junkers, **2013**.

7.1. INTRODUCTION

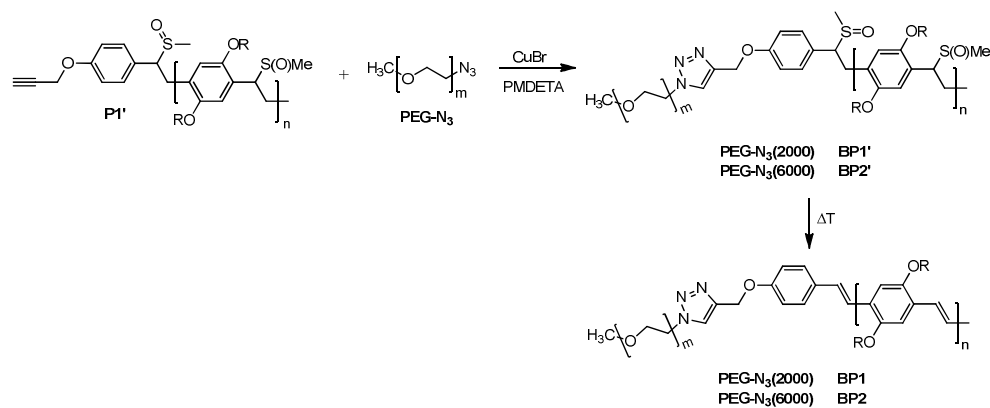
Block copolymers (or more complex structures) containing PPV segments are attractive materials. While the demand for classical (homopolymer) PPV materials is declining in the classical field of organic electronics – especially in photovoltaics – due to limitations in light harvesting capability, new applications can be targeted when polymerizations can be controlled. Block structures allow for self-assembly of materials and thus nanostructuring of the PPV segments, which might find new application in organic transistors or for example in the field of light emitting diodes. Also, biomedical applications can be envisaged where the superior fluorescence properties of PPV can be exploited for the introduction of specific biomarkers. Also in this case, highly functional materials with precisely defined microstructure are required.

For PPV materials, synthesis of rod-coil block copolymers were already reported, however, these were only produced starting from a PPV block synthesized *via* the Siegrist polycondensation method and hence low molecular weight material.^{1,2} In this approach an aldehyde endgroup functionality is available which can be coupled with a suitable linker in a post-polymerization functionalization process. Block copolymers synthesized *via* this method combined with *Click* chemistry were PPV-*b*-POM (polyoxomethalate)³ and PPV-*b*-PMMA (poly(methyl methacrylate)).⁴ Polycondensation reactions are often used to make PPVs, but suffer however from low efficacies and severe limitations in molecular weight. Sulfinyl precursor polymerizations as in our approach follow chain-growth mechanisms and allow for the facile design of higher molecular weight materials.⁵

For the synthesis of block copolymers containing one PPV block synthesized from the sulfinyl precursor route, two different strategies were already described in

this thesis. The PPV block used for these studies was the symmetrically 2-ethylhexyloxy substituted poly[2,5-bis(2-ethylhexyloxy)*p*-phenylene vinylene] (BEH-PPV). By chain extension in consecutive anionic polymerization, a *tert*-butyl acrylate (*t*-BuA) block could be attached to the PPV (as described in Chapter 5), but efficiency of the method was, however, limited, leaving significant amounts of homopolymer PPV in the product mixture behind. The block copolymer could only be isolated using preparative recycle GPC.^{6,7} More successful was the incorporation of a bromine-functionality on the anionic initiator end, which could in a second step be used to reinitiate the polymerization of a vinyl monomer in a single electron transfer – living radical polymerization (SET-LRP) reaction (described in Chapter 6).^{8,9} By using this technique, BEH-PPV-*b*-P(*t*-BuA) block copolymers with different *t*-BuA chain lengths could successfully be synthesized in a robust manner. After hydrolysis of the acrylate block, amphiphilic polymers were obtained that displayed micelle formation and which featured pH-responsive morphologies.^{10,11}

While the SET-LRP approach was very successful, it still limits the choice of the second block to vinyl monomers that undergo radical polymerization. Thus, the development of a modular approach that allows for *any* combination of building blocks is highly attractive. For that aim, the well-known copper assisted azide-alkyne cycloaddition (CuAAC) can be employed,¹²⁻¹⁴ in which a polymer block containing an alkyne functionality is coupled with a polymer block containing an azide functionality (Scheme 7.1).

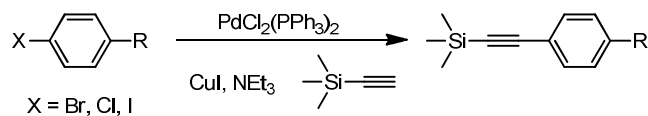


Scheme 7.1: Synthesis of PPV-*b*-PEG block copolymers **BP1** and **BP2** with different PEG chain lengths using CuAAC

In this chapter, the synthesis of BEH-PPV-*b*-PEG block copolymers with different PEG block lengths is presented using this *Click* chemistry approach. The PPV block was synthesized using the anionic sulfinyl precursor route with an alkyne functional anionic initiator, for which was observed that a spacer between the alkyne function and the aromatic core of the initiator is a key figure to success. Thus, no post-polymerization modification is required in order to create the desired *Click* functionality. *Via* this approach an easy handle is created to access the introduced alkyne functionality for coupling with an azide-functionalized polymer block, in the present case poly(ethylene glycol), PEG-N₃. In a last part of this chapter, self-assembly for these PPV-*b*-PEG block copolymers with different PEG block lengths is discussed based on DLS analysis of the formed micelles in aqueous solution.

7.2. EXPERIMENTAL SECTION

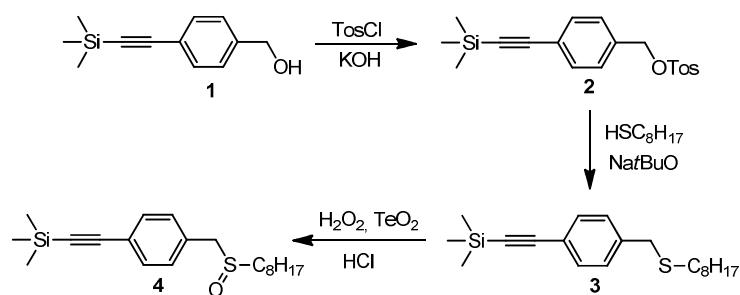
7.2.1. General procedure for Sonogashira reaction^{15,16}



Scheme 7.2: General reaction scheme for Sonogashira reaction

The starting product was dissolved in THF or DMF ($1 \text{ mL} \cdot \text{mmol}^{-1}$) and bis(triphenylphosphine)palladium(II) dichloride ($\text{PdCl}_2(\text{PPh}_3)_2$; 0.03 eq), triethylamine (NEt_3 ; 2.7 eq), Cu(I)I (0.02 eq) and NaI (0.2 eq) were added. In a last step trimethylsilyl acetylene (1.1 eq) was added after bringing the solution under nitrogen atmosphere. The reaction mixture was stirred for several hours at room temperature and poured in H_2O . The water layer was extracted with CH_2Cl_2 , dried over MgSO_4 and filtered. After removal of the solvent under reduced pressure, the reaction product was characterized using ^1H NMR.

7.2.2. Synthesis of anionic initiator with TMS-protected alkyne functionality, trimethyl[(4-[(octylsulfinyl)methyl]phenyl)ethynyl]silane (4)



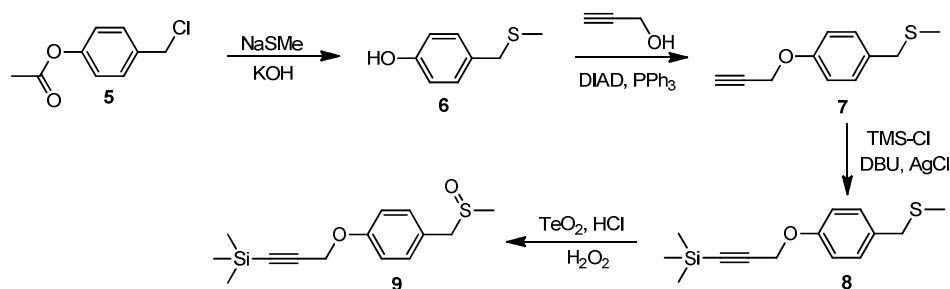
Scheme 7.3: Synthesis of anionic initiator with alkyne functionality **4**

A mixture of **1** (2.00 g, 9.8 mmol) and *p*-toluenesulfonyl chloride (1.92 g, 10.1 mmol) in dichloromethane (40 mL) was cooled in a CHCl₃/liquid N₂ bath under nitrogen atmosphere. KOH (2.20 g, 39.2 mmol) was slowly added so that the temperature did not exceed 5 °C. The reaction mixture was stirred for 3 h at 0 °C, quenched with ice water and extracted with CH₂Cl₂. The combined organic layers were dried over MgSO₄, filtered and the solvent was removed under reduced pressure. Pure **2** was purified by recrystallization from a hexane/ethyl acetate (3/1) mixture and isolated as yellow needle-like crystals. Yield: 41% (1.45 g). Mp: 89 °C; ¹H NMR (300 MHz, CDCl₃, δ): 7.77 (d, *J* = 8.5 Hz, 2H; ArH), 7.38 (d, *J* = 8.2 Hz, 2H; ArH), 7.31 (d, *J* = 8.2 Hz, 2H; ArH), 7.15 (d, *J* = 8.5 Hz, 2H; ArH), 5.01 (s, 2H; CH₂O), 2.43 (s, 3H; ArCH₃), 0.22 (s, 9H; SiCH₃); ¹³C NMR (75 MHz, CDCl₃, δ): 145.6 (C4), 134.1 (C4), 133.8 (C4), 132.8 (CH), 130.6 (CH), 128.9 (CH), 128.6 (CH), 124.6 (C4), 104.9 (C4), 96.0 (C4), 72.0 (CH₂), 22.4 (CH₃), 0.6 (CH₃); FT-IR (NaCl, cm⁻¹): 3583, 2920, 2851, 2159, 1506, 1361, 1250, 1218, 1189, 1176; DIP MS (EI, *m/z*): 358 [M⁺], 203 [M⁺ - Tos], 187 [M⁺ - OTos].

A solution of octanethiol (0.55 g, 3.7 mmol) and Na^tBuO (0.37 g, 3.9 mmol) in methanol (10 mL) was stirred for 1 h under nitrogen atmosphere. This solution was added dropwise to a solution of **2** (1.33 g, 3.7 mmol) in MeOH (5 mL), stirred at room temperature and followed on TLC (hexane/CH₂Cl₂ 7/3). The reaction mixture was poured in water and extracted three times with CH₂Cl₂. The combined organic layers were dried over MgSO₄ and filtered. The solvent was evaporated under reduced pressure and the product used without further purification. **3** (0.87 g, 2.6 mmol) was dissolved in 1,4-dioxane (15 mL) after which TeO₂ (0.08 g, 0.52 mmol) and HCl (2M, 0.1 mL) were added. In the last step H₂O₂ (35 wt%, 0.44 mL, 5.2 mmol) was added dropwise. The reaction was

followed on TLC and quenched with a saturated NaCl solution when overoxidation became apparent. The reaction mixture was extracted three times with CH_2Cl_2 . The organic layers were dried over MgSO_4 , filtered and the solvent was removed under reduced pressure. The gained product was purified using column chromatography (silica, eluent hexane/ CHCl_3 7/3) and subsequently recrystallized twice from hexane. Initiator **4** was isolated as white crystals. Yield: 14% (0.23g). Mp: 76 °C; ^1H NMR (300 MHz, CD_2Cl_2 , δ): 7.45 (d, $J = 8.2$ Hz, 2H; ArH), 7.25 (d, $J = 8.2$ Hz, 2H; ArH), 3.90 (s, 2H; ArCH_2S), 2.54 (t, $J = 7.8$ Hz, 2H; SCH_2), 1.69 (m, 2H; CH_2), 1.49 – 1.21 (m, 10H; CH_2), 0.88 (t, $J = 6.8$ Hz, 3H; CH_3), 0.24 (s, 9H; SiCH_3); ^{13}C NMR (300 MHz, CD_2Cl_2 , δ): 132.6 (CH), 131.8 (C4), 130.6 (CH), 123.5 (C4), 104.9 (C4), 95.5 (C4), 58.4 (CH_2), 51.9 (CH_2), 32.3 (CH_2), 29.7 (CH_2), 29.6 (CH_2), 29.3 (CH_2), 23.1 (CH_2), 23.0 (CH_2), 14.4 (CH_3), 0.1 (CH_3); FT-IR (NaCl, cm^{-1}): 3583, 2955, 2921, 2850, 2158, 1506, 1467, 1413, 1248, 1026; DIP MS (CI, m/z): 349 [MH^+], 187 [$\text{M}^+ - \text{SO}_2\text{C}_8\text{H}_{17}$].

7.2.3. Synthesis of alkyne initiator with spacer, trimethyl[3-(4-[(methylsulfinyl)methyl]phenoxy)propynyl]silane (**9**)



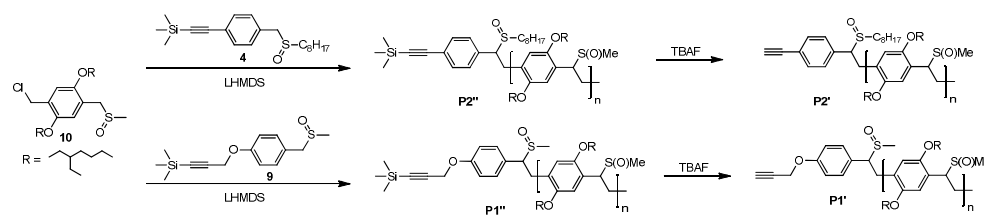
Scheme 7.4: Synthesis of anionic initiator **9** with alkyne functionality

Synthesis of compound **6** was performed as already described in Chapter 6. Compound **7** was synthesized using the Mitsunobu reaction.^{17,18} To a solution of **6** (1.41 g, 9.14 mmol) in THF (0.1 M solution of **6**, 91.4 mL), propargyl alcohol (0.53 mL, 9.14 mmol) and triphenylphosphine (PPh₃; 2.40 g, 9.14 mmol) were added. In a last step, the reaction was cooled to 0 °C and DIAD (diisopropyl azodicarboxylate; 1.80 mL, 9.14 mmol) was added dropwise. The reaction was stirred at room temperature for 24 hours after which the solvent was evaporated. Cold hexane was added to the reaction mixture to remove the triphenylphosphine oxide byproduct by filtration. The solvent was again removed under reduced pressure. The pure compound was isolated using flash chromatography (silica, eluent hexane/ethyl acetate 19/1) as a yellowish oil. Yield: 88% (2.13 g). ¹H NMR (300 MHz, CDCl₃, δ): 7.21 (d, *J* = 9.0 Hz, 2H; ArH), 6.90 (d, *J* = 9.0 Hz, 2H; ArH), 4.66 (d, *J* = 2.4 Hz, 2H; CH₂O), 3.62 (s, 2H; SCH₂), 2.50 (t, *J* = 2.4 Hz, 1H; alkyneH), 1.97 (s, 3H; SCH₃); ¹³C NMR (75 MHz, CDCl₃, δ): 157.2 (C4), 131.9 (C4), 130.6 (CH), 115.5 (CH), 79.2 (C4), 76.2 (CH), 56.5 (CH₂), 38.4 (CH₂), 15.6 (CH₃); FT-IR (NaCl, cm⁻¹): 3288, 2981, 2915, 2121, 1722, 1609, 1510, 1438, 1375, 1302, 1218, 1177, 1108, 1029; DIP MS (EI, *m/z*): 192 [M⁺], 145 [M⁺ - SCH₃].

To a solution of **7** (1 g, 5.22 mmol) in CH₂Cl₂ (25 mL), AgCl (0.15 g; 1.04 mmol) and DBU (1,8-diazabicyclo[5.4.0]undec-7-ene; 1.56 mL, 10.44 mmol) were added. The resulting mixture was heated till 40 °C and trimethylsilyl chloride (1.99 mL, 15.66 mmol) was added dropwise. The reaction was stirred for 2 days under nitrogen atmosphere at 40 °C.¹⁹ After addition of water, the reaction mixture was extracted with CH₂Cl₂ and the organic layer washed with a saturated NaHCO₃ solution, a 2M HCl solution and water. The organic phase was dried over MgSO₄, filtered and the solvent was evaporated. Oxidation of **8**, to

yield **9** was performed as described before and without purification of **8**. Pure **9** was obtained as a yellowish oil after two column chromatography purifications (silica, eluent $\text{CH}_2\text{Cl}_2 \rightarrow \text{CH}_2\text{Cl}_2/\text{MeOH}$ 9/1). Yield: 29% (0.4 g). ^1H NMR (300 MHz, CDCl_3 , δ): 7.21 (d, $J = 8.6$ Hz, 2H; ArH), 6.96 (d, $J = 8.6$ Hz, 2H; ArH), 4.66 (s, 2H; CH_2O), 3.96 (q, $J = 12.9$ Hz, 2H; ArCH_2S), 2.46 (s, 3H; SCH_3), 0.15 (s, 9H; SiCH_3). ^{13}C NMR (75 MHz, CDCl_3 , δ): 158.7 (C4), 131.8 (CH), 122.9 (C4), 116.2 (CH), 100.3 (C4), 93.7 (C4), 60.1 (CH_2), 57.5 (CH_2), 37.7 (CH_3), 0.4 (CH_3); FT-IR (NaCl, cm^{-1}): 3584, 2958, 2923, 2855, 2361, 2341, 2156, 1608, 1511, 1301, 1249, 1219, 1178, 1037, 842; DIP MS (CI, m/z): 281 [MH^+], 217 [$\text{M}^+ - \text{SOCH}_3$].

7.2.4. Synthesis of PPV block with alkyne functionality

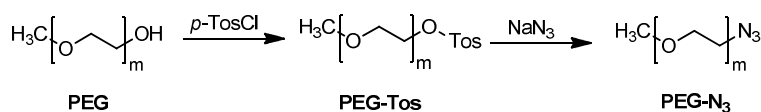


Scheme 7.5: Synthesis of PPV block with alkyne functionality

Synthesis of monomer **10** and all polymerization and elimination reactions were carried out as described before.²⁰ The synthesis of precursor polymers **P2''/P1''** was performed using 0.1 eq of the desired anionic initiator (**4** and **9** respectively; $\text{B} \rightarrow \text{M} + \text{I}$) and quenched after 5 minutes of reaction time by addition of 0.2 mL concentrated HCl solution (37%). After synthesis of the precursor polymer, deprotection of the alkyne functionality was performed by dissolving polymers **P2''** and **P1''** in THF and shielding them from light. Tetra-*n*-butylammonium fluoride (TBAF, 1 M in THF; 10 eq relative to calculated amount

of initiator groups present in polymer chain, based on GPC measurements) was added and the reaction mixture was stirred for 4 h at room temperature. The mixture was poured in water and extracted with CH₂Cl₂. The solvent was evaporated under reduced pressure and polymers **P2'** and **P1'** were dried under vacuum. Deprotection of the alkyne functionality was easily checked by means of ¹H NMR spectroscopy.

7.2.5. Synthesis of PEG block with azide functionality



Scheme 7.6: Synthesis of azide-functionalized poly(ethylene glycol) (**PEG-N₃**)

The PEG blocks with azide functionality were synthesized as described before.²¹ Reactions were started with commercially available poly(ethylene glycol) monomethyl ether with average molecular weights of 2000 and 6000 Da. In a first step a tosylate function was attached to the polymer which in a second step was converted into an azide functionality. Purity and functionalization were checked by means of ATR FT-IR and ¹H NMR measurements.

7.2.6. Synthesis of BEH-PPV-*b*-PEG *via* CuAAC Coupling

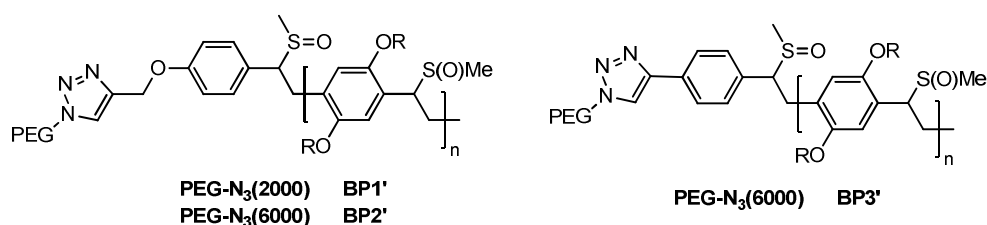


Figure 7.1: PPV-*b*-PEG block copolymers starting from **P1'** (**BP1'/2'**) or **P2'** (**BP3'**)

To a solution of **P1'** (or **P2'**) (40 mg, 12.5 μmol), **PEG-N₃** (1 eq) and Cu(I)Br (8.9 mg, 62.5 μmol) in dry DMF (5 mL), PMDETA (N,N,N',N'',N''-pentamethyldiethylenetriamine 10.8 mg, 62.5 μmol) was added under nitrogen atmosphere. The reaction mixture was stirred for 3 days at room temperature. The solution was passed through a neutral alumina column in order to remove the copper salts and concentrated under reduced pressure. Toluene (5 mL) was added to **BP1'/2'** and the solution was stirred for 3 hours at 110°C in order to eliminate the PPV block. After cooling, block copolymers **BP1** and **BP2** were precipitated in ice cold hexane, filtered, washed with water and the resulting red powder was dried under vacuum.

For dispersion and DLS measurements, **BP1** and **BP2** were dissolved in a minor amount of THF, added to water and filtered (0.45 μm); measurements were performed at an average count rate of approximately 80 kcps (kilocounts per second); pH = 7.

7.3. RESULTS AND DISCUSSION

7.3.1. Synthesis of anionic initiator with alkyne functionality

For the synthesis of anionic initiator **4**, synthesis was started using the Sonogashira reaction. In literature it was found that this reaction is straightforward with high yields.^{15,16} The Sonogashira reaction was tested for different starting products (see Figure 7.2) but the desired compound **4** (or precursor for **4**) was not formed (see Table 7.1).

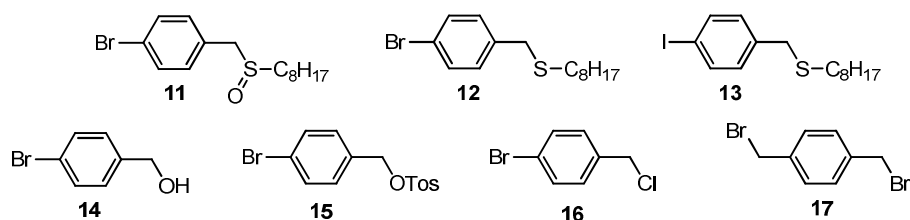


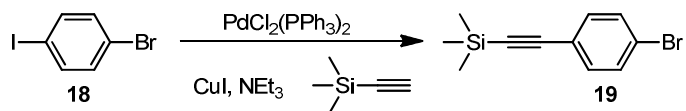
Figure 7.2: Different starting compounds used in the Sonogashira reaction

Table 7.1: Trials for Sonogashira reaction to synthesize a precursor for anionic initiator **4**

Starting compound	Solvent	Reaction time / h	Result
11	DMF	5	Starting material
11	DMF	6	Starting material
11	THF	120	Starting material
12	THF	18	Starting material
13^a	THF	18	Starting material
14	DMF	1	Formation of aldehyde
15	THF	18	?
16	DMF	18	Reaction on $-\text{CH}_2\text{Cl}$ instead of $-\text{Br}$
17	DMF	2	?

^a Similar procedure described in literature for meta-substituted compound²²

Since none of the Sonogashira reactions appeared to yield the desired products, a literature example²³ (Scheme 7.7) was repeated to check for possible defects in the reaction itself or in the starting materials used.



Scheme 7.7: Literature example for Sonogashira reaction

From ^1H NMR experiments it could be concluded that an almost 100% efficiency was reached for the synthesis of compound **19** leading to the conclusion that a methyl-sulfinyl or thioether substituted aromatic core (or related compound) is not favorable for a Sonogashira reaction. For this reason, synthesis of initiator **4** (Figure 7.3) was started using the commercially available 4-(trimethylsilylethynyl) benzyl alcohol (**1**, see Scheme 7.3).

For the synthesis of initiator **9** (Figure 7.3), an alkyne functionalized anionic initiator with a spacer between the aromatic core and the triple bond, an easy 4-step reaction pathway was followed starting from 4-(chloromethyl)phenyl acetate (**5**, see Scheme 7.4).

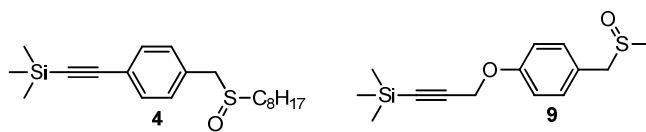


Figure 7.3: Anionic initiators **4** and **9** with alkyn functionality

7.3.2. Synthesis of block copolymers *via Click* coupling of an alkyne-functionalized PPV block (no spacer) and an azide-functionalized PEG block

Initiator **4** was used (0.1 eq) during the synthesis of the alkyne-functionalized PPV block **P2''** which was reacted with **PEG-N₃** ($M_n^{\text{app}} = 6200$) after deprotection of the alkyne functionality using TBAF. Precursor polymer **P2'** was gained in high yield with comparable molecular weights for experiments with the 'standard' used *tert*-butyl functionalized initiator.²⁴

Table 7.2: Results regarding MWD and *PDI* measured on conventional GPC for different precursor PPV polymers **P2''** and **P2'** and conjugated polymer **P2** with alkyne functionality

P2''		P2'		P2	
$M_n^{\text{app}} / \text{g}\cdot\text{mol}^{-1}$	<i>PDI</i>	$M_n^{\text{app}} / \text{g}\cdot\text{mol}^{-1}$	<i>PDI</i>	$M_n^{\text{app}} / \text{g}\cdot\text{mol}^{-1}$	<i>PDI</i>
6100	1.3	6000	1.4		
6400	1.3	6300	1.3	8800	1.4

For the coupling between the alkyne-functionalized PPV block and the azide functionalized PEG block, a *Click* reaction was performed using three different reaction strategies (Figure 7.4).

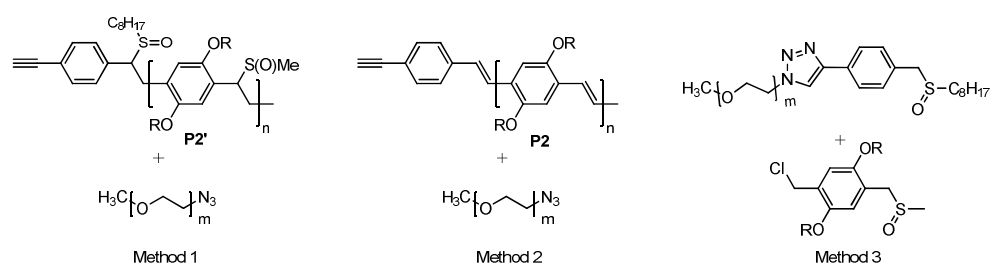


Figure 7.4: Overview of used *Click* reaction methods

The first method (method 1) is the *Click* coupling of the precursor PPV polymer **P2'** with the azide-functionalized PEG. Reaction time and solvent were varied in these tests. The second strategy (method 2) consists of a *Click* reaction starting from the conjugated PPV block **P2** using an earlier published method.²⁵ The last test performed (method 3) was the CuAAC coupling of **PEG-N₃** with deprotected anionic initiator **4** (using TBAF) which in a second step could be used as a macroinitiator for PPV polymerization with monomer **10** (Table 7.3).

Table 7.3: Different reaction methods and conditions for *Click* reactions starting from a PPV block synthesized with anionic initiator **4**

Method	Cu(I)Br / eq	PMDETA / eq	Solvent	T / °C	t / h
1	5	5	THF	50	4
1	5	5	THF	50	24
1	5	5	DMF	50	24
2^a			THF	35	24
3	5	5	THF	RT	12

^a Literature procedure using Cu(I)I and DBU (1,8-diazabicyclo [5.4.0]undec-7-ene) as the ligand²⁵

For all different methods and reactions tested, results regarding molecular weight and polydispersity can be found in Table 7.4 and GPC profiles are depicted in Figure 7.5.

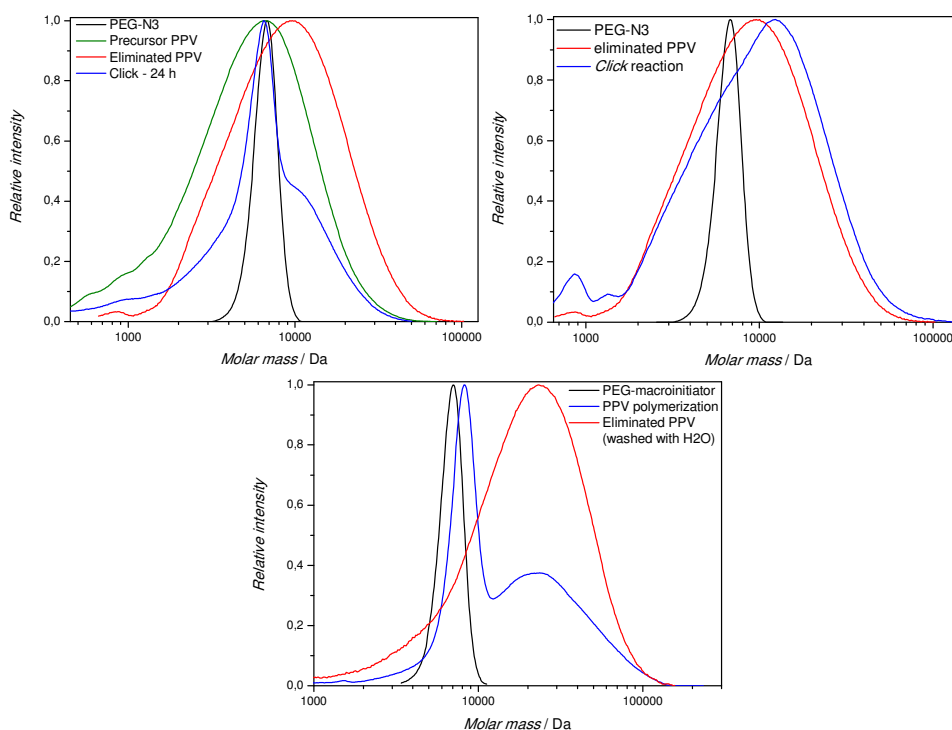


Figure 7.5: GPC profiles for *Click* polymerizations performed using method 1 (upper left), 2 (upper right) and 3 (bottom).

Table 7.4: Results regarding molecular weight and polydispersity for different *Click* methods investigated towards PPV-*b*-PEG block copolymers using anionic initiator **4** for the synthesis of the PPV block

Polymer	Method 1		Method 2		Method 3	
	$M_n^{\text{app}} / \text{g}\cdot\text{mol}^{-1}$	<i>PDI</i>	$M_n^{\text{app}} / \text{g}\cdot\text{mol}^{-1}$	<i>PDI</i>	$M_n^{\text{app}} / \text{g}\cdot\text{mol}^{-1}$	<i>PDI</i>
PEG-N ₃	6200	1.02	6200	1.02		
Pre PPV	4400	1.8				
Conj PPV			6600	1.7		
PEG-macroinit					6600	1.03
PPV- <i>b</i> -PEG	3400 ^a	2.6	7200	1.8	9500	1.9

^a Result given in for reaction time of 4 h in THF, similar results for other test reactions (24 h in THF or DMF, see Table 7.3)

As is clear from the data in Table 7.4 and Figure 7.5, all tested reaction methods and conditions did not lead towards a successful *Click* reaction. For method 1, elimination of the PPV block is observed because the reaction is performed at 50 °C for 4 or 24 h (see similarity in molecular weight for the shoulder of the blue GPC profile with the red curve in the upper left figure). For the CuAAC coupling, starting from the already eliminated PPV block (method 2), only a minor shift is seen in the SEC results compared to the starting PPV block, with a shoulder referring to the PEG block that was present in the reaction mixture. Also here, no 'Clicked' product was found. For the third method, where the **PEG-N₃** was first *Clicked* with deprotected anionic initiator **4**, a bimodal SEC chromatogram was found according to a mixture of two polymers, namely the PEG-macroinitiator and the PPV block. This was also confirmed using ¹H NMR spectroscopy (see Figure 7.6) after washing of the sample with water (removal of the water-soluble PEG block).

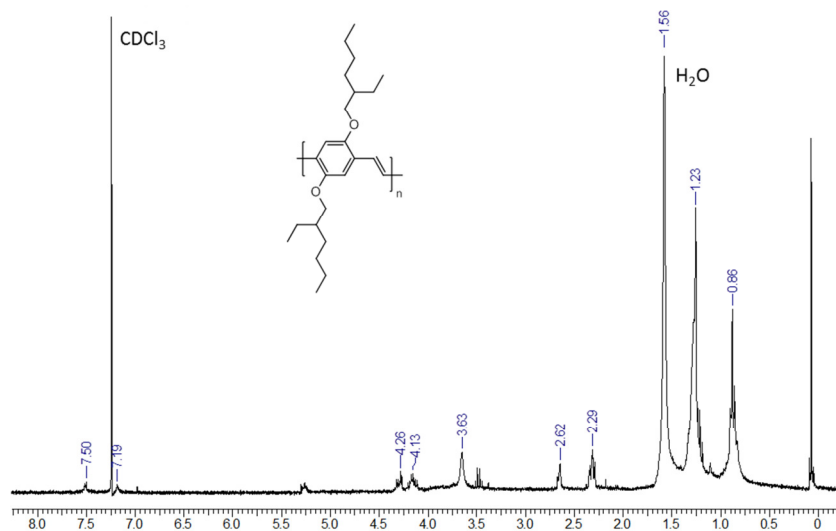


Figure 7.6: ¹H NMR spectrum for the resulting polymer of method 3 after washing with water.

From Figure 7.6 it can be concluded that only signals for the PPV block are present in the NMR spectrum and no signals according to the PEG block can be found after washing with water. Thus for this third method, no PPV was grown to the macroinitiator, and an independent PPV homo-polymerization found place in the reaction mixture.

7.3.3. Synthesis of block copolymers *via Click* coupling of an alkyne-functionalized PPV block (with spacer) and an azide-functionalized PEG block

In order to reach a successful CuAAC reaction, it seemed to be necessary to have a spacer built in between the alkyne functionality and the aromatic core of the anionic initiator (**9**). Polymerizations were again performed *via* the anionic sulfinyl precursor route and good control over polymerizations was achieved for a reaction time of 5 min at 0 °C under nitrogen atmosphere and a monomer concentration ($[M]_i$) of 50 mmol·L⁻¹. To make sure that also this TMS-protected anionic initiator is an efficient species to initiate the anionic polymerization pathway, three different initiator concentrations were tested in order to make sure that molecular weight can be tuned and that the control is as efficient as for the previously employed *tert*-butyl functionalized anionic initiator.^{7,20} Results regarding average molecular weight and polydispersity for these polymerizations (to full conversion, since premature stop of polymerization is difficult to achieve) are given in Table 7.5.

Table 7.5: Molecular weights and *PDI*s for the anionic polymerization of monomer **10** with different amounts of anionic initiator **9**

[In] / mmol·L ⁻¹	Precursor polymer		Conjugated polymer	
	M_n^{app} / g·mol ⁻¹	<i>PDI</i>	M_n^{app} / g·mol ⁻¹	<i>PDI</i>
5	2500	1.9	4700	1.5
15	1800	1.5	4000	1.3
25	1300	1.3	3000	1.2

As is evident from Table 7.5, with the use of a higher initiator content, polymers with lower molecular weights and more narrow distributions were obtained as expected. When the initiator concentration is increased by a factor of 5, roughly half the molecular weight is achieved on the precursor stage. While on first glance this indicates limited influence of the initiator, good agreement with earlier reported results on bromine and *tert*-butyl functionalized anionic initiators^{7,11} is found, for which quantitative endgroup functionalization was unambiguously demonstrated by mass spectrometry. A very similar initiator efficiency can thus be assumed for initiator **9** in the present case and the deviations in molecular weights can be attributed to using a polystyrene calibration of the SEC setup.

With a BEH-PPV precursor polymer of 2500 g·mol⁻¹ and *PDI* of 1.9 (measured against polystyrene standards, which was shown before to give reasonable estimates for M_n^{app} , concomitantly largely overestimating *PDI*),^{6,7} *Click* reactions were performed with two commercially available PEGs that were functionalized with an azide group. For the coupling Cu(I)Br and PMDETA in dry DMF as the solvent were used as standard recipe. Results regarding molecular weight and dispersity for the different starting blocks (elimination of the PPV block resulted in a polymer with a MWD of 4700 g·mol⁻¹) and block copolymers (also

eliminated to obtain the conjugated PPV block) can be found in Table 7.6 and GPC profiles are plotted in Figure 7.7.

Table 7.6: Molecular weights and polydispersities for (conjugated) polymer blocks and PPV-*b*-PEG block copolymers (**BP1** and **BP2**)

	$M_n^{\text{app}} / \text{g}\cdot\text{mol}^{-1}$	<i>PDI</i>	$M_n^{\text{app}} / \text{g}\cdot\text{mol}^{-1}$	<i>PDI</i>
BEH-PPV	4700	1.5	4700	1.5
PEG-N ₃	2700	1.03	6200	1.02
PPV- <i>b</i> -PEG	9200	1.4	14600	1.3

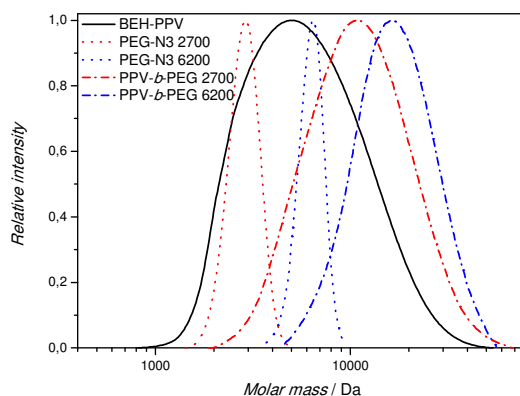


Figure 7.7: GPC profiles for the different BEH-PPV and PEG-N₃ blocks and PPV-*b*-PEG block copolymers with different PEG segment lengths

As is evident from the data in Table 7.6, number average molecular weights for block copolymers are higher than the addition of the separate PPV and PEG blocks. These differences occur because of shifts in hydrodynamic volumes (synthesis of rod-coil block copolymers with stiff PPV block and flexible PEG block) and measurement towards polystyrene standards, which necessarily gives a somewhat erroneous result. The distributions of the coupled products, however, display no bimodality or residual shoulders in the low molecular weight side, thus nicely demonstrating the completion of the CuAAC reaction. It can

thus be safely concluded that the reactions were successful.

Previously, for PPV-*b*-P(*t*-BuA) block copolymers¹¹ shifts in the maximum absorption wavelength (λ_{max}) of the material was seen depending on the chain length of the attached acrylate block. From the UV-Vis spectra for the PPV-*b*-PEG block copolymers (Figure 7.8) it can be concluded that the length of the attached PEG block does in the present case not have an influence on the maximal wavelength and thus on the conjugation length of the PPV block. λ_{max} for the polymer with the short PEG chain is equal to 494 nm and for the long PEG chain is 491 nm (compared to 494 nm for pure PPV).

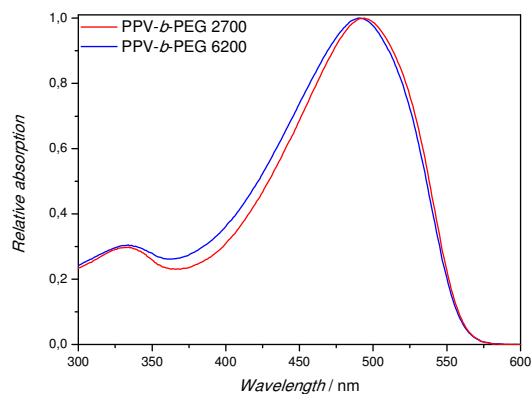


Figure 7.8: UV-Vis spectra for **BP1** and **BP2**

To study self-assembly for these materials, DLS measurements on aqueous micellar solutions of the block copolymers were performed in order to detect formation of self-assembled structures. Results regarding mean hydrodynamic diameter and polydispersity (*PD*) for the measured nanoparticles are given in Table 7.7.

Table 7.7: Mean hydrodynamic diameter and polydispersity for PPV-*b*-PEG block copolymers **BP1** and **BP2** measured *via* DLS^a

Block copolymer	Diameter / nm	PD
BP1	76.0	0.105
BP2	21.1	0.034

^a Average count rate \sim 80 kcps

As is clear from Table 7.7, smaller structures could be found for the block copolymer with the highest PEG content. These results are in agreement with results on PS-*b*-PEG block copolymers. For this system, it was shown that micelles were formed at high PEG content, while a decrease in the PEG chain length caused a change in the dominant morphologies that were obtained towards spherical micelle-like aggregates, rods, lamellae and vesicles. This is believed to be related to the degree of stretching of the PS blocks in the core regions^{26,27} and similar mechanisms might be in play in the PPV-PEG system as well. PPV is generally known to self-aggregate due to the rod-like structure of the chains in combination with the ability to undergo effective π -stacking.

As no PPV-*b*-PEG block copolymers were described in literature using the presented polymerization strategy and with study of self-assembly using DLS measurements in aqueous environment, the earlier described PS-*b*-PEG block copolymers are the best polymers to make a comparison towards formation of different morphologies in the PPV-*b*-PEG system. From the size of the measured particles, and from comparison to the former study, it can be assumed that spherical micellar structures are formed for **BP1** (longest PEG chain). For **BP2** (where the PEG chain is shorter than the PPV segment), bigger particles – with a mean diameter of around 76 nm – were found which relate more to rod-like or lamellar structures. Overall, this initial study demonstrates how the self-

assembly of the PPV materials can be guided in a facile manner. More in-depth studies are, however, required to elucidate the exact shape of the formed micelles because the gained results could only be compared to the results described for the PS-*b*-PEG block copolymers. So far it can only be concluded that for both block copolymers comparable results are found for DLS measurements in aqueous solution and thus similar structures are assumed.

7.4. CONCLUSIONS

PPV-*b*-PEG block copolymers are successfully synthesized with different PEG block lengths based on the well-established CuAAC protocol. BEH-PPV blocks are synthesized *via* the anionic sulfinyl precursor route in a well-controlled manner, employing a functional anionic initiator. A $-\text{CH}_2\text{-O}-$ spacer between the aromatic core and the alkyne functionality is required in order to allow for a successful *Click* reaction with the azide-functionalized PEG polymer blocks (or any other azide functional macromolecule). *Via* DLS measurements, formation of different micellar morphologies can be demonstrated for both block copolymers. For the block copolymer containing the longest PEG block, smaller micelles are identified, most likely of spherical structure. For the block copolymer containing a lower PEG content, larger assemblies are identified, which can be related to rod-like or lamellar structures. Further studies (e.g. atomic force microscopy (AFM) or electron microscopy) would be necessary to reveal the true morphology of the self-assembled PPV-*b*-PEG block copolymers in this aqueous environment.

The successful functionalization of PPV chains with *Clickable* alkyne end terminus opens up a general pathway towards highly complex macromolecular architectures. PPV surface grafts, star polymers and terpolymers of basically any material combination are therewith now available, giving rise to application of these materials not only in optoelectronics, but also for example in bioimaging in biomedical research.

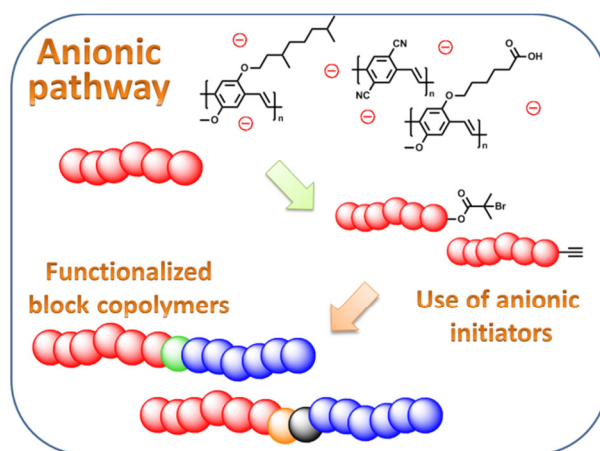
7.5. REFERENCES

- ¹ G. Kossmehl, *J. Phys. Chem.* **1979**, *83*, 417–426.
- ² H. Kretzschmann, H. Meier, *Tetrahedron Lett.* **1991**, *32*, 5059–5062.
- ³ S. Chakraborty, A. Keightley, V. Dusevich, Y. Wang, Z. Peng, *Chem. Mater.* **2010**, *22*, 3995–4006.
- ⁴ C.-C. Ho, Y.-H. Lee, C.-A. Dai, R. A. Segalman, W.-F. Su, *Macromolecules* **2009**, *42*, 4208–4219.
- ⁵ T. Junkers, J. Vandenbergh, P. Adriaensens, L. Lutsen, D. Vanderzande, *Polym. Chem.* **2012**, *3*, 275–285.
- ⁶ Described in Chapter 5.
- ⁷ I. Cosemans, J. Vandenbergh, V. S. D. Voet, K. Loos, L. Lutsen, D. Vanderzande, T. Junkers, *Polymer* **2013**, *54*, 1298–1304.
- ⁸ V. Percec, T. Guliashvili, J. Ladislaw, A. Wistrand, A. Stjerndahl, M. Sienkowska, M. Montiero, S. Sahoo, *J. Am. Chem. Soc.* **2006**, *128*, 14156–14165.
- ⁹ B. Rosen, V. Percec, *Chem. Rev.* **2009**, *109*, 5069–5119.
- ¹⁰ Described in Chapter 6.
- ¹¹ I. Cosemans, J. Vandenbergh, L. Lutsen, D. Vanderzande, T. Junkers, *Polym. Chem.* **2013**, *4*, 3471–3479.
- ¹² L. Liang, D. Astruc, *Coord. Chem. Rev.* **2011**, *255*, 2933–2945.
- ¹³ H. C. Kolb, M. G. Finn, K. B. Sharpless, *Angew. Chem. Int. Ed.* **2001**, *40*, 2004–2021.
- ¹⁴ C. Barner-Kowollik, F. E. Du Prez, P. Espeel, C. J. Hawker, T. Junkers, H. Schlaad, W. Van Camp, *Angew. Chem. Int. Ed.* **2011**, *50*, 60–62.
- ¹⁵ R. Chinchilla, C. Najera, *Chem. Rev.* **2007**, *107*, 874–922.

- ¹⁶ R. Chinchilla, C. Najera, *Chem. Soc. Rev.* **2011**, *40*, 5084–5121.
- ¹⁷ O. Mitsunobu, *Synthesis* **1981**, *1*, 1–28.
- ¹⁸ S. D. Lepore, Y. He, *J. Org. Chem.* **2003**, *68*, 8261–8263.
- ¹⁹ J. T. Wiltshire, G. J. Qioa, *J. Polym. Sci., Part A: Polym. Chem.* **2009**, *47*, 1485–1498.
- ²⁰ I. Cosemans, J. Wouters, T. Cleij, L. Lutsen, W. Maes, T. Junkers, D. Vanderzande, *Macromol. Rapid Commun.* **2012**, *33*, 242–247.
- ²¹ C. Detrembleur, A. Debuigne, O. Altintas, M. Conradi, E. Wong, C. Jérôme, C. Barner-Kowollik, T. Junkers, *Polym. Chem.* **2012**, *3*, 135–147.
- ²² Y. Shirai, L. Cheng, B. Chen, J. M. Tour, *J. Am. Chem. Soc.* **2006**, *128*, 13479–13489.
- ²³ F. Smeets, K. Van den Bergh, J. De Winter, P. Gerbaux, T. Verbiest, G. Koeckelberghs, *Macromolecules* **2009**, *42*, 7638–7641.
- ²⁴ See Chapters 3 and 4
- ²⁵ C.-C. Ho, Y.-H. Lee, C.-A. Dai, R. A. Segalman, W.-F. Su, *Macromolecules* **2009**, *42*, 4208–4219.
- ²⁶ K. Yu, A. Eisenberg, *Macromolecules* **1996**, *29*, 6359–6361.
- ²⁷ T. Patel, L. Abezgauz, D. Danino, V. Aswal, P. Bahadur, *J. Dispersion Sci. Technol.* **2011**, *32*, 1083–1091.

CHAPTER 8

Anionic Polymerization *via* the Sulfinyl Precursor Route for Other PPV Premonomers and Outlook Towards Functional Block Copolymers



The anionic polymerization pathway that is proven before to be a successful route towards well-defined polymers starting from a symmetrically substituted 2-ethylhexyloxy sulfinyl monomer is extended in this chapter towards other sulfinyl premonomers. Unsymmetrically alkyloxy-, ester-substituted and cyano-functionalized premonomers are also polymerized following the anionic pathway which is confirmed using TEMPO (2,2,6,6-tetramethylpiperidin-1-oxyl) as an additive (to make sure no radical pathway was present) or various anionic initiator concentrations during the polymerization reaction. As an outlook for further research, synthetic possibilities towards functionalized block copolymers are described. A first example makes use of an ester-functionalized PPV block in a dual-initiator strategy combined with SET-LRP after which ester-functionalized-PPV-*b*-acrylate block copolymers can be obtained. A second example is the synthesis of an all-PPV p-type-n-type block copolymer synthesized using the *Click* approach for which only preliminary results are presented.

8.1. INTRODUCTION

As a starting point of this thesis, the anionic polymerization route was distinguished from the radical pathway exploring the reaction conditions to obtain well-defined plain-PPV (Chapters 2 and 3). In further research, the anionic polymerization pathway for poly[2,5-bis(2-ethylhexyloxy)-*p*-phenylene vinylene], (BEH-PPV), was explored towards the use of anionic initiators with high initiation efficiencies, the addition mode and different reaction times and temperatures used. Also three different strategies to synthesize block copolymers were described, namely the direct coupling of a second monomer (*t*-BuA) to the anionic chain end,¹ a dual-initiator strategy where the anionic initiator was reinitiated towards a SET-LRP of *tert*-butyl acrylate² and, as a last example, a CuAAC (copper assisted azide-alkyne cycloaddition) coupling between an alkyne-functionalized PPV block and an azide-functionalized PEG (poly(ethylene glycol)) block.³ To prove that this anionic pathway may be used as a general polymerization method for all substituted sulfinyl premonomers, three different monomer systems were tested towards anionic polymerization conditions (LHMDS (lithium hexamethyldisilazide) as the base and THF as the solvent) in this chapter. The different polymers synthesized were poly[2-methoxy-5-(3,7-dimethyloctyloxy)-*p*-phenylene vinylene], (MDMO-PPV), poly[2-methoxy-5-(carboxypentyloxy)-*p*-phenylene vinylene], (CPM-PPV) and poly[2,5-dicyano-*p*-phenylene vinylene], (CN-PPV) (see Figure 8.1).

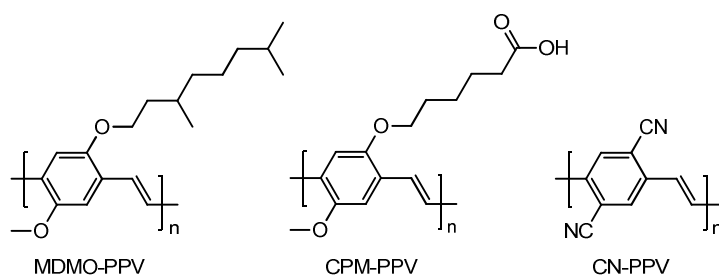


Figure 8.1: Different polymers synthesized *via* the anionic sulfinyl precursor route

In order to reach functionalized side chains on the PPV block, the acid-functionalized polymer (synthesized *via* hydrolysis of the ester-functionalized polymer) is very interesting. For an MDMO-CPM-PPV copolymer (9/1) further post-polymerization functionalization became possible with different functional alcohols using an optimized DCC/DMAP (*N,N'*-dicyclohexylcarbodiimide/4-(*N,N'*-dimethylamino-pyridine) procedure.⁴ It will be demonstrated in this chapter that also for the ester-functionalized precursor polymer, block copolymer synthesis *via* SET-LRP was possible using *tert*-butyl acrylate and methyl acrylate. For styrene as the second monomer, no successful block copolymer could be formed so far and further research on this matter, regarding reaction conditions, will still be required.

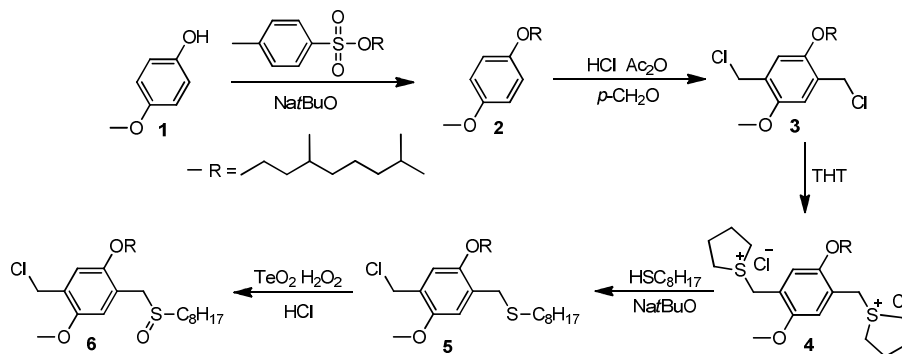
In a last part of this chapter synthesis towards p-type-n-type block copolymers containing a donor BEH-PPV block and an acceptor CN-PPV block will be described. As already mentioned in Chapter 1, p-type-n-type block copolymers are interesting materials for photovoltaic applications because phase separation of the donor-acceptor interface is prevented. By employing self-assembly, which is found for all block copolymers with distinct block properties, controlled layers can be obtained to reach efficient charge transport through the polymer layers.⁵

With using an n-type polymer instead of PCBM ([6,6]-phenyl-C₆₁-butyric acid methyl ester) as the acceptor material in devices, it is expected that a better geometry can be formed throughout the layers and phase separation is slowed down or prevented. For PPV materials, no block copolymer examples were reported on this matter. The most interesting PPV example is a reported solar cell device fabricated from a MEH-PPV (poly[2-methoxy-5-(2-ethylhexyloxy)-*p*-phenylene vinylene]) and PP(CN)V blend (PPV synthesized *via* the Knoevenagel polycondensation with CN-functionalities on the double bond).⁶ In order to reach p-type–n-type block copolymers consisting of two PPV blocks, an alkyne-functionalized BEH-PPV block will be coupled with an azide-functionalized CN-PPV block using CuAAC ligation. Preliminary results will be shown in this chapter and it will be revealed that, by means of ESI–MS (electrospray ionization – mass spectrometry)^{7,8} experiments, no 100% efficiency could be reached so far for the use of anionic initiators in the anionic polymerization reaction with CN-substituted sulfinyl premonomers.

8.2. EXPERIMENTAL SECTION

8.2.1. Monomer synthesis

8.2.1.1. Synthesis of 1-chloromethyl-2-methoxy-5-(3,7-dimethyloctyloxy)-4-[(octylsulfinyl)methyl] benzene (**6**)

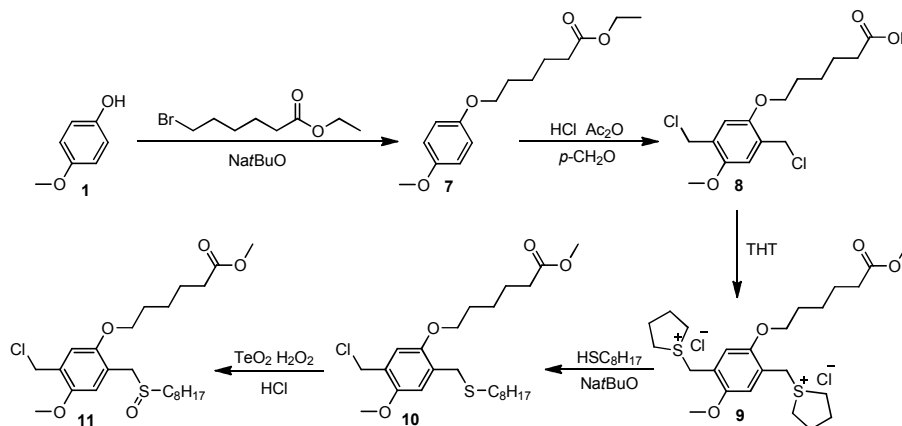


Scheme 8.1: Synthesis of MDMO premonomer **6**

Synthesis of MDMO premonomer **6** was performed as earlier described.⁹⁻¹²

Compound purity was checked by means of ¹H and ¹³C NMR spectroscopy.

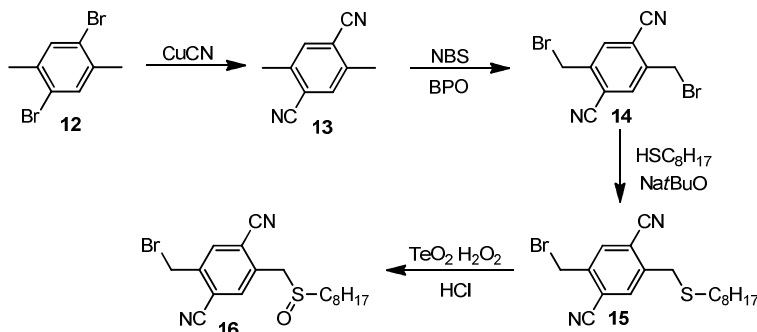
8.2.1.2. Synthesis of 6-(2-chloromethyl-4-methoxy-5-[(octylsulfinyl)methyl]-phenoxy) hexanoic acid methyl ester (**11**)



Scheme 8.2: Synthesis of CPM premonomer **11**

Synthesis of CPM premonomer **11** was performed as earlier described⁴ and optimized performing five azeotropic *n*-octane cycles for the synthesis of compound **10** to prevent the equilibrium to shift again towards the THT-salt. Compound purity was checked by means of ¹H and ¹³C NMR spectroscopy.

8.2.1.3. *Synthesis of 1-bromomethyl-2,5-dicyano-4-[(octylsulfinyl)methyl] benzene (16)*



Scheme 8.3: Synthesis of cyano premonomer **16**

Compound **13** was synthesized by means of a substitution reaction with CuCN on compound **12**.^{13,14} Crude **13** could easily be purified *via* recrystallization in ethanol to obtain white needle-like crystals. After radical bromination of **13**, using NBS combined with dibenzoylperoxide (BPO) as an initiator in CCl₄ (carbon tetrachloride) as the solvent, compound **14** was reached and isolated as white crystals after crystallization from CCl₄ when cooling down the reaction mixture after filtration (to remove succinimide).¹⁵ The last two steps of the synthesis were performed as described before for all other sulfinyl monomers.^{11,16} Crude **16** was purified by means of two recrystallizations in EtOAc/petroleum ether (1/1) and obtained as white fluffy crystals. The purity of compound **16**^{17,18} was checked by means of ¹H and ¹³C NMR spectroscopy.

8.2.2. Synthesis of anionic initiators

8.2.2.1. Synthesis of anionic initiators **17**, **18** and **19**

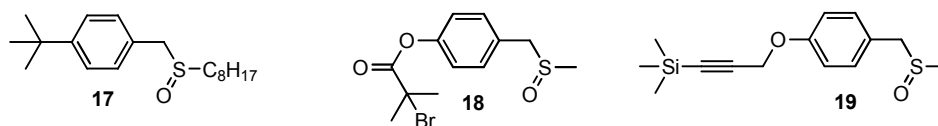
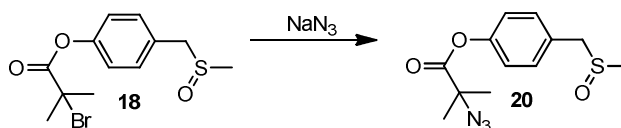


Figure 8.2: Anionic initiators with *tert*-butyl (**17**), bromine (**18**) or TMS- protected alkyne functionality (**19**)

Synthesis and characterization of anionic initiators **17**, **18** and **19** was performed as already described in Chapters 3, 6 and 7 respectively.

8.2.2.2. Synthesis of azide-functionalized anionic initiator **20**

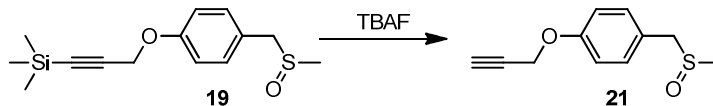


Scheme 8.4: Synthesis of anionic initiator **20**

To a solution of **18** (0.2 g, 0.63 mmol) in DMF (3 mL), NaN_3 (45 mg, 0.7 mmol) was added and the resulting mixture was stirred for 3 hours at room temperature. After addition of H_2O , extraction was performed using CH_2Cl_2 . The organic layer was dried over MgSO_4 , filtered and the solvent was removed under reduced pressure. After recrystallization in hexane/EtOAc (3/1), pure **20** was obtained as white/transparent flake-like crystals. Yield: 55% (0.1 g). Mp: 83.5 °C; ^1H NMR (300 MHz, CDCl_3 , δ): 7.33 (d, J = 8.6 Hz, 2H; ArH), 7.14 (d, J = 8.6 Hz, 2H; ArH), 3.97 (q, J = 13.1 Hz, 2H; ArCH₂S), 2.46 (s, 3H; SCH₃), 1.61 (s, 6H; CH₃); ^{13}C NMR (75 MHz, CDCl_3 , δ): 171.7 (C4), 151.1 (C4), 131.8 (CH), 128.3 (C4), 122.4 (CH), 63.7 (C4), 59.9 (CH₂), 38.0 (CH₃), 24.9 (CH₃); FT-IR

(NaCl, cm^{-1}): 3005, 2977, 2925, 2111, 1755, 1600, 1503, 1467, 1248, 1196, 1167, 1115, 1044; DIP MS (CI, m/z): 282 [MH^+], 218 [$\text{M}^+ - \text{SOCH}_3$].

8.2.2.3. Synthesis of anionic initiator **21** with deprotected alkyne function

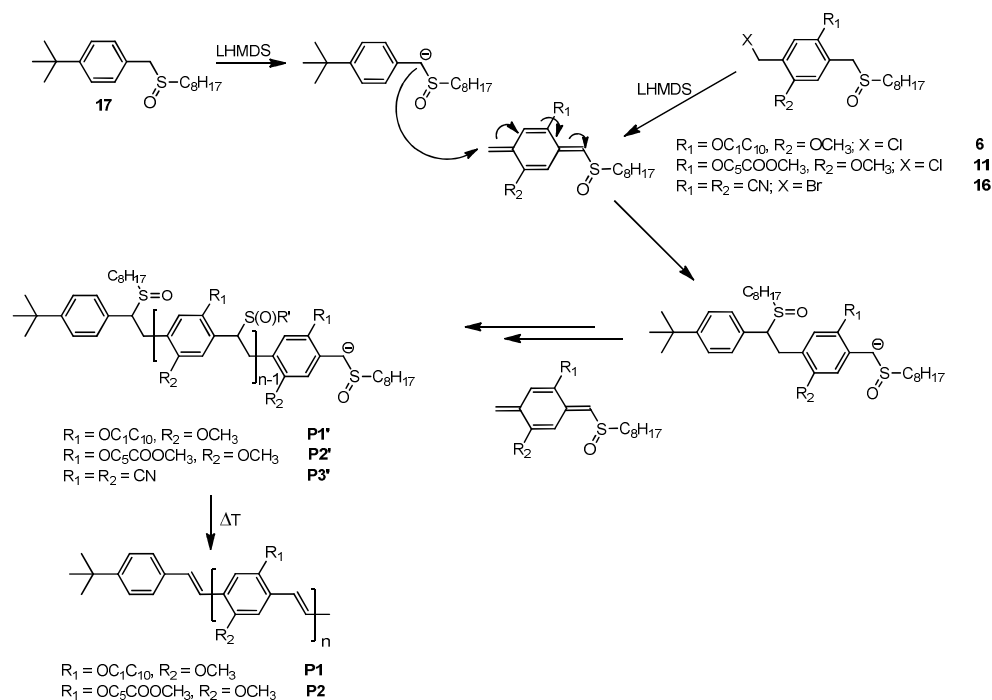


Scheme 8.5: Synthesis of anionic initiator **21**

A solution of **19** (0.1 g, 0.36 mmol) in THF (5 mL) was shielded from the light and brought under nitrogen atmosphere. After addition of TBAF (1M in THF; 1.44 mL, 1.44 mmol) the solution was stirred for 4 h at room temperature. The reaction was quenched with water, extracted with CH_2Cl_2 and dried over MgSO_4 . After filtration, the solvent was removed under reduced pressure. The crude product was purified using column chromatography (silica, eluent $\text{CH}_2\text{Cl}_2/\text{MeOH}$ 9/1) followed by recrystallization in hexane/EtOAc (3/1). Pure **21** was isolated as white crystals. Yield: 53% (39 mg). Mp: 85 °C; ^1H NMR (300 MHz, CDCl_3 , δ): 7.22 (d, $J = 8.8$ Hz, 2H; ArH), 6.97 (d, $J = 8.8$ Hz, 2H; ArH), 4.68 (d, $J = 2.4$ Hz, 2H; OCH_2), 3.93 (q, $J = 13.1$ Hz, 2H; ArCH_2S), 2.51 (t, $J = 2.4$ Hz, 1H; alkyneH), 2.43 (s, 3H; SCH_3); ^{13}C NMR (75 MHz, CDCl_3 , δ): 158.3 (C4), 131.9 (CH), 123.1 (C4), 116.0 (CH), 78.9 (C4), 76.5 (CH), 60.1 (CH_2), 56.5 (CH_2), 37.8 (CH_3); FT-IR (NaCl, cm^{-1}): 3165, 2361, 2341, 2104, 1608, 1511, 1301, 1265, 1217, 1184, 1020, 822; DIP MS (CI, m/z): 209 [MH^+], 145 [$\text{M}^+ - \text{SOCH}_3$].

8.2.3. Anionic polymerization procedure

8.2.3.1. General method



Scheme 8.6: General polymerization procedure for the anionic sulfinyl precursor route towards PPV with introduction of anionic initiator **17**

All glassware was dried overnight in a drying oven at 110 °C and flamed under vacuum prior to use. The premonomer and the given amount of initiator were dissolved in dry THF providing a premonomer concentration of 0.05 M and brought at 0 °C under nitrogen atmosphere. The polymerization was started by adding 1.3 equivalents of LHMDS (1M in THF) by syringe ($B \rightarrow M + I$). After a reaction time of 15 minutes, the reaction mixture was quenched with HCl, poured in water and extracted with CH_2Cl_2 . The organic layer was evaporated under reduced pressure and the obtained sticky yellow oil was analyzed without further purification.

For CN-PPV precursor polymer **P3'**, (reaction time of 5 min) no elimination was performed due to insolubility of the conjugated polymer because no long substituents are present on the aromatic core to ensure solubility. The polymer was obtained as an orange/brown solid.

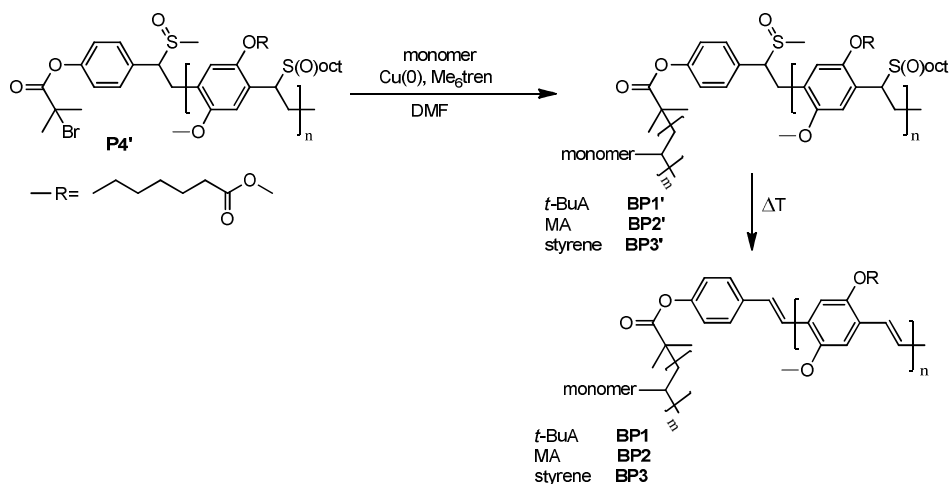
To obtain a conjugated polymer, the precursor polymer (**P1'** or **P2'**) was dissolved in toluene and heated at 110 °C for 3 h. After cooling down, the polymer was precipitated in cold methanol (100 mL) and filtered on a Teflon® filter. The polymer was obtained as a red powder.

8.2.3.2. Test the anionic nature of the polymerization with TEMPO

The procedure was similar to the standard polymerization procedure (without the use of initiator), with the addition of 0.5 equivalents of TEMPO to the premonomer solution before addition of the base.

8.2.4. Synthesis of block copolymers

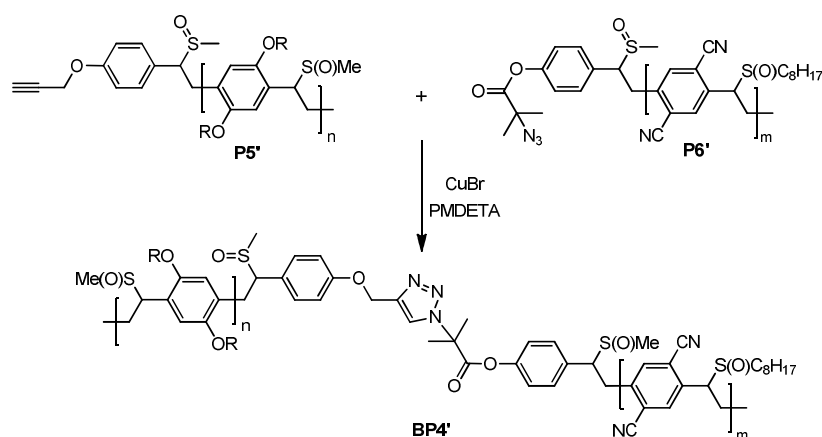
8.2.4.1. Block copolymers via SET-LRP



Scheme 8.7: Synthesis of block copolymers containing one CPM-PPV block via SET-LRP

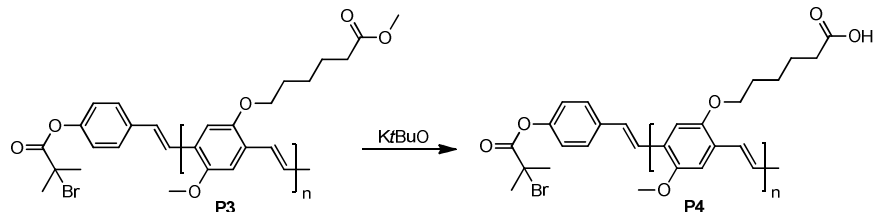
For the introduction of the second polymer block, ester-functionalized precursor polymer **P4'** – synthesized *via* the general anionic sulfinyl method starting from premonomer **11** and 0.2 eq of anionic initiator **18** – was used as the starting block. In the SET-LRP reaction (performed as described in Chapter 6; 1 eq Cu(0) and 1 eq of Me₆tren in DMF) three different monomers were tested: *tert*-butyl acrylate, methyl acrylate (MA) and styrene (50 eq; all filtered over alumina to remove the inhibitors).

8.2.4.2. Block copolymers via Click chemistry



Scheme 8.8: Synthesis of p-type-n-type block copolymer **BP4'** *via* CuAAC coupling

The synthesis of p-type-n-type block copolymer **BP4'** *via* the use of CuAAC chemistry, was performed as described in Chapter 7 (5 eq PMDETA (N,N,N',N'',N'''-pentamethyldiethyleentriamine) as the ligand and 5 eq of Cu(I)Br in DMF as the solvent). Synthesis was started from BEH-PPV¹⁶ with an alkyne- functionality **P5'** (0.1 eq of anionic initiator **19**),¹⁹ and a CN-PPV block with azide functionality **P6'** (0.1 eq of anionic initiator **20**).

8.2.5. Hydrolysis of P3 to reach poly[1,4-(2-(5-carboxypentyloxy)-5-methoxyphenylene) vinylene] (CPM-PPV) P4Scheme 8.9: Hydrolysis of ester-functionalized PPV towards CPM-PPV (**P4**)

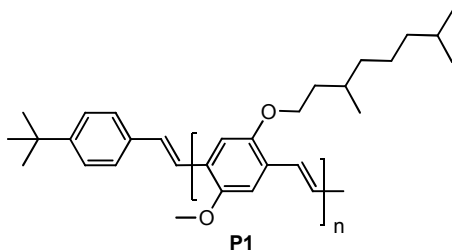
Conjugated polymer **P3** was synthesized *via* elimination of **P4'** following the general procedure.¹⁶ To obtain the acid-functionalized polymer **P4**, conjugated polymer **P3** (0.06g, 0.19 mmol of ester functionalities) was dissolved in dioxane (20 mL) and heated to reflux.⁴ A mixture of K^tBuO (0.22g, 1.94 mmol) in water (1 mL) was added and the resulting reaction mixture was refluxed for 4 h. After cooling down, HCl (1M solution in H₂O, 100 mL) and CH₂Cl₂ were added and the organic phase was extracted with water. After evaporating the water layer, polymer **P4** was obtained as a red solid.

8.3. RESULTS AND DISCUSSION

8.3.1. Testing the anionic nature of the polymerization reactions for different sulfinyl monomers

For the MDMO-, ester-functionalized- and CN-substituted premonomers (**6**, **11** and **16** respectively) the anionic nature of the sulfinyl precursor route, using LHMDS as the base and THF as the solvent, was tested. Therefore two polymerization reactions were performed each, a first one following the general anionic polymerization procedure with LHMDS as the base and THF as the solvent and a second one using this general procedure with the addition of TEMPO. In this second test all potentially present radicals are killed and molecular weight and yield will drop dramatically because no polymerization can take place. If no radicals are present, molecular weights and yields are comparable for both tests and a pure anionic polymerization is obtained as previously reported for plain-PPV and BEH-PPV (symmetrically bis(2-ethylhexyloxy) substituted PPV).^{16,20} As a second confirmation for the anionic nature of the polymerization reaction for the different monomers, anionic initiators were used in different equivalents towards the monomer. If a linear correlation between the inverse of the degree of polymerization and the initial initiator concentration is observed, independent indication for the anionic polymerization is given.

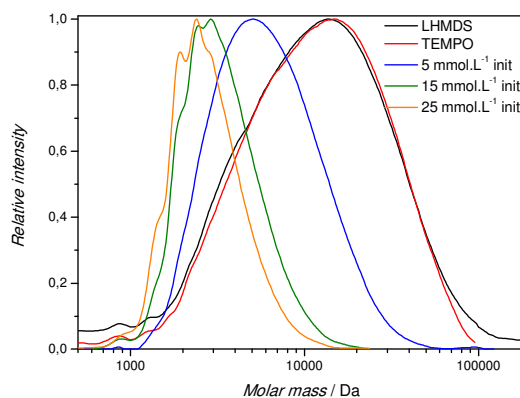
8.3.1.1. Anionic polymerization to obtain well-defined MDMO-PPV


 Figure 8.3: MDMO-PPV **P1**

For MDMO-PPV five polymerization reactions were performed. A first one being the normal anionic polymerization with LHMDS as the base in THF as the solvent and a second one being a polymerization with the addition of TEMPO. The last tests performed, were three polymerization reactions with addition of 0.1, 0.3 and 0.5 eq of anionic initiator **17**. Results regarding molecular weights, *PDI*s and yields can be found in Table 8.1 and the SEC chromatograms are plotted in Figure 8.4.

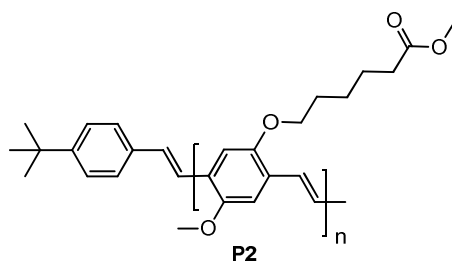
 Table 8.1: Results regarding MWD, *PDI* and yield for the anionic polymerization of MDMO-premonomer **6** with LHMDS in THF (15 min; 0 °C; $[M]_i = 0.05$ M)

Additive	[X] / mmol·L ⁻¹	Precursor polymer		Conjugated polymer		
		M_n^{app} / g·mol ⁻¹	<i>PDI</i>	M_n^{app} / g·mol ⁻¹	<i>PDI</i>	Yield / %
None		4100	2.4	7600	2.3	86
TEMPO	25	4100	2.4	8200	2.1	88
Init 17	5	2600	1.8	4900	1.6	61
Init 17	15	1800	1.3	2900	1.3	58
Init 17	25	1300	1.3	2500	1.2	46

Figure 8.4: SEC profiles for conjugated polymers **P1**

As is clear from Table 8.1 and Figure 8.4, molecular weights are comparable for the polymerization with no additive or with TEMPO as an additive and both with high yields. From these results it could undoubtedly be concluded that an anionic polymerization pathway is followed. By using an anionic initiator, the molecular weight could be tuned and lower *PDI*s were reached. If the gained results for MDMO-PPV were compared to the results obtained for BEH-PPV (see Tables 3.2 and 3.3 in Chapter 3), overall lower molecular weights were reached for the anionic polymerization of MDMO-PPV (this could be due to e.g. the different monomer structure or slight monomer impurities present).

8.3.1.2. Anionic polymerization to obtain well-defined ester-functionalized PPV

Figure 8.5: Ester-functionalized PPV **P2**

For monomer **11**, exactly the same anionic polymerization reactions were tested as described for monomer **6** in order to prove the anionic polymerization pathway. Results regarding molecular weights, polydispersities and yields can be found in Table 8.2 and GPC profiles for the conjugated polymers are plotted in Figure 8.6.

Table 8.2: Results regarding MWD, *PDI* and yield for the anionic polymerization of premonomer **11** to yield ester-functionalized PPV with LHMDS in THF (15 min; 0 °C; $[M]_i = 0.05 \text{ M}$)

Additive	$[X] / \text{mmol}\cdot\text{L}^{-1}$	Precursor polymer		Conjugated polymer		
		$M_n^{\text{app}} / \text{g}\cdot\text{mol}^{-1}$	<i>PDI</i>	$M_n^{\text{app}} / \text{g}\cdot\text{mol}^{-1}$	<i>PDI</i>	Yield / %
None		4700	2.9	9300	2.1	95
TEMPO	25	3700	3.0	7700	2.4	95
Init 17	5	3000	2.1	4800	1.8	72
Init 17	15	1700	1.9	3800	1.5	68
Init 17	25	1300	1.7	2800	1.3	44

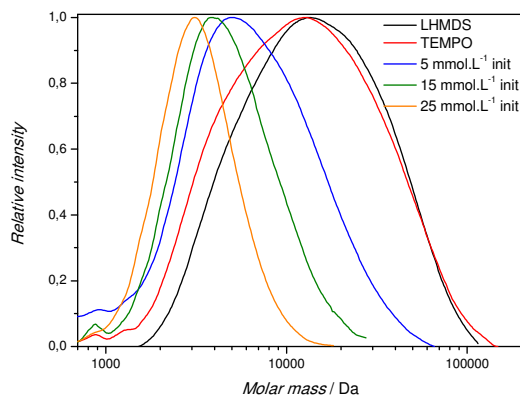


Figure 8.6: GPC profiles for conjugated ester-protected CPM-PPV polymers **P2**

From Figure 8.6, it can clearly be concluded that the GPC profiles for both the pure anionic test reaction and the reaction with addition of TEMPO, are very similar and polymers were obtained in high yields. From these results, it can be

concluded that a pure anionic polymerization reaction also takes place for monomer **11**. Upon addition of anionic initiator **17**, lower molecular weights could be reached, which could be tuned using different amounts of initiator during the polymerization reaction.

8.3.1.3. Anionic polymerization to obtain well-defined CN-PPV

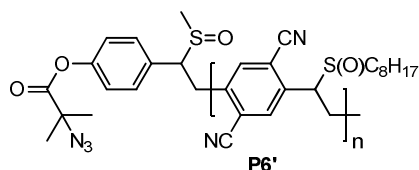


Figure 8.7: Precursor CN-PPV **P6'**

For CN-substituted monomer **16**, the same polymerizations were again performed as for MDMO- and CPM-premonomers **6** and **11**, but here anionic initiator **20** was used instead of **17** (only for synthetic reasons). For CN-PPV **P6'**, no elimination reaction was performed because of the insoluble conjugated polymer that would result due to the short functionalities built in on the aromatic core. Results towards MWD and *PDI* for these polymerization reactions (precursor polymers) can be found in Table 8.3 and GPC profiles are given in Figure 8.8.

Table 8.3: Results regarding MWD and *PDI* for the anionic polymerization of CN-substituted premonomer **16** with LHMDS in THF (5 min; 0 °C; $[M]_i = 0.05$ M)

Additive	[X] / mmol·L ⁻¹	Precursor polymer	
		M_n^{app} / g·mol ⁻¹	<i>PDI</i>
None		4900	3.1
TEMPO	25	3100	3.1
Init 20	5	4600	2.1
Init 20	15	2000	2.1
Init 20	25	1300	2.0

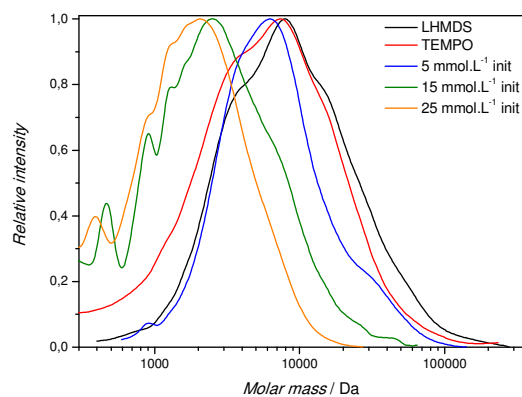


Figure 8.8: GPC profiles for CN-PPV precursor polymers **P6'**

For the cyano-substituted monomer **16** (see Table 8.3), rather low molecular weights were reached with high polydispersities. As is clear from Table 8.3 and Figure 8.8, molecular weights for the polymers obtained in the standard anionic polymerization reaction and the reaction with addition of TEMPO, were very similar (all with quantitative yields). With using higher initiator content, lower molecular weights could be reached and an anionic polymerization pathway is also found for this premonomer, even if the control seems to be somewhat more limited.

8.3.1.4. General overview for the anionic polymerization of different premonomers

To compare the results gained for all different monomers at different initiator concentrations, the inverse of the degree of polymerization ($1/DP_n$) was plotted against the initiator concentration for the (unpurified) precursor polymers **P1'**, **P2'** and **P6'** (see Figure 8.9).

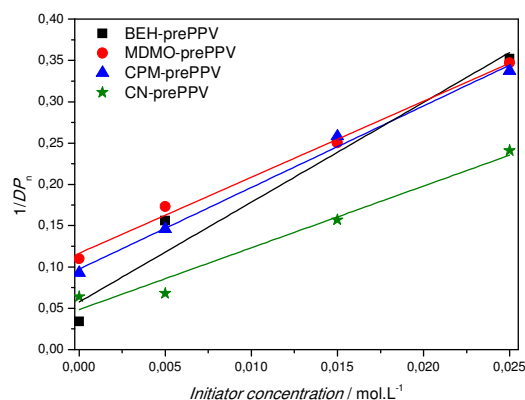
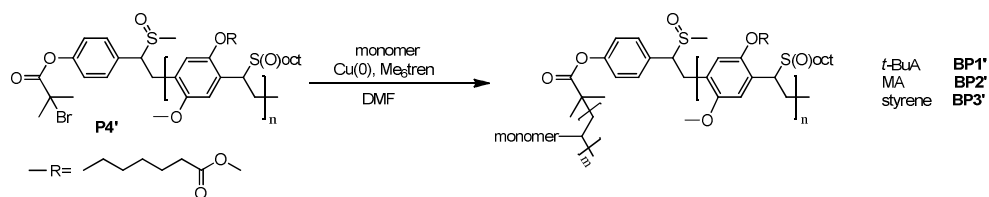


Figure 8.9: Inverse of degree of polymerization (precursor polymer) versus the initiator concentration for the anionic polymerization of different premonomers

It can be concluded that the polymerization for BEH-PPV, MDMO-PPV and CPM-PPV results in comparable degrees of polymerization, with the slope for the BEH-PPV polymerization being a bit steeper as for the other two (because higher molecular weights are reached when no initiator is used). For the cyano-substituted monomer, overall the polymerizations result in a higher degree of polymerization but comparable molecular weights as for the p-type monomers were obtained.

8.3.2. Outlook towards functionalized block copolymers

8.3.2.1. Block copolymers containing an ester-functionalized PPV polymer block



Scheme 8.10: Synthesis of block copolymers starting from **P4'**

As described in Chapter 6, BEH-PPV-*b*-P(*t*-BuA) block copolymers could be synthesized starting from a bromine-functionalized BEH-PPV block which could reinitiate the polymerization of the second monomer *via* SET-LRP. In this way a block copolymer was reached which, after hydrolysis of the acrylate block, could self-assemble in methanolic conditions as confirmed using DLS measurements.² With using the same anionic initiator (**18**) for the synthesis of a well-defined ester-protected CPM-PPV with bromine-functionality (**P4'**), the same strategy towards block copolymers could be followed. Three different monomers were tested in the SET-LRP reaction, namely *tert*-butyl acrylate (*t*-BuA), methyl acrylate (MA) and styrene (Scheme 8.10). Molecular weights and polydispersities for the starting block (precursor) as well as the block copolymers (PPV precursor blocks) are given in Table 8.4 and the GPC profiles are displayed in Figure 8.10.

Table 8.4: MWDs and *PDI*s for different block copolymers containing one ester-precursor CPM-PPV precursor block

Polymer		$M_n^{\text{app}} / \text{g}\cdot\text{mol}^{-1}$	<i>PDI</i>
prePPV	P4'	1900	1.7
prePPV- <i>b</i> -P(<i>t</i> -BuA)	BP1'	3600	2.4
prePPV- <i>b</i> -PMA	BP2'	3400	2.2
prePPV- <i>b</i> -PS	BP3'	2200	2.6

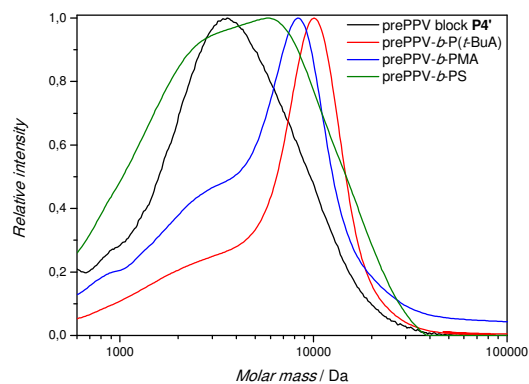


Figure 8.10: GPC profiles for block copolymers containing one ester-functionalized PPV block (precursors)

From the GPC profiles in Figure 8.10, it is clear that for both acrylates (*t*-BuA and MA), block copolymer formation is found, but still pure PPV precursor polymer is present (see low molecular weight shoulder that can be compared to the black curve of the starting PPV precursor block). A second conclusion that can be drawn from the GPC profiles is that the polymerization of styrene as the second block, was not successful. Possible solutions to gain a fully successful block copolymer *via* SET-LRP could be to perform a purification of the precursor PPV polymer and/or further improvement of the reaction conditions for the SET-LRP reaction.

In order to obtain functionalized PPV chains, it was earlier reported that the acid-functionality of the CPM units could easily be converted with different functional alcohols *via* an optimized DCC/DMAP procedure for a MDMO-CPM-PPV (9/1) copolymer.⁴ After hydrolysis of **P3**, CPM-PPV **P4** was reached (as confirmed with ATR FT-IR measurements, Figure 8.11) as a water soluble PPV material for which no further DCC/DMAP functionalization was possible in CH₂Cl₂ (because of this solubility limitation).

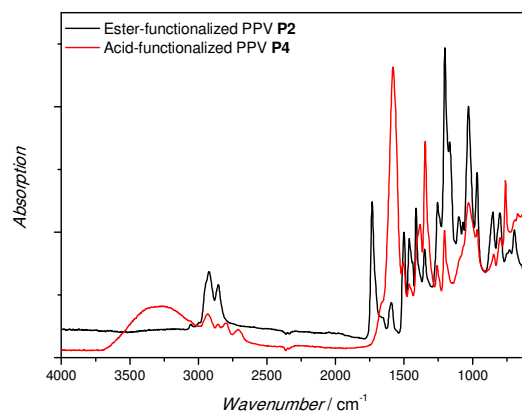


Figure 8.11: ATR FT-IR spectra for **P2** compared to **P4**

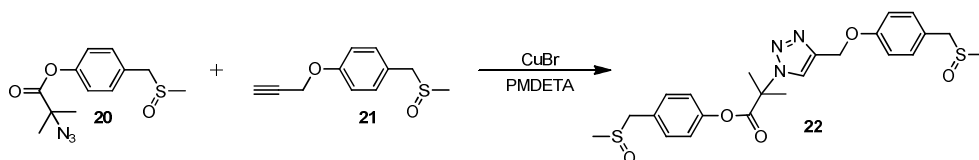
As an outlook for this project, synthesis of e.g. CPM-PPV-*b*-PS block copolymers with relative long PS blocks (to ensure solubility in organic solvents for the CPM block) could be interesting. In this way the acid function becomes available for functionalization with functional alcohols in a post-polymerization DCC/DMAP process in organic solvents such as CH₂Cl₂ in order to obtain block copolymers for new applications.

8.3.2.2. *P*-type-*n*-type block copolymers consisting of two PPV blocks via CuAAC coupling

As already mentioned, *p*-type-*n*-type block copolymers could be interesting materials to introduce in oPVs (organic photovoltaics) because of their corresponding structure and therewith the absence or limitation of phase segregation. Because both blocks should be attached to each other with a spacer (conjugation between both blocks would result in a charge trap), *Click* chemistry is an excellent method to use for this approach.

In order to make sure that an efficient *Click* reaction is obtained between the alkyne-functionalized *p*-type and azide-functionalized *n*-type block, a test

reaction was performed on anionic initiators **20** and **21** (see Scheme 8.11) using the same reaction conditions as for the CuAAC ligation that would be used to couple both polymer blocks (DMF as the solvent, 5 eq Cu(I)Br and 5 eq PMDETA).



Scheme 8.11: *Click* test reaction between azide- and alkyne-functionalized anionic initiators **20** and **21**

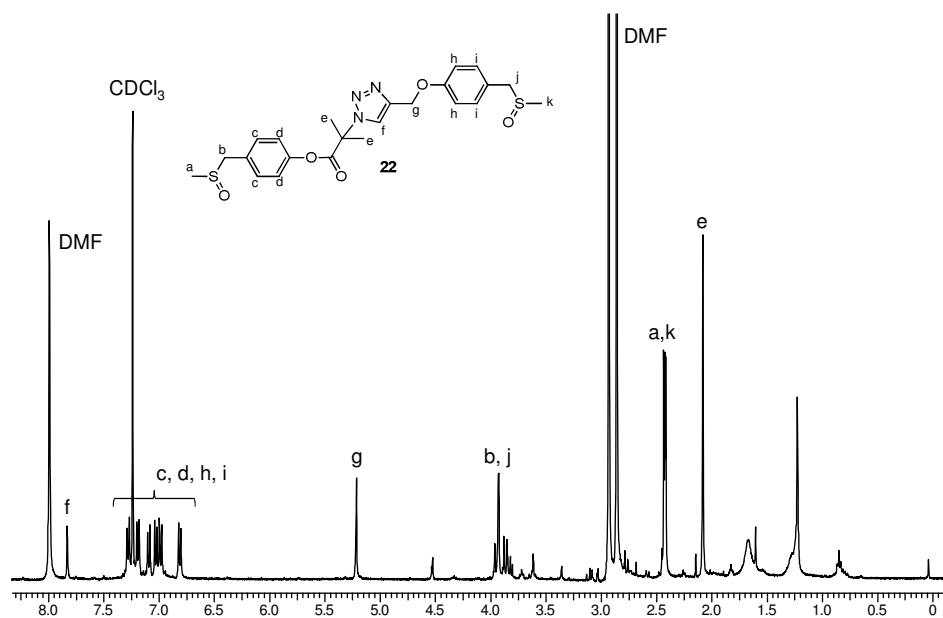


Figure 8.12: ¹H NMR spectrum for CuAAC between anionic initiators **20** and **21** (unpurified)

As is clear from the (unpurified) ^1H NMR spectrum of compound **22** (Figure 8.12), a successful *Click* reaction was obtained between both anionic initiators as the signal for the proton on the triazole ring is clearly present and no signals of the starting compounds were present anymore.

In order to obtain a p-type–n-type block copolymer, a BEH-PPV block with an alkyne functionality was coupled with an azide-functionalized CN-PPV block. In earlier ESI-MS studies (described in Chapter 6), very high initiator efficiency was proven for the BEH-PPV block. To make sure that also this high efficiency is found for the CN-PPV, two low molecular weight polymers (0.5 eq of initiator) were synthesized (Table 8.5) with different anionic initiators and the ESI-MS spectra (azide-functionalized initiator **20**, Figure 8.13, and initiator **17** with *tert*-butyl functionality, Figure 8.14) were compared.

Table 8.5: Molecular weights and polydispersities for CN-substituted precursor polymers used in ESI-MS study with different initiators (0.5 eq init; 5 min; 0 °C; $[\text{M}]_i = 0.05 \text{ M}$)

Initiator	$M_n^{\text{app}} / \text{g}\cdot\text{mol}^{-1}$	<i>PDI</i>
20	1300	2.0
17	1400	2.2

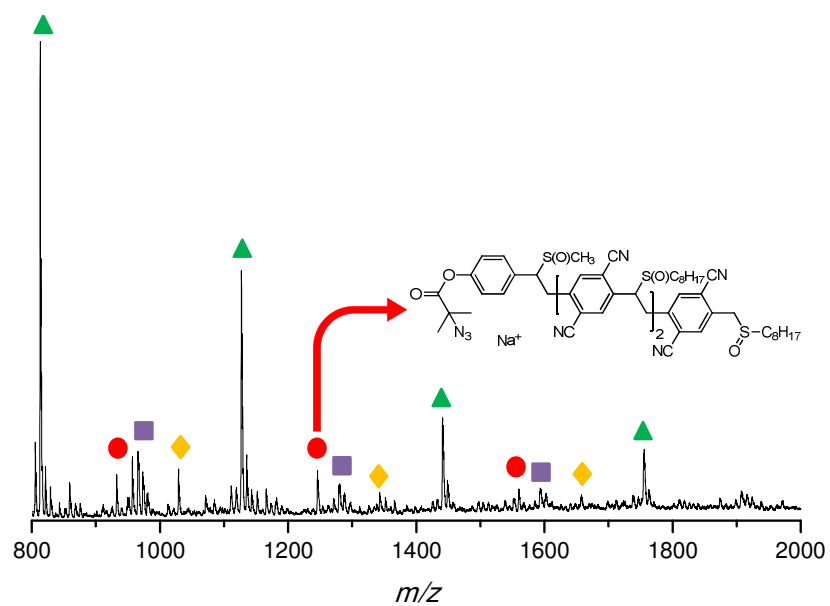


Figure 8.13: ESI-MS spectrum for CN-PPV precursor polymer with azide-functionality

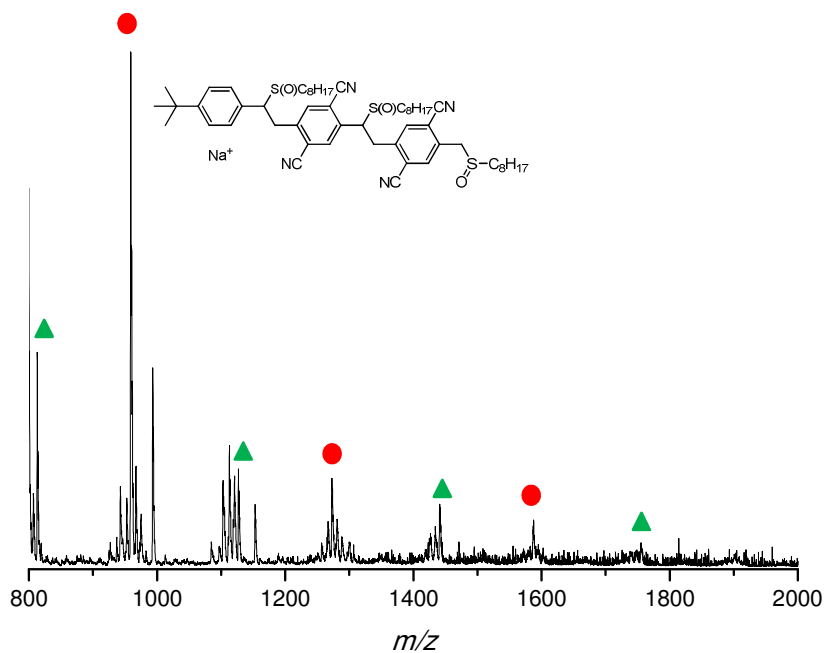


Figure 8.14: ESI-MS spectrum for CN-PPV precursor polymer with *tert*-butyl functionality

It is clear that the desired product (assigned with red circle), with the anionic initiator in α -position of the polymer chain and a sulfinyl group in ω -position, was present in both spectra (although in low intensity for the azide-functionalized polymer). The peaks indicated with purple squares and orange diamonds in Figure 8.13, could not be assigned so far. The peaks assigned with the green triangles (structure of the polymer unknown so far), appear in both spectra with exactly the same m/z values for both polymers and because both anionic initiators are substituted with a different sulfinyl group (methyl for **20** and octyl for **17**) a second confirmation is thereby found indicating that no initiator is incorporated in this polymer chain. All these findings lead to the conclusion that the anionic initiation for the CN-PPV is less efficient as proven for BEH-PPV. For this reason the CuAAC reactions performed to synthesize p-type-n-type block copolymers, did not result in successful coupling of both blocks. As a preliminary example, with the use of a low molecular weight CN-PPV precursor block gained from precipitation in cold MeOH, a semi-successful coupling could be reached (see Table 8.6 and Figure 8.15).

Table 8.6: MWDs and *PDI*s for starting PPV blocks, **P5'** and **P6'**, and p-type-n-type block copolymer **BP4'**

Polymer	$M_n^{\text{app}} / \text{g}\cdot\text{mol}^{-1}$	PDI
BEH-PPV P5'	3200	2.0
CN-PPV P6'	3600	2.1
BP4'	3200	6.2

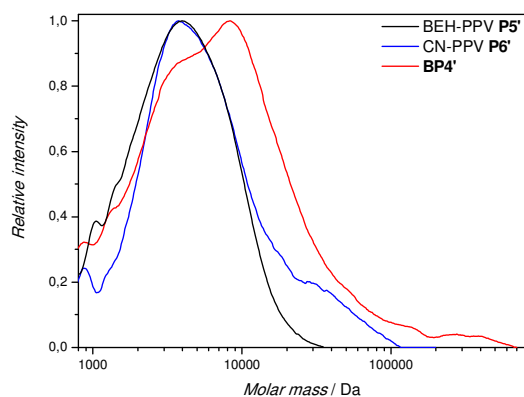


Figure 8.15: GPC profiles for p- and n-type PPV compared to the *Clicked* product **BP4'**

As is clear from the GPC profiles presented in Figure 8.15, still a rather big amount of both PPV homopolymers were present after *Click* reaction, which is off course due to the low initiation efficiency that was found for the n-type block. More research on this topic will be required in first place on the anionic initiation of the CN-PPVs and only then it will be possible to proceed towards the successful synthesis of a p-type–n-type block copolymer (potentially followed by a separation of the block copolymer from the homopolymers using preparative recycling GPC) that can be tested in an organic photovoltaic device.

8.4. CONCLUSION

In conclusion it can be stated that the anionic polymerization pathway for the sulfinyl precursor route can be extended to all kinds of premonomers (different alkyloxy side chains and cyano-functionalized cores). The substituents on the aromatic core do have an influence on the molecular weight that could be reached in the anionic pathway, but upon addition of TEMPO, for all different monomers tested in the anionic route, comparable molecular weights and yields are obtained as for the polymerization without addition of TEMPO. This clearly proves the absence of radicals during the polymerization reaction performed with LHMDS as the base and THF as the solvent. With addition of different amounts of anionic initiator, a linear behavior between the inverse of the degree of polymerization and the initiator concentration is identified, leading to the conclusion that well-defined PPVs, with preselectable molecular weights, can be produced for all different monomers.

For the synthesis of functionalized block copolymers, starting from an ester-functionalized PPV block, SET-LRP is possible for the addition of an acrylate (either *tert*-butyl acrylate or methyl acrylate) as the second block, although, still a low molecular weight shoulder was present in the GPC profiles referring to an incomplete reinitiation. Optimization for the built-in of this second block, also using styrene as the second block, is still matter of further research. In order to obtain a p-type-n-type block copolymer, an alkyne-functionalized BEH-PPV block is coupled in a CuAAC coupling reaction with an azide-functionalized CN-PPV block. Also here further research is still necessary on the anionic initiation of the CN-PPV block. Using ESI-MS experiments, it is shown to be less efficient and thus no successful CuAAC coupling could be obtained between the p-type and n-type polymer blocks yet.

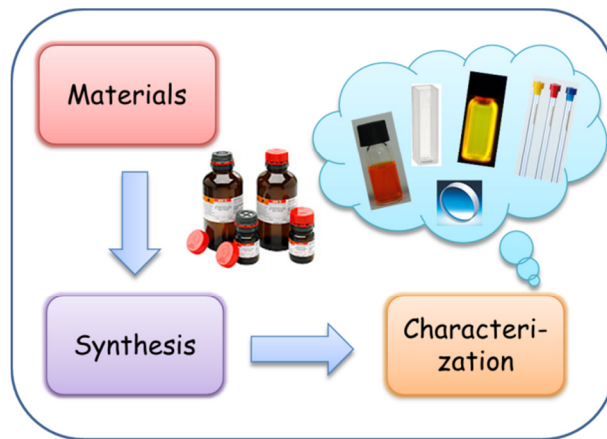
8.5. REFERENCES

- ¹ I. Cosemans, J. Vandenberg, V. S. D. Voet, K. Loos, L. Lutsen, D. Vanderzande, T. Junkers, *Polymer* **2013**, *54*, 1298–1304.
- ² I. Cosemans, J. Vandenberg, L. Lutsen, D. Vanderzande, T. Junkers, *Polym. Chem.* **2013**, *4*, 3471–3479.
- ³ I. Cosemans, J. Vandenberg, L. Lutsen, D. Vanderzande, T. Junkers, **2013**, to be submitted.
- ⁴ J. Duchateau, L. Lutsen, W. Guedens, T. J. Cleij, D. Vanderzande, *Polym. Chem.* **2010**, *1*, 1313–1322.
- ⁵ R. A. Segalman, B. McCulloch, S. Kirmayer, J. J. Urban, *Macromolecules* **2009**, *42*, 9205–9216.
- ⁶ J. J. M. Halls, C. A. Walsh, N. C. Greenham, E. A. Marseglia, R. H. Friend, S. C. Moratti, A. B. Holmes, *Nature* **1995**, *376*, 498–500.
- ⁷ S. J. Gaskell, *J. Mass Spectrom.* **1997**, *32*, 677–688.
- ⁸ S. D. Hanton, *Chem. Rev.* **2001**, *101*, 527–569.
- ⁹ J.-J. Cid, C. Ehli, C. Atienza-Castellanos, A. Gouloumis, E.-M. Maya, P. Vázquez, T. Torres, D. M. Guldi, *Dalton Trans.* **2009**, 3955–3963.
- ¹⁰ H. Becker, H. Spreitzer, K. Ibrom, W. Kreuder, *Macromolecules* **1999**, *32*, 4925–4932.
- ¹¹ F. Louwet, D. Vanderzande, J. Gelan, J. Mullens, *Macromolecules* **1995**, *28*, 1330–1331.
- ¹² A. J. J. M. van Breemen, *PhD thesis*, Limburgs Universitair Centrum, **1999**.
- ¹³ L. Friedman, H. Shechter, *J. Org. Chem.* **1961**, *26*, 2522–2524.
- ¹⁴ G. P. Ellis, T. M. Romney-Alexander, *Chem. Rev.* **1987**, *87*, 779–794.
- ¹⁵ R. K. McCoy, F. E. Karasz, *Chem. Mater.* **1991**, *3*, 941–947.

- ¹⁶ I. Cosemans, J. Wouters, T. Cleij, L. Lutsen, W. Maes, T. Junkers, D. Vanderzande, *Macromol. Rapid Commun.* **2012**, *33*, 242–247.
- ¹⁷ S. Gillissen, L. Lutsen, D. Vanderzande, J. Gelan, *Synth. Met.* **2001**, *119*, 137–138.
- ¹⁸ S. Gillissen, *PhD thesis*, Limburgs Universitair Centrum, **2002**, Chapter 2.
- ¹⁹ Synthesis of the BEH-PPV block , see Chapter 7.
- ²⁰ I. Cosemans, L. Hontis, D. Van Den Berghe, A. Palmaerts, J. Wouters, T. Cleij, L. Lutsen, W. Maes, T. Junkers, D. Vanderzande, *Macromolecules* **2011**, *44*, 7610–7616.

CHAPTER 9

Materials and Characterization



9.1. MATERIALS

All solvents and reagents were purchased from VWR, Acros or Aldrich and were used without further purification. THF was dried by distillation from Na/benzophenone for polymerizations described in Chapter 2, 3 and 4. THF, used in polymerizations described in Chapters 5 – 8, DMF and CH₂Cl₂ were dried on a MB-SPS 800 system (if indicated as dry solvent). *Tert*-butyl acrylate was distilled over CaH₂ and kept in the freezer under nitrogen atmosphere.

On the specialized setup, used at the University of Groningen (Chapter 5), THF was dried over *tert*-butyl lithium (1.9 M in pentane) and condensed under reduced pressure. *Tert*-butyl acrylate was dried over calcium hydride, distilled under reduced pressure and stored under nitrogen at 6 °C.

9.2. CHARACTERIZATION

9.2.1. Standard characterization techniques for monomers and initiators

¹H and ¹³C NMR spectra were recorded in CDCl₃ or CD₂Cl₂ on a Varian Inova 300 spectrometer at 300 and 75 MHz respectively using a 5 mm probe.

Direct insertion probe/mass spectrometry (DIP MS) analyses were obtained with a Varian TSQ-70 and Voyager mass spectrometer (Thermoquest). The capillary column was a Chrompack Cpsil5CB or Cpsil8CB.

FT-IR and ATR FT-IR spectra were collected on a Bruker Tensor 27 FT-IR spectrophotometer (nominal resolution 4 cm⁻¹).

Melting points were determined using a Electrothermal IA9000 series Digital Melting Point Apparatus.

9.2.2. Specialized NMR measurements: (semi-)quantitative ^{13}C NMR and APT NMR

Semi-Quantitative ^{13}C and Attached Proton Test (APT) liquid-state NMR spectra were recorded on a Varian Inova 300 spectrometer in a 5 mm four-nucleus PFG probe ($B_0 = 7.2$ Tesla; Larmor frequency for ^{13}C about 75 MHz). Experimental parameters for the ^{13}C liquid-state NMR spectra were a spectral width of 17 kHz, a 90° pulse length of 12 μsec , an acquisition time of 0.7 sec and a preparation delay time of 75 sec. A broad-band (BB) proton decoupling was only applied during the 90° pulse and acquisition time (inverse gated decoupling) in order to ensure a quantitative spectrum. In this rather short time span the Nuclear Overhauser Effect (NOE) cannot build up. However, by applying BB decoupling all information regard to the carbon multiplicity is lost. Therefore an APT experiment was performed to regain the carbon multiplicity information. As for many pulse sequences, the refocusing 180°_{X} pulse is very essential for an APT pulse sequence. Depending on the number of hydrogen atoms bound to a particular ^{13}C atom, the corresponding magnetic moments will evolve differently after the initial 90°_{X} pulse. The delay τ is set to the inverse of the carbon proton coupling constant $^1J_{\text{CH}}$. For aliphatic sp^3 carbon atoms this $^1J_{\text{CH}}$ is at average about 140 Hz so the delay τ is around 7 msec. In that way non-protonated and CH_2 carbons show positive intensities while CH and CH_3 carbons show negative intensities in the APT spectrum.

9.2.3. Spectroscopic techniques: UV-Vis and fluorescence spectroscopy

UV-Vis spectra were recorded on a Varian Cary 500 UV-Vis-NIR spectrophotometer (scan rate $600 \text{ nm}\cdot\text{min}^{-1}$, continuous run from 200 to 800 nm).

Fluorescence measurements were performed using a 'Fluorolog[®] Tau-3 Lifetime System' spectrofluorometer from Horiba Group, USA. The entire system was controlled by DataMax software. The excitation wavelength was kept at 466 and 495 nm and the emission was scanned between respectively 490 or 520 and 800 nm. The sample was placed at an angle of 22.5°, resulting in the highest fluorescence signal with a minimum of scattering and reflection coming from the glass. The slits of both monochromators were adjusted to 5 nm.

9.2.4. Size exclusion chromatography (SEC) / Gel permeation chromatography (GPC) / Multi angle laser light scattering (MALLS)

Analytical SEC (polymers described in Chapters 2 – 4) was performed using a Spectra Series P100 (Spectra Physics) pump equipped with two mixed-B columns (10 µm, 2 cm × 30 cm, Polymer Labs) and a refractive index detector (Shodex) at 70 °C. THF was used as the eluent at a flow rate of 1.0 mL·min⁻¹. Molecular weight distributions were determined relative to polystyrene standards because Mark-Houwink parameters are not available for the polymers under investigation.

Analysis of the MWDs of the polymer samples described in Chapter 5 – 8 were performed on a Tosoh EcoSEC System, comprising an autosampler, a PSS guard column SDV (50 × 7.5 mm), followed by three PSS SDV analytical linear XL columns (5 µm, 300 × 7.5 mm) and a differential refractive index detector (Tosoh EcoSEC RI) using THF as the eluent at 40 °C with a flow rate of 1 mL·min⁻¹. The SEC system was calibrated using linear narrow polystyrene standards ranging from 474 to 7.5 × 10⁶ g·mol⁻¹ (PS (K = 14.1 × 10⁻⁵ dL·g⁻¹ and α = 0.70)). Polymer concentrations were in the range of 3–5 mg·mL⁻¹. Because

Mark-Houwink parameters are not available for the polymers under investigation, only apparent values are discussed.

Analysis of the MWDs of the polymers with UV detection at λ_{\max} of the polymer was performed using a Spectra Series P100 (Spectra Physics) pump equipped with two mixed-B columns (10 μm , 2 cm x 30 cm, Polymer Laboratories) and an Agilent 1100 DAD UV detector at 60 °C. Chlorobenzene (CB) was used as the eluent at a flow rate of 1.0 mL \cdot min $^{-1}$. Molecular weights were determined relative to polystyrene standards.

MALLS (multi angle laser light scattering) measurements were obtained using a Wyatt DAWN HELIOS 18 angle light scattering device with fused silica cells and a laser wavelength of 658.0 nm. THF was used as the eluent at a flow rate of 1.0 mL \cdot min $^{-1}$ at 40 °C.

9.2.5. Electrospray ionization – mass spectrometry (ESI–MS)

ESI–MS spectra were recorded on a LCQ Fleet mass spectrometer (ThermoFischer Scientific) equipped with an atmospheric pressure ionization source operating in the nebulizer assisted electro spray mode. The instrument was calibrated in the m/z range 220–2000 using a standard solution containing caffeine, MRFA and Ultramark 1621. A constant spray voltage of 5 kV was used and nitrogen at a dimensionless auxiliary gas flow-rate of 10 and a dimensionless sheath gas flow-rate of 3 were applied. The capillary voltage, the tube lens offset voltage and the capillary temperature were set to 25 V, 120 V, and 275 °C respectively. A 250 μL aliquot of a polymer solution with concentration of 10 $\mu\text{g}\cdot\text{mL}^{-1}$ was injected. A mixture of CH_2Cl_2 and methanol (1/3), all HPLC grade, was used as the solvent.

9.2.6. Thermal analysis, DSC and TGA

Differential scanning calorimetry (DSC) measurements were performed on a TA instruments Q200 DSC, purged with nitrogen. About 5 mg samples were sealed in aluminum crucibles (Tzero, 40 μL). The scan rate was 20 $^{\circ}\text{C}\cdot\text{min}^{-1}$ for temperatures ranging from -90 $^{\circ}\text{C}$ – 120 $^{\circ}\text{C}$. Three heating-cooling cycles were run to check the reproducibility.

Thermo gravimetric analysis (TGA) was performed on a TA instruments HiRes TGA 2950 Thermo gravimetric analyzer with a heating rate of 10 $^{\circ}\text{C}\cdot\text{min}^{-1}$.

9.2.7. Dynamic light scattering (DLS) for determination of hydrodynamic diameter of nanoparticles

The average hydrodynamic diameter and the polydispersity index of the nanoparticles were determined using a ZetaPALS equipment (Brookhaven Instruments Cooperation).

SUMMARY

Tailor-made poly(*p*-phenylene vinylene)s (PPVs) are presented in this thesis with their ability to be polymerized in an anionic fashion starting from sulfinyl premonomers. For this sulfinyl precursor route, it is shown that with the use of lithium hexamethyldisilazide (LHMDS) as the base and THF as the solvent, the polymerization mechanism can be shifted towards a pure anionic pathway leading towards well-defined polymers. Further it is shown that this anionic mechanism can be applied to plain-PPV as well as different substituted premonomers (symmetrical and (ester-functionalized) unsymmetrical alkyloxy- and cyano side groups incorporated on the aromatic core). The most studied polymer in this thesis is the symmetrically substituted poly[2,5-bis(2-ethylhexyloxy)*p*-phenylene vinylene] (BEH-PPV).

With the use of anionic initiators, with a structure similar to the premonomer structure, efficient control is reached over molecular weight (between 15500 and 3000 g·mol⁻¹ for conjugated material) and *PDI* (1.5 – 1.1). The high efficiency of incorporation of these units with different functionalities, is proven using electrospray ionization – mass spectrometry (ESI-MS). Because of the linear correlation that is found between molecular weight versus amount of initiator used, this high initiator efficiency is assumed to translate to all polymers synthesized using this method, underpinning the living nature of the polymerization. The ω -chain end cannot be controlled as confirmed *via* either ESI-MS or using a ¹³C-labeled end-capper. In further experiments the addition mode of the initiator to the reaction mixture and reaction temperature and time are explored. These experiments reveal that the polymerization reaction is very

fast, even at reaction time "zero" and reaction temperature $-78\text{ }^{\circ}\text{C}$ high molecular weight ($5900\text{ g}\cdot\text{mol}^{-1}$) is reached for a polymerization reaction with addition of 0.1 eq of initiator, and thus no kinetics are studied for this system so far. In a last attempt to enhance the control over the anionic pathway, a specialized anionic polymerization setup – in collaboration with the University of Groningen – is used to perform the polymerization reactions. As is shown in this work, the obtained results are in good agreement with the results gained using the regular Schlenk lines (vacuum/ N_2).

In order to obtain self-assembled structures, different block copolymer synthesis approaches are studied in this thesis. The first method that is tested is the direct coupling of an acrylate block to the anionic chain end of the PPV chain. Using this method, PPV-*b*-P(*t*-BuA) block copolymers can only be achieved after separation from the PPV homopolymer using preparative recycle GPC. A second – more promising method that was used to obtain these PPV-*b*-P(*t*-BuA) block copolymers – makes use of a dual-initiator strategy. To reach this goal, a bromine-functionalized anionic initiator is incorporated in the PPV chain which, in a consecutive step, can be reinitiated with a vinyl monomer polymerization like SET-LRP (single electron transfer – living radical polymerization). Using this method, block copolymers with different acrylate chain lengths can be obtained for which – after hydrolysis of the acrylate block – self-assembly is demonstrated *via* DLS (dynamic light scattering) measurements in methanolic solution. This method is also extended towards a PPV polymer with an ester-functionalized side chain (precursor for CPM-PPV), resulting in block copolymers with either *tert*-butyl acrylate or methyl acrylate as comonomer.

A last method to obtain block copolymers, and probably also the most universal one, is to make use of the well-known CuAAC (copper assisted azide-alkyne

cycloaddition) or *Click* coupling reaction. With using this method an alkyne-functionalized PPV block can be coupled with azide-functionalized PEG (poly(ethylene glycol)) blocks in order to obtain well-defined PPV-*b*-PEG block copolymers with different PEG chain lengths. Also for these block copolymers DLS measurements are performed in aqueous solution yielding different micellar structures with sizes depending on the PEG chain length.

With this successful CuAAC reaction in hands for PPV materials, the synthesis of a p-type–n-type block copolymer is envisaged consisting of two PPV blocks. The p-type block is a BEH-PPV block with alkyne-functionality and the n-type block a CN-PPV block with an azide-functional group. With using ESI-MS it becomes evident that for these cyano-functionalized monomers, anionic initiation is less efficient and thus no CuAAC coupling can be performed in order to obtain pure p-type–n-type block copolymers.

To conclude, the anionic pathway for the sulfinyl precursor route is successfully established for different monomers and with the use of functionalized anionic initiators, defined α -chain ends are obtained. Using this strategy, the synthesis of block copolymers, either *via* SET-LRP (for vinyl monomers) or *via Click* chemistry, is available and opens pathways towards a wide variety of materials and application of these block copolymers.

SAMENVATTING

In deze thesis worden op maat gemaakte poly(*p*-fenyleen vinyleen) (PPV) materialen beschreven en de mogelijkheid om deze polymeren te synthetiseren via een anionische route, uitgaande van sulfinyl premonomeren. Als er gebruik gemaakt wordt van lithium hexamethyldisilazide (LHMDS) als base en THF als oplosmiddel in deze sulfinyl precursor route, kan het polymerizatiemechanisme volledig omgebogen worden naar een zuivere anionische route die leidt tot goed gedefiniëerde polymeren. Ook is aangetoond dat dit anionisch mechanisme zowel op ongesubstitueerd PPV als op verschillende, gesubstitueerde premonomeren (symmetrische en (ester-gefunctionaliseerde) asymmetrische alkyloxy- en cyano-zijketens ingebouwd op de aromatische kern) toegepast kan worden. Het meest bestudeerde polymer in deze thesis is het symmetrisch gesubstitueerde poly[2,5-bis(2-ethylhexyloxy)*p*-fenyleen vinyleen] (BEH-PPV).

Door gebruik te maken van anionische initiatoren, met een vegelijkbare structuur als die van het premonomeer, wordt een efficiënte controle bereikt over zowel het molecular gewicht (tussen 15500 en 3000 g·mol⁻¹ voor de geconjugeerde polymeren) als de polydispersiteit (1.5 – 1.1) van de bekomen polymeren. Ook is aangetoond via electrospray ionisatie – massaspectrometrie (ESI-MS) dat de inbouw van deze eenheden, met een grote verscheidenheid aan functionaliteiten, gebeurt met een hoge efficiëntie. Door het lineaire verband dat gevonden wordt tussen het moleculaire gewicht en de hoeveelheid gebruikte initiator, wordt aangenomen dat deze hoge initiator efficiëntie vertaald kan worden naar alle polymeren die gesynthetiseerd worden via deze methode en is dus een extra bevestiging voor de levende natuur van deze anionische

polymerisatieroute. Via ESI-MS enerzijds en een ^{13}C -gelabelde eindgroep anderzijds is bevestigd dat het ω -keteneinde niet gecontroleerd kan worden. Verder onderzoek concentreert zich op de volgorde van toevoegen van de verschillende reagentia aan het reactiemengsel, reactietemperatuur en -tijd. Deze experimenten tonen aan dat de polymerisatiereactie zeer snel verloopt, want zelfs bij "nul" minuten reactietijd en een temperatuur van $-78\text{ }^\circ\text{C}$, voor een reactie met toevoeging van 0.1 equivalenten initiator, wordt een hoog moleculair gewicht ($5900\text{ g}\cdot\text{mol}^{-1}$) bereikt. Hierdoor is het tot dusver onmogelijk om de kinetica voor deze anionische route te bestuderen. Een laatste mogelijkheid die aangewend wordt om de controle over deze anionische polymerisatieroute te verbeteren, is het gebruik van een gespecialiseerde anionische polymerisatie opstelling – in samenwerking met Rijksuniversiteit Groningen – voor het uitvoeren van de reacties. Zoals aangetoond in dit werk, zijn de resultaten die met deze methode bereikt worden, in goede overeenkomst met de resultaten bereikt met Schlenk lijnen (vacuüm/ N_2), die normaler wijze gebruikt worden.

Om zelfgeassembleerde structuren te verkrijgen, worden in deze thesis verschillende benaderingen beschreven om blok copolymeren te synthetiseren. Een eerste methode die getest wordt, is de directe koppeling van een acrylaat blok aan het levende anionische keteneinde van de PPV keten. Door gebruik te maken van deze methode, kunnen PPV-*b*-P(*t*-BuA) blok copolymeren enkel bereikt worden als het blok copolymeer van het homopolymeer gescheiden wordt gebruik makend van preparatieve *recycle* GPC. Een tweede – en meer veelbelovende – strategie om deze PPV-*b*-P(*t*-BuA) block copolymeren te bereiken is gebruik te maken van een tweevoudige-initiator strategie. Hiertoe wordt een broom-gefunctionaliseerde initiator ingebouwd in de PPV keten die, in een volgende stap, gereïniëerd kan worden met een vinyl monomeer

polymerisatiereactie zoals bijvoorbeeld SET-LRP (*single electron transfer – living radical polymerization*). Door gebruik te maken van deze methode kunnen blok copolymeren met verschillende acrylaat blok lengtes bekomen worden die – na hydrolyse van het acrylaat blok – zelfassemblage vertonen in een oplossing van methanol, zoals aangetoond gebruik makend van DLS (*dynamic light scattering*) metingen. Deze tweevoudig-initiator strategie is verder uitgebreid naar een PPV polymeer met ester-gefunctionaliseerde zijketens (precursor voor CPM-PPV) en resulteert in blok copolymeren met enerzijds een *tert*-butyl acrylaat en anderzijds een methyl acrylaat als comonomeer.

Een laatste methode die beschreven is voor de synthese van blok copolymeren, en waarschijnlijk ook de meest universele, maakt gebruik van de welbekende CuAAC (*copper assisted azide-alkyne cycloaddition*) of *Click* koppelingsreactie. Door gebruik te maken van deze methode kan een alkyn-gefunctionaliseerd PPV blok gekoppeld worden met azide-gefunctionaliseerde PEG (poly(ethyleen glycol)) blokken van verschillende lengte om zo goed gedefiniëerde PPV-*b*-PEG blok copolymeren te bekomen. Ook voor deze blok copolymeren worden, in DLS metingen uitgevoerd in waterig midden, verschillende micellaire structuren waargenomen afhankelijke van de ketenlengte van het PEG blok.

Met deze succesvolle *Click* reactie in handen voor PPV materialen, wordt de synthese van een p-type–n-type blok copolymeer beoogd, opgebouwd uit twee PPV blokken. Het p-type blok bestaat uit een BEH-PPV blok met een alkyn-functionaliteit en het n-type blok is een cyano-PPV blok met een azide functie ingebouwd in de polymeerketen. Voor dit cyano-gefunctionaliseerd monomeer wordt echter een minder efficiënte inbouw van de anionische initiator waargenomen zoals vastgesteld via ESI-MS metingen. Hierdoor kan er dus geen

CuAAC koppeling uitgevoerd worden die een zuiver p-type-n-type blok copolymer oplevert.

Algemeen kan dus besloten worden dat de anionische polymerisatie voor de sulfinyl precursorroute succesvol bevestigd is voor verschillende monomeren en dat, gebruik makend van anionische initiatoren, gedefiniëerde α -keteneindes bereikt kunnen worden. Dankzij deze efficiënte inbouw wordt de synthese van blok copolymeren, via SET-LRP (voor vinyl monomeren) enerzijds of via *Click* chemie anderzijds, bereikt en is de weg geopend voor de synthese van verscheidene blok copolymeren en toepassing ervan.

LIST OF ABBREVIATIONS

°C	Degrees celcius
ΔT	Elevated temperature
δ	Chemical shift
λ	Wavelength
λ_{\max}	Wavelength at maximum absorbance
$[\eta]$	Intrinsic viscosity
a	Mark-Houwink constant
Ac ₂ O	Acetic anhydride
ADMET	Acyclic diene metathesis
AFM	Atomic force microscopy
APT	Attached proton test
Ar	Phenyl
ATR	Attenuated total reflectance
ATRP	Atom transfer radical polymerization
- <i>b</i> -	<i>Block</i>
BB	Broad-band
$[B]_i$	Initial base concentration
BEH-PPV	Poly[2,5-bis(2-ethylhexyloxy)- <i>p</i> -phenylene vinylene]
BPO	Dibenzoylperoxide
CB	Chlorobenzene
CBr ₄	Carbon tetrabromide
CCl ₄	Carbon tetrachloride
CD ₂ Cl ₂	Deuterated dichloromethane
CDCl ₃	Deuterated chloroform
CH ₂ Cl ₂	Dichloromethane
CHCl ₃	Chloroform
CI	Chemical impact ionization
C _i	Initiator concentration
C _m	Monomer concentration
CN	Cyano
CN-PPV	Poly[2,5-dicyano- <i>p</i> -phenylene vinylene]
CPM-PPV	Poly[2-methoxy-5-carboxypentyloxy)- <i>p</i> -phenylene vinylene]
Cu	Copper
CuAAC	Copper assisted azide-alkyne cycloaddition
Cu(I)Br	Copper(I) bromide
CuCN	Copper cyanide

Cu(I)I	Copper(I) iodide
d	Doublet
D ₂ O	Deuterium oxide
Da	Dalton
DBU	1,8-diazabicyclo[5.4.0]undec-7-ene
DCC	N,N'-Dicyclohexylcarbodiimide
DIAD	Diisopropyl azodicarboxylate
DIP MS	Direct insertion probe mass spectrometry
DLS	Dynamic light scattering
DMAP	Dimethylaminopyridine
DMF	Dimethylformamide
DNA	Deoxyribonucleic acid
<i>dn/dc</i>	Specific refractive index increment for a change of solute concentration
DPMK	Diphenylmethyl potassium
<i>DP_n</i>	Degree of polymerization
DSC	Differential scanning calorimetry
e ⁻	Electron
E _g	Bandgap
EI	Electron impact ionization
eq	Equivalent
ESI-MS	Electrospray ionization – mass spectrometry
Et ₂ O	Diethylether
EtOAc	Ethylacetate
EtOH	Ethanol
eV	Electron volt
FT-IR	Fourier transform-infrared spectroscopy
GPC	Gel permeation chromatography
h	Hour
h ⁺	Hole
H ₂ O	Water
H ₂ O ₂	Hydrogenperoxide
HSC ₈ H ₁₇	<i>n</i> -Octane thiol
H ₂ SO ₄	Sulfuric acid
HCl	Hydrochloric acid
HOMO	Highest occupied molecular orbital
HPLC	High-performance liquid chromatography
In	Initiator
[In]	Initiator concentration
<i>J</i>	Coupling constant

K	Mark-Houwink constant
kcps	Kilocounts per second
k_i	Rate constant for initiation
KOH	Potassium hydroxide
k_p	Propagation rate constant
K t BuO	Potassium <i>tert</i> -butoxide
L	Leaving group
LDA	Lithium diisopropylamide
LHMDS	Lithium hexamethyldisilazide
LUMO	Lowest unoccupied molecular orbital
m	Multiplet
M	Molar
$[M]_i$	Initial monomer concentration
m/z	Mass-to-charge ratio
M^+	Molecular ion
MA	Methyl acrylate
MALLS	Multi angle laser light scattering
MDMO-PPV	Poly[2-methoxy-5-(3,7-dimethyloctyloxy)- <i>p</i> -phenylene vinylene]
MEH-PPV	Poly[2-methoxy-5-(2-ethylhexyloxy)- <i>p</i> -phenylene vinylene]
Me ₆ tren	Tris[2-(dimethylamino)ethyl]amine
MeOH	Methanol
*MeOH	¹³ C-labeled methanol
MgSO ₄	Magnesium sulfate
MHKS	Mark-Houwink constants
MHz	MegaHertz
min	Minutes
MIP	Molecular imprinted polymer
MMPP·6H ₂ O	Magnesium bis(monoperoxyphthalate) hexahydrate
M_n	Number-average molecular weight
M_n^{app}	Apparent number-average molecular weight
Mp	Meltingpoint
MS	Mass spectrometry
M_w^{app}	Apparent weight-average molecular weight
MW, M or MWD	Molecular weight
N ₂	Nitrogen
Na	Sodium
NaCl	Sodium chloride
NaHCO ₃	Sodium bicarbonate

NaI	Sodium iodine
NaN ₃	Sodium azide
NaOH	Sodium hydroxide
NaSMe	Sodium thiomethoxide
Na ^t BuO	Sodium <i>tert</i> -butoxide
NBS	N-bromosuccinimide
NEt ₃	Triethylamine
NMP	N-methyl-2-pyrrolidone
NMR	Nuclear magnetic resonance
NOE	Nuclear Overhauser effect
oFET	Organic field effect transistor
oLED	Organic light emitting diode
OM	Oligomeric material
oPV	Organic photovoltaic
P	Polarizer group
<i>p</i> -	<i>Para</i>
<i>p</i> -CH ₂ O	<i>Para</i> -formaldehyde
P(<i>t</i> -BuA)	Poly(<i>tert</i> -butyl acrylate)
PAA	Poly(acrylic acid)
PAV	Poly(arylene vinylene)
PBA	Poly(<i>n</i> -butyl acrylate)
PCBM	[6,6]-phenyl-C ₆₁ -butyric acid methyl ester
PdCl ₂ (PPh ₃) ₂	Bis(triphenylphosphine)palladium(II) dichloride
<i>PDI</i>	Polydispersity index
PEG	Poly(ethylene glycol)
PFS	Poly(ferrocenyldimethylsilane)
PI	Polyisoprene
PLA	Poly(lactic acid)
PM	Polymeric material
PMA	Poly(methyl acrylate)
PMDETA	N,N,N',N'',N'''-pentamethyldiethylenetriamine
PMMA	Poly(methyl methacrylate)
POM	Polyoxomethalate
PP(CN)V	PPV synthesized <i>via</i> Knoevenagel polycondensation
PPG	Poly(propylene glycol)
PPh ₃	Triphenylphosphine
ppm	Parts per million
PPV	Poly(<i>p</i> -phenylene vinylene)
PPyV	Poly(pyridine vinylene)
<i>p</i> -QM	<i>Para</i> -quinodimethane

PS	Polystyrene
P(S-stat-C ₆₀ MS)	Statistical polymer of PS and C ₆₀ decorated PS
P2VP	Poly(2-vinylpyridine)
q	Quadruplet
RI	Refractive index
ROMP	Ring opening metathesis polymerization
RT	Room temperature
s	Singulet
sec	Seconds
SEC	Size exclusion chromatography
sec-BuLi	Sec-butyl lithium
sec-BuOH	Sec-butanol
SET-LRP	Single electron transfer – living radical polymerization
t	Triplet
T	Temperature
TBAF	Tetra- <i>n</i> -butylammonium fluoride
<i>t</i> -BuA	<i>Tert</i> -butyl acrylate
TEMPO	2,2,6,6-tetramethylpiperidin-1-oxyl
TeO ₂	Tellurium dioxide
TFA	Trifluoroacetic acid
<i>T_g</i>	Glass transition temperature
TGA	Thermogravimetric analysis
THF	Tetrahydrofuran
THT	Tetrahydrothiophene
TLC	Thin layer chromatography
TMS	Tetramethylsilane
TosCl	<i>p</i> -Toluenesulfonyl chloride
UV	Ultraviolet
UV-Vis	Ultraviolet-visible
B → M + I	Addition mode of base to monomer and initiator mixture
I + B → M	Addition mode of initiator and base mixture to monomer
M → I + B	Addition mode of monomer to initiator and base mixture

PUBLICATIONS AND PERSONAL CONTRIBUTION

PUBLICATIONS

"Discovery of an anionic polymerization mechanism for high molecular weight PPV derivatives *via* the sulfinyl precursor route" **I. Cosemans**, L. Hontis, D. Van Den Berghe, A. Palmaerts, J. Wouters, T. Cleij, L. Lutsen, W. Maes, T. Junkers and D. Vanderzande, *Macromolecules*, 2011, 44, 7610.

- Article writing

"Living polymerization *via* anionic initiation for the synthesis of well-defined PPV materials" **I. Cosemans**, J. Wouters, T. Cleij, L. Lutsen, W. Maes, T. Junkers and D. Vanderzande, *Macromol. Rapid Commun.*, 2012, 33, 242.

- Article writing
- Synthetic work on substituted monomer and BEH-PPV, characterization and analysis

"Controlled synthesis of MDMO-PPV and block copolymers made thereof" J. Vandenberg, **I. Cosemans**, L. Lutsen, D. Vanderzande and T. Junkers, *Polym. Chem.*, 2012, 3, 1722.

- Synthetic work: MDMO-PPV synthesis with different amounts of CBr₄
- Not presented in this thesis

"Anionic PPV polymerization from the sulfinyl precursor route: Block copolymer formation from sequential addition of monomers" **I. Cosemans**, J. Vandenberg, V. S. D. Voet, K. Loos, L. Lutsen, D. Vanderzande and T. Junkers, *Polymer*, 2013, 54, 1298.

- Article writing
- All synthetic work, characterization and analysis

"Synthesis of well-defined PPV containing block copolymers with precise endgroup control from a dual-initiator strategy" **I. Cosemans**, J. Vandenberg, L. Lutsen, D. Vanderzande and T. Junkers, *Polym. Chem.*, 2013, 4, 3471.

- Article writing
- All synthetic work, characterization and analysis
- ESI-MS measurements: Joke Vandenberg
- DLS measurements: Linny Baeten

"Synthesis of PPV-*b*-PEG block copolymers using *Click* chemistry" **I. Cosemans**, J. Vandenberg, L. Lutsen, D. Vanderzande and T. Junkers, 2013, to be submitted.

- Article writing
- All synthetic work, characterization and analysis
- DLS measurements: Linny Baeten

CONFERENCES: oral presentations

"Anionic polymerization of PPVs" **I. Cosemans**, J. Vandenberg, L. Lutsen, D. Vanderzande and T. Junkers, KVCV Chemistry Conference for Young Scientists, March 2012, Blankenberge.

"Anionic polymerization of PPVs, use of ESI-MS to prove initiator efficiency"
I. Cosemans, J. Vandenberg, L. Lutsen, D. Vanderzande and T. Junkers, Belgian Polymer Group annual meeting, May 2012, Blankenberge.

CONFERENCES: poster presentations

"Anionic polymerization of PPVs and use of anionic initiators" **I. Cosemans**, L. Lutsen, T. Junkers and D. Vanderzande, Belgian Polymer Group annual meeting, May 2011, Houffalize.

"Anionic polymerization of PPVs: initiation vs propagation" **I. Cosemans**, L. Lutsen, T. Junkers and D. Vanderzande, NanoPV, October 2011, Universiteit Hasselt.

"Anionic polymerization of PPVs: initiation vs propagation" **I. Cosemans**, L. Lutsen, T. Junkers and D. Vanderzande, 1st P2M conference Precision Polymer Materials, December 2011, Obernai, France.

"Synthesis of well-defined PPV polymers with precise endgroup control and block copolymer synthesis" **I. Cosemans**, J. Vandenberg, L. Lutsen, D. Vanderzande and T. Junkers, BeGe Macromolecular meeting, December 2012, Houffalize.

"Synthesis of well-defined PPV polymers *via* the anionic route and block copolymer synthesis" **I. Cosemans**, J. Vandenberg, L. Lutsen, D. Vanderzande and T. Junkers, Belgian Polymer Group annual meeting, May 2013, Houffalize.

"Anionic pathway toward well-defined polymers with precise endgroup control and synthesis of block copolymers" **I. Cosemans**, J. Vandenberg, L. Lutsen, D. Vanderzande and T. Junkers, EPF conference Pisa, June 2013, Pisa – Italy.

Awarded 'Best Poster'

DANKWOORD

Ik ben er geraakt, aan het dankwoord! Iedereen heeft altijd gezegd: "wacht maar, dat wordt nog een moeilijk stukje" en ze lijken nog gelijk te krijgen ook... Want natuurlijk wil ik nu niemand vergeten, zorgen dat iedereen stuk voor stuk zijn of haar bedankje krijgt want vier jaar onderzoek, dat is heel wat. Dus bij deze, moest ik je toch vergeten zijn: Dank je wel! Zo, dat is dus al in orde ☺

Eerst en vooral wil ik Thomas bedanken. Thomas, danke für die Energie, die du in mich und meine Arbeit investiert hast. Durch deine Hilfe wurde meine Doktorarbeit zu dem was sie ist und worüber ich sehr glücklich bin. Vielen Dank auch für dein Vertrauen und deine motivierenden Worte. Dirk, promotor van het eerste uur, als het van jou afhing zou ik nog een jaartje verder doen, maar dat maakt het des te duidelijker hoe snel 4 jaar voorbij vliegen. Dank je wel voor alle hulp en input en voor de vele ideeën, al dan niet verwezenlijkt tijdens mijn onderzoek! Laurence, thanks for your help during my work at the university. Also thanks for the 'clean hood award' as the colleagues like to call it here! Wouter, ook jou mag ik zeker niet vergeten voor de hulp bij mijn eerste twee publicaties, de gezellige babbels en het lesgeven. Iets wat ik nooit echt graag gedaan heb, maar waar ik wel enorm in ben kunnen groeien! Peter, dank je wel voor het opnemen van en de hulp bij het ontrafelen van een aantal NMR spectra. Richard en Katja, dank je wel om in mijn jury te zitten. Katja, bedankt voor de fijne twee weken die ik heb mogen doorbrengen in jouw labo in Groningen (en deze 'dank je wel' mag zeker ook doorgegeven worden aan Vincent!).

Het financiële plaatje is ook niet te vergeten, 4 jaar onderzoek, daar kruipen heel wat centjes in. Graag wil ik het BOF (Bijzonder OnderzoeksFonds) van de UHasselt bedanken voor de financiering van mijn doctoraat. Ook het ESF (European Science Foundation) wil ik bedanken omdat het mij de mogelijkheid gaf om gedurende twee weken naar Groningen te gaan om daar mijn onderzoek verder te zetten en te verbreden. Het FWO (Fonds Wetenschappelijk Onderzoek) wil ik graag bedanken voor financiering van het congres in Pisa.

Voor al mijn collega's, zowel de 'oude' als de 'nieuwe', merci, bedankt, dank je wel, voor de fijne tijd in het labo. Ik heb er mij altijd thuis kunnen voelen en gewoon mezelf kunnen zijn! Joke (samen naar Straatsburg en Pisa, ik vond het altijd gezellig!!), Sarah (positiviteit!), Hanne (veel van je geleerd! ☺), Ans (veel geluk met jullie kindje!), Toon (buurman, pintjes... Altijd gezellig!), Suleyman (altijd meelachen met onze Nederlandse mopjes), Lidia (doing columns in the hood next to mine...), Iris (gezellige babbeltjes en merci voor de eerste GPC metingen), Tom (altijd klaar met een grappig katten-filmpje of wat flauwe zever!), Matthias (veel succes, jij bent ongeveer volgende in rij!), Jurgen (nieuwe buurman en zuurkast-deler, gelukkig was die heel groot :p), Pieter (langs mij leek jij misschien nog meer rommel te maken dan het eigenlijk was..), Kayte (yummy cakes!), Julija (nice and quite, sorry for the noise sometimes ☺), Rafaël (met dank aan de Mitsunobu reactie!), Neomy (eindelozes babbels, tot de mannen er gek van werden, dank je wel meid! Ik ga je missen als ik hier weg ben!!), Benjamin (thanks for the translation ☺), Stephan (de atypisch stille Nederlander, zeker in vergelijking met Neomy), Veronique (ja, de mannen hier hebben nog veel te leren, zeker als het over jasjes gaat!), Linny (mooie DLS metingen en gezellige babbels!), de bio-afdeling (Erik, David,

Brecht, Duy Tien, Rebecca), Evelien (dankzij jouw werk is een groot deel van hoofdstuk 4 er! Veel succes, het ga je goed!), Jasmien, Geert, Jeroen, Sanne, Matthias en Gaël (veel succes allemaal, voor jullie begint het nog maar pas...!).

De studenten die ik heb mogen begeleiden: Mieke, Evelien (nogmaals ☺) en Annelies, dank je wel voor jullie harde werk!

Gunter en Koen, dank je wel voor het opnemen van mijn vele NMRs. Gunter, een extra bedankje is hier op zijn plaats voor je antwoord op mijn vele vragen! Huguette, bedankt voor je hulp bij de vele UV-Vis, FT-IR en fluorescentie metingen, zeker als de computers weer eens een vervelende foutmelding gaven. Jan ('de-massa-man'), dank je wel voor het opnemen van de vele massaspectra, Guy en Martine, bedankt voor de TGA en DSC metingen en ook Jenny, dank je wel voor je hulp bij de GPC (zeker die oude...).

Hilde (mmm, koude kersentaart!), Gène en Rita van didactiek, ook jullie wil ik bedanken voor het lenen van materiaal (en de afwas ervan in de afwasmachine) en de hulp bij het geven van de labo's.

Anke (en Tim), Brecht (en Jorinde) en Katrien, mijn studiegenootjes! Dank jullie wel voor de fijne avondjes die we zijn blijven houden, ik hecht er veel belang aan en hoop dat we dit zeker gaan blijven doen! Hopelijk kan ik binnenkort van jullie doctoraat een exemplaar in mijn kast zetten!! ☺

Natuurlijk hebben de voorbije vier jaren niet alleen een chemische insteek gehad, maar zijn er ook nog heel veel mensen van buitenuit die ik moet bedanken! Al snapten ze er eigenlijk niet zo heel veel van, toch bleef iedereen vaak genoeg naar mijn onderzoek vragen (en zelfs geïnteresseerd luisteren)!

Eerst en vooral Sofie!!! Altijd klaar voor een knuffel als het wat minder goed ging, een babbel als het nodig was, een ontspannen reisje naar eender waar,

een 'zotte doos in crime'. Alles wat wij al samen meegemaakt hebben is niet in het kort samen te vatten. Ik zie je graag! Veel geluk nog samen met Wim (als je nog eens werkershanden nodig hebt... Je weet mij te vinden hè! En ik jou ook!). Lien en David (en de kleine Louise), dank je wel voor alles! Jullie zijn super vrienden!!

Ook niet te vergeten zijn Daisy, Kevin, Dorien, Marijke en Thomas, de EVA's en de leden van Vocal Fun. Dank je wel voor alle fijne momenten die we al hebben kunnen delen, en de vele die er hopelijk nog gaan komen! ☺

Een opsomming zou misschien te ver gaan, maar de 'Cosemannekes' verdienen hier zeker ook een plaats! Moeke, tantes en nonkels, nichten en neven (en de vele achterneven en -nichtjes ondertussen ook al)! Dank je wel voor alle fijne ontspannen familiemomenten, familieweekends en nichten- en nevendagen. Ik heb van allemaal evenveel genoten en hopelijk mogen er nog veel volgen!

Ma en pa, nonke Luc, tante, nonke Bart, Marthe en Wouter, ook voor jullie zeker een woordje van dank voor alle fijne familiemomenten en steun! En ja Marthe, voor jou een extra vermelding, dat gaat niet anders! Je bent een super-nichtje!!!! ☺

André en Kristien, Koen en Annelies (en Arne), Pieter, Stijn en Elke (en Wolf), dank je wel om mij zo snel op te nemen in jullie familie!

Mama en papa, jullie verdienen hier zeker ook een belangrijk plaatsje! Dank jullie wel voor alle steun de voorbije jaren, voor jullie luisterend oor, aanmoedigingen, interesse in de chemie, de gezellige uitstapjes, spinnen komen doodkloppen, plantjes verzorgen,... Ik zou uren kunnen doorgaan met opsommen maar woorden zijn er toch niet genoeg om te beschrijven wat jullie voor mij betekenen! Ik zie jullie graag!

Nele en Lotte, mijn liefste zussen, Maarten, mijn tofste schoonbroer, en Warre, het schattigste metekindje dat ik mij kan voorstellen... Dank jullie wel voor alles! Jullie zijn de beste!

De belangrijkste mensen komen altijd onderaan een dankwoord, en als je het laatste plaatsje verdient in de rij, ben je echt wel de allerbelangrijkste! Schatje, Liefje, Wouter, dank je wel voor alle steun, de knuffels als het even tegenzat, de aanmoedigingen, het nalezen... Niets is zo geweldig geweest als het laatste half jaartje samen met jou en ik hoop dat we er zo nog veel aan elkaar gaan breien! Liefje, ik zie je graag, met heel mijn hart!!

DANK JE WEL ALLEMAAL!!!!

*With a smile in your heart,
You can climb the highest mountain*